Spatio-temporal transcriptome analysis of surface-associated multicellular assemblages of Bacillus subtilis

Yasmine Dergham

université PARIS-SACLAY

Analyse spatio-temporelle du transcriptome d'assemblages multicellulaires de *Bacillus subtilis* associés aux surfaces

Spatio-temporal transcriptome analysis of surface-associated multicellular assemblages of *Bacillus subtilis*

Thèse de doctorat de l'université Paris-Saclay

École doctorale n°581 agriculture, alimentation, biologie, environnement et santé (ABIES)
Spécialité de doctorat: Microbiologie
Unité de recherche : Université Paris-Saclay, INRAE, AgroParisTech, Micalis Institute, 78350, Jouy-en-Josas, France.
Référent : AgroParisTech

Thèse présentée et soutenue à Paris-Saclay,

le 13/12/2021, par

Yasmine DERGHAM

Composition du Jury

Matthieu JULES Professeur, AgroParisTech (Université Paris-Saclay)	Président
Ivan MIJAKOVIC Professeur, Technical University of Denmark	Rapporteur & Examinateur
Nicola STANLEY-WALL Professeure, University of Dundee	Rapporteur & Examinatrice
Ken-Ichi YOSHIDA Professeur, Kobe University	Examinateur

Direction de la thèse

Romain BRIANDET Directeur de Recherche, INRAE (Université Paris-Saclay)	Directeur de thèse
Kassem HAMZE Professeur, Lebanese University	Co-directeur de thèse & Examinateur
Dominique LE COQ Chargé de Recherche, CNRS (Université Paris-Saclay)	Invité

Thèse de doctorat

NNT : 2021UPASB064

Maison du doctorat de l'Université Paris-Saclay
2ème étage aile ouest, Ecole normale supérieure Paris-Saclay
4 avenue des Sciences,
91190 Gif sur Yvette, France

Acknowlegments

This thesis was funded by the Union of Southern Suburbs Municipalities of Beirut, INRAE (Micalis, Jouy-en-Josas center, and INRAE DRH), Campus France, AgroParisTech foundation and was mainly carried out within the Micalis Institute (Food Microbiology in the service of health), a mixed unit between INRAE, AgroParisTech and the Université Paris-Saclay.

I want to express my gratitude for the jury members Mr. Ivan MIJAKOVIC, Mrs. Nicola STANLEY-WALL, Mr. Matthieu JULES, and Mr. Ken-Ichi YOSHIDA for their acceptance to evaluate my thesis work.

My sincere gratitude goes to my thesis director Mr. Romain BRIANDET for his continuous support, academically and personally, the great availability despite his many responsibilities, motivation, enthusiasm, and immense knowledge. His guidance, scientific rigor and his advices have taught me a lot during these three years of research and thesis writing. I could not have imagined having a better mentor and advisor for my Ph.D. study.

I expand my gratitude to my thesis co-director Mr. Kassem HAMZE for his limitless trust and confidence that he has placed in me. I would like to thank him for having encouraged me to carry out a M2 internship on the swarming ability of *B. subtilis* from which I have learned a lot. His guidance and continuous support afterwards have allowed me to have this excellent opportunity to conduct and carry out this thesis project. Working with you was a pleasure and I am grateful and thankful for all what you have provided.

My deepest thanks goes also to Mr. Dominique LE COQ for all his help, his permanent support, encouragement and all the positive vibes I was always receiving. I thank him for all the productive discussion, persistent help, effective correction recommendations and proofreading for my writings, which allowed me to improve my skills to gain more clarity.

I take this opportunity to thank my thesis committee members Mr. Adrian DAERR for the valuable discussions and Mr. Arnaud BRIDIER for the positive contribution in this work and sharing the expertise.

I would like to thank all of whom I have collaborated with during my Ph.D.: Pierre NICOLAS for all the help and the fruitful discussions we had concerning the transcriptome data analysis; Eugenie HUILLET for her advice and for the emotional back up every time I was disappointed from the RNA extraction results; Pilar SANCHEZE-VIZUETE for the direct participation to the progress of this work; Julien DESCHAMPS, thank you very much for your help and patience while training me to use the confocal microscopy, Imaris and BiofilmQ software; it was a pleasure working with such a good mood and humor person.

I thank all the members of the Micalis Institute, and in particular all B3D team: Marie-Françoise NOIROT-GROS, Florence DUBOIS-BRISSONNET, Maud DARSONVAL, Jean-Christophe PIARD, Marina GREGOIRE, Cédric SAINT-MARTIN, Virgile GUENEAU, and Aurore QUILLERE for your kindness, support, and above all for being as my second family abroad. I also like to thank former members in the team: Samia ALMOUGHRABIE and Agathe DUTOIT, for your friendship, your kindness and all the good times we had together inside and outside the laboratory.

Thanks to all the doctoral students, post-docs and trainees with whom I exchanged and spent good times: Malak, Youssra, Marwa, Jana, Hasna, Cassandre, Nay. I forgot probably a lot, so thank you all.

My sincere thanks also go to the members of the MIMA2 platforms, @BriDge, MaIAGE unit, and I2BC without whom this work would not have been possible.

I would like to extend my heartiest thanks with a deep sense of gratitude to my parents, my sister and brothers, without whom nothing would have been possible, for their unconditional love, support and always being there by my side.

TABLE OF CONTENTS

GENERAL INTRODUCTION

Bacteria perform an essential beneficial role to ultimately sustain life on this planet. With the constant environmental fluctuations, bacteria need to evolve adaptive strategies to survive, often by the formation of spatially structured aggregates enclosed by a self-produced extracellular matrix, known as biofilms [1], [2]. This collective microbial behavior gives rise to several emergent important properties, such as the formation of physical and social interactions, an increased rate of genetic exchange, and an enhanced tolerance to antimicrobials, which questions the fundamental role played by the biofilm extracellular matrix [2]. This matrix - mainly composed of water, polysaccharides, proteins, lipids, and extracellular DNA- is not only involved in the establishment and maintenance of the spatial architecture of a biofilm, but also contributes to the protection of cells from harsh environmental conditions such as dehydration, and tolerance against the action of antimicrobial agents. Besides the beneficial aspects of biofilm formation in several human applications (agricultural biocontrol, bioremediation, production of energy…), it is also responsible for deleterious clogging or biocorrosion of industrial pipes, and even for dramatic public health problems. It is estimated that nearly 80% of human chronic infections would be associated with biofilm formation and about 60-70% of the hospital-acquired (nosocomial) infections to the presence of biofilms on the surface with indwelling medical devices [3]–[5].

Within the spatial organization of a biofilm, cells respond differently to their local environmental conditions, *i.e.* different concentration gradients of chemical and nutrients, resulting in physiological heterogeneity [6]. The microscale gradients depend on the spatial localization of a biofilm, e.g. with a nutrient gradient through a submerged biofilm adherent to an abiotic surface oppositely oriented to that for a colony grown on a nutrient agar surface. As a pure culture evolves towards biofilm formation, cells need to adapt to these microenvironmental alterations, resulting in cellular physiological differentiations with each cell type displaying a distinct phenotype. Thus, a same genetically homogeneous biofilm can include surfactin producers, matrix producers, protease producers, cannibals, competent, as well as spore-forming cells [7]–[10]. Hence, in order to control these surface bounded communities, a deeper understanding of their formation is essential to originate appropriate strategies to manage the development of these complex structures.

In this context, a *Bacillus subtilis* NDmed strain, isolated from a hospital washer-disinfector [11], formed spatially organized architecture submerged biofilm with the highest biovolume when compared to seven other strains of *B. subtilis* [12]. Moreover, this strain by itself is not a pathogenic

bacteria but in mixed biofilms Briandet and his co-workers have found that the NDmed protects pathogenic bacteria, such as *Staphylococcus aureus*, from the action of biocides used to disinfect medical devices [13]. This protection has been shown to be related to the formation of highly structured biofilms with a high production capacity of extracellular matrix. Genetically the *ypqP* gene showed a potential involvement in the polysaccharide synthesis and participates in the spatial organization and thereby indirectly in the tolerance against biocide actions [14]. Thus, understanding how these surface bounded communities are formed is crucial for their contorl.

This thesis work was carried out under the co-direction of Romain Briandet (team 'Biofilms & Spatially Organized Communities' (B3D) of the Micalis Institute, a mix unit between INRAE, AgroParisTech and the Université Paris-Saclay; with the co-supervision of Dominique Le Coq) and Kassem Hamze (team 'Applied Plant Biotechnology' (APB) at the Lebanese University). It benefitted from fundings from the 'Union of Southern Suburbs Municipalities of Beirut', AgroParisTech Fondation, and INRAE (Micalis, MICA and DG). It is a French PhD from the ABIES Doctoral School (Université Paris-Saclay), mainly realized at the Jouy-en-Josas INRAE research center. A 'Campus France Cedre' program allowed me to spend 2 months in the Lebanese team at the end of the first year.

Using a multidisciplinary approach based on the skills of the two host laboratories (*B. subtilis* genetic regulation and spatial analysis of biofilms in the B3D team; genetic regulation of *B. subtilis* swarming in the APB team), we sought to identify whether genes are implicated similarly through the different surface-associated microbial communities, with special emphasis on the submerged model. Moreover, we are interested to compare spatially the different biofilm models, from which we have selected genetic determinants involved in *B. subtilis* different subpopulations encountering the various surface-associated communities to be observed *in situ* spatiotemporally.

To answer these questions, we have used different laboratory culturing approaches of surface-associated multicellular assemblages and performed a genetic comparative study with genes known to be involved in the formation and the regulation of 3D structures of *B. subtilis*. We have demonstrated that specific gene inactivation could exhibit similar impact on the different surface-associated communities, but also could differ due to their localization associated with various heterogeneity levels. Moreover, real-time confocal imaging coupled with fluorescently reported strains revealed a novel discontinuous submerged biofilm development in *B. subtilis* that is

sequentially followed by pellicle formation at the liquid-air interface after several hours of incubation and massive population redistribution. Finally, we carried out, using RNA-seq, a whole transcriptome analysis for nine different spatio-physiological conditions, from a 24 hour swarming model (four different localized compartments; the colony, base, dendrites and tips) and a 24 hour static liquid culture (three localized compartments; the pellicle, the detached cells, and the submerged biofilm), as well as the exponential and stationary phases of a planktonic culture under agitation. RNA-seq results allowed us to have a global view on the different genetic profiles for each of the differently spatial populations. Comparison between the transcriptome profiles allowed us to identify, fluorescently report differentially expressed genes, and visualize *in situ* at a cell level or over a temporal scale the genetic heterogeneity in subpopulations encountered in a biofilm model.

This thesis is thus composed of three main parts.

The **first part** corresponds to a bibliographical summary presenting the context of the main axes of this work: i) an overview of the importance of the biofilm mode of life; ii) the emerging properties associated with the spatial architecture of surface-associated communities; iii) *B. subtilis* surface-associated communities and their regulations; iv) *B. subtilis* NDmed, a strain hyper-resistant to the action of biocides and capable of protecting pathogenic bacteria in mixed biofilm.

The **second part** presents the results obtained during this work. The first chapter describes the comparison of the genetic features involved in *B. subtilis* biofilm formation using multi-culturing approaches (Article 1). The second chapter presents the coordinated population redistribution between *B. subtilis* submerged biofilm and liquid-air pellicle (Article 2). The final chapter, devoted to the multi-scale spatial transcriptome unveils the heterogeneity between subpopulations of *B. subtilis* surface-associated communities (Article 3 in preparation, with additional results presented).

This thesis concludes in a **third part** with a discussion putting into perspective all the results obtained and the avenues of research opened in *B. subtilis* multicellular mode of life and their applications.

BIBLIOGRAPHIC STUDIES

1- Biofilms are everywhere

Bacteria are frequently found living in dense communities associated with surfaces or interfaces and are usually enclosed in self-generated extracellular polymeric substances [15]–[18]. Surface bounded communities were first described in the seventeenth century, from aggregates scraped from teeth and tongue [18], [19]. Primitive microscopy techniques made it more possible to study such microbial communities. Observed samples were usually aquatic planktonic organisms colonizing surfaces such as submerged leaves, rocks, or sediments colonized by animals, algae, protists or only uncommonly large bacteria, like phototrophic, possible to be described at that time [18]. By these studies, the term "film" was first introduced and used to describe the biological layer formed on the solid surfaces particularly in biological wastewater treatment, marine biofouling and dental microbiology [18], [20]. The microbial sessile lifestyle was then recognized as an ubiquitous and predominant mode in nature, in engineered aquatic ecosystems, and in the different (commensal or pathogenic) interactions with plants, animals and humans [15], [17], [18]. These observations have led to the establishment of the term "biofilm", aroused only in the 1960s, as a general term for sessile growth of microorganisms in diverse niches [18], [21]. In the last few decades, several spatial models were proposed for the diverse appearances of the microbial biofilms associated with a surface, *i.e*, the heterogeneous biofilm model, the dense confluent biofilm model, beanstalk-like model [12], and mushroom-like biofilm model [18]. The heterogeneous biofilm model corresponds to biofilms having a thin basal layer of microorganisms with tall stacks of microcolonies raised from the surface, and was analyzed from the biofilms formed in the oligotrophic drinking water systems. For medical or aquatic environmental importance, the dense confluent biofilm model has been proposed. Moreover, certain undomesticated *Bacillus subtilis* strains, from the medical environment, were capable of forming the beanstalk-like structure on the submerged level that could reach a height of more than 300μm [12]. The mushroom-like biofilm model was proposed based on observations of bacterial strains, like *Pseudomonas aeruginosa*, grown in flow cells supplemented with relatively high nutrient conditions, forming microcolonies attached by stalks of extracellular polymeric substances (EPS) which could merge to each other and still be penetrated by water channels. The later laboratory-grown biofilms described may not represent environmental biofilms; however, these biofilm types could share several spectra [18]. For example, a transition from sparsely colonized surfaces with heterogeneous biofilms to a dense

biofilm, corresponding to the initial notion of biofilms as surface-covering biological layers, after an increased nutrient supplementation [18].

Biofilms are cell aggregates frequently embedded in a self-producing extracellular matrix that allow cells to adhere to each other and/or to develop on solid-liquid, liquid-liquid, liquid-air or solid-air interfaces [17], [18], [22]. This formation is a common characteristic throughout a diverse range of prokaryotic organisms for the most ancient lineages of the phylogenetic tree, the Archeae and the Bacteria [15]. Around 40% of these prokaryotes are above the subsurface, mostly in the biofilm form found in the soil and the upper oceanic sediments, and only a minority are as planktonic cells in oceans. Under the subsurface, in the deep oceanic and continental subsurface, almost all of the remaining 60% of the bacteria and archaea population are surface-attached cells [23]. Microbial communities are also present in association with plants, animals, and humans. To end up by an estimation of ~40-80% of cells in the largest abiotic and biotic habitats on earth reside in biofilms [23].

These microbial communities growing in biofilms provide homeostasis for cells to face harsh stressful environmental conditions, such as nutrient depletion, drought or extreme pH values [1], [24], [25] In addition, these spatial communities have been identified as facilitating cell-cell interaction that could lead to beneficial interactions with other organisms, such as symbiosis. In nature, cohabitation of microbiota (archaea, bacteria, fungi and protists) with plants promotes beneficial effects on plants' health from disease suppression, boosting plant immune system, increasing the tolerance to abiotic stresses and environmental variations [26]. For example, the rhizosphere of the ancient African crop, finger millet, is inhabited by biofilm-mediated microcolonies of a bacterial endophyte (*Enterobacter* sp.) which confers both chemical and physical barriers against the colonization by a pathogenic bacteria (*Fusarium graminearum*) [27]. Another example of symbiotic biofilm is the colonization of a host squid by the bioluminescent bacteria *Vibrio fischeri,* which allows the squid to camouflage the moonlight shadow by modulating the bacterial light [28], [29]. Moreover, biofilms have been posited to drive biogeochemical cycles involved in the processing of organic matter or the degradation of contaminants [23].

In several engineering applications, biofilms are essential and play a useful role including wastewater treatment, bioremediation, historical building preservation, in the food industry (Figure 1), production of electricity using microbial batteries, or as a biocontrol agent [30]–[34]. On the

other hand, these microbial communities are responsible for unpleasant effects on human activities such as clogging and biocorrosion of industrial pipelines, leading to huge economic losses every year [35], [36]. Biofilm-residing bacteria are well known to be resilient to host defense mechanisms, have a high level of antimicrobial resistance and to other treatments. In fact, it has been estimated that around 80% of all microbial infections are related to biofilms [37].

Figure 1: Biofilms encounter all habitats. *Biofilms are central in natural biogeochemical cycles (left column). They protect microorganisms from erosion forces in rivers and from extreme environmental conditions in Yellowstone hot springs. They contribute to the biogenic formation of mineral structures called stromatolites. Biofilms can have deleterious activity in our daily life (central column). Microbial fooling can increase the consumption of petrol by boat, or be at the origin of the grimy black substance that has been spreading over the monument's signature dome, the roof of the Jefferson memorial in the USA. Such microbial structures are also involved in chronic infections in plants, animals and humans when they involve pathogens. But biofilms can also be controlled for positive processes (right column). They can be used on fermented foodstuff for preservation and taste, as well as in several bioprocesses such as toxic compounds degradation, and biogas or electricity production.*

Chronic infections and bacterial pathogenicity are linked to bacterial biofilm formation, including recurrent urinary tract infections by enteropathogenic *Escherichia coli*, chronic rhinosinusitis or chronic wound colonization by *Staphylococcus aureus,* chronic otitis media by *Haemophilus influenzae* or *Streptococcus pneumoniae*, and cystic fibrosis pneumonia by *P. aeruginosa.* For medical concern, this latter pathogen has grabbed researchers working on biofilms

for its significant cause of chronic lung and wound infections [38]. These infections are due to the biofilm lifestyle of bacteria, which makes it difficult to eradicate either by the host immune system or even by standard antibiotic treatments, leading to increased morbidity and mortality levels [38]–[41]. Extensive studies on this bacterium allowed researchers to understand further the mechanisms, biological and physico-chemical, that take place during biofilm development, intercellular interactions and antimicrobial resistance [42], [43].

Residing in biofilms, these microorganisms are protected from host immune response or antibiotic treatment by producing extracellular polymeric substances that lead to the formation of 3D structures acting as a protective shield surrounding a congregation of bacteria [44]. This structural organization causes different microenvironments generating subpopulations of various physiological cell types responding differently to local environmental conditions (such as nutrient and oxygen accessibility, antimicrobial treatments...). Under stress conditions, bacteria slow down the metabolism by downregulating their gene expression to stop cell growth and cell division. Slow growing subpopulations of cells have enhanced tolerance and better survival rates under the action of certain antibiotics. When the conditions are back to normal, these persistent strains will propagate and regain the sensitivity against stresses[45]–[50]. In mixed biofilms, it has been shown that the interaction and co-existence of both *P. aeruginosa* and *S. aureus* during the early colonization of wound surfaces, for example, is a beneficial process for both bacteria. *S. aureus* acts as a pioneer for the attachment of *P. aeruginosa*, which in turn promotes an invasive phenotype in *S. aureus* [51]. Hence, biofilms encountering mixed bacterial populations may be an important trait for colonization, pathogenicity and their resistance [51].

Microbial infections associated with implanted medical devices are an additional important public health problem, as estimated to represent around 60 to 70% of nosocomial infections [5]. These microbial biofilms adhering on medical devices, such as intravascular or urinary catheters, pacemakers, heart valves, stents, and orthopedic implants, initially used to save lives, could be a cause of serious illness and death when being colonized by bacterial biofilms [41], [52], [53]. For example, in the USA the Agency for Healthcare Research and Quality reported that nosocomial infections are the most common complications during hospital care and one of the top ten leading causes for death [54].

Today (2021), the hot topic is the Sars-Cov-2 coronavirus (CoVs) responsible for the deadly pneumonia pandemic. Viruses, like other microorganisms, could encounter and settle within pre-existing biofilms [55]. In addition, extracellular viral assemblages were observed and proposed to correspond to viral biofilms, in which similarities were detailed between them, their composition and organization, and bacterial biofilms [56], [57]. Thus, understanding how biofilms are acting as reservoirs for highly pathogenic viruses, such as CoVs, could help in answering questions related to the persistence and ways of its transmission.

For instance, biocides used to disinfect surfaces are highly effective on planktonic microbes, although their efficacy decreases by a thousand-fold when applied over a mature spatially organized biofilm [58]–[60]. For better control, new strategies are therefore required to disinfect surfaces, treat biofilms and prevent their dispersal. The interest of biofilm communities continues to increase for a better understanding of the molecular mechanisms involved in this lifestyle.

2- Spatial organization triggers emerging properties

Typically bacteria are thought to be unicellular, however, in nature, most microorganisms live in dense and complex communities, one of the most successful modes of life [24]. Generally, biofilm development progresses in several stages (Figure 2 presenting the model for *Pseudomonas aeruginosa*). Initially, bacterial cells begin to adhere and attach to a nearby surface, then adherent cells will eventually stop separating and form chains of cells exuding extracellular polymeric substance (EPS) resulting in cell aggregation and biofilm maturation. In mature biofilms, a maximum cell density is reached and a 3D structure is considered. In old biofilms, a molecule is secreted, such as D-amino acids and polyamines, to break down the extracellular matrix around the biofilm and cells are then dispersed in the environment. In case the bacteria is a pathogenic one the latter stage will allow the migration of infection to new locations [9], [24].

Figure 2: The biofilm cycle of P. aeruginosa. *Motile cells attach to the surface and start to produce EPS. After growth and maturation, a subpopulation of cells return to the planktonic stage by active and highly regulated mechanisms. (From: [61]).*

Spatial biofilms composed of high cell density with different heterogeneity levels can build between members of the same or different species co-inhabiting the same environment. These microbial spatial biofilm communities offer new and different properties, such as novel structures, activities, and patterns arising during the process [2]. These properties were not predictable by studies on free-living bacterial cells constantly mixed together in the same environment [2]. Cells in spatially structured communities tend to interact with the same neighbours for extended periods of time that could influence the growth, survival and diverse metabolic activities [62]. Hence, from these emerging properties, sessile spatially structured aggregates of cells can acquire or develop physical and social interactions, enhanced rate of gene exchange, and increased tolerance against harsh environmental conditions [2].

Social interactions within spatial structures

Natural selection could favour or disfavour the social phenotype, depending on the fitness costs, the effect on other cells, and the genotype of the affected cells. The social phenotype is influenced by the spatial structure of a biofilm and close neighbors are the ones directly affected [63]. Biofilm spatial structures could either be as segregated or mixed lineages (Figure 3).

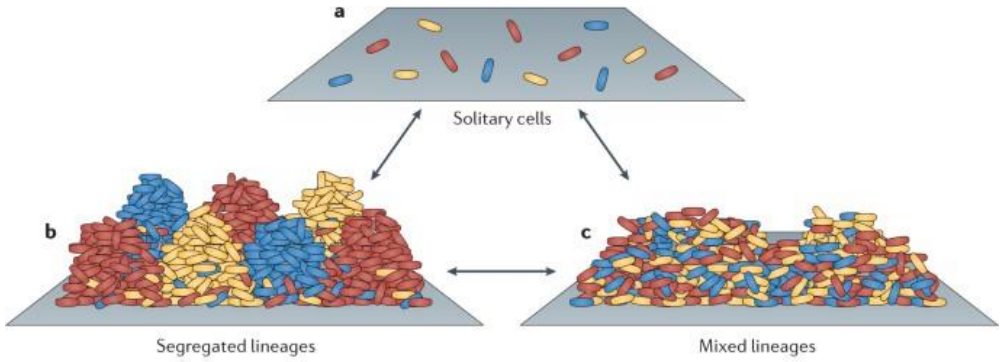

Figure 3: Microbial spatial structure influences the different social phenotypes. *a) Neither cooperative nor antagonistic social phenotype is present when cells are found solitary on a surface. b) In segregated genetic lineages, with high population size, cooperative phenotype is often favoured and sharing of public goods that exclusively benefit the close neighbouring cells. c) In mixed genetic lineages, with high population size, antagonistic phenotype is often expected to be the predominant one, however, other interactions such as commensalism and mutualism could also occur. The transition from solitary to either segregated or mixed lineages depends on several factors or vice versa by dispersal or disturbance by events that destroy the spatial structure formed. Populations can be shifted towards segregation either by default as adherent cells to a surface divide, favored by spatial bottlenecks due to limited growth, or by mother-daughter cell attachment mechanisms. Populations can form mixed lineage due to physical perturbation, diffusive cell movement, spatial homogeneous growth rates, rapid population turnover due to migration, and mutualistic cross-feeding interactions. (From: [63]).*

Spatial segregation increases the frequency of interactions between monospecies cells by favoring cooperative behaviors to enhance the ecological productivity for the biofilm as a whole [63]. For example, as *Clostridium difficile* secretes an exoenzyme with cellulolytic activity, neighboring cells can use cellulose from host tissue as a nutrient source, taking advantage of this nutrient reservoir as a public good [63], [64]. The question that arises here is when does this cooperative behavior turn out to become competitive? When the public goods are costly to be produced and how far they are shared through the clone, their evolutionary fate and maintenance depends on whether or not they benefit clonemates rather than competing species [65]–[67].

Spatial cells may become mixed lineages when they are dispersed and seeking for recolonization by means of motility in a homogenous abundant nutrient environment [68]. Hence, a competitive phenotype between several strains or species will predominate [63]. Among the different responses that could take place is the rapid growth and resource acquisition [69], or even secretion of toxins coupled with antitoxins to prevent self-poisoning [63]. On the other hand, spatial

mixed structures could promote cooperative interactions between different strains or species (reviewed in [63]). These cooperative interactions include the exchange of various metabolites compounds such as carbon sources, vitamins, amino acids and nucleotides [70]. These exchanges could be either by direct contact of the cellular membranes, by nanotubes or vesicles, or indirectly through the release and uptake of molecules from the environment [70]–[73].

In fact, well mixed different species or strains growing together in limited nutrient growth conditions often experience strong spatial bottlenecks. This leads to spatial segregation where some cell lineages are cut off by the actively growing front, with subdivision of the population into monoclonal sectors, a process known as spatial genetic drift [63], [68]. On agar surface, this process has been observed for *Escherichia coli*, *Bacillus subtilis*, *Pseudomonas aeruginosa*, and *Saccharomyces cerevisiae* [63].

Spatial architecture determined by the social interactions

Social interactions, cooperation or completion, can modify the fitness of neighboring cells by changing the population structure through the increase or decrease of the local abundance of different strains [63]. Biofilm growth often depends on individual cells on the edge of the colony involved in reproductive fitness [74]. For example, *Saccharomyces cerevisiae* secretes an enzyme 'invertase' catalyzing hydrolysis of sucrose to glucose and fructose, that can then diffuse away from cells as public goods [75]. A co-inoculation of *S. cerevisiae* wild type and an invertase-null mutant on agar surface induces a spontaneous population subdivision into monoclonal sectors where the wild type favors to benefit its own clone mates that will expand more rapidly and dominate all the colony borders [75] (Figure 4).

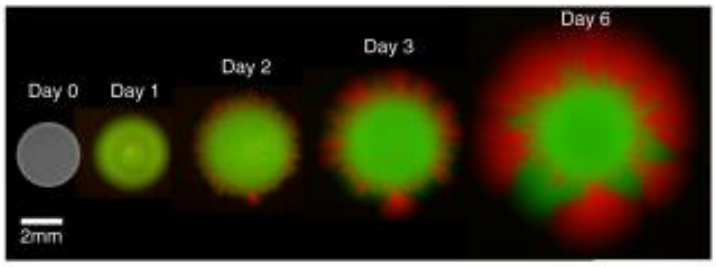

Figure 4: Public good diffusion induces cell lineage segregation in Saccharomyces cerevisiae. *Wild type cells (red), able to secrete an invertase enzyme as public goods, and invertase-null mutant (green), illustrating the evolution of cooperation promoted by spatial expansion on a surface. (From: [75]).*

These interactions between microorganisms, with same or different genotypes, could be modified through adhesion and matrix secretion that directly influence the organization of the biofilm architecture [63]. Cells remain close to their own genotype, for example, *Neisseria gonorrhoeae* can self-assort from initially mixed populations exploiting differences in the adhesion properties of cell surface pili [76]. Moreover, cells can also remain close to other genotypes when a beneficial exchange could take place between them. For instance, a co-culture of two mutualistic genotypes evolves to cell aggregation, contrary to cells grown solely in monocultures [77].

The biofilm matrix is a core key involved in the spatial phenotypes

For a three-dimensional spatial arrangement, biofilm cells produce extracellular polymeric substances (EPS) that hold them together [78]. Intermolecular interactions between the self-organized EPS components define the spatial organization by filling the gaps between the cells providing a mechanical stability for the biofilm [2], [79]. The matrix is mainly composed of water (around 97%) containing other components such as polysaccharides, proteins, eDNA, lipids, amyloids, cellulose…[2], [16], [80]. This composition provides structural and functional benefits and could differ depending on the environmental conditions and on the species if they are of the same or different strains. Several emergent properties for the biofilm is conferred by the heterogeneous, highly organized matrix: i) protection against desiccation as a water-retaining hydrogel, ii) acting as a sponge-like, capturing resources such as nutrients, gasses and other molecules and influencing their exchange between the different environmental scales, iii) trapping and long-term stabilizing, as an external digestive system, extracellular enzymes secreted by cells in the biofilm [2]. Moreover, dead cell debris also remains in the matrix and acts as a nutrient source for the alive encountering cells. DNA also has been shown to be a source of phosphorus, carbon and energy [81]. For example, *P. aeruginosa* secretes extracellular DNase to degrade DNA in the biofilm matrix and use it as a nutrient [82]. Moreover, eDNA in the matrix facilitates the horizontal gene transfer between species, which enables them to acquire new genetic material such as antimicrobial resistance allowing their persistence in the encountered stressful environment [83], [84].

Social phenotype regulated by quorum sensing

Biofilm population density is controlled by signaling mechanisms between cells to prevent an overflow of unsustainable cell level, a process known as quorum sensing [85], [86]. This

microbial regulatory mechanism is driven by autoinducers signaling molecules, such as acyl-homoserine lactones (AHLs) used for intra-species cell-to-cell communication in Gram-negative microorganisms [87], [88]. As bacterial cells constantly produce these autoinducers, their concentration in a developing community increases up to a specific threshold known as quorum level [41], [89]. At that point, autoinducers can bind to and thus activate or repress specific target genes. Hence, bacteria in the biofilm exhibit a unified response to maintain a well-coordinated adequate size biofilm [89]. Quorum sensing could also be used to time the secretion of public goods to avoid their usage by cells that do not produce them [90]. Hence, this process can regulate competitive traits such as the production of matrix that will allow the limitation of space or even of bacteriocin, a toxin secreted by *Streptococcus* spp. and *Lactobacillus* spp [91]–[93] This corresponds well to the hypothesis that microorganisms secreting toxins are effective pathogens only above a sufficient high cell density [63], [94].

Different heterogeneity levels in a 3D community

Clonal populations in a certain environment can promote phenotypic differentiation due to variations in gene expression and/or physiological adaptation to local environments [95]–[97]. In spatial 3D structures, cells can modify their microenvironment by the consumption or secretion of metabolites, thereby creating spatial gradients of nutrient concentrations leading to phenotype diversity by physiological adaptations [98], [99]. In a biofilm, a spatio-temporal correlation could take place between the phenotype and the patterns of gene expression, which can lead to subpopulations with different functions in coordination with time. For example, various types of *B. subtilis* cells are present at the same time in a biofilm, such as motile cells, surfactant producers, matrix producers and sporulating ones (Figure 5). These subpopulations with distributed different tasks are important for the growth and migration of cells seeking nutrients [7], [10], [100], [101].

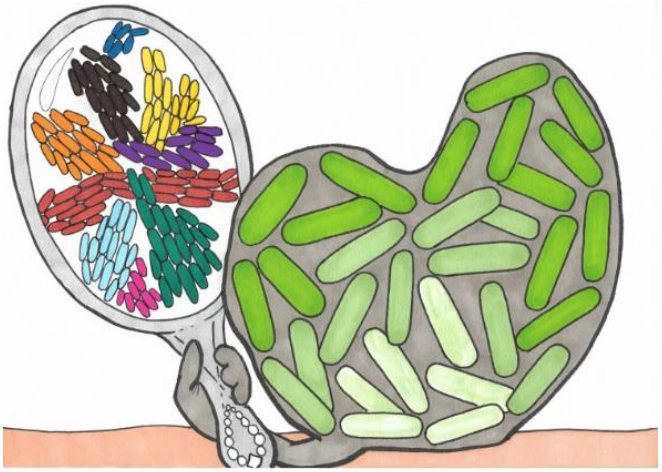

Figure 5: Diverse heterogeneity levels in a biofilm. *A schematic illustration showing bacterial surface aggregates (green) embedded in an extracellular matrix (grey). These bacterial cells represent either a mixed biofilm combining different strains of bacteria or a mono-culture of cells with different physiological cell types. (From: [101]).*

As the biofilm develops, bacterial cells growing in this community are not only physiologically different from planktonic cells, but also from each other on both the local and temporal levels. Thus, there is a correlation between the physiological and chemical heterogeneity in a biofilm, such as the microscale concentration gradients of oxygen, nutrients, as well as the accumulation of acidic waste products that lead to changes in pH values (Figure 6) [2], [6], [102]. Among these gradients, oxygen is the best studied one since the concentration profiles could be measured by microelectrodes [103], [104]. In submerged biofilms, formed on the solid-liquid interface, oxygen is present in the liquid part and the top layer of cells are mainly under aerobic respiration. The biofilm matrix is essentially an aqueous solution in which oxygen diffusion rate is approximately 60% of that in pure water [6], [105]. Hence, oxygen is unable to reach the deep cell layers in a biofilm, not because the diffusion rate is low but because the cells in the upper layers of biofilm are actively respiring it. These gradient phenomena generate different spatial subpopulations that could be separated by only a few micrometers, both in mono- and multi-species biofilms [6], [106].

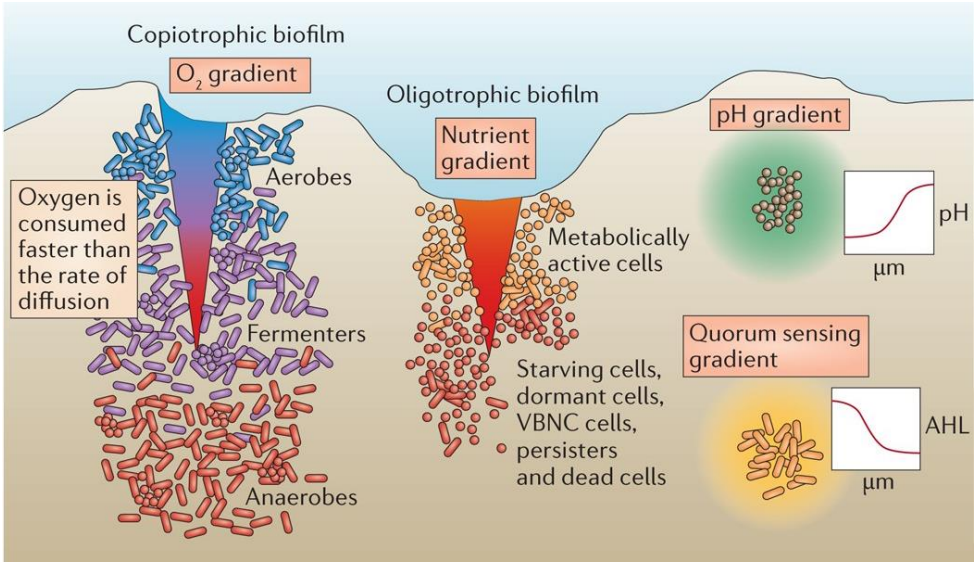

Figure 6: Different heterogeneity levels in a biofilm. *The formation of multilayered biofilm embedded in the extracellular matrix leads to the formation gradients and therefore different spatial subpopulations formed within a small scale. For example in submerged biofilms, oxygen and nutrients concentrations are higher on the top of the biofilm, which becomes depleted in the lower layers near to the abiotic surface due to their consumption from microbial organisms during their diffusion. In addition, other chemical gradients present in a biofilm such as pH and quorum sensing molecules all lead to stratified cells with physiological heterogeneity. (From: [2]).*

Microscopic methods to study and visualize *in situ* physiological heterogeneity of cells in biofilm

Biofilm visualization techniques to observe and monitor different heterogeneity levels are in fast progress. Most of these experimental techniques depend on the use of fluorescent dyes or on the construction of fluorescent transcriptional reporter gene fusions, coupled with either epifluorescence or confocal scanning laser microscopy [6]. Images then require to be treated by different softwares such as BiofilmQ, Imaris, and ImageJ to visualize, monitor, or quantify several biofilm parameters (biovolume, fluorescence intensity, trace cell movement...).

In thick spatially organized materials such as biofilms, conventional epifluorescence microscopy is no longer compatible with single-cell resolution, due to the accumulation of out-of-focus background fluorescence signals. Laser scanning microscopy (LSM) combines a set of techniques that overcomes this strong optical limitation (Figure 7).

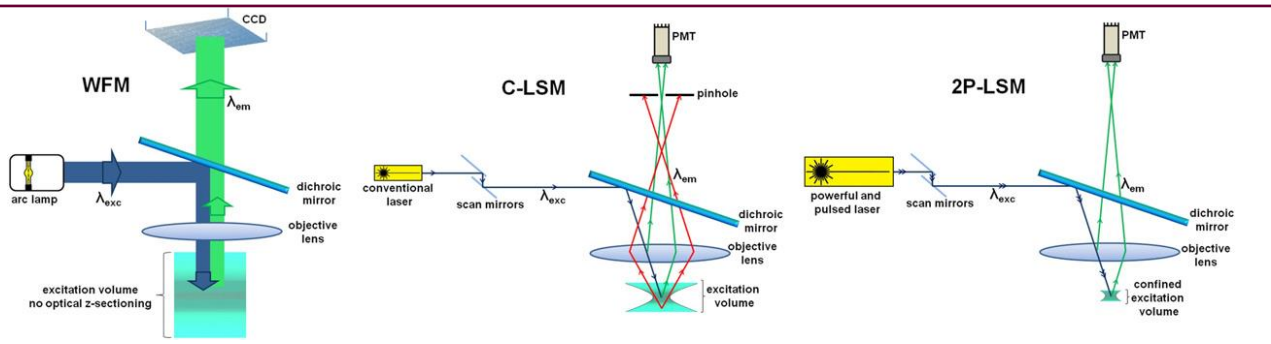

Figure 7: The direction of the optical paths in the different microscopy modes. *Wide field microscopy (WFM), confocal laser scanning microscopy (C-LSM), two photons laser scanning microscopy (2P-LSM). Illumination light is blue (excitation wavelength: λexc), in focus fluorescence emission is green (emission wavelength: λem), out of focus emission fluorescence is red. Detector: Charge Coupled Device camera (array) or PhotoMulTiplier tube (point source). (From: [107]).*

Confocal scanning laser microscopy (CSLM) has been used extensively to characterize biofilms, compare spatial organisation between strains, and also to observe the reactivity of a biocide on a biofilm over time [14], [108]–[111]. The development of technical features in the confocal microscopy provided new prospects to observe, explain and unravel the complexity of a biofilm [112], [109]**.** This technique is usually coupled with a high diversity of fluorescent markers that are able to label specifically cells, such as Syto9 or SYBER Green as nucleic acid stains used to visualize the architecture of a biofilm [12]. Staining components of a biofilm such as the extracellular matrix compounds is possible by fluorescently labeled lectins (such as ConcanavalinA), which binds to glycoconjugates of extracellular polymeric substances and thus allows to better characterize the nature and organization of biofilm matrix [113], [114]. Congo Red or thioflavin-T have been used to contrast specific matrix components [112], [115].

For spatial-temporal observation of gene expression in a biofilm, a frequent genetic approach consists in using fluorescent transcriptional fusions to genes of interest [8], [116]. Moreover, multispecies interactions in a biofilm could be also observed by reporting strains expressing constitutively different fluorescent proteins such as the green fluorescent protein (GFP) in one strain, and a red fluorescent protein (mCherry) in the other [117] (Figure 8).

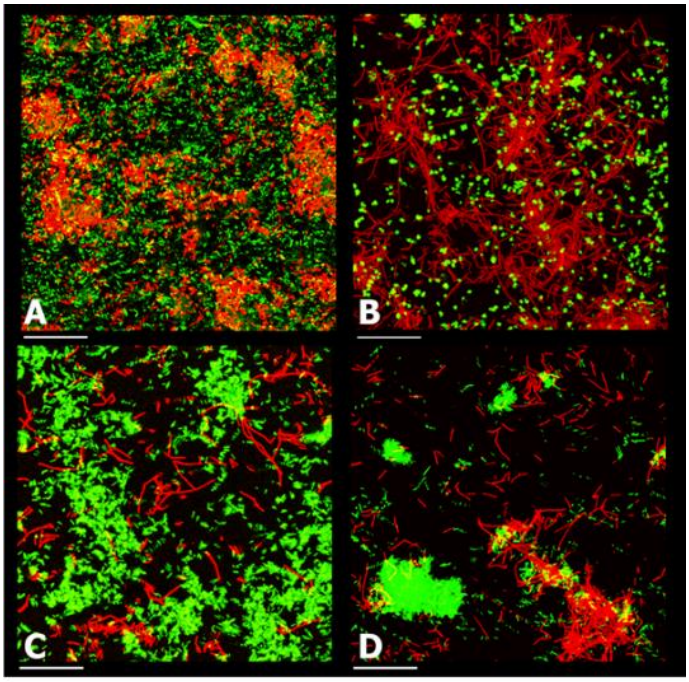

Figure 8: Multispecies spatial organization on surface associated multicellular communities. *The images display Bacillus subtilis NDmed strain reported by mCherry (red) mixed with a pathogenic strain reported by GFP (green). B. subtilis grown with A) Salmonella enterica, B) Staphylococcus aureus, C) Escherichia coli K12, and D) Escherichia coli SS2. (From: [117]).*

Fluorescent *in situ* hybridization (FISH) is another approach to localize gene expression in biofilms, both for laboratory or environmental samples [118], [119] Fluorescently labeled nucleic acid probes, designed specifically for individual species of highly conserved regions, hybridize to bacterial ribosomal RNA molecules. Fluorophores labeled with different colors and probes designed specifically for either highly conserved or divergent regions of rRNA sequence could be used to detect the distribution of different domains (Bacteria or Archaea) or specific species in a biofilm [120], [121]. One of the difficulties for this technique is the inability of the probes to diffuse within the biofilm, to penetrate the cells and bind to the nucleic acids [119], [122]. With advances in FISH new peptide nucleic acid (PNA) probes have been designed, which have greater penetration ability in the biofilm and thereby better visualization [123].

Membrane integrity is considered as a critical discriminator between alive and dead cells [124]. To estimate the efficiency of cell inactivation in biofilms [109] under stressful environments such as acidity, biocides, detergents…, a commercial nucleic acid staining kit LIVE/DEAD

*Bac*Light is frequently used [125], [126]. This kit contains a membrane permeable green fluorescent stain (Syto9) that stains all the cells and a membrane impermeable red fluorescent stain (propidium iodide: IP) that stains cells with damaged membranes. Commonly this technique allows the spatial visualization of alive cells from dead cells in a biofilm. However, by such an approach, a fake signal could be produced due to a non-specific binding when both stains are used together [126]–[128]. To limit this, propidium iodide can be used alone with strains reported by GFP when available, an approach often used in real-time visualization (Figure 9) [109], [129], [130].

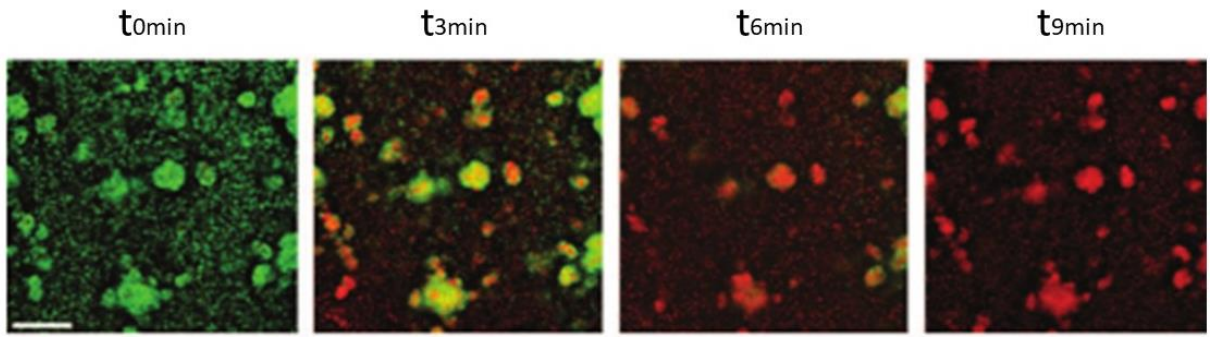

Figure 9: Visualization of Staphylococcus aureus cell inactivation over time after biocide application. *Using a BacLight Live/Dead viability kit, all viable S. aureus cells are stained by Syto9 (green) and permeabilized cells are stained by PI (propidium iodide, red). The images correspond to a horizontal section with a scale of 20µm. (From: [130]).*

3- *Bacillus subtilis* as a model organism to decipher genetic regulation of biofilm formation

Since the dawn of microbiology, the Gram-positive bacterium *Bacillus subtilis* has been the subject of hard-working laborious investigations [9]. *B. subtilis*, a member of the *Firmicutes* phylum, was originally named *Vibrio subtilis* in 1835 by Christian Gottfried Ehrenberg, and renamed *Bacillus subtilis* in 1872 by Ferdinand Cohn, who isolated the bacteria after soaking and then boiling hay [131]. Cohn characterized many of the distinctive features of *B. subtilis*: the development and formation of spores, the transition between motile and filamentous cells, and the formation of a pellicle biofilm floating on a static liquid culture. Cohn described this event clearly when the term “biofilm” was formulated much later [132]. *B. subtilis* was considered as obligate aerobe microorganism, but further studies showed that this bacteria could grow anaerobically by respiring nitrate or nitrite as an electron acceptor [133] or by fermenting pyruvate or glucose as a

carbon source [134]–[136]. It is a rod shaped, motile organism with peritrichous flagella all over the cell surface and ubiquitously found in various ecological niches.

In nature, *B. subtilis* is found in abundance in the soil, considered as its primary reservoir. As a rhizobacterium it promotes beneficial effects on the plant growth by limiting the pathogen species to develop [137], [138]. *B. subtilis* is not just a soil microorganism, but is also a member of the gut microflora in both animals and humans, as its capacity to form spores and biofilms allows this species to pass the hash gastric environment to reach and persist in the intestine [139]–[141]. With no pathogenicity nor toxic effects recorded from its contact, *B. subtilis* is considered as a GRAS (Generally Recognized As Safe) organism by the FDA (Food and Drug Administration). Moreover, with an excellent protein secretion ability, it has been widely used as a cell factory to produce heterologous proteins. *B. subtilis* is found in the agricultural industry as a biocontrol agent and also in the food industry as a probiotic and as a *natto* subspecies in traditional Japanese food from fermented soybeans [142]–[145]. The great capacity to form biofilms results in problematic side effects in industrial pipelines clogging and biofouling. But the most dangerous to human health is their persistence in medical environments and resistance to biocides where *B. subtilis* biofilms can protect pathogenic bacteria [11], [14], [111]. For all the above reasons combined with the fact that *B. subtilis* is naturally competent, easy and safe to be manipulated in the laboratory, thus it became the model for Gram-positive bacteria of studies on the genetic regulations of sporulation, carbon metabolism and biofilm formation [9], [146], [147].

In the laboratory, the experiments began with the original wild type strain, described by Ferdinand Cohn in 1872, and commonly referred to as the “Marburg strain”. This strain was subjected to X-ray and UV (mutagenic treatments) in 1947 at Yale University [148], which led to a variety of mutants, including the 168 strain, highly transformable by exogenous DNA, which allowed later to define conditions for genetic competence in *B. subtilis* [149], [150]. Hence, this strain became a genetic tool, extensively studied and in 1997 its genomic sequence was published that allowed further developments of global experimental approaches such as “omics”, phenotypical, biochemical and physiological data set [151]–[156]. Several databases have been created, among which the *Subtiwiki* database collects all available information and studies on *B. subtilis* current knowledge of the genes, their expression, and the different regulatory pathways [157] (http://www.subtiwiki.uni-goettingen.de/v3/).

Fortunately in 1930, the "Marburg strain" was deposited by Harold J. Conn in the American Type Culture Collection (ATCC) under the number 6051, and after two decades deposited in the British National Collection of Industrial Bacteria (NCIB) under the accession number 3610 [158], [159]. The two strains, ATCC 6051 and NCIB 3610, are similar and considered as the closest to the original Marburg strain and thereby as parental strains of 168 [159]. The latter has had a loss in the genetic background compared to the original ones leading to phenotypic losses such as the ability to swarm, to produce certain antibiotics, and even to form complex spatial biofilms [132], [160]–[163].

The different laboratory models of surface-associated communities for *B. subtilis*

Many bacterial species have developed different strategies to sense environmental signals and to overcome stress conditions. One of the best-studied responses is the process of spore formation by the Gram-positive bacterium *B. subtilis*. All these studies have concentrated on the ability of a single cell to differentiate into metabolically inactive spores in a homogenous planktonic culture. However, in nature, bacteria are most commonly found in the form of multicellular assemblages [25], [164]. In the early 2000s, the ability of *B. subtilis* to form biofilms, surface adherent structured communities encased by self-produced matrix, has been investigated [163]. The switch between a motile to a sessile form has been used to study these surface-associated communities.

In the laboratory, several artificial culturing conditions are used to study *B. subtilis* biofilm formations, including colonies at the air-solid interface and pellicle at the air-liquid interface (Figure 10) [163], [165]. This pioneer work has provided an experimental framework for further studies that aimed to decipher the molecular mechanisms and their regulations involved in biofilm formation for *B. subtilis* [8], [9], [147]. Wild-type strains of *B. subtilis* (e.g. NCIB 3610) has shown to have the ability to form spatially organized colonies and well-structured pellicles, while laboratory strains, such as the reference strain (168), are only able to form smooth colonies and thin pellicles [163], [165]. A genetic comparison between the NCIB3610 and 168 made it possible to identify in 168 mutations responsible for the phenotypic alteration with a loss to form wrinkled and robust biofilms [165]. Most probably these mutations were acquired during the mutagenic treatment of the 'Marburg strain' in the 1950s, which has affected at least five genes the *srf*, *epsC*,

swrA, *degQ* and *rapP*. Moreover, NCIB 3610 possesses a plasmid with 102 genes among which *comI* encoding an inhibitor that prevents the development of genetic competence [166]. This explains the very low natural genetic competence ability of the natural isolate NCIB 3610, which made it more difficult to manipulate for further genetic studies, contrary to 168 which lost this plasmid.

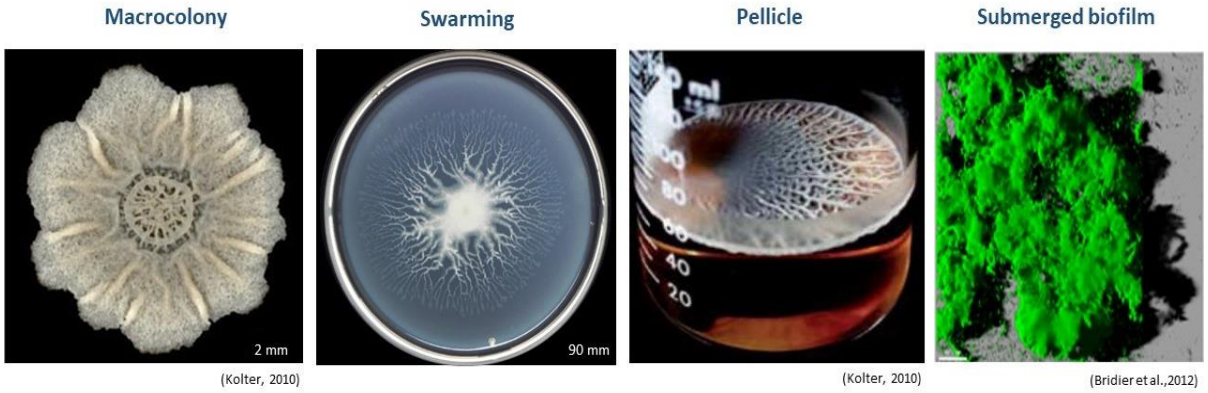

Figure 10: Biofilm models grown on different laboratory culturing conditions. *On solid agar surfaces B. subtilis grows as a macrocolony; on semi-solid media, cells swarm and colonize new niches; in liquid static culture, bacteria either grow at the air-liquid interface and form a pellicle, or adhere to a solid surface and form submerged biofilm at the solid-liquid interface (From: [9], [13]).*

Moreover, studies of surface-associated multicellular behaviors by the motile bacterium *B. subtilis* have also covered the semi-solid culturing state. *B. subtilis* wild type strains have the ability to migrate over semi-solid surfaces by organized collective movements while proliferating and consuming nutrients, a behavior known as swarming. On a rich medium, like LB, *B. subtilis* swarms in the form of a multilayered mass of cells from the site of bacterial inoculation [167]. In contrast, on well optimized synthetic medium and temperature conditions, *B. subtilis* swarms over a semi-solid agar in the form of a highly branched, monolayered dendritic pattern that covers the petri dish in a few hours at a constant rate (up to 10 mm/ hr) [168]–[171]. This system was lately used for kin discriminations among different *B. subtilis* isolates [172]. The optimal defined B-medium is used to mimic conditions for a slow growth of cells in nature and allows a highly reproducible development of swarm on both spatial and temporal levels [171]. The swarming process is as follow: (i) at the site of inoculation bacteria first grow in number and form a multilayered mother colony, (ii) after several hours of incubation bacteria secrete surfactin, which reduces the surface

tension and facilitates the translocation of bacteria on the surface, (iii) and then several small monolayered bud-like structures migrate outward from the edges of the mother colony and elongate to form dendrites [173]. The latter continue to extend in the monolayer form up to at least 1.5cm from the tips of the dendrites, before a switch to a multilayered biofilm form that starts to occur from the base of the dendrites up to the tips [169], [170], [174]. The tips of the dendrites, the final 1 to 2 mm, include hyper-flagellated and highly motile swarmers [168]. Hence, due to the early and rapid switch to a multilayered biofilm form on LB rich medium, single-cell *in situ* spatiotemporal studies for *B. subtilis* have been performed using the synthetic B-medium to identify genes involved in the different stages of swarming [168], [171], [173], [174]. *B. subtilis* NCIB 3610 strain is able to swarm robustly on this semi-solid synthetic medium, contrary to the laboratory strain 168, due to frameshift mutations in the *sfp* gene required for the surfactin synthesis [167], [169].

Surface-associated multicellular aggregates were mainly studied at the interface with air, and only few studies focused on submerged biofilm development. Such studies of surface-associated biofilms at the solid-liquid interface were first carried out by Lazazzera and co-workers [175]–[179] followed by Briandet and co-workers [12], [14], [111], [180]. Studies have focused on aerial models for the technical simplicity to observe differences in the phenotypes (due to genetic differences) between strains, without requiring complex tools to analyze them. For instance, observation of highly wrinkled architectural structures of colonies indicates a high capacity of extracellular matrix production by a particular strain of *B. subtilis*. Wrinkles are formed by a lateral compressive force as a consequence of localized cell death, coupled with the stiffness provided by the extracellular matrix [181]. Beneath the wrinkles is a remarkable network of well-defined channels, which provides the biofilm with an enhanced transport system to exchange water, nutrients, enzymes, and signals, dispose of potentially toxic metabolites, and display enhanced metabolic cooperativity [182].

On the other flip, submerged biofilm monitoring required the use of more customized laboratory tools such as flow chambers, microfluidic circuits, specific microplates or staining techniques. Advanced techniques, such as electron or confocal microscopy, and elaborated software are essential for the visualization of these biofilms and allow a deeper analysis, up to quantification of the 3D structure (thickness, roughness, and biovolume), localization of the

extracellular matrix *in situ*, as well as gene expression monitoring on spatiotemporal levels. An optimized framework for such a system, developed by Briandet and co-workers, consisting in growth of submerged biofilms in microplates, combined with confocal microscopy technique, allows both spatial and temporal monitoring of the submerged biofilms at single-cell level [12]–[14], [183].

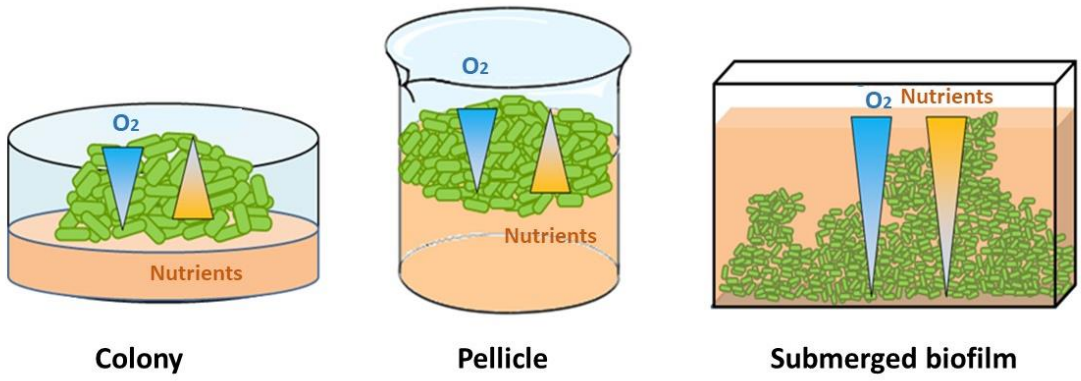

Figure 11: Spatial localization of a biofilm generates different chemical gradients. *Oxygen (O2) and nutrient gradients appearing across the 3D structure of a biofilm can intervene in the cell differentiation within the community. Both gradients are parallel in the submerged biofilm, while they are antiparallel in the colony and the pellicle. (Adapted from: [184]).*

Cells in these models are not only spatially localized in microenvironmental settings different from each other, but also chemical gradients are present within each model [6]. For example, in aerial biofilm models, the permeability of oxygen in the biomass decreases gradually from the outer top layer to the inside bottom layers, whereas the nutrient gradient is opposite, with higher concentration near the surface (nutrient agar or liquid surface). On the other hand, in the submerged model the oxygen and the nutrient gradients are parallel, with gradually decreasing concentrations through the biomass from the top to the bottom inert surface (Figure 11). These chemical gradients generate physiologically heterogeneous subpopulations within each biofilm model. Thus, the biofilm models not only spatially differ from each other, but also harbour within their own biofilm different subpopulations that differ both spatially and temporally.

Bacillus subtilis biofilm matrix

The matrix of *B. subtilis*, important for the stability, survival, and propagation of the surface-attached biofilms, is mainly composed of water, exopolysaccharides, extracellular proteins (*i.e.,* TasA, and BslA), eDNA, and other minimal deposits (Figure 12) [185]. Environmental conditions, including the cultural medium, temperature, humidity.., as well as the *B. subtilis* strain modulate the matrix composition and thereby the biofilm three-dimensional structure.

Figure 12: The biofilm matrix of Bacillus subtilis NDmed. *Scanning electron microscopy, by A. Canette and T. Meyheuc, INRA MICALIS MIMA2 Imaging Center. Cover photograph of AEM Volume 81, Number 1, January 2015, Copyright 2015, American Society for Microbiology, with permission*

Synthesis of the main biofilm extracellular polymeric substances (EPS) involves the products of the *epsA-O* operon [163]. The EPS are essential for the complex 3D structure for the colony and the pellicle, as well as for their function of water retention [186]–[188]. Mutation of this operon leads to structureless biofilms formed with the air interface, while the effect on submerged biofilms has not been studied yet [189]. The first genes of the operon, *epsA* and *epsB* encode a putative transmembrane modulator protein (EspA) and a putative kinase (EpsB), respectively, which interact specifically together to form the tyrosine kinase complex EpsAB regulating the EPS production [190], [191]. Few of the other genes constituting the *epsA-O* operon have been studied in more detail. EpsE is a bifunctional protein involved in the synthesis of the

exopolysaccharides through its glycosyl-transferase activity and also inhibits motility through the interaction with the FliG protein, a flagellar motor switch protein. Hence, the presence of EPS by itself is a signal for the activation of EpsE that synergistically contributes to the stabilization of the biofilm by activating the production of the exopolysaccharides [192], [193]. Although the precise function of certain *epsA-O* encoded proteins remains to be clarified, *i.e.*, EpsL as a sugar transferase that could transfer the first sugar to lipid carrier; EpsC, EpsM, and EpsN as playing a role in the biosynthesis of a modified monosaccharide produced by some bacteria; and EpsG still remaining of unknown function, their synthesis is necessary for the biofilm formation [163], [185], [190], [194].

Besides uncharacterized proteins in the matrix, proteins encoded by the *tapA-sipW-tasA* (*tapA*) operon are involved in the biofilm formation. TapA (previously YqxM) assembles and anchors the TasA protein, although being not essential for the formation nor having any effect on the architecture of the TasA fibers [185], [195]–[198]. Mutation of *tapA*, dramatically affects the TasA level as TapA is an accessory protein required for proper polymerization of the TasA fibers and their binding to the cell wall. Hence, the full function for both TapA and TasA in the matrix requires their associated expression in the cell [195]. The *sipW* gene encodes a signal peptidase required for post-transcriptional modification of both TasA and TapA as they are exported outside the cell [189], [199]. Moreover, SipW controls the expression of the *tapA* and *epsA-O* operons during biofilm formation after cells have adhered to a solid surface, which was not observed for biofilms formed at the liquid-air interface [179].

TasA is involved in biofilm complex structure, in sliding motility, as well as for the signaling and plant colonization [185]. Its presence in the matrix is essential for the biofilm structural integrity [115], [198]. In addition, TasA has an impact on the cell physiology, as its presence in the biofilm matrix stimulates a subpopulation to express motility genes and downregulate the matrix genes contributing in the dispersion of biofilm colony on surfaces [116], [185], [200]. Deletion of *tasA* leads to major gene expression changes: down-regulation of genes related to sporulation, and increased expression levels of genes involved in biofilm formation, antimicrobial secondary metabolite synthesis, anaerobic respiration, fermentative metabolic pathways and overflow metabolism. It has been shown that Δ*tasA* cells exhibit several symptoms indicative of excessive stress. Moreover, as TasA associates to the detergent-resistant fraction of

the cell membrane, and its loss increases membrane fluidity and cell death, it has been proposed that in addition to its structural function during extracellular matrix assembly, TasA contributes to the stabilization of membrane dynamics as cells enter stationary phase [200].

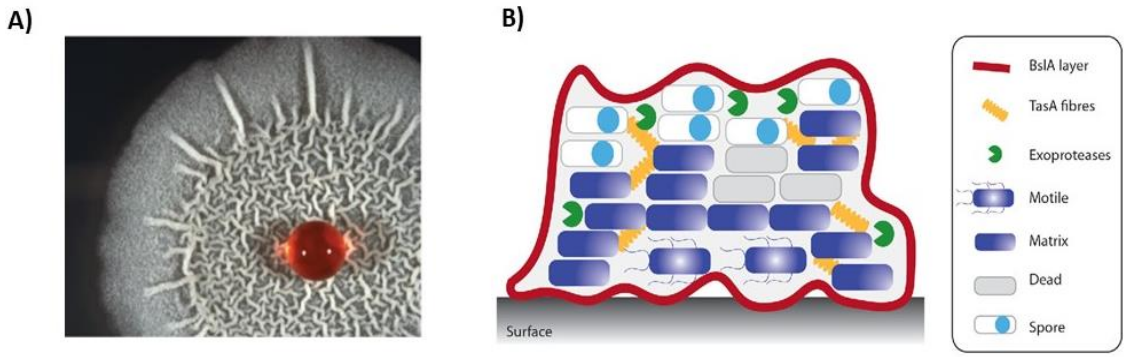

Figure 13: The 3D structure of Bacillus subtilis biofilm. *(A) Mature biofilm grown at the solid-air interface exhibits a complex architecture with emergent properties, such as high hydrophobicity as shown by the spherical form of a stained water droplet placed on the biofilm; (B) B. subtilis biofilm encounters different cell types, including cells producing the hydrophobic protein that coats the surface (From: [16], [147]).*

BslA is another structural protein required for a complex biofilm architecture and biofilm surface hydrophobicity (Figure 13) [201], [202]. This amphiphilic protein is localized to the biofilm periphery and forms a hydrophobic layer at the air interface in colonies and pellicles, even though *bslA* is transcribed evenly in the biofilm population [201], [203]. Although BslA has been shown to act cooperatively with the TasA amyloid fibers and EPS to form structurally complex biofilm, its presence is not essential for the production of these matrix components [204].

Moreover, another biofilm matrix component is the extracellular DNA (eDNA), the presence of which is essential for the 3D architecture of biofilms. The eDNA has been shown to be mainly required for the early phases (as early as 12 hours) of biofilm development, after a DNase treatment over a developing biofilm. This treatment was not affecting developed biofilms after 24 and 48 hours. A 3D evolution over time of a direct interaction between the eDNA and EPS has been observed: after 12 hours of biofilm development, a considerable amount of eDNA was connected to the bacteria; after 24 hours the eDNA was peripherally localized and the EPS were

concentrated more inside the biofilm; and after 48 hours the biofilm was entirely covered by eDNA and EPS [205].

In *B. subtilis*, the anionic polymer poly-γ-glutamic acid (γ-PGA) is a matrix component the synthesis of which relies on the *pgsBCAE* operon, regulated by the DegS-DegU and ComA-ComP two-component systems [177], [206]–[208]. Depending on the strain and the culturing conditions used, the level of γ-PGA varies. Mutations in the *psgBCAE* operon do not affect the pellicle formation [189], [209]. However, other studies performed with different *B. subtilis* strains and biofilm settings have shown that the γ-PGA increases biofilm robustness and its complex morphology [177], [207], [210].

B. subtilis also produces and secretes surfactin, a surface active lipopeptide, encoded by the *srfAA-AD* operon. Although, it has been shown that the production of surfactin triggers the synthesis of extracellular matrix and thereby formation of biofilms [144], [211], [212], it has no impact on the formation of pellicle [213]. It is important for bacterial swarming, a multicellular moving behavior of bacteria over a surface, by reducing the surface tension allowing their coordinated and rapid movement [167]. Recently, surfactin has been shown to facilitate the genetic transformation by horizontal gene transfer [214]. It is notable to mention that beside the importance of the matrix for the biofilm structure and maturation, its production is energetically expensive and the operons involved are subjected to a strict transcriptional control, even if from a social microbial view, these components can be shared by the community as public goods [147], [189], [204], [215].

Cell differentiation is triggered by complex regulatory networks

During biofilm formation, a process with a significant energy cost, *B. subtilis* has a complex regulatory network to ensure a correct timing for the expression of genes involved in producing and assembling the matrix molecules. Cell differentiation from a motile to sessile state involves mutually exclusive regulatory pathways, *i.e. B. subtilis* cells in a population are either expressing genes required for motility or for matrix production (Figure 14) [216]. Thus, the same *B. subtilis* population displays heterogeneity in its gene expression.

Extracellular signals, such as leakage of potassium due to the action of surfactants or biocides, changes in osmotic pressure, or oxygen limitation, are recognized by sensory histidine kinases KinA, KinB, KinC and KinD [217]–[219]. These kinases are indirectly involved in the

activation of the biofilm pathway through phosphorylation of Spo0A, in which the phosphoryl groups are sequentially transferred from the kinases to the proteins Spo0F, Spo0B and finally to Spo0A (Figure 14) [220], [221]. Spo0A is a central transcriptional regulator controlling more than 100 genes, including those related to the production of matrix, killing-factor toxins, and sporulation [222], [223]. The concentration of phosphorylated Spo0A (Spo0A-P) accumulated in a cell determines the gene expression profile and thereby the cell fate [222]. A threshold level of Spo0A instantly represses transcription of *abrB*, encoding a transcriptional repressor of several genes, including the *tapA* operon, involved in biofilm formation [176]. Thus, an intermediate level of Spo0A-P induces matrix production and a higher level triggers the sporulation process.

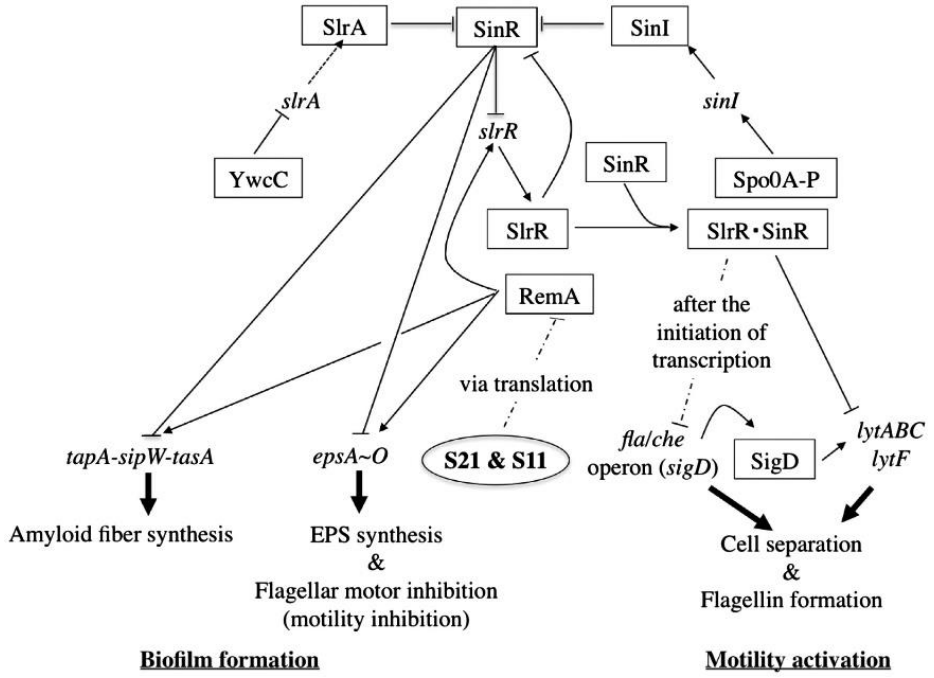

Figure 14: Complex regulatory pathways for motility and biofilm formation. *Arrows indicate activation and T bars indicate repression; transcriptional regulators are presented by squares. (From: [224]).*

Threshold levels of Spo0A-P induces an antirepressor pathway through the activation of SinI that binds directly and form a heterodimer with the transcriptional repressor SinR, thus prevents the latter from inhibiting the transcription of matrix-encoding *epsA-O* and *tapA* operons [216]. For instance, under biofilm-promoting conditions the transcriptional repressor of matrix

production operons *sinR* is expressed in most cells; however, the *sinI* is only expressed in a small subpopulation of cells, those required for extracellular matrix production [225].

SinR is not only sequestered and antagonized by SinI but also by SlrR and SlrA [226]. By a negative feedback loop, SinR represses *slrR* gene and by turn SlrR protein binds to and forms a heterodimer with SinR preventing it from binding to the *tasA* and *eps* promoters as well as inhibit SinR from repressing *slrR* gene [227]–[230]. In addition to the Spo0A/SinI pathway, YwcC/SlrA is another pathway that represses SinR [226], [227], [231]. YwcC is a transcription repressor of the divergently transcribed *slrA* gene, the products of which (SlrA protein) is paralogous to SinI. Thus, the antagonistic interaction between these proteins and SinR is similar [230]. The *tasA* and *eps* operons, as well as *slrR*, are under the positive control of RemA. Hence, SinR represses the matrix operons by antagonizing the binding of RemA [232], [233].

DegU~P like Spo0A~P functions as both activator and repressor of biofilm formation [227]. The DegU regulator controls the synthesis of other matrix components, and other several physiological processes including competence, exoprotease production, and swarming [234]. The level of DegU~P, controlled by its cognate sensor kinase DegS, determines the cell fate. For instance, high level of DegU~P inhibits complex colony architecture and swarming motility, but induces the production of exoproteases and/or triggers sporulation; intermediate level of Deg~U induces the synthesis of BslA and γ-PGA during activation of biofilm formation; non-phosphorylated DegU is required for motility (swimming or swarming) [186], [234]–[238].

EpsE, one of the proteins encoded by the *eps* operon, inhibits motility by interacting with the flagellar motor switch protein FliG in matrix producing cells at a given time point [192]. Motility genes are partly encoded by the *fla/che* operon, which include flagellar genes, chemotaxis genes and *sigD*, encoding the RNA polymerase sigma D factor. High level of sigma D activates expression of *hag* gene (encoding the flagellar filament protein) and *lytC*, *lytD* and *lytF* genes (encoding cell separating autolysins) [216], [239], [240].

The secondary messenger cyclic dimeric adenylate monophosphate (c-di-AMP) modulates Spo0A-mediated regulatory pathway. C-di-AMP controls diverse functions such as bacterial cell division and cell wall synthesis, response to DNA damage, sporulation [241], [242], and also reduces expression of *tapA* and *epsA-O* operons, thereby leading to reduction in the biofilm

formation [243]. Gundlach *et al.* have shown that inactivation of *sinR* restores biofilm formation even under increased intracellular c-di-AMP concentration; however a high intracellular c-di-AMP level was not able to affect the intracellular level of SinR, suggesting that the nucleotide affects the activity of this regulator [243]. Another study by Townsley *et al.* demonstrated that increased intracellular and extracellular c-di-AMP concentration induces expression of the *tapA* operon, required to increase biofilm formation. Moreover, *B. subtilis* can sense and respond to extracellular c-di-AMP, by two putative c-di-AMP transporters, thus revealing a potential role in inter-bacterial communication [244]. The difference in the results between the studies could possibly be due to environmental changes that had an effect on c-di-AMP intracellular levels or its secretion ability [185].

In *B. subtilis*, cyclic dimeric guanosine monophosphate (c-di-GMP) is another secondary messenger controlling diverse cell processes such as motility, biofilm formation, and cell-cell signaling. YpfA, a putative c-di-GMP receptor, interacts with the flagellar motor protein MotA and directly inhibits *B. subtilis* motility. However, the effect of c-di-GMP level on biofilm formation is still unclear [245].

Biofilm aging and dispersal

As the biofilm ages, bacterial cells become more stressed due to the increase in density of the population, nutrients and oxygen limitation, energy depletion or/and accumulations of waste products… Hence, sessile cells in a biofilm need to sense and respond to these environmental stressful signals by triggering motility to escape and to colonize new surfaces, a phenomenon known as biofilm dispersal [246], [247]. This bacterial strategy is a natural step in biofilm life cycle and when used by some pathogenic species, can increase the exacerbation, transmission and spread of infections such as in periodontitis, cystic fibrosis, pneumonia, and catheter-associated endocarditis [15], [247], [248]. Flagella synthesis is a requirement for successful dispersal motility by either swimming in liquid medium or swarming on wet semi-solid surfaces [247]. In *B. subtilis*, motility is controlled by the transcriptional regulator SinR, which activates genes involved in synthesis of flagellin (*hag*) and in cell chain separation (*lytABC* and *lytF*, encoding major autolysins), and represses genes involved in matrix synthesis, required for sessile lifestyle [147]. SinR has been suggested to be the main target of SigB, a general stress transcriptional sigma factor, which is activated during unfavourable conditions [249].

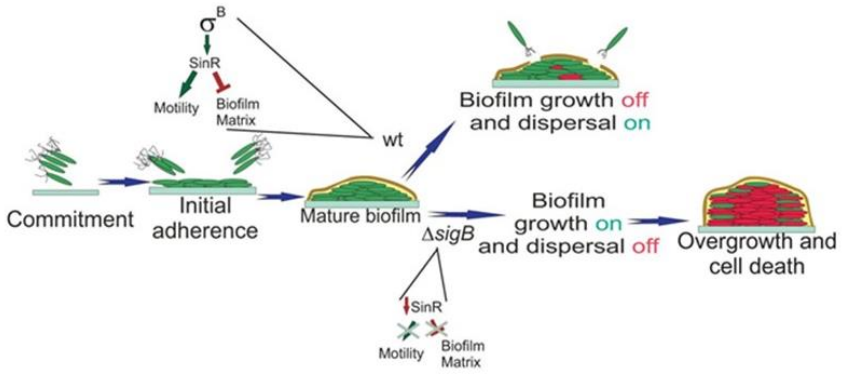

Figure 15: Biofilm dispersal is regulated by SigB. *A proposed schematic model for the role of SigB during the biofilm life cycle and its regulation on sinR. (From: [249]).*

Thus, in a mature biofilm, and in order to stop its overgrowth, stress signals are sensed by SigB. The latter triggers the dispersal phenotype by activating SinR, the master regulator that controls the exclusive expression of genes required for motile and sessile states, as explained above (Figure 15) [227]. It has been shown recently that SigB is activated in a series of stochastic pulses in developing biofilms, with the highest level of expression in *B. subtilis* cells near to the top of the biofilm (colony). These pulses of gene expression could modify the structure of the biofilm during its formation [250].

Transcriptome remodeling during *B. subtilis* biofilm development

Transcriptome studies have been performed on different *B. subtilis* biofilm laboratory models to compare the genetic profile of different strains grown similarly or using the same strain grown in different culturing conditions. Bacteria, commonly found as surface associated multicellular communities, adopt collective behaviors similar to the many processes and properties found in eukaryotes such as cell differentiation, division of labour, cell signaling, programmed cell death, morphogenesis and self-recognition [9], [251], [252]. Phylo-transcriptome tools are successfully used to track evolutionary signatures in animals, plants and fungi [253]–[257]. This approach shows independent evolution occurring during the development of the three major branches (Bacteria, Archaea, and Eukaryotes), but similar phylogeny-ontogeny correlations indicate that all eukaryotic developmental programs have an evolutionary imprint. A time-resolved transcriptome and proteome profiles analysis of a *B. subtilis* colony development selecting several time points during two months showed that biofilm ontology correlates with evolutionary measures

[258]. Three distinct periods of biofilm ontology emerged, linked by two transition stages (Figure 16), during which 99% of genes were differentially expressed when considering all ontology timepoints together. These two most dynamic transition stages between day 1 and 2 and day 7 and 14 of the biofilm development correspond respectively to 30% and 25% of variation in gene expression [258].

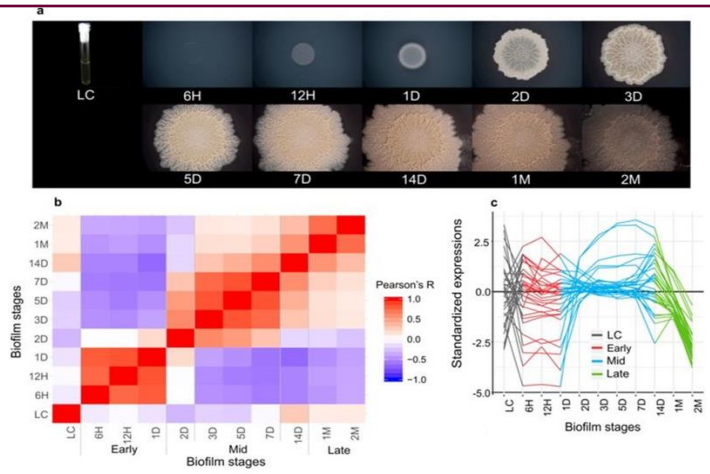

Figure 16: B. subtilis biofilm development is tightly regulated with a phylogeny-ontogeny recapitulation pattern. *a) Morphology of selected samples of B. subtilis; b) Pearson's correlation coefficients between time points of biofilm ontology; c) Average of the transcriptome profiles of the 31 most populated gene clusters. (From: [258]).*

Moreover, a functional category analysis (Figure 17) revealed that biofilm formation is tightly controlled, in which each time point has a discrete hierarchical organization at the functional level. This suggests that biofilm formation in *B. subtilis* is a genuine developmental process comparable to the non-continuous and stage-organized architecture of organismal development in animals, plants and fungi [258].

Figure 17: Biofilm ontology is a tightly controlled process with organized functional divergent stages. *A Subtiwiki functional categories (ontology depth 3) analysis over biofilm growth for genes with transcription of 0.5 of a log_2 scale above the median of their overall transcription profile. The different colors represent biofilm growth periods: liquid culture (grey) early biofilm stage (red), middle biofilm stage (blue) and late biofilm stage (green). (From: [258]).*

Another time-resolved study combining the use of metabolomics, transcriptomic and proteomic on pellicle biofilm development of *B. subtilis* has reported a widespread and dynamic remodeling affecting different metabolic pathways. All measurements were in excellent agreement, indicating that remodeling of metabolism is largely controlled at the transcriptional level during biofilm development. For instance, changes in transcription level are majorly faced by changes in protein abundance (Figure 18), many of which related to metabolism such as fatty acid synthesis, flagellar biogenesis, chemotaxis, sporulation, extracellular matrix production…[259].

Transcriptome studies provide a global comprehensive investigation of genetic remodeling taking place during biofilm development which will serve as a useful track for future studies.

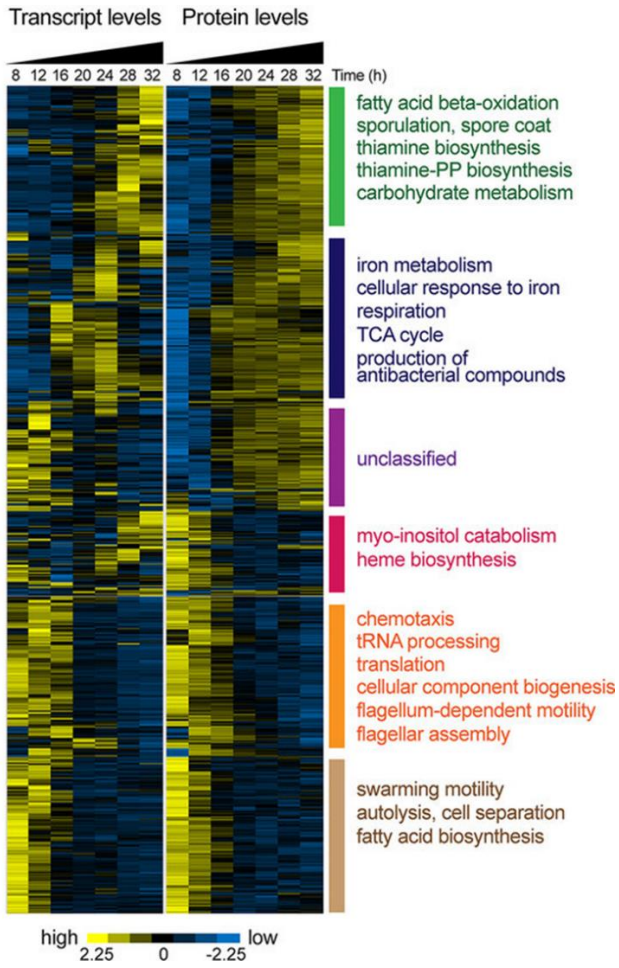

Figure 18: progressive changes on Transcriptome and proteome profiles of B. subtilis during pellicle development. *Relative transcript and protein levels of genes with significant changes in protein abundance are displayed. The high (yellow) and low (blue) color scale indicates relative transcript or protein levels across the time course. (From: [259]).*

Cellular heterogeneity in surface-associated communities of *B. subtilis*

In ideal growth conditions, all cells homogeneously submitted to the same signals would respond equally with identical growth and phenotypic behavior. However, when the conditions become unfavorable, cells need to adapt to these various environmental signals by differentiating into diverse subpopulations (Figure 19). *Bacillus subtilis* is one of the best studied microorganisms for its ability to display a broad range of cell types. For example, under stress conditions, *B. subtilis*

cells can become competent to incorporate exogenous DNA from the environment [260], [261], or can differentiate into producers of killing-factors toxins, i.e. bacteriocins, that aims to kill susceptible cells present in the medium to be cannibalized by alive differentiated cells as nutrient source [262]. The latter physiological cell states can delay the entry into the irreversible sporulation process that leads to a metabolically inactive dormant spore able to highly resist external stressors [263], [264]. Moreover, during the development of spatially organized surface-associated communities a subpopulation of cells produce an extracellular matrix, a material required to hold cells together and form complex structures [8]. Motile cells have also been observed during different stages of biofilm formation. These cell differentiations bring advantages for the bacterial community by promoting the division of labor between the members of the same population, in which different developmental features occur at the same time with a minimal energy cost [265], [266].

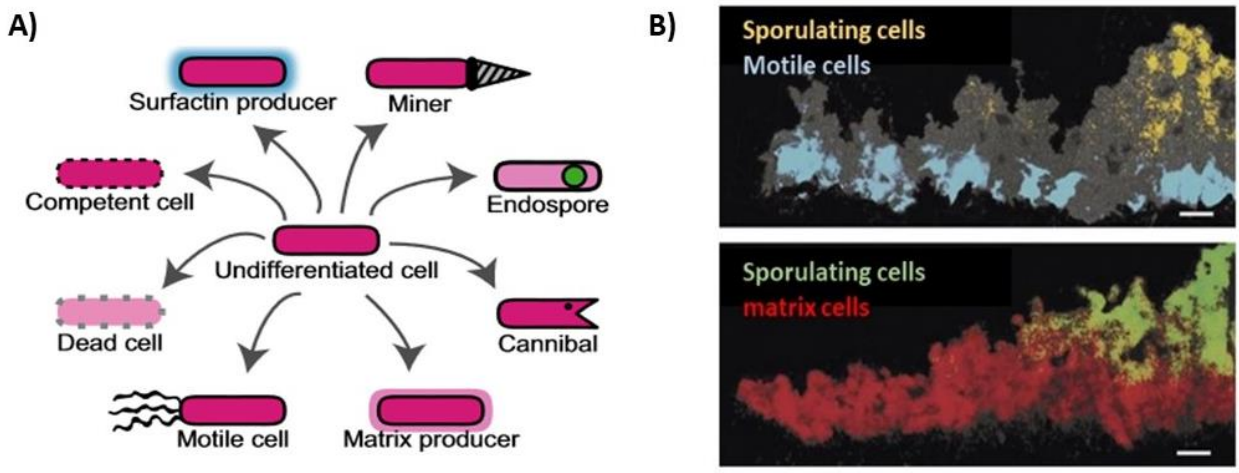

Figure 19: Differentiation of B. subtilis. *(A) Various types of differentiated cells (B) Thin section of colonies showing the different spatial localizations of differentiated cells inside a biofilm. (From: [8], [267]).*

Hidden behind these differentiated subpopulations are sophisticated networks of regulation of gene expression, responding to several different extracellular signals. These signals perceived differently from one cell to another, depending on its particular spatio-temporal location, modulate different gene expression patterns, leading to differently responding sub-populations [6], [8].

Generally, in most representative attributes for a dispersed biofilm morphology motile cells are present, which requires expression of the *hag* gene, encoding a major flagellar protein and also of *lytABC* and *lytF*, encoding autolysins responsible for cell separation. However, in a complex architectural 3D structure, genes involved in matrix production i.e. *tasA*, *eps*, *bslA*, *ypqP* and *pgs* are expressed in a subpopulation of cells.

4- *Bacillus subtilis* NDmed, a hyper-resistant strain to the action of biocides

In a large number of ecological, industrial and hospital settings surface-associated communities are the source of many problems, including public health issues such as nosocomial infections [20], [268]. For example, some studies have reported the persistence of surface-associated bacteria on an endoscope even after cleaning and disinfecting procedures take place [269], [270]. In this context, an undomesticated *B. subtilis* NDmed strain isolated from an endoscope washer-disinfector from a hospital in England [11], has been found to be hyper-resistant to peracetic acid (PAA), a biocide frequently used to disinfect endoscopes [13].

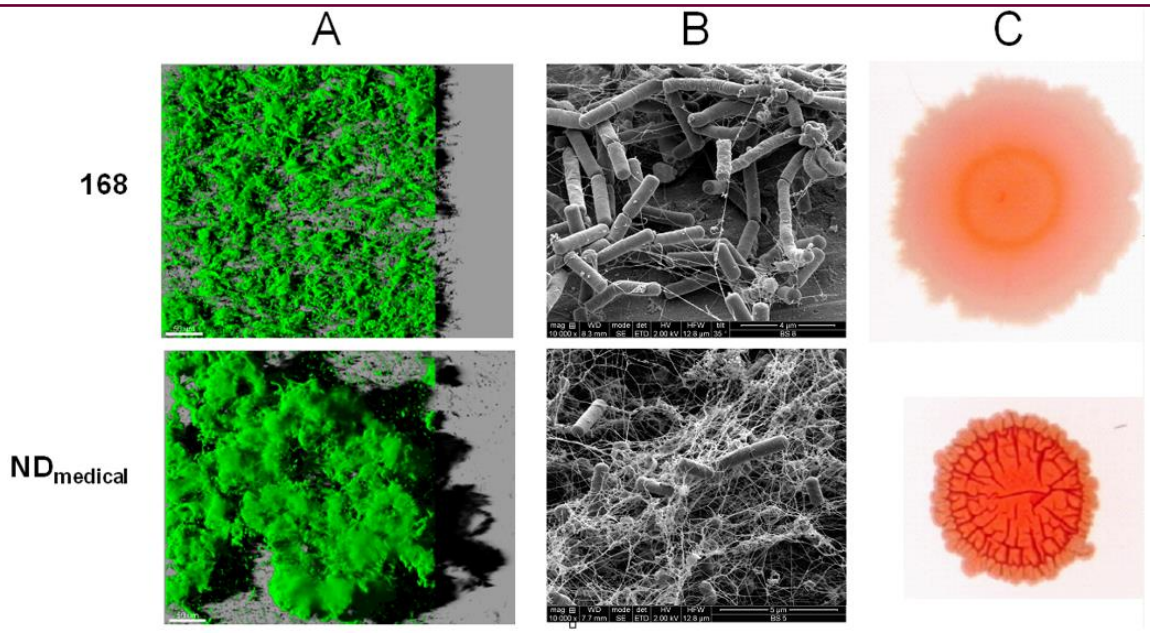

Figure 20: Comparison of architectures of biofilms formed by B. subtilis 168 and NDmed strains. *(A) 3-D projection of biofilms, with aerial view of the structure. (B) Scanning Electron Microscopy images of 24 hours biofilms (C) Dye binding properties of 72 hours macrocolonies grown on Congo red indicator medium. (From :[13]).*

Bridier *et al.* have shown that, within a collection of *B. subtilis* isolates, the NDmed strain displayed the highest biofilm biovolume with a "beanstalk-like" structure that could reach a height up to 300 µm, on the submerged level [12]. By using confocal and electron microscopy techniques, phenotypical characterization of the NDmed strain has been shown to form spatially architectural biofilms, submerged and colony, with high amounts of exopolymeric substances when compared to the *B. subtilis* 168 reference strain (Figure 20) [13]. Moreover, real-time fluorescent visualization of membranes integrity loss indicated cellular inactivation after a treatment with Peracetic acid (PAA) within 30 seconds for the biofilm cells formed by *B. subtilis* 168 strain, while the loss was much more gradual in the biofilm formed by NDmed strain, where pockets of alive cells were still visible even after 10 minutes of exposition (Figure 21) [13].

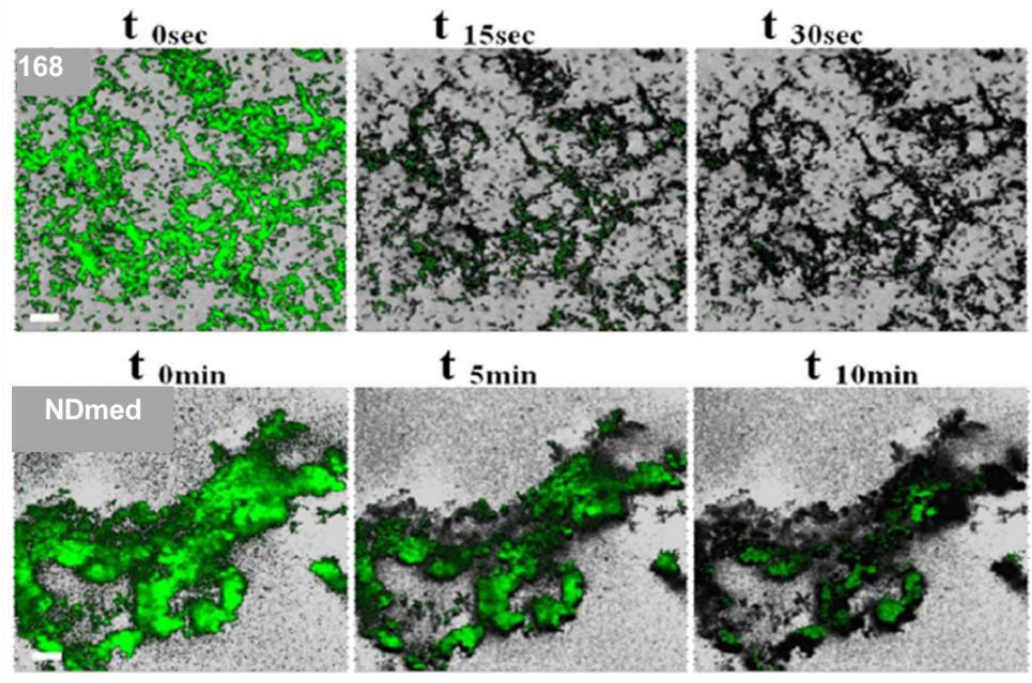

Figure 21: Peracetic acid (PAA) activity in B. subtilis biofilms. *Visualization of the kinetics of membrane permeabilization (Chemchrome V6 fluorescence) in 168 and NDmed biofilms during PAA treatment. (From: [13]).*

Genetically the NDmed sequence is very similar to that of the 168 reference strain, with less than 100 single-nucleotide polymorphism (SNPs) and less than 50 insertions/deletions [271]. Genes defective in strain 168 (*sfp*, *epsC*, *swrA*, and *degQ*) are functional in both NDmed and NCIB3610. Similar to other wild type strains, NDmed has a functional *ypqP* gene (renamed

afterward *spsM* in [272]), whereas this gene is disrupted by the SPβ prophage in both 168 and NCIB3610. The *ypqP* gene, potentially involved in the synthesis of polysaccharide, is involved in the mucoid spatial 3D structure of the biofilm and participates in the resistance against biocidal actions (Figure 22) [14].

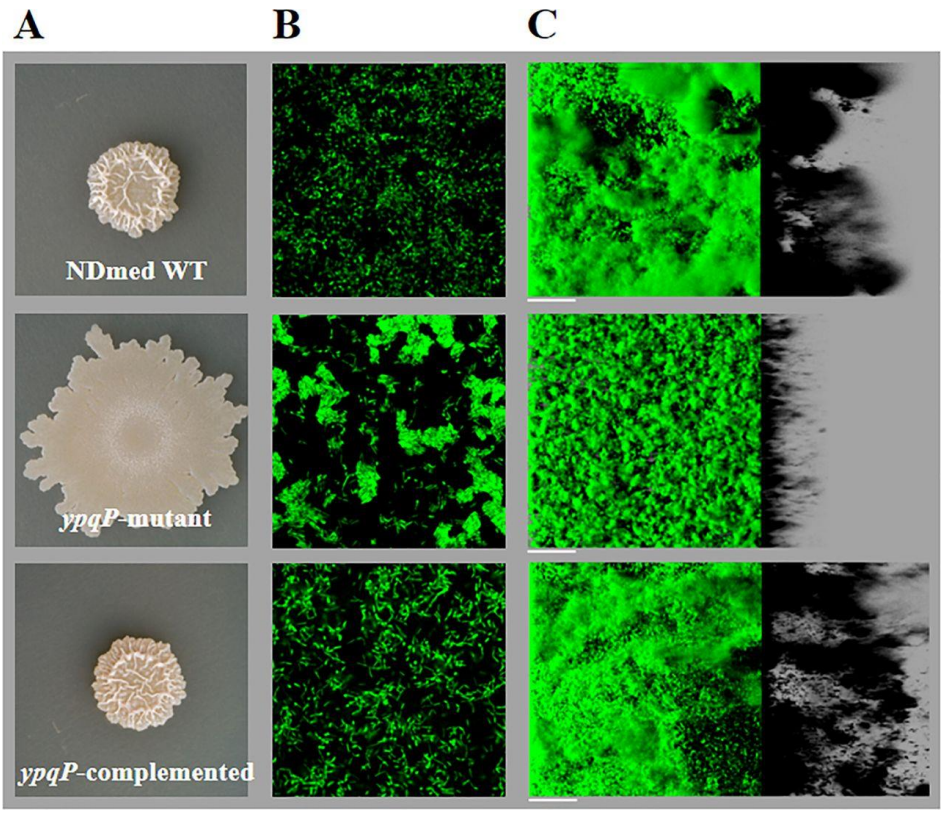

Figure 22: Visualization of the effect of ypqP disruption on submerged-biofilm structure and complex colony morphology in B. subtilis NDmed WT and mutant strains. *(A) 3 days colonies of the NDmed WT, ypqP mutant, and ypqP-complemented strains grown in TSB agar. (B and C) 48 hour biofilms of the three strains stained with SYTO9. (B) Adherent cells in contact with the surface, and (C) Reconstruction of the 3-D structure. (From: [14]).*

NDmed is not a pathogenic bacteria but has been found to protect pathogenic bacteria such as *Staphylococcus aureus* from biocide action when grown together in mixed biofilms. A *ypqP* mutant lost most of its ability to protect pathogens (Figure 23) [14]. In other words, this means that in a mixed species biofilm exposed to a biocide, a gene responsible for the persistence of the pathogen has been identified, but this gene (*ypqP*) is from the genome of the partner, not the pathogen. This observation opens doors to shotgun metagenomic approaches in this area of biofilm control as already explored in the human microbiota [273].

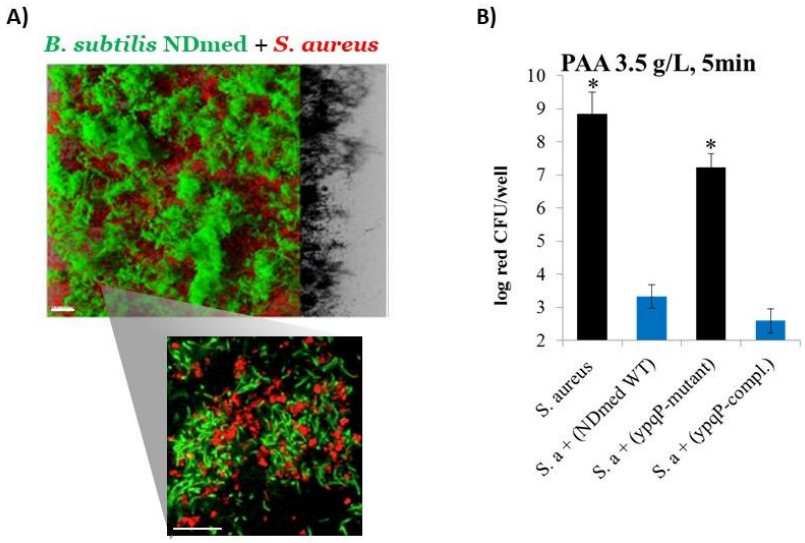

Figure 23: Bacillus subtilis NDmed and Staphylococcus aureus in mixed biofilm. *(A) 3D reconstruction and a section at higher magnification of mixed species biofilm of B. subtilis NDmed-GFP (green) with S. aureus-mCherry (red). Scale bars correspond to 20 µm. (B) A log10 reduction of S. aureus populations, mono- or dual-species (NDmed wild type, NDmed ΔypqP, and ypqP-complemented NDmed), subjected to 3.5g/liter PAA. The results are a mean of at least 8 experiments; error bars indicate the standard errors; and asterisks indicate statistically significant (P<0.05). (From: [13], [14]).*

Important highlights from the bibliography section

B. subtilis is a Gram-positive model organism one of the best studied for surface-associated multicellular communities. These studies have focused on the development of complex macrocolonies on either solid or semi-solid agar and on the formation of pellicles at the air-liquid interface. The knowledge acquired in recent years has shed light on a large number of molecular pathways involved in the surface-associated development and dispersion, including cellular differentiation, matrix production, and motility. Lately, B. subtilis NDmed, isolated from a hospital, was found to form striking submerged biofilms compared to other B. subtilis reference strains, i.e. 168 and NCIB3610, and to be hyper-resistant to the action of biocides. To develop suitable strategies to control these surface-bounded communities, certain aspects still need to be identified. For instance, using the same culture conditions determine the similarity and differences in nature of molecular determinants involved in the surface-bounded communities colonization and the dynamic growth development, with emphasis on the submerged biofilm. Different genetic tools are used to identify the requirement of a gene through phenotypic observation, mainly after 24 or 48 hours of incubation. However, little is known about the difference between these spatially localized surface-associated communities at a specific time point.

RESULTS

Chapter 1. "Comparison of the Genetic Features Involved in *Bacillus subtilis* Biofilm Formation Using Multi-Culturing Approaches"

Most of the studies on the genetic regulation of B. subtilis biofilm are based on the strain NCIB3610 and its well established biofilm phenotypes: macrocolony on agar and floating pellicle. 10 years ago, the B3D team characterized an undomesticated strain of Bacillus subtilis that was isolated from an endoscope washer disinfector in England and that was hyper-resistant to biocides (strain NDmed). It was then demonstrated that this isolate was able to protect pathogens in mixed species biofilms, and that this hyper-resistance was associated with the product of the gene ypqP that is disrupted in the strain NCIB3610. A feature of this isolate was the extended ability to form submerged biofilms on a solid surface, a phenotype that was poorly described for this species. During an international summer school on biofilm in Nice (https://epws.org/summer-school-bacterial-biofilms-nice-france/), Romain Briandet presented the team work on the submerged biofilm formed by this isolate. Rickard Losick, specialist of B. subtilis biofilm regulation from Harvard University, engaged in a constructive discussion on this submerged biofilm phenotype. He had some difficulty connecting these data with what he could observe in well established models (NCIB3610 colony and pellicle). He suggested revisiting with NDmed and the submerged model the role of the major genes described so far in biofilm formation (NCIB3610 colony and pellicle) to connect them with this new phenotype that offers in particular unprecedented imaging possibilities. It is the object of this paper. We constructed a library of NDmed mutants affected in genes previously shown to participate in the formation of macrocolony or floating pellicle by NCIB3610, and phenotyped them systematically in the 3 biofilms models for comparison.

This article has been ***published in Microorganisms 2021, 9(3), 633****;* *https://doi.org/10.3390/microorganisms9030633. It belongs to the Special Issue "Bacillus subtilis as a Model Organism to Study Basic Cell Processes".*

"Comparison of the Genetic Features Involved in *Bacillus subtilis* Biofilm Formation Using Multi-Culturing Approaches"

(Paper 1)

Yasmine Dergham [1,2], Pilar Sanchez-Vizuete [1], Dominique Le Coq [1,3], Julien Deschamps [1], Arnaud Bridier [4], Kassem Hamze [2], Romain Briandet [1,*]

1. Micalis Institute, INRAE, AgroParisTech, Université Paris-Saclay, 78350 Jouy-en-Josas, France; yasmin.dorghamova-dergham@inrae.fr (Y.D.); pilarsanviz@gmail.com (P.S.-V.); dominique.le-coq@inrae.fr (D.L.C.); julien.deschamps@inrae.fr (J.D.)
2. Faculty of Science, Lebanese University, 1003 Beirut, Lebanon; kassem.hamze@ul.edu.lb
3. Centre National de la Recherche Scientifique (CNRS), Micalis Institute, INRAE, AgroParisTech, Université Paris-Saclay, 78350 Jouy-en-Josas, France
4. Fougères Laboratory, Antibiotics, Biocides, Residues and Resistance Unit, Anses, 35300 Fougères, France; arnaud.bridier@anses.fr

***** Correspondence: romain.briandet@inrae.fr

Keywords: *Bacillus subtilis*; NDmed; biofilm; pellicle; complex macrocolonies; swarming; confocal laser scanning microscopy (CLSM)

Abstract

Surface-associated multicellular assemblage is an important bacterial trait to withstand harsh environmental conditions. *Bacillus subtilis* is one of the most studied Gram-positive bacteria, serving as a model for the study of genetic pathways involved in the different steps of 3D biofilm formation. *B. subtilis* biofilm studies have mainly focused on pellicle formation at the air-liquid interface or complex macrocolonies formed on nutritive agar. However, only few studies focus on the genetic features of *B. subtilis* submerged biofilm formation and their link with other multicellular models at the air interface. NDmed, an undomesticated *B. subtilis* strain isolated from a hospital, has demonstrated the ability to produce highly structured immersed biofilms when compared to strains classically used for studying *B. subtilis* biofilms. In this contribution, we have conducted a multi-culturing comparison (between macrocolony, swarming, pellicle, and submerged biofilm) of *B. subtilis* multicellular communities using the NDmed strain and mutated derivatives for genes shown to be required for motility and biofilm formation in pellicle and macrocolony models. For the 15 mutated NDmed strains studied, all showed an altered phenotype for at least one of the different culture laboratory assays. Mutation of genes involved in matrix production (i.e., *tasA*, *epsA-O*, *cap*, *ypqP*) caused a negative impact on all biofilm phenotypes but favored swarming motility on semi-solid surfaces. Mutation of *bslA*, a gene coding for an amphiphilic protein, affected the stability of the pellicle at the air-liquid interface with no impact on the submerged biofilm model. Moreover, mutation of *lytF*, an autolysin gene required for cell separation, had a greater effect on the submerged biofilm model than that formed at aerial level, opposite to the observation for *lytABC* mutant. In addition, *B. subtilis* NDmed with *sinR* mutation formed wrinkled macrocolony, less than that formed by the wild type, but was unable to form neither thick pellicle nor structured submerged biofilm. The results are discussed in terms of the relevancy to determine whether genes involved in colony and pellicle formation also govern submerged biofilm formation, by regarding the specificities in each model.

Keywords: *Bacillus subtilis;* NDmed; biofilm; pellicle; complex macrocolonies; swarming; confocal laser scanning microscopy (CLSM)

Introduction

Bacteria in nature frequently exist in communities that display complex social behavior, which involves intercellular signaling to permit survival and dissemination in a wide variety of habitats [1]. Even within a pure culture biofilm, where cells are genetically identical, different patterns of gene expression co-exist and therefore produce subpopulations of functionally distinct cell types [2]. Surface-associated biofilm develops in a sequential process in which sessile bacterial cells secrete extracellular matrix and aggregate as structured multicellular groups [3,4]. In nature, microbial biofilms participate in many biogeochemical cycling processes for most elements in water, soil, sediments, and subsurface environments [5]. In addition, utilization of microbial antagonists as biological control agents is a promising biotechnological alternative to the use of pesticides, which often accumulate in plants and end up by affecting humans in a direct or indirect way [6]. However, in terms of public health and with the medical science progress, more and more medical devices and/or artificial organs are being applied in the treatment of human diseases. As a consequence, biofilm-associated infections has become also frequent. It has been estimated that many bacterial infections in human are correlated with biofilm formation and are associated with the indwelling medical devices (such as catheters or needles) [7].

Over the last decades, *Bacillus subtilis*, a Gram-positive, motile, spore-forming bacterium has served as a model organism for molecular studies on biofilm formation [5]. These studies were mainly based on the development of complex macrocolonies on the agar-air interface, or floating pellicle at the air-liquid interface, and only few on submerged biofilms [8–14]. These models allowed highlighting that the transition from motile to sessile biofilm lifestyle, and vice versa, is controlled by complex genes regulatory networks. Four pairs of global regulators—the Spo0A/AbrB, SinI/SinR, SlrR/SlrA, and DegS/DegU—have been shown to play major roles, directly and indirectly, on both the formation and development of complex multicellular communities and on expression of the motility-involved genes [8, 12, 15–20]. Flagella required for motility are partly encoded by the *fla/che* operon, which, in addition to flagellar genes, includes chemotaxis genes and the *sigD* gene. In turn, the sigma D factor has been shown to direct transcription of other flagellar genes outside the *fla/che* operon (i.e., *hag* gene and other SigD-dependent motility genes) and genes involved in autolytic enzymes synthesis (*lytC, lytD*, and *lytF*) that mediate the separation of sister cells after cell division [21–24]. On the other hand, Spo0A

phosphorylation represses two negative biofilm formation regulators, AbrB and SinR, therefore leading to expression of genes involved in the synthesis of biofilm matrix (polysaccharide synthesis by *epsA-O*, amyloid like fiber TasA encoded by the *tapA-sipW-tasA* operon, and the amphiphilic matrix protein produced by *bslA*) [2,25].

In specific conditions, cells from a bacterial colony can become highly motile and migrate over the substrate with specific collective patterns, a process known as swarming [4]. Swarming—a remarkable example of cooperative behavior in bacteria—is a mass, coordinated, and rapid migration (2 to 10 mm/hr) of cells on a surface [26]. In *B. subtilis*, this developmental process is observed on semi-solid agar (0.6%–1% agar) and has been shown to be completely dependent on flagella and surfactin production [26–29].

In 2001, Hamon and Lazazzera have shown that *B. subtilis* has the ability to adhere to abiotic surfaces and form structured biofilms [8], which have grabbed biofilm researches to reconsider the importance of the immersed surface-associated biofilm model for this species. In this context, architectural comparative submerged biofilm studies performed on various *B. subtilis* strains from different origins, including NCIB3610 and 168 reference strains, have revealed an undomesticated *B. subtilis* NDmed strain as able to form the highest submerged biofilm biovolume [11, 13].

The NDmed strain, isolated from a hospital endoscope washer-disinfector was found to resist to the action of peracetic acid (an oxidizing agent commonly used in formulations used for the endoscope disinfection) and to have the ability to protect the pathogen *Staphylococcus aureus* in mixed biofilms [30,31]. By the use of confocal and electronic microscopy techniques, it has been shown that the hyper-resistant phenotype was related to the complex architectural biofilm formed and to the large amount of extracellular matrix produced that could prevent the diffusion-reaction of oxidizing agents [30]. Moreover, further genetic comparison between NDmed and other *B. subtilis* reference strains pinpointed that the *ypqP* gene (renamed *spsM* [32]), potentially involved in the synthesis of polysaccharide, was involved indirectly in this resistance by participating to the strong spatial organization of the *B. subtilis* NDmed biofilms, both at air and liquid interfaces [13]. This gene is disrupted by the SPβ prophage in both *B. subtilis* NCIB3610 and 168 strains [13].

These new observations suggested that interfaces between surfaces and liquids could, as for most other bacteria, be a relevant biotope for *B. subtilis* biofilm.

Our knowledge for the molecular mechanisms controlling the formation and the behavior of *B. subtilis* 3D communities is still limited. In this contribution, *B. subtilis* NCIB3610 and 168 strains were compared to NDmed in different laboratory culture conditions. Moreover, 15 mutants derived from the NDmed strain and defective in genes previously described as triggering biofilm formation were compared through a multi-culturing approach using four multicellular models, at the interface with air (solid agar, semi-solid agar, liquid medium) or at the interface between a solid surface (polystyrene) and a liquid medium, submerged model. Thus, this provided a global view over the different biofilm laboratory assays used to study the effect of gene mutation on both motility and biofilm formation in *B. subtilis* wild type.

2. Materials and Methods

2.1. Bacterial Strains and Growth Conditions

All bacterial strains and mutants used in this study are listed in Table 1. The *B. subtilis* NDmed derivatives mutated in various genes were obtained by transformation with chromosomal DNA extracted from strains carrying the corresponding different alleles of interest marked with a suitable antibiotic resistance cassette. Transforming chromosomal DNA was extracted according to the method of Marmur [33], and transformation of *B. subtilis* was performed according to the method of Anagnostopoulos and Spizizen [34], including the use of the MGI and MGII media of Borenstein and Ephrati-Elizur [35]. Transformants were selected on Lysogeny Broth (LB) plates supplemented with the relevant antibiotic at the following concentrations: spectinomycin, 100 µg ml^{-1}; chloramphenicol, 4 µg ml^{-1}; erythromycin, 0.5 µg ml^{-1}; tetracycline, 10 µg ml^{-1}; neomycin and kanamycin, 8 µg ml^{-1}. Before each experiment, cells were subcultured in Tryptone Soya Broth (TSB, BioMérieux, France; pH 7.2) and supplemented with antibiotics when necessary. For biofilm formation, bacteria were grown in TSB at 30 °C for 8 hrs with agitation, then diluted 1/100 in 10 mL TSB incubated overnight at 30 °C. This culture was then used to grow biofilms on different assays. Bacteria for swarming experiments were grown with agitation at 37 °C in synthetic B-medium composed of (all final concentrations; pH 7.2) 15 mM $(NH_4)_2SO_4$, 8 mM $MgSO_4.7H_2O$, 27 mM KCl, 7 mM sodium citrate.$2H_2O$, 50 mM Tris/HCl (pH 7.5), and 2 mM $CaCl_2.2H_2O$, 1 µM

$FeSO_4.7H_2O$, 10 µM $MnSO_4.4H_2O$, 0.6 mM KH_2PO_4, 4.5 mM glutamic acid (pH 8), 862 µM lysine, 784 µM tryptophan, 1 mM threonine and 0.5% glucose were added before use [36]. Antibiotics were added to bacterial cultures when needed.

Table 1. *Bacillus subtilis* strains used in this study.

Strain	Genotype or Isolation Source	Construction [a] or Reference
NDmed	Undomesticated, isolated from endoscope washer-disinfectors	[31]
NCIB3610	Natural isolate, less domesticated	[37]
168	*trpC2* (domesticated strain)	[37]
GM3248	NDmed Δ*ypqP*:: kan	[13]
GM3533	NDmed Δ*sinR*:: cm	Tf NDmed/DNA ABS840 [38]
GM3535	NDmed Δ*epsA-O*:: tet	Tf NDmed/DNA GM3532 [NCIB3610, Δ*tasA*:: kan, Δ*epsA-O::* tet] (our lab collection)
GM3539	NDmed Δ*sinI*:: kan	Tf NDmed/DNA ABS803 [39]
GM3545	NDmed Δ*cap*:: pKPSd/ cm	Tf NDmed/DNA GM3543 [NCIB3610 Δ*cap*:: pKPSd/ cm] (our lab collection)
GM3555	NDmed Δ*abrB*:: cm	Tf NDmed/DNA MM1717 [40]
GM3559	NDmed Δ*degU*:: neo	Tf NDmed/DNA GM719 [41]
GM3561	NDmed Δ*bslA*:: cm	Tf NDmed/DNA NRS2097 [20]
GM3602	NDmed Δ*lytF*:: spec	Tf NDmed/DNA NRS3295 [42]
GM3611	NDmed Δ*lytABC*:: kan	Tf NDmed/DNA NRS3295 [42]
GM3614	NDmed Δ*tasA*:: kan	Tf NDmed/DNA GM3532 [NCIB3610, Δ*tasA*:: kan, Δ*epsA-O::* tet] (our lab collection)
GM3618	NDmed Δ*slrR*:: spec	Tf NDmed/DNA GM3598 [NCIB3610 Δ*slrR::* spec] (our lab collection)
GM3619	NDmed Δ*srfAA*:: ery	Tf NDmed/DNA GM3599 [NCIB3610 Δ*srfAA*:: ery] (our lab collection)
GM3652	NDmed *amyE*:: Phyperspank-GFP / spec, Δ*hag*::cm	Tf NDmedGFP [30]/DNA OMG954 [29]
GM3671	NDmed *amyE*:: Phyperspank-GFP / spec , Δ*spo0A*:: Kan	Tf NDmedGFP [30]/DNA FBT2 [43]

[a] TF NDmed/DNA stands for transformation of NDmed by chromosomal DNA of indicated strains.

2.2. Submerged Biofilm Developmental Assays

Submerged biofilms were grown on the surface of polystyrene 96-well microtiter plates with a µclear® base (Greiner Bio-one, France) enabling high-resolution fluorescence imaging as previously described [44]. An amount of 200 µL of an overnight culture in TSB (adjusted to an OD 600 nm of 0.02) was added in each well. The microtiter plate was then incubated at 30 °C for 90 min to allow the bacteria to adhere to the bottom of the wells. Wells were then rinsed with TSB to

eliminate non-adherent bacteria and refilled with 200 µL of sterile TSB. The plates were incubated at 30 °C for 24 hrs, and 5 µM of the cell permeant nucleic acid dye SYTO 9 (diluted 1:1000 in TSB from a SYTO 9 stock solution at 5 mM in DMSO; Invitrogen, France) were added to the 200 µL culture, obtain green fluorescent bacteria. For each strain, at least 9 to 15 wells were analyzed independently.

2.3. Macrocolony Experimental Conditions

For colony architectural formation, 3 µL of an overnight culture in TSB were inoculated on 1.5% Tryptone Soya Agar (TSA) with 40 µg/mL Congo Red (Sigma-Aldrich, St. Quentin Fallavier, France) and 20 µg/mL Coomassie Brilliant Blue (Sigma-Aldrich, St. Quentin Fallavier, France). Congo Red has been shown to bind extracellular matrix components and allows to compare the ability of different bacterial strains, including *B. subtilis*, which binds to amyloidic proteins [45, 46]. The Coomassie Blue has a high affinity to bind proteins and is commonly used to detect, visualize, and quantify proteins separated on polyacrylamide gels [47, 48]. The plates were then incubated at 30 °C for 6 days. Digital images of the colonies on the plates were taken using a Canon EOS 80D with 24 MP (6000 × 4000 pixels). Macrocolony experiments were performed three to five times independently.

2.4. Swarming Experiment Conditions

Cultures for the swarm inoculum were prepared in 10 mL B-medium inoculated with a single colony and shaken overnight at 37 °C. The culture was then diluted to an OD_{600nm} of approximately 0.1 and grown until it reached an OD_{600nm} of approximately 0.2. This procedure was repeated twice and finally the culture was grown to T4 (4 hrs after the transition from exponential growth). The OD_{600nm} was measured and the culture was diluted, and 2 µL of diluted bacterial culture (10^4 CFU) were inoculated at the center of B-medium agar plate and incubated for 24 hrs at 30 °C with 50% relative humidity. Plates (9 cm diameter) containing 25 mL agar medium (0.7% agar) were prepared 1 hr before inoculation and dried with lids open for 5 min before inoculation. Pictures were taken by a digital Nikon Coolpix P100 (10 MP) camera. Swarming experiments were repeated three to five times independently.

2.5. Pellicle Experiments

After an overnight culture in TSB at 30 °C, 10 µL of the bacterial suspension were used to inoculate 2 mL of TSB in 24-well plates (TPP, Trasadingen, Switzerland). Plates were then incubated at 30 °C for 24 hrs. Digital images of the pellicles were taken using a digital Nikon Coolpix P100 (10 MP) camera. This experiment was repeated three up to five times independently for each condition.

2.6. Non-invasive Confocal Laser Scanning Microscopy (CLSM) of Submerged Biofilms

Immersed biofilms were observed using a Leica SP8 AOBS inverter confocal laser scanning microscope (CLSM, LEICA Microsystems, Wetzlar, Germany) at the INRAE MIMA2 platform (www6.jouy.inra.fr/mima2_eng/). For observation, strains were tagged fluorescently in green with SYTO 9 (1:1000 dilution in TSB), a nucleic acid marker. After 20 min of incubation in the dark at 30 °C to enable fluorescent labeling of the bacteria, plates were then mounted on the motorized stage of the confocal microscope. Biofilms on the bottom of the wells were scanned using a HC PL APO CS2 63x/1.2 water immersion objective lens. SYTO 9 excitation was performed at 488 nm with an argon laser, and the emitted fluorescence was recorded within the range 500–600 nm on hybrids detectors. The 3D (xyz) acquisitions were performed (512 × 512 pixels, pixel size 0.361 µm, 1 image every z = 1µm with a scan speed of 600 Hz). Easy 3D projections were constructed from Z-series images using IMARIS v9.0 software (Bitplane AG, Zurich, Switzerland). Biofilms biomass was estimated through extraction of the biofilm biovolume (in $\mu m^3/\mu m^2$) after isosurfaces automatic detection using the IMARIS quantification module from a minimum of twenty confocal image z-series.

2.7. Statistical Analysis

One-way ANOVA was performed using GraphPad Prism 8 software (GraphPad, La Jolla, California, USA). Significance was defined as a *p* value associated with a Fisher test value lower than 0.05.

3. Results and Discussion

3.1. Bacillus Subtilis NDmed forms Highly Structured Biofilms Compared to the NCIB3610 and 168 Strains

In the last decades, NCIB3610 has been widely used as a model for the "wild type" of *B. subtilis*. This strain has been shown to form more elaborate and robust biofilm communities when compared to the domesticated laboratory stain 168 [49, 50]. However, in both the NCIB3610 and 168 strains, the *ypqP* gene is disrupted by the SPβ prophage, contrary to several sequenced natural isolates of *B. subtilis* [13]. This gene has been shown to be involved in the strong spatial organization of biofilms of the undomesticated *B. subtilis* NDmed strain, both at air and liquid interfaces [13]. In this study, a phenotypical characterization of NDmed grown under different laboratory culture conditions was performed, in comparison with the classical reference strains NCIB3610 and 168.

Macrocolonies of these strains were observed after being grown for 6 days on indicator plates containing both Congo Red (labeling amyloidic proteinaceous compounds in *B. subtilis* biofilm matrix) and Coomassie blue (proteinaceous matrix counterstain) [46, 47]. As shown in Figure 1, the NDmed strain formed a highly structured and more compact macrocolony, contrary to the NCIB3610 and 168 strains that formed flat macrocolonies without or with only very fine wrinkles. In addition, the NDmed macrocolony was more intensely stained by the Congo Red, indicating a higher amount of exopolymeric substances and proteins produced compared to the two other strains.

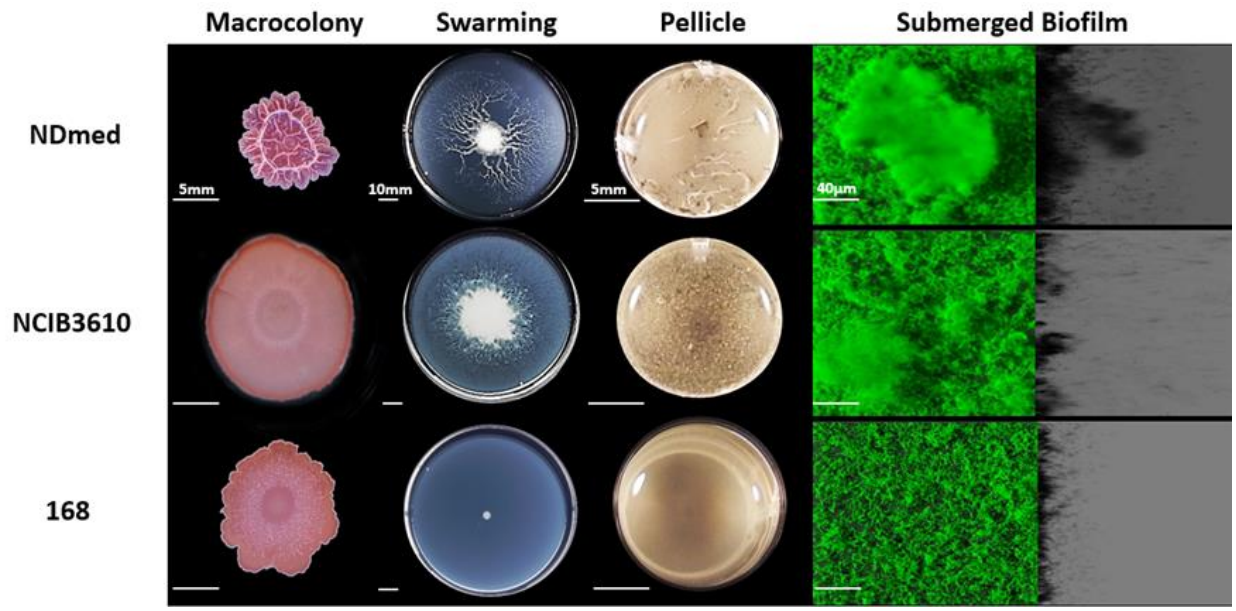

Figure 1. Comparative phenotype for B. subtilis strains on different laboratory assays. *Macrocolonies grown on 1.5% TSA for 6 days at 30 °C after a central spot of 3 µL of an overnight bacterial culture in TSB (scale bars 5 mm). 0.7% of B-synthetic medium is used for swarming plates (9 cm diameter) that are incubated for 24 hrs at 30 °C (scale bars represent 10 mm). For pellicles, bacterial cells have been cultured in a 24-well plate with TSB for 24 hrs at 30 °C (scale bars 5 mm). Macrocolony, swarming, and pellicle images are representative for the majority of the phenotype from at least three replicates for each strain, which reveal variation for the surface architecture. In a 96 well microplate system, immersed biofilms are labeled by SYTO 9 after 24 hrs of incubation at 30 °C. The shadow on the right represents the virtual lateral shadow projection of the submerged biofilm (scale bars represent 40 µm).*

As the biofilms formed by these three strains had such profound architectural differences, we wondered whether they might also present marked differences in another structured multicellular behavior i.e., swarming. Hence, to better visualize differences between them, semi-solid plates (swarming plates) were used as a 2D model to view bacterial surface colonization initiating from a macrocolony. Dendritic swarming pattern of *B. subtilis* was previously best characterized on a synthetic fully defined medium (B-medium) with optimized nutrient and temperature conditions [28]. Figure 1 shows the swarming patterns obtained on the synthetic B-medium (0.7% agar) after 24 hrs of incubation at 30 °C for the studied *B. subtilis* strains. Obviously, both NDmed and NCIB3610 showed swarming on B-medium but with varied dendritic patterns. NCIB3610 displayed a thin highly complex dendritic swarming pattern that spread all over the plate within 24 hrs of incubation, whereas NDmed swarmed with a thick countable less spread

dendritic pattern. The mother colony of the NDmed appears to be highly structured with slimy texture when disrupted mechanically by a loop. On the other hand, a less structured widely spread mother colony was formed by NCIB3610, suggesting that less extracellular polymeric substances are produced in this strain compared to the NDmed strain. The mother colony in a swarm for both NDmed and NCIB3610 closely resembles the structural architecture of the macrocolonies formed. Consistent with previous observation, the 168 *B. subtilis* strain failed to swarm on this synthetic medium, essentially because of a frameshift mutation in the *sfp* gene, required for the surfactin biosynthesis that facilitates the migration over the surface by reducing the surface tension [27].

Other models of biofilm are formed in liquid cultures, either at the air-liquid interface (pellicle) or as submerged biofilms at the solid-liquid interface [8, 10–12]. To characterize the ability of *B. subtilis* to adhere and to form submerged multicellular communities on surface, CLSM has been used to acquire confocal stack images for the submerged biofilms, from which an Easy-3D reconstruction by the IMARIS software could reveal the three-dimensional structure with a lateral virtual shadow projection. As shown in Figure 1, and in accordance with previous reports, *B. subtilis* NDmed formed well-structured air-liquid biofilm (pellicle) and highly spatially organized submerged biofilm at the solid-liquid interface [11, 13, 30].

NCIB3610 strain did not form a thick pellicle within 24 hrs of incubation at 30 °C but produced well-structured biofilms (with a biovolume of 11 $\mu m^3/\mu m^2$, significantly smaller than the 14 $\mu m^3/\mu m^2$ biovolume formed by the NDmed, $p < 0.05$). The 168 strain, as previously been observed [11], was unable to form a pellicle in these conditions and displayed only a much less dense submerged biofilm (with a 6 $\mu m^3/\mu m^2$ biovolume) in comparison with the two other *B. subtilis* strains ($p < 0.05$).

In comparison between the three *B. subtilis* strains studied here, NDmed displayed complex architectural biofilm formation on/in both solid and liquid medium, and had the ability to swarm rather efficiently.

3.2. Mutants Affected in Matrix-Producing Components Fail to form Well-Firmed Surface Cohesive Biofilms

In order to determine whether the genes involved in *B. subtilis* colony and pellicle formation also govern submerged biofilm formation, we constructed a set of derivative mutants of the NDmed strain and analyzed the corresponding phenotypes in the different biofilm models.

Extracellular matrix, mainly composed of polymeric substances, is essential for the biofilm structural formation. In *B. subtilis*, the amyloid-like fiber TasA encoded by the *tapA-sipW-tasA* operon, and the polysaccharides synthesized by the products of the *epsA-O* operon are mainly responsible for the synthesis of biofilm matrix, which bundles cells together and maintains their stability [2,46,49,51,52]. In addition, the BslA protein exhibits amphiphilic properties by forming a hydrophobic layer at the air interface [53] and activates the formation of complex colony development and pellicle formation [20, 54]. Poly-γ-glutamate (γ-PGA), a secreted polymeric substance that accumulates in the culture media like the biofilm matrix [9] and in the capsule, is synthesized by the enzymes encoded by the *cap* operon. Recently it has been shown that in many tested environmental *B. subtilis* isolates γ-PGA production contributed to the complex morphology and robustness by enhancing cell-surface interactions of the colony biofilms [55]. The *ypqP* gene in both *B. subtilis* strains 168 and NCIB3610 is disrupted by the SPβ prophage, whose excision during sporulation phase reconstitutes a functional *ypqP* gene allowing addition of polysaccharides to the spore envelope [32]. In the undomesticated NDmed strain, *ypqP* non-disrupted by the SPβ prophage, has been identified as a requirement for the spatial biofilm organization [13].

Figure 2 shows the effect of matrix gene mutation on different laboratory culture assays. Macrocolonies formed by *tasA*, *epsA-0*, *bslA*, *cap*, and *ypqP* mutants on TSA agar medium were flat contrary to the highly structured and wrinkled wild type NDmed colony (Figure 2). Interestingly, the *tasA* mutant was the least stained, by proteinaceous dyes, indicating a drastic negative effect of the corresponding mutation on extracellular matrix production.

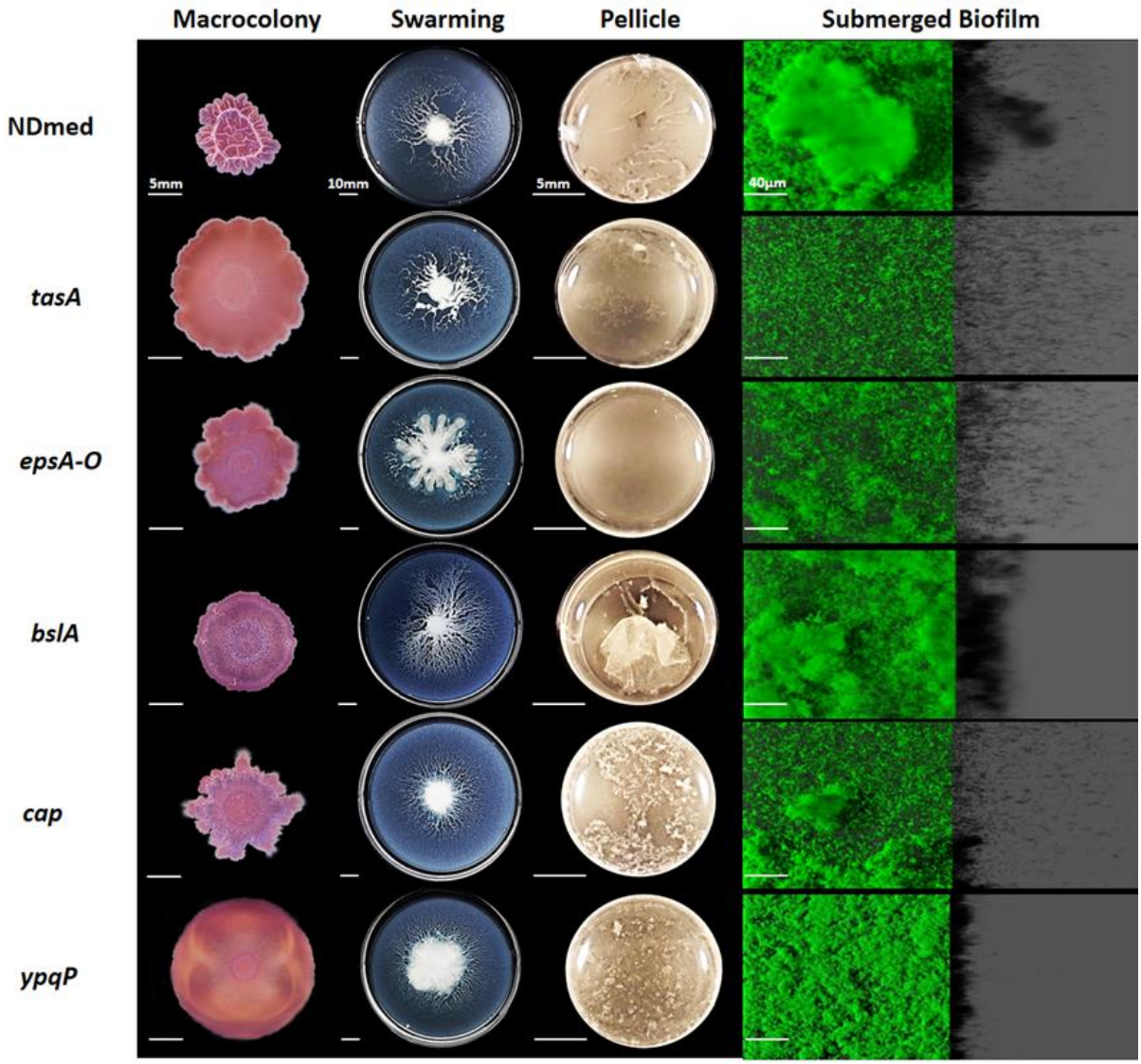

Figure 2. Different B. subtilis NDmed mutants of genes involved in extracellular matrix production on different culture assays. *On 1.5% TSA, macrocolonies grown for 6 days at 30 °C after a central spot of 3 µL of an overnight bacterial culture in TSB. For swarming model, 2µL of bacterial culture (10^4 bacterial dilution) have been inoculated on the middle of 0.7% B-medium plates and cultured for 24 hrs at 30 °C. In a 24-well plate, bacteria in TSB are cultured at 30 °C and pellicles were obtained after 24 hrs. Macrocolony, swarming, and pellicle images are representative for the majority of the phenotype from at least three replicates for each strain revealing the effect of mutations on the biofilm formation. In a microplate system, immersed biofilms are labeled by SYTO 9 after 24 hrs on incubation at 30 °C. The shadow on the right represents the vertical projection of the submerged biofilm (scale bars represent 40 µm).*

Effects of matrix gene mutations on surface motility were visualized through swarming plates. All mutants affected in matrix synthesis tested were observed to swarm better than the wild

type NDmed strain after 24 hrs of incubation on minimal B-medium. The mother colony (place of bacterial inoculation) for the *tasA*, *epsA-O*, and *ypqP* mutants was producing a very viscous and loose matrix. This suggests that all together the TasA (amyloid-like fibers) with the exopolysaccharide synthesized (through the products of *epsA-O* and *ypqP*) are important for the cell interlock and the structural stability in a biofilm.

However, it is difficult to differentiate the importance of each gene individually on the biofilm structural formation on agar. Hence, submerged biofilms revealed how in the *tasA* and *epsA-O* mutants biofilm cells were clearly unbundled and unable to form structured biofilms (Figure 2). Submerged biofilm formed by the *bslA* mutant was not affected at all, and those formed by the *cap* and the *ypqP* mutants were quite less affected after 24 hrs of incubation. Such observation has been numerically confirmed by an estimation of the biovolume and the thickness of submerged biofilms formed for all NDmed mutants studied here, which are represented in Figure 5. Indeed, in this study the *ypqP* mutation had a less effect on submerged biofilm biovolume and thickness after 24 hrs of incubation, however, the effect was more drastic when compared to the wild type NDmed after 48 hrs of incubation [13]. Moreover, *ypqP* was slightly expressed after 24 hrs and strongly transcribed only after 48 hrs (our unpublished data). This could suggest that *ypqP* is involved in the late structural biofilm spatial organization.

Regarding biofilms formed on liquid-air interface, our observations also highlight the importance of amyloid fibers and exopolysaccharides in the biofilm formation. In rich medium after 24 hrs of incubation the *tasA* and *epsA-O* mutants could form only very thin delicate pellicle (Figure 2), similar to what has been shown by previous studies on *B. subtilis* NCIB3610 [46,52]. As for the *ypqP* and *cap* mutants a less structured pellicle was formed. On the other hand, a delicate pellicle formed by the *bslA* mutant was very fragile and sensitive to any small plate movement, and sank to the bottom of the well due to cells lacking the hydrophobic layer that allows the pellicle to be stable at the air-liquid interface. These results suggest that *tasA* and *epsA-O* are crucial matrix genes, required in architectural settlement of *B. subtilis* multicellular communities in the different biofilm models. The genes *cap*, *ypqP*, and *bslA* also play an important role in formation of a highly structured and stable biofilm but in a more model-dependent way.

3.3. Motility and Autolysins are Essentially Required for Architectural Submerged Biofilm Formation of B. subtilis NDmed

In the mid-exponential growth phase of *B. subtilis*, two populations of cells were described: individual motile cells, and long chains of sessile cells [56]. Motility is a way for bacteria to colonize more favorable niches. Bacterial motility has also a positive role in nascent biofilm maturation and spreading, as it has been shown that motile cells can create transient pores that increase the nutrient flow in the matrix of mature biofilms [57]. In *B. subtilis*, flagellar motility studies have focused on both swarming over semi-solid agar plates and swimming in liquid culture [27, 28, 56, 58]. As previously shown, *B. subtilis hag* mutants, affected in a gene encoding flagellin protein for flagellum formation, fail to swarm over different media tested including the B-medium [27,29]. In liquid culture, *B. subtilis hag* mutant was shown to have a delayed flagellar formation [10, 58].

In Figure 3, the NDmed *hag* mutant formed a slightly wrinkled macrocolony on agar plate, while it failed to swarm on an optimal semi-solid plate. In static liquid culture after 24 hrs of incubation, this *hag* mutant was able to produce non-structured submerged compact biofilm with diminished thickness unaffecting the biovolume at the solid-liquid interface (Figure 5). Nevertheless, the *hag* mutant did not form pellicle at the air-liquid interface after 24 hrs of incubation in a rich medium (TSB). This suggested that the inability to swim prevented the cells to reach the air-liquid interface and thus inhibited or caused a delay in the formation of a pellicle, as previously observed [10].

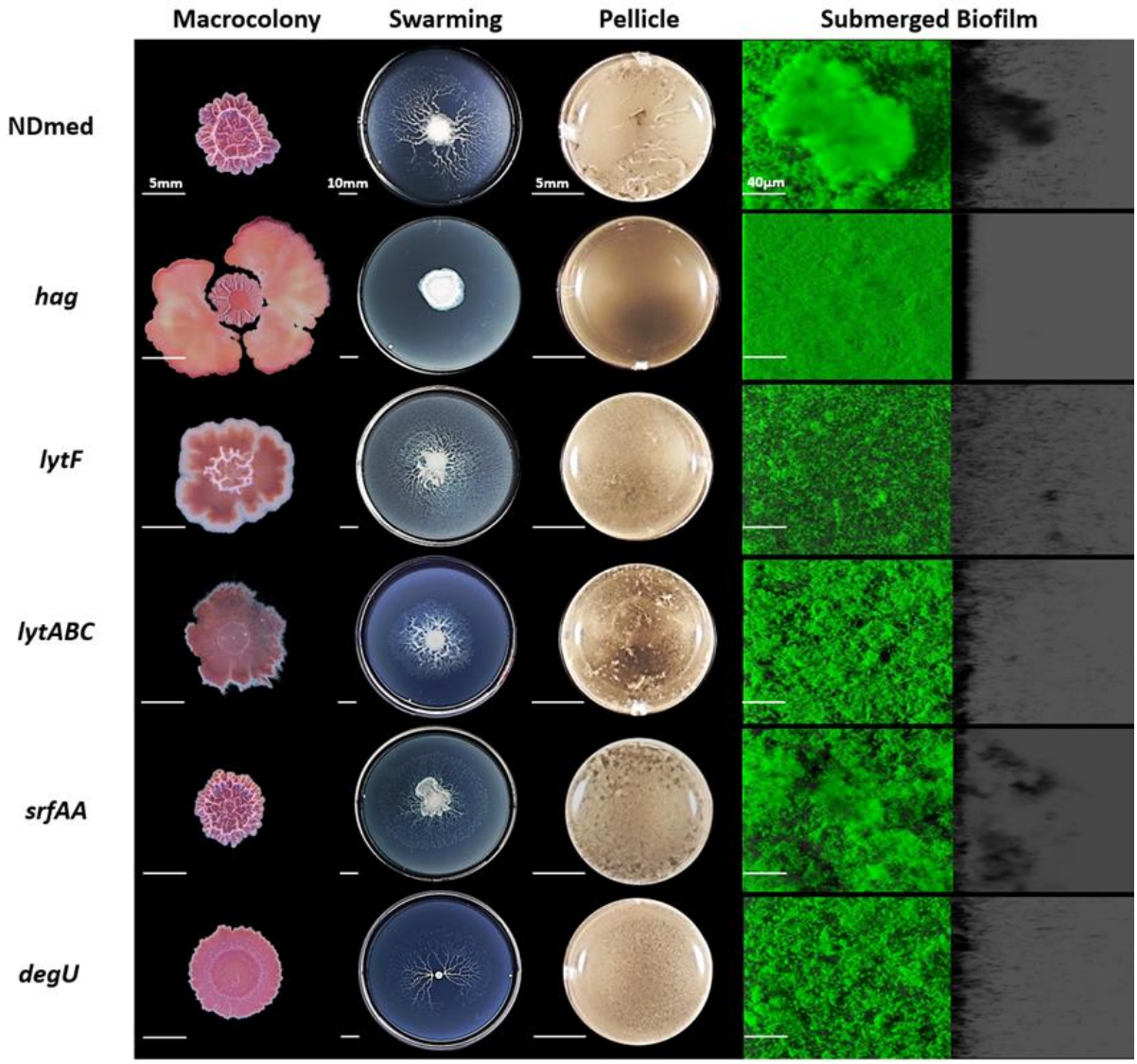

Figure 3. Motility and autolysin genes mutants of B. subtilis NDmed strain on different laboratory assays. *Macrocolonies for mutated regulator genes are cultured on TSA for 6 days at 30 °C. Swarming plates are formed on B-synthetic medium (0.7% agar) that are cultured for 24 hrs at 30 °C. Pellicle and submerged biofilms were formed after 24 hrs of incubation at 30 °C in TSB medium. For submerged images the scale bars represent 40 µm. Macrocolony, swarming, and pellicle images are representative for the majority of the phenotype from at least three replicates for each strain revealing the effect of mutations on the biofilm formation.*

For efficient growth and motility, bacteria need to continuously divide and adapt the cell wall composition (peptidoglycan), thanks to the autolysin system in *B. subtilis.* Expression of two major autolysin genes, *lytF* and *lytC* involved in cell separation is controlled by sigma factor D that also directs the transcription of motility and chemotaxis genes [24, 59]. We have studied the effect

of *lytF* and *lytABC* mutation on the different assays of biofilm formation (Figure 3). The NDmed *lytF* mutants showed better aerial (macrocolony and pellicle) biofilm formation than the *lytABC* autolysin mutant that formed flat and pale color macrocolony (due to the reduced autolytic enzymes produced). However, in submerged biofilm, the *lytF* mutant was more affected and showed reduced biovolume (Figure 5A; $p < 0.05$) while the biofilm biovolume of the *lytABC* mutant was only slightly decreased. To look at the effect on motility, we have tested these mutant strains on swarming plates. Similarly to previous observation with *B. subtilis* NCIB3610 strain [59] the *lytF* mutant was able to swarm better than the *lytABC* mutant, which led to the proposition that *lytF* is principally dedicated in cell separation and *lytC* is more involved in the proper flagellar function [59]. Hence, among the different autolysins, encoded by more than 35 genes encoding peptidoglycan hydrolases, inactivation of only one gene will have an impact on one of the biofilm models studied. However, absolute long chain cells phenotype could not be always seen, since different autolysins could replace each other [24, 60].

Interestingly, the *srfAA* mutation, affecting surfactin production and competence, has no effect on the structural biofilms developed as macrocolonies, pellicle, and submerged one (Figure 3) when compared to the wild type *B. subtilis* NDmed ($p > 0.05$). On swarming plates, surfactin production reduces surface tension during bacterial surface translocation. The 168 strain, carrying a frame-shift mutation in *sfp*, fails to produce surfactin and is thus unable to migrate over the B-medium swarming plate [27, 29]. Moreover, studies with the NCIB3610 *sfrAA* mutant have also shown its inability to swarm [61]. However, either 168 or NCIB3610 *srfAA* mutants, have been shown to regain the ability of swarming, when provided with exogenous surfactin [27, 61]. Interestingly, in our study, the NDmed *srfAA* mutant, which lacks a surfactin ring, displayed a monolayer dendritic swarming pattern having migrated from a more viscous mother colony, suggesting that other extracellular proteases have been secreted to facilitate the translocation.

Previous studies have shown that mutation of *degU* affects transcription of more than 200 genes, which intervene in the genetic network activation for both flagellum and biofilm formation [54]. It has been demonstrated that different levels of DegU~P co-ordinates *B. subtilis* multicellular behavior i.e., low level of DegU~P activates swarming motility and complex architectural colony formation whereas high level of DegU~P inhibits swarming and complex colony formation and is mainly required for the activation of exoprotease production [54, 62]. In *B. subtilis* NCIB3610,

DegU targets two proteins that have been shown to be involved in biofilm formation, YuaB (BslA) and YvcA (a putative membrane-bound lipoprotein). However, for the *B. subtilis* ATCC6051 strain, highly genetically similar to NCIB3610 (they are both descending from the original Marburg strain [37]), YvcA has been shown to be required only for complex colony formation but not for pellicle formation [20, 54, 62]. Hence, multicellular communities differ from strain to strain, which highlights the interest to test *degU* mutation affecting the undomesticated strain NDmed and observe its effect over the different laboratory assays (Figure 3). Such *degU* mutation has a negative impact on the complex architectural macrocolony formed on agar surface and only slightly affects the biovolume formed by the submerged biofilm (Figure 5A, $p > 0.05$). A slight delay was observed in the swarming motility as well as for the pellicle formation indicating that a complex regulatory network, like phosphorylated Spo0A [20], intervenes to ensure a comparable biofilm formation.

3.4. Mutation of B. subtilis NDmed Biofilm Regulators do Not Have the Same Impact on All Biofilm Models

Spo0A, a key regulator of biofilm formation, is driven by exogenous and endogenous signals [63]. Activated Spo0A governs the genetic pathway controlling the matrix production gene expression by inducing SinI which binds and inhibits SinR, a repressor of the *eps* and *tapA-sipW-tasA* operons. Another role for Spo0A is to repress the expression of AbrB, a negative regulator for the initiation of biofilm formation [8, 64]. Hence, the transition from surface-attached cells to three-dimensional biofilm structure is dependent on the activated Spo0A regulator [8]. To determine and clearly visualize the effect of these regulators on biofilm formation, *spo0A*, *abrB*, *sinR*, *sinI*, and *slrR* mutants of NDmed were tested under different biofilm culture conditions (Figure 4).

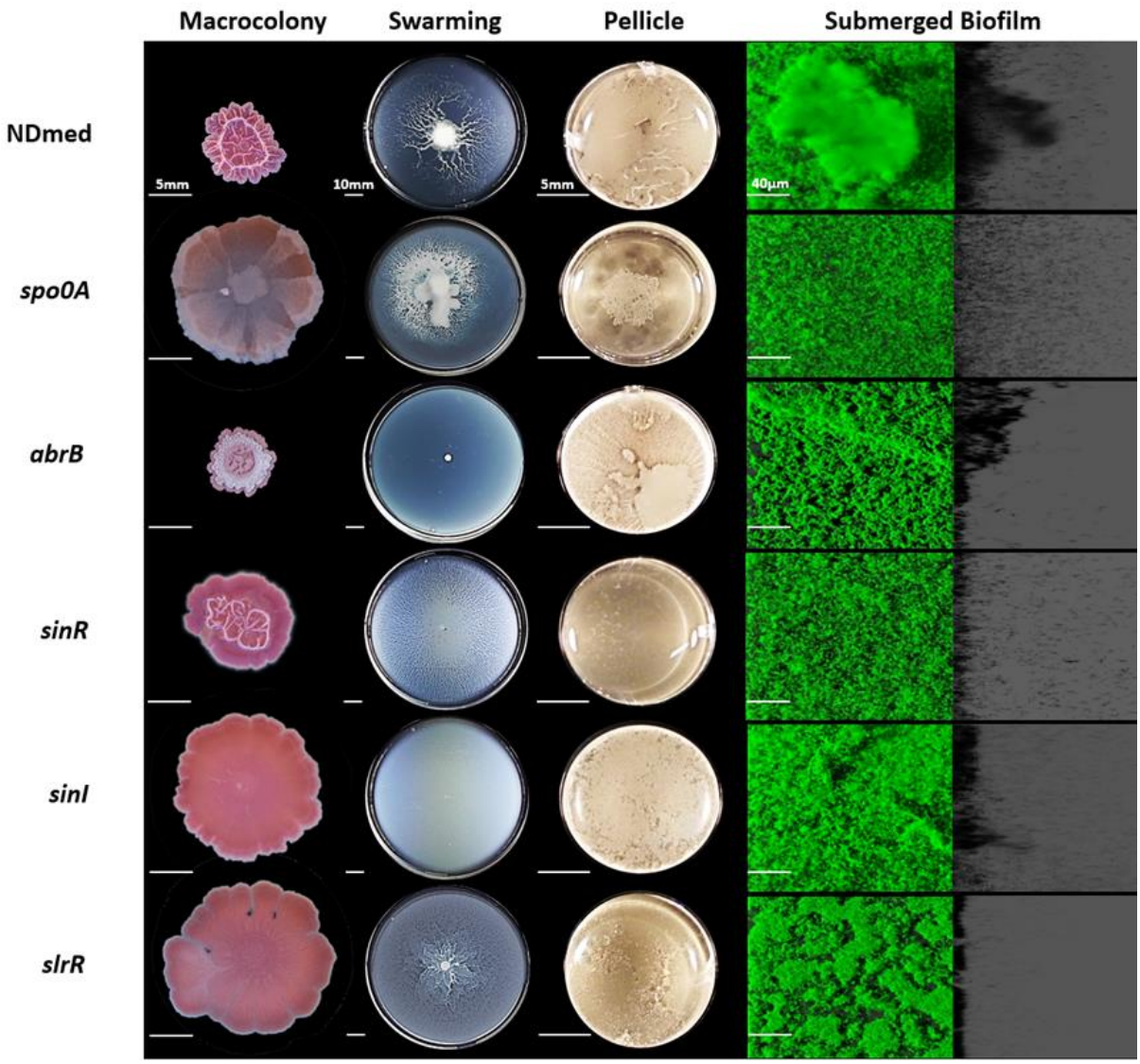

Figure 4. Mutational effect of global regulators required for biofilm development. *Macrocolonies for mutants of regulator genes have been cultured on TSA for 6 days at 30 °C after a central spot of 3µl of an overnight bacterial culture in TSB. Swarming plates are formed by B-synthetic medium (0.7% agar) incubated for 24 hrs at 30 °C. Pellicle formed after 24 hrs of incubation at 30 °C in TSB medium. Macrocolony, swarming, and pellicle images are representative for the majority of the phenotype from at least three replicates for each strain revealing the effect of mutations on the biofilm formation. In a microplate system, immersed biofilms are labeled by SYTO 9 after 24 hrs on incubation at 30 °C. The shadow on the right represents the vertical projection of the submerged biofilm (scale bars represent 40 µm).*

The *spo0A* mutant grew as a structureless spread macrocolony, while the *abrB* mutant showed a very vigorous and structured macrocolony on solid agar medium (Figure 4). In liquid culture, previous studies have shown that *B. subtilis spo0A* mutant cells were able to adhere to a surface and attach only as a monolayer form, suggesting that these mutants lack cell-cell

interactions necessary for multicellular biofilm formation [8]. By using the CLSM, we could observe that the *spo0A* mutant cells did not form any thick submerged biofilm and rather remained essentially dispersed in the medium (Figure 4). These dispersed cells seemed to reach the surface of the liquid-air interface and form a highly disconnected pellicle-like structure in the middle of the well. On the other hand, the *abrB* mutant could form an extremely firm and highly structured pellicle, even more than that formed by the wild type NDmed strain, as well as thick highly structured architectural submerged biofilm (Figures 4 and 5B). Quantification of the submerged biofilm biovolumes (Figure 5A) formed by the *spo0A* and *abrB* mutants assures the role of Spo0A/AbrB pair as the main regulator for biofilm formation. On swarming plates, the *abrB* mutant was strongly affected, where even though producing an extensive surfactin zone, it was only able to form few small bud-like structures that emerged from the mother colony and then failed to proceed further. A similar behavior was observed for the *abrB* mutant of *B. subtilis* (168 *sfp*+) whose cells within the bud accumulate as long-chain forms [29]. Besides this, we could observe that the *spo0A* mutant on the swarming plates (Figure 4) showed extensive motility that filled all the plate rapidly with viscous multicellular biofilm formation in the middle of the plate. This could indicate that this viscous layer is due to an extensive secretion of surfactin or of extracellular proteases from a huge number of bacterial cells that lack cell-cell interaction, facilitating the movement over the surface.

Biofilm formation, under appropriate conditions, is initiated by motile *B. subtilis* cells that adhere to the surface become sessile and form long chains of non-motile cells, held together by extracellular matrix. The transcription factor SinR, a central regulator in the assembly of *B. subtilis* cells into multicellular communities [17], controls both motility and biofilm formation by directly repressing the *eps* and *tapA-sipW-tasA* operons [65]. SinI, induced by phosphorylated Spo0A, binds directly to SinR and causes its inhibition. Moreover, SinI derepresses the action of SlrR [18, 66]. SlrR, an additional regulatory protein, binds to and antagonizes SlrA, and thus constitutes a negative regulatory double loop with SinR, in which the *slrR* gene is repressed by SinR and in turn SlrR prevents SinR from repressing *slrR* [16, 67]. SlrA could play only a minor role in biofilm formation; however, it can be substituted functionally by SinI, its equivalent paralog [16, 18]. Hence, SinR is inhibited by two paralogous antirepressors, SinI and SlrA [16].

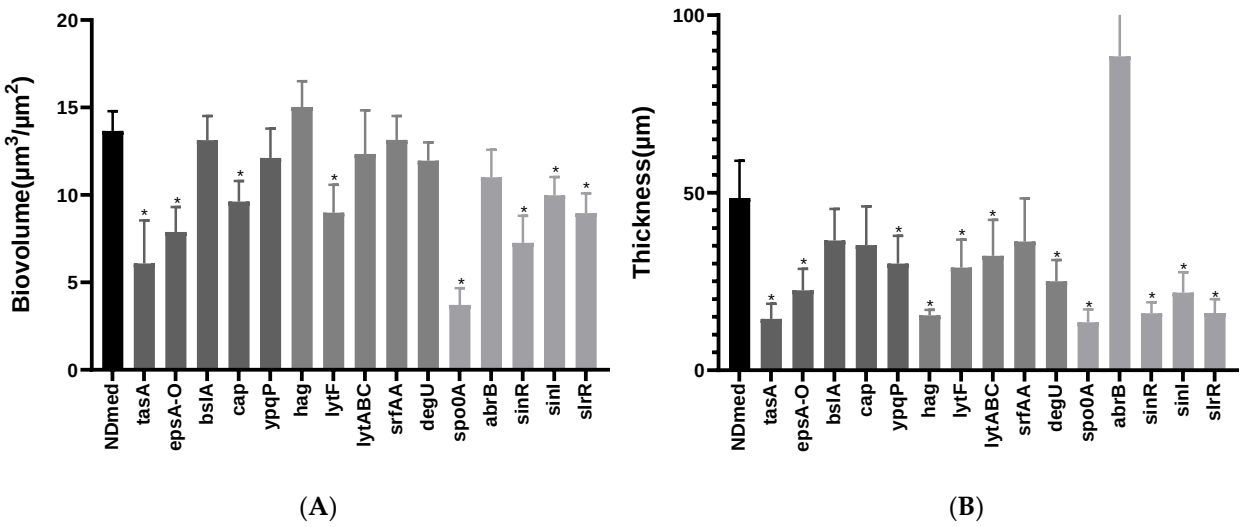

Figure 5. Submerged biofilms biovolumes and maximum thickness of the B. subtilis NDmed mutant strains studied. *Biovolume (**A**) and maximum thickness (**B**) obtained were calculated from twenty confocal image series each. The color of the bars indicate gene categories (black for wild type NDmed, dark grey for matrix genes, grey for motility and autolytic genes, and light grey for global regulators). The error bars indicate the 95% confidence level, and the asterisk indicates the statistically significant differences (* is for $p < 0.05$) with the NDmed wild-type strain.*

A *sinR* mutation, in the NCIB3610 strain has been shown to lead to the formation of extremely thick colony when compared to the wild type, while *sinI* or *slrR* mutants formed flat structureless colonies on agar surface [17, 65]. We have investigated the role of these major gene regulators on submerged biofilm formation and motility in the *B. subtilis* NDmed strain. Figure 4 shows similar phenotype for both *sinI* and *slrR* mutants with flat structureless macrocolonies on agar surface; however, the *sinR* mutant formed wrinkled macrocolony less structured than that formed by the wild type.

Swarming is a phenomenon taking place in two consecutive stages, migration over the surface of highly motile cells followed by their differentiation to less motile matrix producing cells that become stacked in a three-dimensional structure [26, 68]. On swarming plates and after 24 hr of incubation, the NDmed *sinR* mutant swarmed all over the plate with a multilayered biofilm dendritic pattern, which could indicate that swarming cells are unable to separate. In contrast, the NDmed *sinI* mutant eventually swarmed all over the plate in a monolayer form (Figure 4) similar to what has been described for *sinI* mutant in the NCIB3610 context [17]. This suggests that when

matrix production genes are blocked, mutant bacterial strains were only able to reach the first stage of swarming. SlrR stimulates transcription of the *tapA-sipW-tasA* operon but not of the *eps* operon and represses genes that mediate cell separation [10, 18]. Thus, *slrR* mutation affects the expression of TasA but not Eps production and promotes cell separation. On swarming plates, the NDmed *slrR* mutant was able to swarm rapidly in a monolayer form all over the plate with less structured biofilm in the mother colony (place of inoculation) when compared to the wild type (Figure 4).

In liquid culture, a NDmed *sinR* mutant cultivated in TSB medium for 24 hrs of incubation, formed very thin pellicle (Figure 4). This could be due to cells unable to reach easily the surface. The NDmed *sinI* mutant was able to form a rather good pellicle, suggesting that the motile swimmer cells were able to reach the surface. These phenotypes are similar to what has been observed previously for ATCC6051 *sinR* and *sinI* mutant strains [10, 18]. A defect in flagellar formation in the *sinR* mutant [10, 18] and a functional complementation between SinI and SlrA [16] in the *sinI* mutant could account for these phenotypes. Another hypothesis could be the occurrence of natural frameshift mutations within the *sinR* open reading frame, which suppress the blocking biofilm formation effects of a *sinI* mutation, as shown by Kearns *et al.* [17]. A NDmed *slrR* mutant could form a thin pellicle at the air-liquid interface, similarly to what has been observed in the NCIB3610 context [65].

The submerged biofilm biovolume of the NDmed *sinR* mutant (Figure 5A) was more negatively affected than that of the *sinI* or the *slrR* mutants when compared to the wild type NDmed (with a $p < 0.05$ for these three mutated genes compared to the wild type). This could stress the importance of motility and autolysin in the formation of biofilm and suggest that mutation in one gene could be overcome and controlled by other regulatory pathways. Thus, these results further indicate that the SinI/SinR pair are the main regulators controlling the mode of bacterial life, motile or sessile, cells.

4. Conclusions

Overall, this study highlights the value of the NDmed strain as an undomesticated, naturally competent *B. subtilis* isolate, to point out the effect of gene mutation on the different structural biofilm communities formed. Gene mutation could exhibit a similar impact on all the different biofilm models formed on different culturing conditions. For instance, the *tasA* and *epsA-O* gene

mutation affected all the surface associated communities formed but improved surface translocation. However, the *bslA* gene mutation has a negative effect just on the aerial biofilm models, structural microcolonies, and the pellicle stability, and no effect on the submerged biofilm formation. Our results emphasize the importance of the submerged model to further understand the molecular mechanisms during biofilm formation. Biofilm development throughout different environmental culturing conditions could have similar genetic profile, but these multicellular communities can also display considerable differences on the structural, chemical, and biological heterogeneity levels across different biofilm models. A whole transcriptional analysis could be done for the differently localized heterogeneous compartments of a biofilm to further understand the core of the transcriptional network that takes place between and during the biofilm development.

Author Contributions: Conceptualization, R.B., D.L.C., P.S.V., Y.D., and K.H.; methodology, Y.D., P.S.V., and J.D.; formal analysis, Y.D.; writing—original draft preparation, Y.D.; writing—review and editing, R.B., K.H., D.L.C., A.B., P.S.V., and J.D.; supervision, R.B. and K.H.; funding acquisition, K.H. and R.B. All authors have read and agreed to the published version of the manuscript.

Funding: Yasmine Dergham is the recipient of fundings from the Union of Southern Suburbs Municipalities of Beirut, INRAE, Campus France PHC CEDRE 42280PF and Fondation AgroParisTech.

Data Availability Statement: Not applicable.

Acknowledgments: We thank Arnaud Chastanet, Etienne Dervyn, Michal Obuchowski, Nicola R. Stanley-Wall, and Roberto Kolter for providing strains, and the MIMA2 INRAE imaging platform for microscopic analysis.

Conflicts of Interest: The authors declare no conflicts of interest.

References

1. Shapiro, J.A. Thinking about bacterial populations as multicellular organisms. *Annu. Rev. Microbiol.* **1998**, *52*, 81–104, doi:10.1146/annurev.micro.52.1.81.
2. Vlamakis, H.; Chai, Y.; Beauregard, P.B.; Losick, R.; Kolter, R. Sticking together: Building a biofilm the *Bacillus subtilis* way. *Nat. Rev. Microbiol.* **2013**, *11*, 157–168, doi:10.1038/nrmicro2960.
3. Kearns, D.B. A field guide to bacterial swarming motility. *Nat. Rev. Microbiol.* **2010**, *8*, 634–644, doi:10.1038/nrmicro2405.
4. Verstraeten, N.; Braeken, K.; Debkumari, B.; Fauvart, M.; Fransaer, J.; Vermant, J.; Michiels, J. Living on a surface: Swarming and biofilm formation. *Trends Microbiol.* **2008**, *16*, 496–506, doi:10.1016/j.tim.2008.07.004.
5. Lemon, K.P.; Earl, A.M.; Vlamakis, H.C.; Aguilar, C.; Kolter, R. Biofilm Development with an Emphasis on *Bacillus subtilis*. *Curr. Top. Microbiol. Immunol.* **2008**, *322*, 1–16, doi:10.1007/978-3-540-75418-3_1.

6. Nagórska, K.; Bikowski, M.; Obuchowski, M. Multicellular behaviour and production of a wide variety of toxic substances support usage of *Bacillus subtilis* as a powerful biocontrol agent. *Acta Biochim. Pol.* **2007**, *54*, 495–508.
7. Jamal, M.; Ahmad, W.; Andleeb, S.; Jalil, F.; Imran, M.; Nawaz, M.A.; Hussain, T.; Ali, M.; Rafiq, M.; Kamil, M.A. Bacterial biofilm and associated infections. *J. Chin. Med. Assoc.* **2018**, *81*, 7–11, doi:10.1016/j.jcma.2017.07.012.
8. Hamon, M.A.; Lazazzera, B.A. The sporulation transcription factor Spo0A is required for biofilm development in *Bacillus subtilis*. *Mol. Microbiol.* **2002**, *42*, 1199–1209, doi:10.1046/j.1365-2958.2001.02709.x.
9. Stanley, N.R.; Lazazzera, B.A. Defining the genetic differences between wild and domestic strains of *Bacillus subtilis* that affect poly-γ-dl-glutamic acid production and biofilm formation. *Mol. Microbiol.* **2005**, *57*, 1143–1158, doi:10.1111/j.1365-2958.2005.04746.x.
10. Kobayashi, K. *Bacillus subtilis* Pellicle Formation Proceeds through Genetically Defined Morphological Changes. *J. Bacteriol.* **2007**, *189*, 4920–4931, doi:10.1128/jb.00157-07.
11. Bridier, A.; Le Coq, D.; Dubois-Brissonnet, F.; Thomas, V.; Aymerich, S.; Briandet, R. The Spatial Architecture of *Bacillus subtilis* Biofilms Deciphered Using a Surface-Associated Model and In Situ Imaging. *PLoS ONE* **2011**, *6*, e16177, doi:10.1371/journal.pone.0016177.
12. Hamon, M.A.; Stanley, N.R.; Britton, R.A.; Grossman, A.D.; Lazazzera, B.A. Identification of AbrB-regulated genes involved in biofilmformation by *Bacillus subtilis*. *Mol. Microbiol.* **2004**, *52*, 847–860.
13. Sanchez-Vizuete, P.; Le Coq, D.; Bridier, A.; Herry, J.M.; Aymerich, S.; Briandet, R. Identification of *ypqP* as a new *Bacillus subtilis* biofilm determinant that mediates the protection of *Staphylococcus aureus* against antimicrobial agents in mixed-species communities. *Appl. Environ. Microbiol.* **2015**, *81*, 109–118.
14. Ostrov, I.; Sela, N.; Belausov, E.; Steinberg, D.; Shemesh, M. Adaptation of Bacillus species to dairy associated environment facilitates their biofilm forming ability. *Food Microbiol.* **2019**, *82*, 316–324, doi:10.1016/j.fm.2019.02.015.
15. Chu, F.; Kearns, D.B.; Branda, S.S.; Kolter, R.; Losick, R. Targets of the master regulator of biofilm formation in *Bacillus subtilis*. *Mol. Microbiol.* **2006**, *59*, 1216–1228, doi:10.1111/j.1365-2958.2005.05019.x.
16. Chai, Y.; Kolter, R.; Losick, R. Paralogous antirepressors acting on the master regulator for biofilm formation in *Bacillus subtilis*. *Mol. Microbiol.* **2009**, *74*, 876–887, doi:10.1111/j.1365-2958.2009.06900.x.
17. Kearns, D.B.; Chu, F.; Branda, S.S.; Kolter, R.; Losick, R. A master regulator for biofilm formation by *Bacillus subtilis*. *Mol. Microbiol.* **2004**, *55*, 739–749, doi:10.1111/j.1365-2958.2004.04440.x.
18. Kobayashi, K. SlrR/SlrA controls the initiation of biofilm formation in *Bacillus subtilis*. *Mol. Microbiol.* **2008**, *69*, 1399–1410, doi:10.1111/j.1365-2958.2008.06369.x.
19. Murray, E.J.; Kiley, T.B.; Stanley-Wall, N.R. A pivotal role for the response regulator DegU in controlling multicellular behaviour. *Microbiology* **2009**, *155*, 1–8, doi:10.1099/mic.0.023903-0.
20. Verhamme, D.T.; Murray, E.J.; Stanley-Wall, N.R. DegU and Spo0A Jointly Control Transcription of Two Loci Required for Complex Colony Development by *Bacillus subtilis*. *J. Bacteriol.* **2008**, *191*, 100–108, doi:10.1128/jb.01236-08.
21. Márquez-Magaña, L.M.; Chamberlin, M.J. Characterization of the *sigD* transcription unit of *Bacillus subtilis*. *J. Bacteriol.* **1994**, *176*, 2427–2434, doi:10.1128/jb.176.8.2427-2434.1994.
22. Marquez, L.M.; Helmann, J.D.; Ferrari, E.; Parker, H.M.; Ordal, G.W.; Chamberlin, M.J. Studies of σ(D)-dependent functions in *Bacillus subtilis*. *J. Bacteriol.* **1990**, *172*, 3435–3443.
23. Serizawa, M.; Yamamoto, H.; Yamaguchi, H.; Fujita, Y.; Kobayashi, K.; Ogasawara, N.; Sekiguchi, J. Systematic analysis of SigD-regulated genes in *Bacillus subtilis* by DNA microarray and Northern blotting analyses. *Gene* **2004**, *329*, 125–136.

24. Margot, P.; Pagni, M.; Karamata, D. *Bacillus subtilis* 168 gene *lytF* encodes a γ-D-glutamate-meso-diaminopimelate muropeptidase expressed by the alternative vegetative sigma factor, σD. *Microbiology* **1999**, *145*, 57–65, doi:10.1099/13500872-145-1-57.
25. Ostrowski, A.; Mehert, A.; Prescott, A.; Kiley, T.B.; Stanley-Wall, N.R. YuaB Functions Synergistically with the Exopolysaccharide and TasA Amyloid Fibers to Allow Biofilm Formation by *Bacillus subtilis*. *J. Bacteriol.* **2011**, *193*, 4821–4831, doi:10.1128/jb.00223-11.
26. Harshey, R.M. Bacterial Motility on a Surface: Many Ways to a Common Goal. *Annu. Rev. Microbiol.* **2003**, *57*, 249–273, doi:10.1146/annurev.micro.57.030502.091014.
27. Julkowska, D.; Obuchowski, M.; Holland, I.B.; Séror, S.J. Comparative Analysis of the Development of Swarming Communities of *Bacillus subtilis* 168 and a Natural Wild Type: Critical Effects of Surfactin and the Composition of the Medium. *Society* **2005**, *187*, 65–76, doi:10.1128/jb.187.1.65-76.2005.
28. Julkowska, D.; Obuchowski, M.; Holland, I.B.; Séror, S.J. Branched swarming patterns on a synthetic medium formed by wild-type *Bacillus subtilis* strain 3610: Detection of different cellular morphologies and constellations of cells as the complex architecture develops. *Microbiology* **2004**, *150*, 1839–1849, doi:10.1099/mic.0.27061-0.
29. Hamze, K.; Julkowska, D.; Autret, S.; Hinc, K.; Nagorska, K.; Sekowska, A.; Holland, I.B.; Séror, S.J. Identification of genes required for different stages of dendritic swarming in *Bacillus subtilis*, with a novel role for *phrC*. *Microbiology* **2009**, *155*, 398–412, doi:10.1099/mic.0.021477-0.
30. Bridier, A.; Sanchez-Vizuete, M.d.P.; Le Coq, D.; Aymerich, S.; Meylheuc, T.; Maillard, J.-Y.; Thomas, V.; Dubois-Brissonnet, F.; Briandet, R. Biofilms of a *Bacillus subtilis* Hospital Isolate Protect *Staphylococcus aureus* from Biocide Action. *PLoS ONE* **2012**, *7*, e44506, doi:10.1371/journal.pone.0044506.
31. Martin, D.; Denyer, S.; McDonnell, G.; Maillard, J.-Y. Resistance and cross-resistance to oxidising agents of bacterial isolates from endoscope washer disinfectors. *J. Hosp. Infect.* **2008**, *69*, 377–383, doi:10.1016/j.jhin.2008.04.010.
32. Abe, K.; Kawano, Y.; Iwamoto, K.; Arai, K.; Maruyama, Y.; Eichenberger, P.; Sato, T. Developmentally-Regulated Excision of the SPβ Prophage Reconstitutes a Gene Required for Spore Envelope Maturation in *Bacillus subtilis*. *PLoS Genet.* **2014**, *10*, e1004636, doi:10.1371/journal.pgen.1004636.
33. Marmur, J. A procedure for the isolation of deoxyribonucleic acid from micro-organisms. *J. Mol. Biol.* **1961**, *3*, 208–218, doi:10.1016/s0022-2836(61)80047-8.
34. Anagnostopoulos, C.; Spizizen, J. Requirements for Transformation in *Bacillus subtilis*. *J. Bacteriol.* **1961**, *81*, 741–746.
35. Borenstein, S.; Ephrati-Elizur, E. Spontaneous release of DNA in sequential genetic order by *Bacillus subtilis*. *J. Mol. Biol.* **1969**, *45*, 137–152, doi:10.1016/0022-2836(69)90216-2.
36. Antelmann, H.; Engelmann, S.; Schmid, R.; Sorokin, A.; Lapidus, A.; Hecker, M. Expression of a stress- and starvation-induced *dps*/*pexB*-homologous gene is controlled by the alternative sigma factor σ(B) in *Bacillus subtilis*. *J. Bacteriol.* **1997**, *179*, 7251–7256.
37. Zeigler, D.R.; Prágai, Z.; Rodriguez, S.; Chevreux, B.; Muffler, A.; Albert, T.; Bai, R.; Wyss, M.; Perkins, J.B. The Origins of 168, W23, and Other *Bacillus subtilis* Legacy Strains. *J. Bacteriol.* **2008**, *190*, 6983–6995, doi:10.1128/jb.00722-08.
38. Bidnenko, V.; Nicolas, P.; Grylak-Mielnicka, A.; Delumeau, O.; Auger, S.; Aucouturier, A.; Guérin, C.; Repoila, F.; Bardowski, J.; Aymerich, S.; Bidnenko, E. Termination factor Rho: From the control of pervasive transcription to cell fate determination in *Bacillus subtilis*. *PLoS Genet.* **2017**, *13*, e1006909, doi:10.1371/journal.pgen.1006909.
39. Monteferrante, C.G.; MacKichan, C.; Marchadier, E.; Prejean, M.-V.; Van Dijl, J.M.; Carballido-López, R. Mapping the twin-arginine protein translocation network of *Bacillus subtilis*. *Proteomics* **2013**, *13*, 800–811, doi:10.1002/pmic.201200416.

40. Nagórska, K.; Hinc, K.; Strauch, M.A.; Obuchowski, M. Influence of the σB Stress Factor and *yxaB*, the Gene for a Putative Exopolysaccharide Synthase under σB Control, on Biofilm Formation. *J. Bacteriol.* **2008**, *190*, 3546–3556, doi:10.1128/jb.01665-07.
41. Crutz, A.M.; Steinmetz, M. Transcription of the *Bacillus subtilis sacX* and *sacY* genes, encoding regulators of sucrose metabolism, is both inducible by sucrose and controlled by the DegS-DegU signalling system. *J. Bacteriol.* **1992**, *174*, 6087–6095.
42. Murray, E.J.; Stanley-Wall, N.R. The sensitivity of *Bacillus subtilis* to diverse antimicrobial compounds is influenced by Abh. *Arch. Microbiol.* **2010**, *192*, 1059–1067, doi:10.1007/s00203-010-0630-4.
43. Dervyn, E.; Poncet, S.; Klier, A.; Rapoport, G. Transcriptional regulation of the cryIVD gene operon from *Bacillus thuringiensis* subsp. israelensis. *J. Bacteriol.* **1995**, *177*, 2283–2291, doi:10.1128/jb.177.9.2283-2291.1995.
44. Bridier, A.; Dubois-Brissonnet, F.; Boubetra, A.; Thomas, V.; Briandet, R. The biofilm architecture of sixty opportunistic pathogens deciphered using a high throughput CLSM method. *J. Microbiol. Methods* **2010**, *82*, 64–70, doi:10.1016/j.mimet.2010.04.006.
45. Friedman, L.; Kolter, R. Genes involved in matrix formation in *Pseudomonas aeruginosa* PA14 biofilms. *Mol. Microbiol.* **2003**, *51*, 675–690, doi:10.1046/j.1365-2958.2003.03877.x.
46. Romero, D.; Aguilar, C.; Losick, R.; Kolter, R. Amyloid fibers provide structural integrity to *Bacillus subtilis* biofilms. *Proc. Natl. Acad. Sci. USA* **2010**, *107*, 2230–2234, doi:10.1073/pnas.0910560107.
47. Kiersztyn, B.; Siuda, W.; Chróst, R. Coomassie Blue G250 for Visualization of Active Bacteria from Lake Environment and Culture. *Pol. J. Microbiol.* **2017**, *66*, 365–373, doi:10.5604/01.3001.0010.4867.
48. Neumann, U.; Khalaf, H.; Rimpler, M. Quantitation of electrophoretically separated proteins in the submicrogram range by dye elution. *Electrophoresis* **1994**, *15*, 916–921, doi:10.1002/elps.11501501132.
49. Branda, S.S.; González-Pastor, J.E.; Ben-Yehuda, S.; Losick, R.; Kolter, R. Fruiting body formation by *Bacillus subtilis*. *Proc. Natl. Acad. Sci. USA* **2001**, *98*, 11621–11626, doi:10.1073/pnas.191384198.
50. McLoon, A.L.; Guttenplan, S.B.; Kearns, D.B.; Kolter, R.; Losick, R. Tracing the Domestication of a Biofilm-Forming Bacterium. *J. Bacteriol.* **2011**, *193*, 2027–2034, doi:10.1128/jb.01542-10.
51. Branda, S.S.; González-Pastor, J.E.; Dervyn, E.; Ehrlich, S.D.; Losick, R.; Kolter, R. Genes Involved in Formation of Structured Multicellular Communities by *Bacillus subtilis*. *J. Bacteriol.* **2004**, *186*, 3970–3979, doi:10.1128/jb.186.12.3970-3979.2004.
52. Branda, S.S.; Chu, F.; Kearns, D.B.; Losick, R.; Kolter, R. A major protein component of the *Bacillus subtilis* biofilm matrix. *Mol. Microbiol.* **2006**, *59*, 1229–1238, doi:10.1111/j.1365-2958.2005.05020.x.
53. Kobayashi, K.; Iwano, M. BslA(YuaB) forms a hydrophobic layer on the surface of *Bacillus subtilis* biofilms. *Mol. Microbiol.* **2012**, *85*, 51–66.
54. Kobayashi, K. Gradual activation of the response regulator DegU controls serial expression of genes for flagellum formation and biofilm formation in *Bacillus subtilis*. *Mol. Microbiol.* **2007**, *66*, 395–409, doi:10.1111/j.1365-2958.2007.05923.x.
55. Yu, Y.; Yan, F.; Chen, Y.; Jin, C.; Guo, J.-H.; Chai, Y. Poly-γ-Glutamic Acids Contribute to Biofilm Formation and Plant Root Colonization in Selected Environmental Isolates of *Bacillus subtilis*. *Front. Microbiol.* **2016**, *7*, 1811, doi:10.3389/fmicb.2016.01811.
56. Kearns, D.B.; Losick, R. Cell population heterogeneity during growth of *Bacillus subtilis*. *Genes Dev.* **2005**, *19*, 3083–3094.
57. Houry, A.; Gohar, M.; Deschamps, J.; Tischenko, E.; Aymerich, S.; Gruss, A.; Briandet, R. Bacterial swimmers that infiltrate and take over the biofilm matrix. *Proc. Natl. Acad. Sci. USA* **2012**, *109*, 13088–13093, doi:10.1073/pnas.1200791109.
58. Hölscher, T.; Bartels, B.; Lin, Y.-C.; Gallegos-Monterrosa, R.; Price-Whelan, A.; Kolter, R.; Dietrich, L.E.P.; Kovács, Á.T. Motility, Chemotaxis and Aerotaxis Contribute to Competitiveness during Bacterial Pellicle Biofilm Development. *J. Mol. Biol.* **2015**, *427*, 3695–3708, doi:10.1016/j.jmb.2015.06.014.

59. Chen, R.; Guttenplan, S.B.; Blair, K.M.; Kearns, D.B. Role of the σD-dependent autolysins in *Bacillus subtilis* population heterogeneity. *J. Bacteriol.* **2009**, *191*, 5775–5784.
60. Smith, T.J.; Foster, S.J. Characterization of the involvement of two compensatory autolysins in mother cell lysis during sporulation of *Bacillus subtilis* 168. *J. Bacteriol.* **1995**, *177*, 3855–3862, doi:10.1128/jb.177.13.3855-3862.1995.
61. Kearns, D.B.; Chu, F.; Rudner, R.; Losick, R. Genes governing swarming in *Bacillus subtilis* and evidence for a phase variation mechanism controlling surface motility. *Mol. Microbiol.* **2004**, *52*, 357–369, doi:10.1111/j.1365-2958.2004.03996.x.
62. Verhamme, D.T.; Kiley, T.B.; Stanley-Wall, N.R. DegU co-ordinates multicellular behaviour exhibited by *Bacillus subtilis*. *Mol. Microbiol.* **2007**, *65*, 554–568, doi:10.1111/j.1365-2958.2007.05810.x.
63. Mielich-süss, B.; Lopez, D. Molecular mechanisms involved in *Bacillus subtilis* biofilm formation. *Environ. Microbiol.* **2015**, *17*, 555–565.
64. Strauch, M.; Webb, V.; Spiegelman, G.; Hoch, J.A. The Spo0A protein of *Bacillus subtilis* is a repressor of the *abrB* gene. *Proc. Natl. Acad. Sci. USA* **1990**, *87*, 1801–1805, doi:10.1073/pnas.87.5.1801.
65. Takada, H.; Morita, M.; Shiwa, Y.; Sugimoto, R.; Suzuki, S.; Kawamura, F.; Yoshikawa, H. Cell motility and biofilm formation in *Bacillus subtilis* are affected by the ribosomal proteins, S11 and S21. *Biosci. Biotechnol. Biochem.* **2014**, *78*, 898–907, doi:10.1080/09168451.2014.915729.
66. Chu, F.; Kearns, D.B.; McLoon, A.; Chai, Y.; Kolter, R.; Losick, R. A novel regulatory protein governing biofilm formation in *Bacillus subtilis*. *Mol. Microbiol.* **2008**, *68*, 1117–1127, doi:10.1111/j.1365-2958.2008.06201.x.
67. Chai, Y.; Kolter, R.; Losick, R. Reversal of an epigenetic switch governing cell chaining in *Bacillus subtilis* by protein instability. *Mol. Microbiol.* **2010**, *78*, 218–229, doi:10.1111/j.1365-2958.2010.07335.x.
68. Copeland, M.F.; Weibel, D.B. Bacterial swarming: A model system for studying dynamic self-assembly. *Soft Matter* **2009**, *5*, 1174–1187, doi:10.1039/b812146j.

Chapter 2. "The coordinated population redistribution between *Bacillus subtilis* submerged biofilm and liquid-air pellicle"

In this contribution, we investigated the dynamic of colonization of Bacillus subtilis growing statically in a microplate well. Taking advantage of 4D-CLSM, we could describe a non-linear biphasic process with brutal population relocalisation between the two interfaces (liquid-surface and liquid-air). Adherent cells first form chains associated with the bottom surface of the well. After around 3 hours, chains coordinately fragment in a few minutes to liberate individual free motile cells in the medium. This motile population actively migrates to the liquid air interface to initialize a second biofilm community floating on the liquid medium (pellicle). A time course transcriptome analysis supported by gene reporter assays allows us to pinpoint oxygen depletion as a trigger for this switching cell fate. This switching cell fate was observed for the B. subtilis strains tested, but not for close relative species. In a second kinetic and under anaerobic metabolism, residual adherent cells initiate after 7h the typical biofilm protruding structures by massively producing the matrix components.

This phenomenon of massive population redistribution was discovered in the framework of Arnaud Bridier's PhD, deepened in Pilar Sanchez Vizuete's PhD, and finalized here with my contributions. Taking advantage of my experience to manipulate transcriptomic data, I revisited the tiling array data to demonstrate a temporal functional structure within the data set (Figure S1). I also performed all the CLM imaging of Figure 3, and contributed with Julien Deschamps to the establishment of the 4D Kymographs presented in Figure 4.

The article has been ***published in Biofilm 2021, 100065;***
http://doi.org/10.1016/j.biofilm.2021.100065. The Biofilm journal is from Elsevier.

"The coordinated population redistribution between *Bacillus subtilis* submerged biofilm and liquid-air pellicle"

(Paper 2)

Pilar Sanchez-Vizuete[a,1], Yasmine Dergham[a,b], Arnaud Bridier[c], Julien Deschamps[a], Etienne Dervyn[a], Kassem Hamze[b], Stéphane Aymerich[a], Dominique Le Coq[a,d], Romain Briandet[a,*]

[a] Université Paris-Saclay, INRAE, AgroParisTech, Micalis Institute, 78350 Jouy-en-Josas, France,
[b] Faculty of Science, Lebanese University, 1003 Beirut, Lebanon,
[c] Fougères Laboratory, Antibiotics, Biocides, Residues and Resistance Unit, Anses, 35300 Fougères, France,
[d] Université Paris-Saclay, Centre National de la Recherche Scientifique (CNRS), INRAE, AgroParisTech, Micalis Institute, 78350 Jouy-en-Josas, France.

*corresponding author: romain.briandet@inrae.fr
[1] present address: pilarsanviz@gmail.com

Keywords: *Bacillus subtilis*, biofilm, pellicle, 4D-CLSM, motility, oxygen sensing, metabolism.

ABSTRACT

Bacillus subtilis is a widely used bacterial model to decipher biofilm formation, genetic determinants and their regulation. For several years, studies were conducted on colonies or pellicles formed at the interface with air, but more recent works showed that non-domesticated strains were able to form thick and structured biofilms on submerged surfaces. Taking advantage of time-lapse confocal laser scanning microscopy, we monitored bacterial colonization on the surface and observed an unexpected biphasic submerged biofilm development. Cells adhering to the surface firstly form elongated chains before being suddenly fragmented and released as free motile cells in the medium. This switching coincided with an oxygen depletion in the well which preceded the formation of the pellicle at the liquid-air interface. Residual bacteria still associated with the solid surface at the bottom of the well started to express matrix genes under anaerobic metabolism to build the typical biofilm protruding structures.

INTRODUCTION

In their natural habitat, bacteria mostly live in biofilms, associated with surfaces and embedded in a complex mixture of exopolymers (Karygianni *et al.*, 2020). These structures provide to their inhabitants a protective environment in which they can resist harsh conditions such as desiccation, nutrients starvation or the action of toxic compounds (Flemming *et al.*, 2016). Microbial biofilms can be considered useful since they are involved in natural biogeochemical cycles and increasingly used in biotechnologies for wastewater treatments or the production of green energies (Mukherjee and Cao, 2021). However, biofilms also facilitate pathogen persistence despite antimicrobial treatments and thus have a severe negative impact in human health being involved in up to 80% of chronic and recurrent infections (Mah, 2012).

These infectious concerns have driven the international research efforts for more than 30 years to unravel the mechanisms of biofilm formation and their control (Nickel *et al.*, 1985; Costerton et al., 1999; da Silva *et al.*, 2021). Most of the pioneer studies in this field have been carried out with axenic biofilms of pathogenic strains, such as *Pseudomonas aeruginosa*, grown in flow-cells and observed by *in situ* confocal imaging (Pamp *et al.*, 2009). In the early 2000s, *Bacillus subtilis* emerged as a model of Gram-positive bacteria for the dissection of the genetic determinants of biofilm formation and their regulation (Branda *et al.*, 2001; Piggot and Hilbert, 2004). Most of

these studies used the strain NCIB3610, that has been shown to form spatially organized multicellular structures *i.e.* colony on agar, floating pellicle at the liquid-air interface, and submerged biofilm at the solid-liquid interface (Branda *et al.*, 2001; Kobayashi, 2007; Vlamakis *et al.*, 2013; Sanchez-Vizuete *et al.*, 2015). These experimental models have then been successfully used to dissect the complexity of *B. subtilis* multicellularity and their genetic circuits to identify the regulators controlling biofilm development, maturation and dispersion (e.g. Spo0A, SinR, SinI, AbrB, SlrR or SigB) (Kearns *et al.*, 2005; Vlamakis *et al.*, 2013; Cairns *et al.*, 2014; Bartolini *et al.*, 2019; Milton *et al.*, 2020; Nishikawa and Kobayashi, 2021; Arnaouteli *et al.*, 2021). In response to external signals, individual motile cells switch to sessile chains by inactivating expression of the motility genes (*hag*, encoding the principal flagellar protein and *lytABC* and *lytF*, encoding the autolysins responsible of cell separation) and by activation of the matrix production genes (Chai *et al.*, 2010; López and Kolter, 2010; Diethmaier *et al.*, 2011). This matrix of *B. subtilis* biofilms is essentially composed of the polysaccharides synthesized by the products of the 15-genes operon *epsA-O* (*eps* operon), the amyloid-like protein TasA, synthesized from the *tapA-sipW-tasA* operon, and the amphiphilic protein BslA (Romero *et al.*, 2010; Ostrowski *et al.*, 2011; Kobayashi and Iwano, 2012; Roux *et al.*, 2015; El Mammeri *et al.*, 2019).

Focusing on non-domesticated *B. subtilis* strains isolated from food or from medical environments, we showed that some strains, especially the NDmed strain isolated from an endoscope washer-disinfector, were able to form thick and structured biofilms on submerged surfaces (Bridier *et al.*, 2011). Moreover, NDmed was able to protect *Staphylococcus aureus* from biocide action in a submerged mixed-species biofilm (Bridier *et al.*, 2012). The gene *ypqP* (renamed *spsM*, (Abe *et al.*, 2014)) likely involved in the synthesis of polysaccharide, is inactivated in both the model strain NCIB3610 and the lab strain 168, and was identified as being responsible for these features of NDmed submerged biofilms (Sanchez-Vizuete *et al.*, 2015).

These works point out the importance of the submerged biofilm as a model of growth in the study of *B. subtilis* social behavior. Moreover *B. subtilis* submerged biofilms are also considered to be representative of other *B. subtilis* natural habitats such as soil and plant roots surface (Chen *et al.*, 2013; Pandin *et al.*, 2017). Nevertheless, little is still known about the genetic pathways involved in the formation of *B. subtilis* submerged biofilms (Bridier *et al.*, 2011; Terra *et al.*, 2012; Dergham *et al.*, 2021).

To better understand the molecular strategies that bacteria undergo to build biofilms, we used 4D confocal laser scanning imaging (4D-CLSM) to visualize, *in situ,* in time-lapse and at cell level, the biofilm structural dynamics. By this approach, we have discovered that the transition from sessile cells to a highly structured biofilm of *B. subtilis* on the submerged level involves an unexpected sudden and coordinated fragmentation of the sessile population to a motile one. The latter event has been shown to be closely connected with the pellicle formation at the liquid-air interface and with transition from aerobic to anaerobic metabolisms. This work points out sophisticated programs of cellular specialization and cell-cell communication within the microbial community.

MATERIALS AND METHODS

Bacterial strains and growth conditions

The strains used during this study are listed in Table 1. *B. subtilis* NDmed derivative strains were obtained by transformation with chromosomal DNA of various strains to introduce the corresponding suitable reporter fusion. Extraction of chromosomal DNA and transformation of *B. subtilis* were performed as described previously (Dergham *et al.*, 2021); transformants were selected on Luria-Bertani (LB, Sigma, France) plates supplemented with appropriate antibiotics at the following concentrations: spectinomycin (spec), 100µg/mL; chloramphenicol (cm), 5 µg/mL kanamycin (kan), 8µg/ml. The *B. subtilis* strain GM2938 expressing mCherry was obtained by transforming for spectinomycin resistance strain BSB168, a *trp+* derivative of the reference strain 168 Marburg (Rühl *et al.*, 2012) with plasmid pIC630. This results in the integration by a double crossing over into the chromosomal *amyE* locus of the *mCherry* gene placed under the control of the $P_{hyperspank}$ promoter, an isopropyl β-D-1-thiogalactopyranoside (IPTG)-inducible promoter derived from the *Escherichia coli lac* operon. Plasmid pIC630 was constructed by placing the *mCherry* gene (codon-optimized for *B. subtilis*) under the control of $P_{hyperspank}$ through cloning into pDR111 of a *Hind*III–*Sph*I restriction fragment obtained from a PCR on plasmid pDR201 with primers DC014 (5'-CCCAAGCTTACATAAGGAGGAACTACTATG-3') and DC015 (5'-ACATGCATGCTTATTTGTATAATTC-3') (both pDR111 and pDR201 are kind gifts from D. Rudner, Harvard Medical School). A similar IPTG-inducible fusion of the *gfpmut2* gene under the control of the $P_{hyperspank}$ promoter was introduced into NDmed to give the *B. subtilis* strain NDmed-GFP expressing GFPmut2. The transcriptional fusions of the *fnr* or *gapB* promoter with *gfpmut3*

were constructed within the pBaSysBioII plasmid using ligation-independent cloning prior to integration into the chromosome of BSB168 in a non-mutagenic manner, resulting in strains BBA0184 and BBA9006, respectively (Botella *et al.*, 2010; Rühl *et al.*, 2012). Bacterial stock cultures were kept at -20°C in Tryptone Soy Broth (TSB, bioMerieux, France) containing 20% (vol/vol) glycerol. Prior to each experiment, frozen cells were sub-cultured twice in TSB at 30°C. The final overnight culture was used as an inoculum for the growth of biofilms.

Table 1. Strains used in this study

Strain	Relevant genotype or isolation source	Reference or construction[a]
B. subtilis NDmed	Undomesticated, isolated from endoscope washer-disinfectors	(Martin et al., 2008)
B. subtilis NDmed GFP	NDmed *amyE::P$_{hyperspank}$-gfpmut2* (spec)	(Bridier et al., 2012)
B. subtilis GM2938	BSB168 *amyE::P$_{hyperspank}$-mCherry* (spec)	This work
B. subtilis NDmed mCherry	NDmed *amyE::P$_{hyperspank}$-mCherry* (spec)	TF NDmed/DNA GM2938
B. subtilis TMN547	NCIB3610 *amyE::Phag-gfp* (cm) *sacA::PtapA-mKate2* (kan)	(Norman et al., 2013)
B. subtilis NDmed 547	NDmed *amyE::Phag-gfp* (cm) *sacA::PtapA-mKate2* (kan)	TF NDmed/DNA TMN547
B. subtilis BBA9006	BSB168 *PgapB-gfpmut3* (spec)	(Rühl et al., 2012)
B. subtilis GM3378	NDmed *PgapB-gfpmut3* (spec)	TF NDmed/DNA BBA9006
B. subtilis BBA0184	BSB168 *Pfnr-gfpmut3* (spec)	(Botella et al., 2010)
B. subtilis GM3361	NDmed *Pfnr-gfpmut3* (spec)	TF NDmed/DNA BBA0184
B. subtilis 168	*trpC2* (Domesticated strain)	*Bacillus* genetics Stock Center
B. subtilis BSB168	*trp+* derivative of 168	(Rühl et al., 2012)
B. subtilis NCIB3610	Less domesticated strain	(Branda et al., 2001)
B. subtilis NDfood	Isolated from a dairy product	(Bridier et al., 2011)
B. subtilis BSn5	Isolated from a plant	(Deng et al., 2011)
B. subtilis BSP1	Isolated from poultry	(Schyns et al., 2013)
B. cereus 407		(Houry et al., 2010)
B. licheniformis LMG7559	Isolated from flour	(De Clerck and De Vos, 2004)
B. amyloliquefaciens 20P6	Isolated from lettuce	This work

[a]TF NDmed/DNA stands for transformation of NDmed by chromosomal DNA of indicated strains

Biofilm development in 96 well microplates

Submerged biofilms were grown on the surface of polystyrene 96-well microtiter plates with a µclear® base (Greiner Bio-one, France) enabling high-resolution fluorescence imaging (Bridier *et al.*, 2010). 200 µL of an overnight culture in TSB (adjusted to an OD 600nm of 0.02) were added in each well. The microtiter plate was then incubated at 30°C for 90 min to allow the bacteria to adhere to the bottom of the wells. Wells were then rinsed with TSB to eliminate non-adherent bacteria and refilled with 200 µL of sterile TSB. When appropriate, the medium was supplemented with 200µM IPTG to induce the expression of the fluorescent reporters GFP or mCherry from the $P_{hyperspank}$ promoter. The vital stain FM4-64 (Invitrogen), added to the medium at a final concentration of 1µg/mL, and was used to label bacteria membranes when appropriate.

In order to acquire high resolution images of pellicle (Fig. 3B), floating biofilms grown in a 12-well microplate (Greiner bio-one, Germany) were detached by a tip from the sides of the well and placed on a slide to be observed under confocal microscopy.

4D-CLSM

After the initial adhesion and washing steps, the 96 well microtiter plate was mounted on the motorized stage of a Leica SP8 AOBS inverter confocal laser scanning microscope (CLSM, LEICA Microsystems, Germany) at the MIMA2 platform (www6.jouy.inra.fr/mima2_eng/). Temperature was maintained at 30°C during all experiments. 4D (xyzt) acquisitions were performed with the following parameters: images of 246 x 246 µm were acquired at 600 Hz using a 63×/1.2 N.A. with a z-step of 1µm and a thickness of 120µm at intervals of 15 min. To detect GFP, an argon laser at 488 nm set at 10% of the maximal intensity was used, and the emitted fluorescence was collected in the range 495 to 550 nm using hybrid detectors (HyD LEICA Microsystems, Germany). To detect the red fluorescence of mKate2 or FM4-64, a 561 nm helium-neon laser set at 25% and 2% of the maximal intensity respectively was used, and fluorescence was collected in the range 590 to 720 nm and 605 to 705 nm respectively, using hybrid detectors.

To visualize simultaneously submerged biofilm and liquid-air pellicle dynamic (Fig. 1), the control software was set to take xyzt series of 1.5 x 1.5 mm images scanned at 600 Hz using a low-resolution long range 10×/0.3 N.A. air objective with a z-step of 5µm and a thickness of 4.5mm at intervals of 60 min. To detect mCherry emitted fluorescence, a 561 nm helium-neon laser set at

20% of the maximal intensity was used, and fluorescence was collected in the range 580 to 700 nm using hybrid detectors. High resolution imaging of 24h culture biofilms (Fig. 3B) was obtained with a HCX APO L U-V-I 40x/0.80 WATER objective lens in well filled only 100 µL of growth media to reduce the distance between both interfaces.

CLSM image analysis

Projections of the biofilm structural dynamic were constructed from xyzt images series using IMARIS 9.3 (Bitplane, Switzerland). Individual cell length and numbers were extracted from 4D-CLSM with the ImageJ (v1.53) particle analysis function. Space-time kymographs were constructed with the BiofilmQ visualisation toolbox (Hartmann *et al.*, 2021). Local density color code was calculated with BiofilmQ after Otsu segmentation and visualized with Paraview 5.9 (Ayachit, 2015).

Temporal transcriptome analysis

Biofilms were grown as previously explained. Briefly, 200 µL of an overnight culture of NDmed in TSB (adjusted to an OD 600nm of 0.02) were added in each well. The microtiter plate was then incubated at 30°C for 90 min to allow the bacteria to adhere to the bottom of the wells. Wells were then rinsed with TSB to eliminate non-adherent bacteria and refilled with 200 µL of sterile TSB. For each time point (1h, 3h, 4h, 5h, 7h, 24h and 48h) 96-well plates were prepared. At each time point, the content of the wells was recovered and put into contact with the same volume of killing buffer (Nicolas *et al.*, 2012).

Then, RNA was extracted following the method described by Nicolas *et al.*, 2012. The RNA concentration was measured using Nanodrop and RNA quality was determined using an Agilent 2100 Bioanalyzer. Synthesis and Cy3-labelling of cDNA, and hybridization of the sample to the *B. subtilis* T3 2x400K tiling array (Agilent-044473) were performed following Agilent Technologies protocols, as previously described (Rath *et al.*, 2020). The microarray was scanned with Agilent Technologies Scanner, model G2505C. Grid: 044473_D_F_20121025. Protocol: GE1_107_Sep09. The tiling array data set is available from NCBI's Gene Expression Omnibus (GEO) database (accession number GSE190460).

Measurement of dissolved oxygen in the wells

A pO_2 microelectrode (Lazard research laboratories, Inc) was used to measure over time oxygen concentration in the microtiter plate wells. Zero calibration was performed with a 2% sodium bisulfite solution and the results were expressed in ppm.

RESULTS

1. Coexistence of submerged biofilms and floating pellicles in microplates wells

In order to confirm that a *B. subtilis* non-domesticated strain was able to grow both as submerged biofilms and floating pellicles in microscopic grade microplate wells, we have combined 4D-CLSM and a long-range objective to monitor both interfacial communities simultaneously. For this, we used a *B. subtilis* NDmed strain derivative constitutively expressing mCherry red fluorescent protein to monitor its growth during 24 hours starting from a single layer of adherent cells (Fig. 1, movies S1 and S2 in the supplemental material).

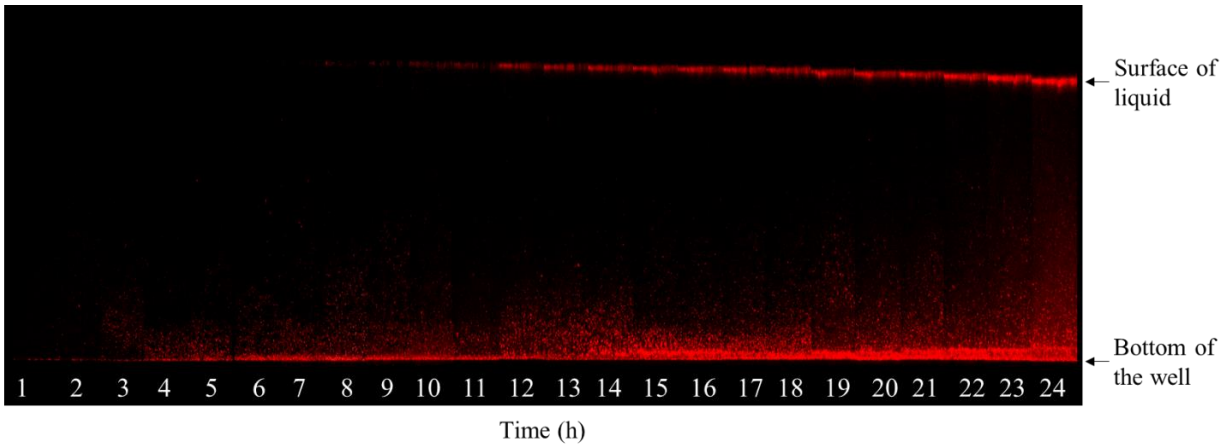

Fig.1. CLSM Section view of a microplate well colonized by B. subtilis NDmed-mCherry showing the relative dynamics of formation of submerged biofilm (bottom of the well) and the floating pellicle (surface of liquid); *a representative experiment of three replicates is presented. Note that pellicle slightly falls over time due to liquid evaporation. The distance between the bottom of the well and the surface of the liquid is around 4.5 mm.*

We observed an increase of red fluorescence from the bottom of the well up to a couple of hundred micrometers which corresponds to the development of the submerged biofilm. Increase in

fluorescence intensity at the liquid-air interface occurred 7-8 hours after the incubation starting point of the adhering cells, corresponding to the formation of the pellicle. It can be seen in Figure 1 that the distance between the surface and the floating pellicle was initially 4.5 mm, but slightly decreased over time corresponding to liquid evaporation in the well and thereby a consequent drop of the liquid-air interface. Our observations demonstrate that a submerged biofilm and a floating pellicle can form consecutively in the same system. In addition, the fluorescent cells observed in the space between the attached submerged biofilm and the floating pellicles are swimming free cells (see movies S1 and S2), suggesting the existence of an interplay between both communities.

2. A brutal and coordinated fragmentation of sessile elongating chains precede floating pellicle formation

Development of adherent *B. subtilis* NDmed GFP cells on the bottom of the microtiter plates wells was monitored by time-lapse confocal laser scanning microscopy (4D-CLSM) with images taken every 15 minutes during 14 hours (Fig.2 and movies S3 and S4 in the supplemental material). Figure 2A represents tile images from the movie S3 at specific time points illustrating the two stages in the surface colonization. In a first stage, sessile cells proliferate as a dense network of long filaments covering the surface. Between 2 and 4 hours after they started to proliferate, elongated chains with an average length of around 9 µm suddenly fragment and liberate a cloud of shorter free-swimming cells with an average length of 3 µm (Fig. 2B and 2C, movie S4). This transition occurred reproducibly in less than 30 minutes, and the construction of the typical *B. subtilis* protruding structures of sessile cells was visible only in a second kinetic, after 7 to 9 hours (Fig. 2A and 2B, movie S3).

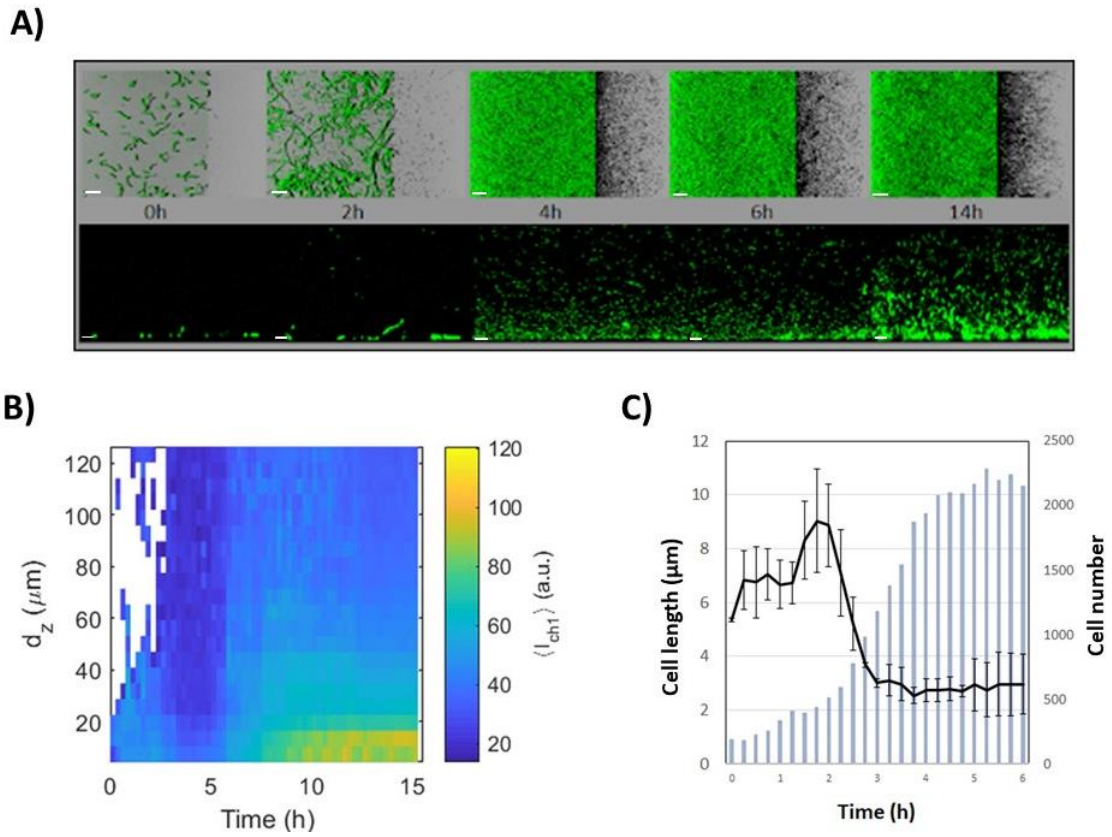

Fig. 2. The biphasic process of submerged biofilm formation by B. subtilis NDmed. A) *4D-CLSM of B. subtilis NDmed GFP on submerged surfaces. Imaris Easy 3D reconstructions (top) and sections views as an XZ projection (bottom) at specific time points of a representative experiment of three independent experiments. The shadow on the right represents a vertical (YZ) projection of the submerged biofilm (scale bars represent 20µm).* ***B)*** *Space-time kymograph generated with BiofilmQ from 4D-CLSM series showing the brutal apparition of free cell in all the well 3h after biofilm initiation and the late initiation of submerged biofilm after 7h. dz represents the distance to the surface in µm and Ich1 the GFP fluorescence intensity in relative arbitrary units. Representative of n = 3 independent biofilms.* ***C)*** *Individual cell length coordinately and brutally drop during chain fragmentation 2 to 3 h after biofilm initiation. Chains fragmentation is correlated with an increased number of detected individual objects in the medium. Mean cell length +/- SD calculated from n=3 experiments.*

Similar 4D-CLSM observations were acquired for other *B. subtilis* strains (movies S5-9 in the supplemental material), and strains of other related species (movies S10-12), using the vital FM4-64 fluorescent dye instead of GFP (see details of the strains in Table 1). The reference strains 168 and NCIB3610 displayed a similar behavior to that of the NDmed strain, as well as all other non-domesticated *B. subtilis* isolates tested (NDfood, BsN5 or BSP1). On the contrary, closely related but distinct *Bacillus* species strains such as *Bacillus cereus* 407, *Bacillus licheniformis* LMG7559

or *Bacillus amyloliquefaciens* 20P6 showed a continuous monophasic colonization of the surface without any coordinated liberation of free motile cells (movies S10-12 in the supplemental material).

3. Temporal transcriptome analysis

To understand the mechanism behind sessile cells fragmentation into highly motile ones, a transcriptome analysis by tiling array was done for *B. subtilis* over a temporal scale. A global view of the results indicates that the genes encoding basic functions essential for cellular growth are expressed at a constant rate during the first hours (from 1h to 7h), with variation not exceeding at most a factor of 2 (see supplementary data S1). These ensure replication (DNA polymerase, primase, gyrase, topoisomerase, helicase, initiation/termination factors), transcription (RNA polymerase, sigma A factor, elongation/pause/termination factors), translation (ribosomal proteins, aminoacyl-tRNA synthetases, initiation elongation factors) or central carbon metabolism (enzymes of glycolysis and TCA cycle). Thus, this indicates that the process of fragmentation occurs while cells are growing at a constant rate. Results represented in Figure S1 confirm the initial microscopic observations, where genes required for autolysis and motility start to be upregulated after 3 hours to reach their maximum level after 4 hours of incubation, the time in which elongated sessile chains fragment into motile short cells.

Nutrient or/and oxygen depletion were hypothesized to be possible signals triggering the early fragmentation of the sessile chains cells. To investigate the carbon source depletion as a triggering signal, we have monitored expression of *gapB*, a gene encoding a Glyceraldehyde-3-Phosphate-Dehydrogenase derepressed only under gluconeogenic conditions (supplementary data S1) (Fillinger *et al.*, 2000). The *gapB* gene expression was extremely downregulated during the first 7 hours of incubation, and appeared strongly upregulated only in the late samples from 24 hours and 48 hours, indicating that glycolytic carbon source limitation occurred much later than the fragmentation process.

For oxygen sensing and respiration we have monitored the *hemAT* gene (encoding a soluble chemotaxis receptor oxygen sensor protein) (Hou *et al.*, 2000), the *cydABCD* operon (encoding cytochrome bd oxidase induced under low oxygen tensions, represented as *cydA* in Fig. S1), and the *qoxABCD* operon (encoding cytochrome aa3 quinol oxidase, the major oxidase in aerated

cultures, represented as *qoxA* gene in Fig. S1) (Sachla *et al.*, 2021). For efficient aerobic growth, cells require either CydABCD or QoxABCD (Sachla *et al.*, 2021). In the first hour only *cydA* appears to be upregulated (Fig. S1) and after 3 hours none of the aerobic respiratory genes are expressed. Meanwhile, *hemAT* starts to be upregulated, in synchrony with the fragmentation of sessile cells to motile ones, to reach its maximum expression after 4 hours. Aerobic respiration is regained and observed by the upregulation of *qoxA*. Shortly after, anaerobic respiration can be observed (Fig. S1) by upregulation of the self-regulated operon *nark-fnr*, encoding the Fnr transcriptional regulator for anaerobically induced genes, i.e. the *narGHJI* operon and the *arfM* gene encoding another anaerobic regulator. In addition, upregulation is also observed for the *nasBCDEF* operon (represented in Figure S1 with *nasD* and *nasF*) encoding a nitrate- and a nitrite reductase (Nakano and Zuber, 1998).

Then after 7 hours of incubation, biofilm matrix genes (*i.e. epsA*, *tasA*, *dhbA*, *yvcA*, *pgsB*, and *bslA*) are upregulated, the time where the biofilms (submerged and pellicle) are in the process of formation and stabilization. Expression follows of late biofilm genes (*i.e. yxaB*, *veg*, *ymcA*, and *ypqP*) for the complex architectural biofilm formation after 24 and 48 hours, as well as genes related to sporulation.

4. *In situ* cell visualization for the fate switching with fluorescent reporters

Using the NDmed547 strain harboring two transcriptional reporter constructions, we could monitor both motility and matrix production (*Phag-gfp* reporting the expression of flagella genes in green and *PtapA-mKate2* reporting the expression of matrix genes in red). The submerged biofilm formation was monitored over 14 hours (image every 15 minutes) for the spatio-temporal patterns of these two subpopulations of cell fate (Fig. 3A and movie S13 in the supplementary material). Promoter activities are illustrated in Figure 4A and 4B, as a kymograph representing the fluorescence intensity as a function of time and altitude above. Moreover, the GM3361 strain allowed to report in the NDmed context expression of *fnr*, encoding a regulator of the global response to oxygen depletion (*Pfnr-gfpmut3)* (Fig. 4C).

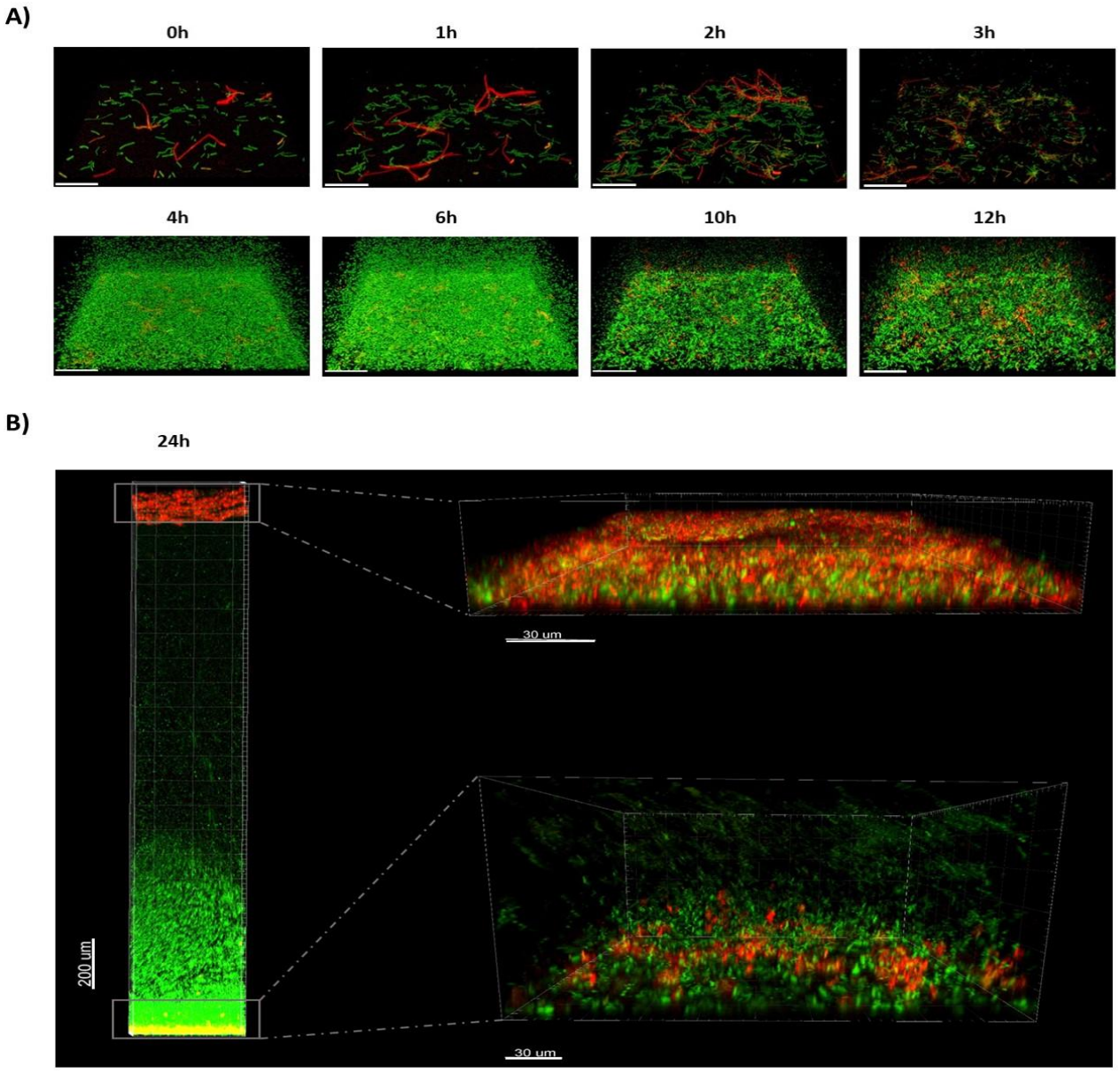

Fig.3 CLSM of NDmed547 [amyE::Phag-gfp sacA::PtapA-mKate2] reporting in green the expression of the hag gene (motility) and in red the expression of tapA (matrix synthesis). A) *4D-CLSM of the biphasic submerged biofilm formation process. See also movie S13. The scale bars represent 50µm.* ***B)*** *CLSM visualization of the well colonization after 24h, both on the surface (with a zoom on submerged biofilm on the bottom right with a scale bar of 30µm) and at the liquid air interface (with a zoom on a floating pellicle on the up right with a scale bar of 30µm).*

Initially, a subpopulation of sessile chains of cells expressing *tapA* (red) coexists with a subpopulation of motile cells expressing *hag* (green). During the first 3 hours of submerged biofilm formation, sessile chains have elongated and propagated, discern visually by the high fluorescent intensity recorded in Figure 4B, while the fraction of cells expressing *hag* was less abundant (Fig.

3A and 4A). After 3 hours, red cell chains (expressing *tapA*) suddenly and coordinately fragment into green individual motile cells (expressing *hag)*, corresponding to the sudden change of the fluorescent intensity color observed in Figure 4A to a more intense one. In parallel, a clear signal of fluorescence was detectable as early as 3-4 hours with GM3361 *[Pfnr-gfpmut3]*), indicating that oxygen limitation occurred in early stages of the biofilm development (Fig. 4C). This was confirmed by a direct and continuous measurement of oxygen concentration using a microelectrode (Fig. 4D). Oxygen concentration in the well strictly decreased below the detection limit as early as four hours after incubation of adherent cells. This oxygen limitation was correlated to trigger the population of red elongated chains, expressing the *tapA* operon, to fragment and acquire motility (Fig. 4). The *tapA* expression was highly regained after ~7h (Fig. S1 and Fig. 4B) to structure the typical surface-associated protruding submerged biofilm and initiate the floating pellicle of *B. subtilis*, which leads to two biofilms in a same well of static liquid culture (Fig. 3B).

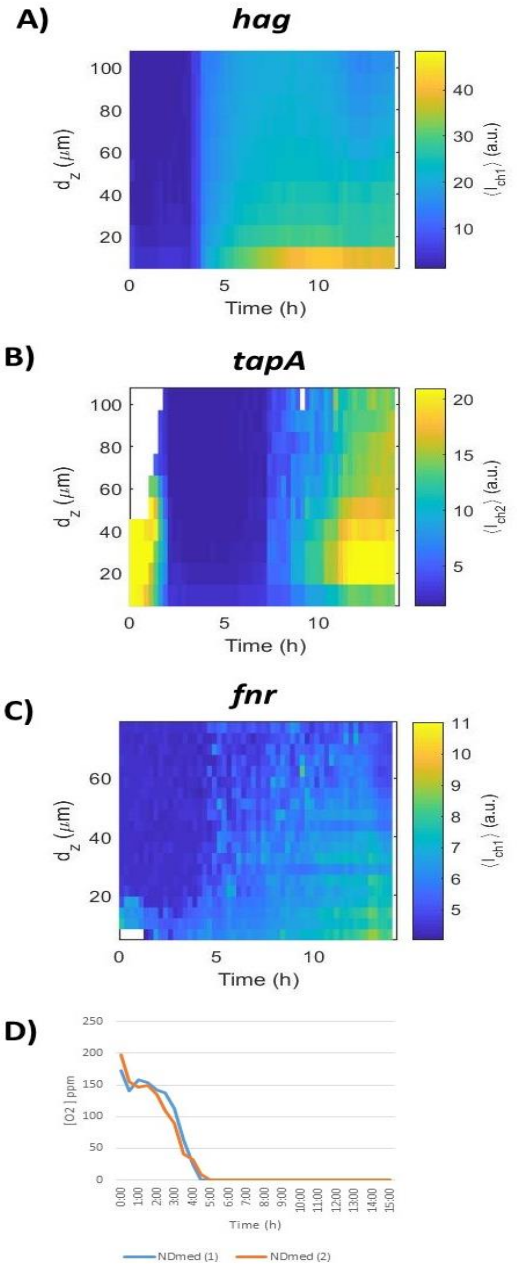

Fig.4 Space-time kymographs *for reporters* ***(A)*** *hag,* ***(B)*** *tapA,* ***(C)*** *fnr transcription during submerged biofilm formation of B. subtilis NDmed. Representative of n = 3 independent biofilms for each reporter. Kymographs were constructed with BiofilmQ visualization toolbox from 4D-CLSM image sequences with fluorescent transcriptional fusions (NDmed547 [amyE::Phag-gfp sacA::PtapA-mKate2] and GM3361 [Pfnr-gfpmut3]). dz represents the distance to the surface in µm and Ich1 the fluorescent reporter intensity in relative arbitrary units. The graph in panel* ***(D)*** *represents the oxygen concentration measured in two wells with a microelectrode showing a sharp decrease of oxygen concentration that drops from around 185 ppm at t=0 below the probe detection limit after less than 5 hours.*

DISCUSSION

We observed previously that the non-domesticated *B. subtilis* NDmed strain was able to form robust submerged biofilms in the bottom of microtiter-plates under static conditions (Bridier *et al.*, 2011). In the present work, using 4D-CLSM, we visualized the formation dynamics of these submerged biofilms, which surprisingly appeared to be a discontinuous process. After a first stage of development on the surface, and concomitantly with oxygen limitation, sessile chains suddenly fragment, liberating a massive number of free motile cells. These planktonic cells partially migrate towards the liquid-air interface to initiate a floating pellicle. It is only in a second kinetics that the characteristic surface-associated protruding structures of *B. subtilis* NDmed rise, along with strong expression of the *tapA-sipW-tasA* matrix operon. To our knowledge, such biphasic biofilm formation has never been explored and when pellicles and submerged biofilms have been studied, it was frequently under different conditions.

In other bacterial species like *Pseudomonas aeruginosa*, detachment from the surface and dispersion has been described as a possible end to the biofilm lifestyle cycle. The active cells scattering from biofilm to new habitats seem to be driven by limitations of resources or the emergence of stressful conditions in the cell microenvironment. Depletion in nutrient availability or the accumulation of waste metabolic products (such as acids issuing from fermentation in oxygen-depleted zones) have been demonstrated to induce biofilm dispersal (Rumbaugh and Sauer, 2020). In the work presented here, we demonstrate that early oxygen limitation in the well is concomitant with massive liberation of planktonic cells from early submerged biofilm after approximately 4 hours of development. In *B. subtilis*, oxygen depletion has been shown previously to induce matrix production by increasing transcription of the *tapA* operon in NCIB3610 colonies (Kolodkin-Gal *et al.*, 2013). In our submerged system, expression in NDmed of *tapA* was also correlated with that of *fnr*, a gene induced under deep oxygen depletion. These observations suggest that, after a first step of proliferation of sessile cells as filaments covering the surface, the limitation of oxygen triggered their fragmentation into motile cells able to migrate to the air-medium interface to form the pellicle. Indeed, a temporal transcriptome analysis of biofilm showed that genes involved in oxygen sensing, autolysis and motility were highly expressed after 4 hours of development, which corresponded to the sudden transition between filaments and motile cells observed with 4D-CLSM. This is in accordance with a previous report identifying oxygen as a

putative trigger for active movement towards the air–liquid interface of *B. subtilis* NCIB3610 cells, since a *ΔhemAT* mutant was outcompeted by the wild type during pellicle formation in static co-cultures (Hölscher *et al.*, 2015). Similar behaviors were also described for the Gram-negative lake sediment bacterium *Shewanella oneidensis* MR-1, as biofilms formed by this species showed a rapid detachment from the surface upon a sudden downshift in oxygen concentration (Thormann *et al.*, 2005).

Interestingly, all other *B. subtilis* strains tested, including thick biofilm-forming isolates such as NDfood, BsN5 and BsP1, or weaker submerged biofilm-forming strains 168 and NCIB3610, showed a similar biphasic submerged biofilm dynamics (Movies S5-9). In contrast, other related species, such as *B. cereus*, *B. amyloliquefaciens* or *B. licheniformis* exhibited a continuous colonization of the surface (Movies S10-12). Some of these *Bacilli* are also able to form chains of cells, but which did not fragment during the time the biofilm formation was monitored. *B. subtilis* chain formation was first visualized in pellicles (Kobayashi, 2007), however without observation of coordinated return to planktonic state in these conditions. The relation between submerged biofilm and liquid-air pellicle shown here could suggest an interplay, with co-metabolism between the populations of both interfaces: the population in contact with air could liberate metabolites used by the surface-associated population to grow in anaerobic condition. This is consistent with the described ability of *B. subtilis* to grow without oxygen, respiring nitrate or nitrite instead of oxygen as electrons acceptor (Nakano and Hulett, 1997). Nevertheless, this potential relation between populations requires further investigation.

Understanding the triggers and effectors of this coordinated multicellular behavior could also contribute to identifying new actors involved in biofilm disruption. This has been largely studied in recent years because of its potential as an alternative treatment to promote biofilm cell detachment (Kostakioti *et al.*, 2013; Cascioferro *et al.*, 2021). Some natural molecules produced by mature biofilms have been found to induce biofilm disassembly, such as nitric oxide in *Pseudomonas spp.* biofilms (Barraud *et al.*, 2015) or acidic amino acids in *S. aureus* biofilms (Warraich *et al.*, 2020). The combination of such biofilm disruptors with antibiotics treatment to improve drug effectiveness could be a promising approach to tackle biofilm chronic infections.

The experimental approach proposed in this work allowed visualization, at the cell level, of the dynamic interactions between subpopulations in a *B. subtilis* community. The

multidimensional description of spatio-temporal patterns of gene expression has been recently facilitated by the availability to biologists of advanced quantitative microscopic analysis tools (Hartmann *et al.*, 2021). The implementation of this system to more complex samples, such as multispecies biofilms, could provide an experimental approach for the study of spatial interactions between species, co-metabolism or cell-to-cell signaling.

ACKNOWLEDGMENTS

This work was supported by INRAE. P. Sanchez-Vizuete was the recipient of a PhD grant from the Région Ile-de-France (DIM ASTREA). Y. Dergham is the recipient of fundings from the Union of Southern Suburbs Municipalities of Beirut, INRAE, Campus France PHC CEDRE 42280PF and Fondation AgroParisTech. L. Tournier and V. Fromion (INRAE) are acknowledged for fruitful discussions, R. Losick for the gift of the strain TMN547, and M. Jules for the gift of strains BBA0184 and BBA9006.

CREDIT AUTHOR STATEMENT

PSV: Conceptualization, experiments, writing original draft preparation reviewing and editing, **YD**: Conceptualisation, experiments, data curation, draft preparation, reviewing and editing, **AB**: Conceptualisation, experiments, writing- reviewing and editing, **JD***:* Assistance with 4D-CLSM microscopy and image analysis, **ED**: Transcriptomic experiments, **KH:** Supervision and reviewing, **SA**: Conceptualisation and reviewing, **DLC**: Conceptualization, methodology, supervision, writing- reviewing and editing, **RB**: Conceptualization, methodology, supervision, writing-reviewing and editing.

REFERENCES

Abe, K., Kawano, Y., Iwamoto, K., Arai, K., Maruyama, Y., Eichenberger, P., *et al.* (2014). Developmentally-regulated excision of the SPβ prophage reconstitutes a gene required for spore envelope maturation in *Bacillus subtilis*. *PLoS Genet* 10, e1004636. doi:10.1371/journal.pgen.1004636.

Arnaouteli, S., Bamford, N. C., Stanley-Wall, N. R., and Kovács, Á. T. (2021). *Bacillus subtilis* biofilm formation and social interactions. *Nat Rev Microbiol*. doi:10.1038/s41579-021-00540-9.

Ayachit, U. (2015). "The ParaView Guide: A Parallel Visualization Application," in (Clifton Park, USA: Kitware).

Barraud, N., Kelso, M. J., Rice, S. A., and Kjelleberg, S. (2015). Nitric oxide: a key mediator of biofilm dispersal with applications in infectious diseases. *Curr Pharm Des* 21, 31–42. doi:10.2174/1381612820666140905112822.

Bartolini, M., Cogliati, S., Vileta, D., Bauman, C., Rateni, L., Leñini, C., et al. (2019). Regulation of Biofilm Aging and Dispersal in *Bacillus subtilis* by the Alternative Sigma Factor SigB. *J Bacteriol* 201, e00473-18. doi:10.1128/JB.00473-18.

Botella, E., Fogg, M., Jules, M., Piersma, S., Doherty, G., Hansen, A., et al. (2010). pBaSysBioII: an integrative plasmid generating gfp transcriptional fusions for high-throughput analysis of gene expression in *Bacillus subtilis*. *Microbiology (Reading)* 156, 1600–1608. doi:10.1099/mic.0.035758-0.

Branda, S. S., González-Pastor, J. E., Ben-Yehuda, S., Losick, R., and Kolter, R. (2001). Fruiting body formation by *Bacillus subtilis*. *Proc Natl Acad Sci U S A* 98, 11621–11626. doi:10.1073/pnas.191384198.

Bridier, A., Dubois-Brissonnet, F., Boubetra, A., Thomas, V., and Briandet, R. (2010). The biofilm architecture of sixty opportunistic pathogens deciphered using a high throughput CLSM method. *J Microbiol Methods* 82, 64–70. doi:10.1016/j.mimet.2010.04.006.

Bridier, A., Le Coq, D., Dubois-Brissonnet, F., Thomas, V., Aymerich, S., and Briandet, R. (2011). The spatial architecture of *Bacillus subtilis* biofilms deciphered using a surface-associated model and in situ imaging. *PLoS One* 6, e16177. doi:10.1371/journal.pone.0016177.

Bridier, A., Sanchez-Vizuete, M. D. P., Le Coq, D., Aymerich, S., Meylheuc, T., Maillard, J.-Y., et al. (2012). Biofilms of a *Bacillus subtilis* hospital isolate protect Staphylococcus aureus from biocide action. *PLoS One* 7, e44506. doi:10.1371/journal.pone.0044506.

Cairns, L. S., Hobley, L., and Stanley-Wall, N. R. (2014). Biofilm formation by *Bacillus subtilis*: new insights into regulatory strategies and assembly mechanisms. *Mol Microbiol* 93, 587–598. doi:10.1111/mmi.12697.

Cascioferro, S., Carbone, D., Parrino, B., Pecoraro, C., Giovannetti, E., Cirrincione, G., et al. (2021). Therapeutic Strategies To Counteract Antibiotic Resistance in MRSA Biofilm-Associated Infections. *ChemMedChem* 16, 65–80. doi:10.1002/cmdc.202000677.

Chai, Y., Kolter, R., and Losick, R. (2010). Reversal of an epigenetic switch governing cell chaining in *Bacillus subtilis* by protein instability. *Mol Microbiol* 78, 218–229. doi:10.1111/j.1365-2958.2010.07335.x.

Chen, Y., Yan, F., Chai, Y., Liu, H., Kolter, R., Losick, R., et al. (2013). Biocontrol of tomato wilt disease by *Bacillus subtilis* isolates from natural environments depends on conserved

genes mediating biofilm formation. *Environ Microbiol* 15, 848–864. doi:10.1111/j.1462-2920.2012.02860.x.

Costerton, J. W., Stewart, P. S., and Greenberg, E. P. (1999). Bacterial biofilms: a common cause of persistent infections. *Science* 284, 1318–1322. doi:10.1126/science.284.5418.1318.

da Silva, R. A. G., Afonina, I., and Kline, K. A. (2021). Eradicating biofilm infections: an update on current and prospective approaches. *Curr Opin Microbiol* 63, 117–125. doi:10.1016/j.mib.2021.07.001.

De Clerck, E., and De Vos, P. (2004). Genotypic diversity among *Bacillus licheniformis* strains from various sources. *FEMS Microbiol Lett* 231, 91–98. doi:10.1016/S0378-1097(03)00935-2.

Deng, Y., Zhu, Y., Wang, P., Zhu, L., Zheng, J., Li, R., et al. (2011). Complete genome sequence of *Bacillus subtilis* BSn5, an endophytic bacterium of Amorphophallus konjac with antimicrobial activity for the plant pathogen Erwinia carotovora subsp. carotovora. *J Bacteriol* 193, 2070–2071. doi:10.1128/JB.00129-11.

Dergham, Y., Sanchez-Vizuete, P., Le Coq, D., Deschamps, J., Bridier, A., Hamze, K., et al. (2021). Comparison of the Genetic Features Involved in *Bacillus subtilis* Biofilm Formation Using Multi-Culturing Approaches. *Microorganisms* 9, 633. doi:10.3390/microorganisms9030633.

Diethmaier, C., Pietack, N., Gunka, K., Wrede, C., Lehnik-Habrink, M., Herzberg, C., et al. (2011). A novel factor controlling bistability in *Bacillus subtilis*: the YmdB protein affects flagellin expression and biofilm formation. *J Bacteriol* 193, 5997–6007. doi:10.1128/JB.05360-11.

El Mammeri, N., Hierrezuelo, J., Tolchard, J., Cámara-Almirón, J., Caro-Astorga, J., Álvarez-Mena, A., et al. (2019). Molecular architecture of bacterial amyloids in *Bacillus* biofilms. *FASEB J* 33, 12146–12163. doi:10.1096/fj.201900831R.

Fillinger, S., Boschi-Muller, S., Azza, S., Dervyn, E., Branlant, G., and Aymerich, S. (2000). Two glyceraldehyde-3-phosphate dehydrogenases with opposite physiological roles in a nonphotosynthetic bacterium. *J Biol Chem* 275, 14031–14037. doi:10.1074/jbc.275.19.14031.

Flemming, H.-C., Wingender, J., Szewzyk, U., Steinberg, P., Rice, S. A., and Kjelleberg, S. (2016). Biofilms: an emergent form of bacterial life. *Nat Rev Microbiol* 14, 563–575. doi:10.1038/nrmicro.2016.94.

Hartmann, R., Jeckel, H., Jelli, E., Singh, P. K., Vaidya, S., Bayer, M., et al. (2021). Quantitative image analysis of microbial communities with BiofilmQ. *Nat Microbiol* 6, 151–156. doi:10.1038/s41564-020-00817-4.

Hölscher, T., Bartels, B., Lin, Y.-C., Gallegos-Monterrosa, R., Price-Whelan, A., Kolter, R., et al. (2015). Motility, Chemotaxis and Aerotaxis Contribute to Competitiveness during Bacterial Pellicle Biofilm Development. *J Mol Biol* 427, 3695–3708. doi:10.1016/j.jmb.2015.06.014.

Hou, S., Larsen, R. W., Boudko, D., Riley, C. W., Karatan, E., Zimmer, M., et al. (2000). Myoglobin-like aerotaxis transducers in Archaea and Bacteria. *Nature* 403, 540–544. doi:10.1038/35000570.

Houry, A., Briandet, R., Aymerich, S., and Gohar, M. (2010). Involvement of motility and flagella in *Bacillus cereus* biofilm formation. *Microbiology (Reading)* 156, 1009–1018. doi:10.1099/mic.0.034827-0.

Karygianni, L., Ren, Z., Koo, H., and Thurnheer, T. (2020). Biofilm Matrixome: Extracellular Components in Structured Microbial Communities. *Trends Microbiol* 28, 668–681. doi:10.1016/j.tim.2020.03.016.

Kearns, D. B., Chu, F., Branda, S. S., Kolter, R., and Losick, R. (2005). A master regulator for biofilm formation by *Bacillus subtilis*. *Mol Microbiol* 55, 739–749. doi:10.1111/j.1365-2958.2004.04440.x.

Kobayashi, K. (2007). *Bacillus subtilis* pellicle formation proceeds through genetically defined morphological changes. *J Bacteriol* 189, 4920–4931. doi:10.1128/JB.00157-07.

Kobayashi, K., and Iwano, M. (2012). BslA(YuaB) forms a hydrophobic layer on the surface of *Bacillus subtilis* biofilms. *Mol Microbiol* 85, 51–66. doi:10.1111/j.1365-2958.2012.08094.x.

Kolodkin-Gal, I., Elsholz, A. K. W., Muth, C., Girguis, P. R., Kolter, R., and Losick, R. (2013). Respiration control of multicellularity in *Bacillus subtilis* by a complex of the cytochrome chain with a membrane-embedded histidine kinase. *Genes Dev* 27, 887–899. doi:10.1101/gad.215244.113.

Kostakioti, M., Hadjifrangiskou, M., and Hultgren, S. J. (2013). Bacterial biofilms: development, dispersal, and therapeutic strategies in the dawn of the postantibiotic era. *Cold Spring Harb Perspect Med* 3, a010306. doi:10.1101/cshperspect.a010306.

López, D., and Kolter, R. (2010). Extracellular signals that define distinct and coexisting cell fates in *Bacillus subtilis*. *FEMS Microbiol Rev* 34, 134–149. doi:10.1111/j.1574-6976.2009.00199.x.

Mah, T.-F. (2012). Biofilm-specific antibiotic resistance. *Future Microbiol* 7, 1061–1072. doi:10.2217/fmb.12.76.

Martin, D. J. H., Denyer, S. P., McDonnell, G., and Maillard, J.-Y. (2008). Resistance and cross-resistance to oxidising agents of bacterial isolates from endoscope washer disinfectors. *J Hosp Infect* 69, 377–383. doi:10.1016/j.jhin.2008.04.010.

Milton, M. E., Draughn, G. L., Bobay, B. G., Stowe, S. D., Olson, A. L., Feldmann, E. A., et al. (2020). The Solution Structures and Interaction of SinR and SinI: Elucidating the Mechanism of Action of the Master Regulator Switch for Biofilm Formation in *Bacillus subtilis*. *J Mol Biol* 432, 343–357. doi:10.1016/j.jmb.2019.08.019.

Mukherjee, M., and Cao, B. (2021). Engineering controllable biofilms for biotechnological applications. *Microb Biotechnol* 14, 74–78. doi:10.1111/1751-7915.13715.

Nakano, M. M., and Hulett, F. M. (1997). Adaptation of *Bacillus subtilis* to oxygen limitation.

FEMS Microbiol Lett 157, 1–7. doi:10.1111/j.1574-6968.1997.tb12744.x.

Nakano, M. M., and Zuber, P. (1998). Anaerobic growth of a "strict aerobe" (*Bacillus subtilis*). *Annu Rev Microbiol* 52, 165–190. doi:10.1146/annurev.micro.52.1.165.

Nickel, J. C., Ruseska, I., Wright, J. B., and Costerton, J. W. (1985). Tobramycin resistance of *Pseudomonas aeruginosa* cells growing as a biofilm on urinary catheter material. *Antimicrob Agents Chemother* 27, 619–624. doi:10.1128/AAC.27.4.619.

Nicolas, P., Mäder, U., Dervyn, E., Rochat, T., Leduc, A., Pigeonneau, N., et al. (2012). Condition-dependent transcriptome reveals high-level regulatory architecture in *Bacillus subtilis*. *Science* 335, 1103–1106. doi:10.1126/science.1206848.

Nishikawa, M., and Kobayashi, K. (2021). Calcium Prevents Biofilm Dispersion in *Bacillus subtilis*. *J Bacteriol* 203, e0011421. doi:10.1128/JB.00114-21.

Norman, T. M., Lord, N. D., Paulsson, J., and Losick, R. (2013). Memory and modularity in cell-fate decision making. *Nature* 503, 481–486. doi:10.1038/nature12804.

Ostrowski, A., Mehert, A., Prescott, A., Kiley, T. B., and Stanley-Wall, N. R. (2011). YuaB functions synergistically with the exopolysaccharide and TasA amyloid fibers to allow biofilm formation by *Bacillus subtilis*. *J Bacteriol* 193, 4821–4831. doi:10.1128/JB.00223-11.

Pamp, S. J., Sternberg, C., and Tolker-Nielsen, T. (2009). Insight into the microbial multicellular lifestyle via flow-cell technology and confocal microscopy. *Cytometry A* 75, 90–103. doi:10.1002/cyto.a.20685.

Pandin, C., Le Coq, D., Canette, A., Aymerich, S., and Briandet, R. (2017). Should the biofilm mode of life be taken into consideration for microbial biocontrol agents? *Microb Biotechnol* 10, 719–734. doi:10.1111/1751-7915.12693.

Piggot, P. J., and Hilbert, D. W. (2004). Sporulation of *Bacillus subtilis*. *Curr Opin Microbiol* 7, 579–586. doi:10.1016/j.mib.2004.10.001.

Rath, H., Sappa, P. K., Hoffmann, T., Salazar, M. G., Reder, A., Steil, L., *et al.* (2020). Impact of high salinity and the compatible solute glycine betaine on gene expression of *Bacillus subtilis*. *Environ. Microbiol.* 22, 3266-3286. doi:org/10.1111/1462-2920.15087

Romero, D., Aguilar, C., Losick, R., and Kolter, R. (2010). Amyloid fibers provide structural integrity to *Bacillus subtilis* biofilms. *Proc Natl Acad Sci U S A* 107, 2230–2234. doi:10.1073/pnas.0910560107.

Roux, D., Cywes-Bentley, C., Zhang, Y.-F., Pons, S., Konkol, M., Kearns, D. B., et al. (2015). Identification of Poly-N-acetylglucosamine as a Major Polysaccharide Component of the *Bacillus subtilis* Biofilm Matrix. *J Biol Chem* 290, 19261–19272. doi:10.1074/jbc.M115.648709.

Rühl, M., Le Coq, D., Aymerich, S., and Sauer, U. (2012). 13C-flux analysis reveals NADPH-balancing transhydrogenation cycles in stationary phase of nitrogen-starving *Bacillus subtilis*. *Journal of Biological Chemistry* 287, 27959–27970. doi:10.1074/jbc.M112.366492.

Rumbaugh, K. P., and Sauer, K. (2020). Biofilm dispersion. *Nat Rev Microbiol* 18, 571–586. doi:10.1038/s41579-020-0385-0.

Sachla, A. J., Luo, Y., and Helmann, J. D. (2021). Manganese impairs the QoxABCD terminal oxidase leading to respiration-associated toxicity. *Mol Microbiol*. doi:10.1111/mmi.14767.

Sanchez-Vizuete, P., Le Coq, D., Bridier, A., Herry, J.-M., Aymerich, S., and Briandet, R. (2015). Identification of *ypqP* as a New *Bacillus subtilis* biofilm determinant that mediates the protection of Staphylococcus aureus against antimicrobial agents in mixed-species communities. *Appl Environ Microbiol* 81, 109–118. doi:10.1128/AEM.02473-14.

Schyns, G., Serra, C. R., Lapointe, T., Pereira-Leal, J. B., Potot, S., Fickers, P., et al. (2013). Genome of a Gut Strain of *Bacillus subtilis*. *Genome Announc* 1, e00184-12. doi:10.1128/genomeA.00184-12.

Terra, R., Stanley-Wall, N. R., Cao, G., and Lazazzera, B. A. (2012). Identification of *Bacillus subtilis* SipW as a bifunctional signal peptidase that controls surface-adhered biofilm formation. *J Bacteriol* 194, 2781–2790. doi:10.1128/JB.06780-11.

Thormann, K. M., Saville, R. M., Shukla, S., and Spormann, A. M. (2005). Induction of rapid detachment in Shewanella oneidensis MR-1 biofilms. *J Bacteriol* 187, 1014–1021. doi:10.1128/JB.187.3.1014-1021.2005.

Vlamakis, H., Chai, Y., Beauregard, P., Losick, R., and Kolter, R. (2013). Sticking together: building a biofilm the *Bacillus subtilis* way. *Nat Rev Microbiol* 11, 157–168. doi:10.1038/nrmicro2960.

Warraich, A. A., Mohammed, A. R., Perrie, Y., Hussain, M., Gibson, H., and Rahman, A. (2020). Evaluation of anti-biofilm activity of acidic amino acids and synergy with ciprofloxacin on *Staphylococcus aureus* biofilms. *Sci Rep* 10, 9021. doi:10.1038/s41598-020-66082-x.

SUPPLEMENTARY MATERIAL

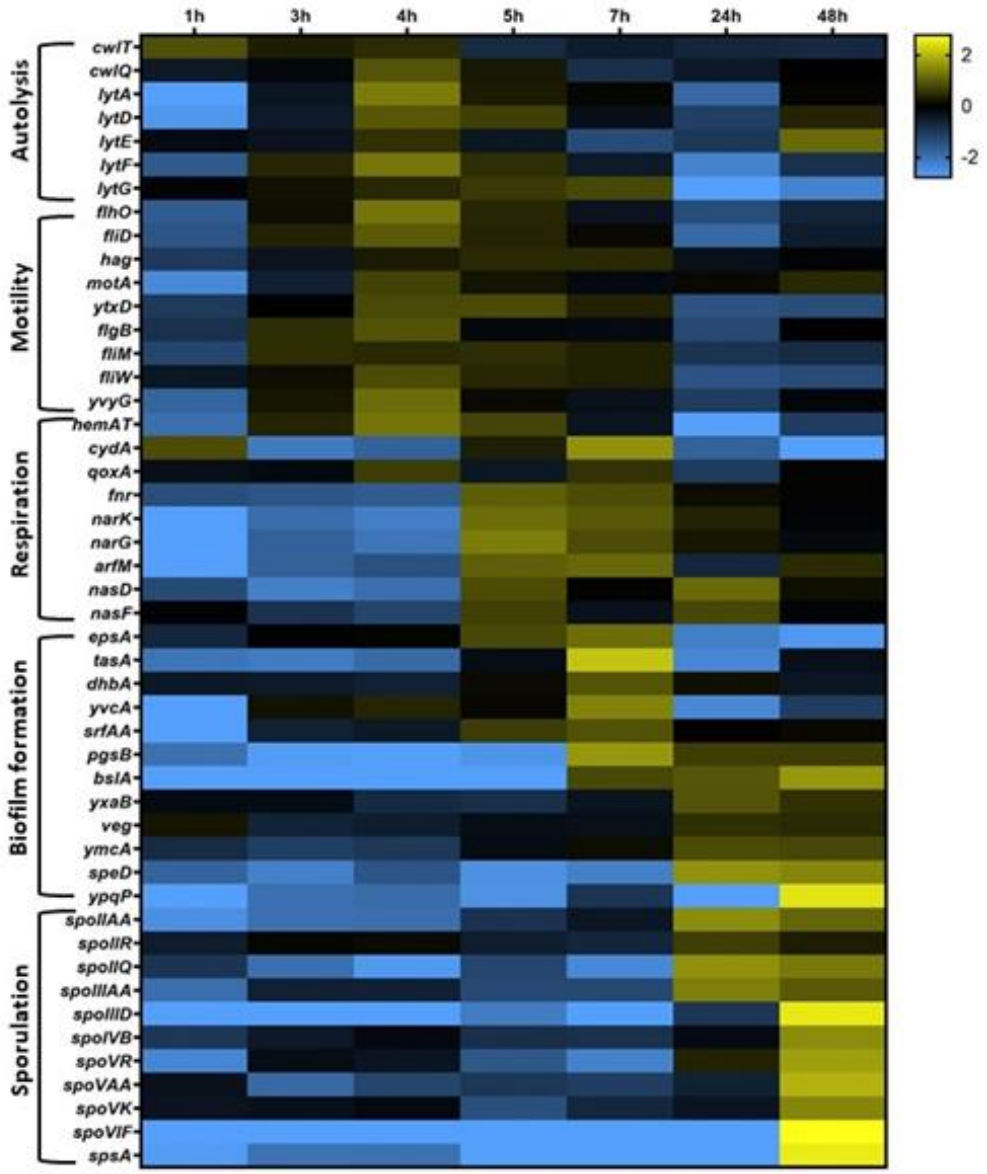

Fig. S1 Temporal tiling array transcriptome of *Bacillus subtilis* NDmed colonizing microplate wells. All the biomass from the wells was collected for the transcriptome analysis after 1, 3, 4, 5, 7, 24, and 48h. A log2 fold change (log2FC) of expression was calculated for the genes from the ratio of expression over the average of expression across all temporal samples. The heatmap elaborated using GraphPad Prism 8 software (Graphpad, CA, USA) displays data for 48 genes selected from *Subtiwiki* categories (http://subtiwiki.uni-goettingen.de/), as representatives for the different functional categories. The yellow and the blue represent respectively an upregulation or a downregulation of a gene compared to its average expression over the time course, with a scale adjusted to a log2FC of +/-2.8. Full dataset of the tiling array is available in the **Supplementary Data S1**.

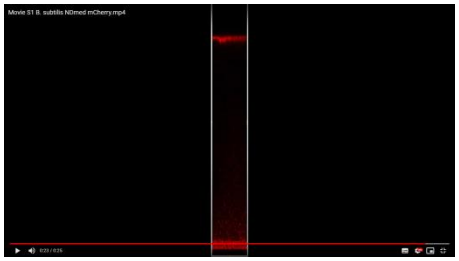

Movie S1: Visualisation of the interplay between *B. subtilis* NDmed-mCherry submerged biofilm and pellicle formation in a well of microplate (1 image every hour for 24h, each image 1.5 x 1.5 mm)

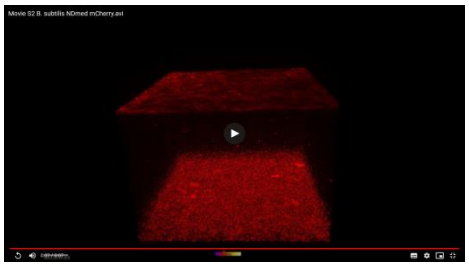

Movie S2: 4D-CLSM of *B. subtilis* NDmed-mCherry submerged biofilm and pellicle formation in a microplate (1 image every hour for 14 hours, Imaris 3D projection representation, each image 246 x 246 µm).

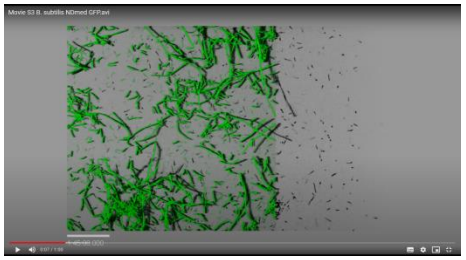

Movie S3: 4D-CLSM of *B. subtilis* NDmed-GFP submerged biofilm (1 image every 15 min for 15 hours, Imaris Easy 3D projection representation, each image 246 x 246 µm).

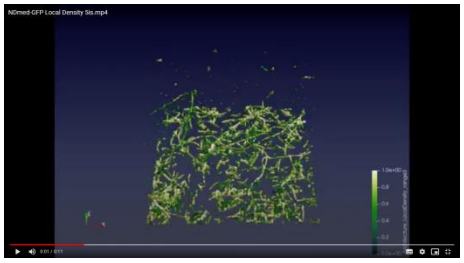

Movie S4: *B. subtilis* NDmed-GFP submerged biofilm dynamic with a local density color code (BiofilmQ) (1 image every 15 min for 15 hours, each image 246 x 246 µm).

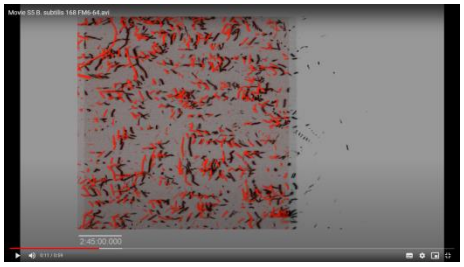

Movie S5. 4D-CLSM of *B. subtilis* 168 labelled with the red membrane vital dye FM4-64 (1 image every 15 min for 15 hours, each image 246 x 246 µm).

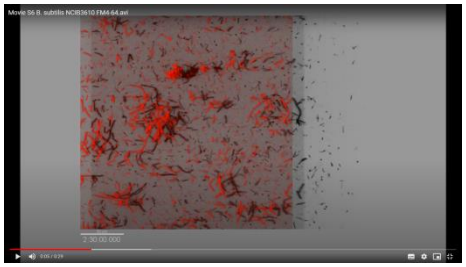

Movie S6. *B. subtilis* NCIB3610 labelled with the red membrane vital dye FM4-64 (1 image every 15 min for 15 hours, each image 246 x 246 µm).

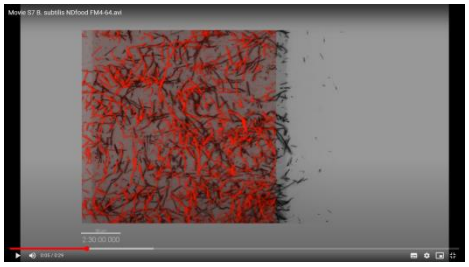

Movie S7. *B. subtilis* NDfood labelled with the red membrane vital dye FM4-64 (1 image every 15 min for 15 hours, each image 246 x 246 µm).

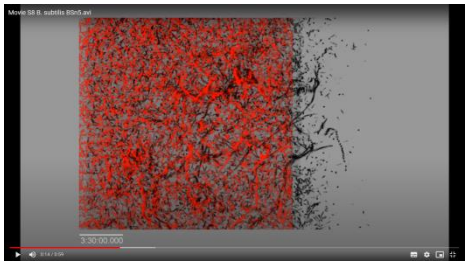

Movie S8. *B. subtilis* BsN5 labelled with the red membrane vital dye FM4-64 (1 image every 15 min for 15 hours, each image 246 x 246 µm).

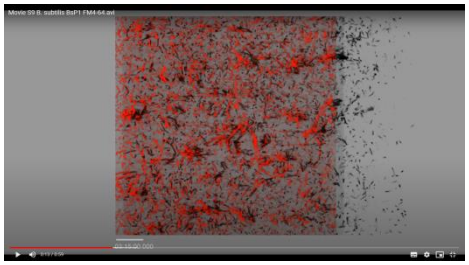

Movie S9. *B. subtilis* BsP1 labelled with the red membrane vital dye FM4-64 (1 image every 15 min for 15 hours, each image 246 x 246 µm).

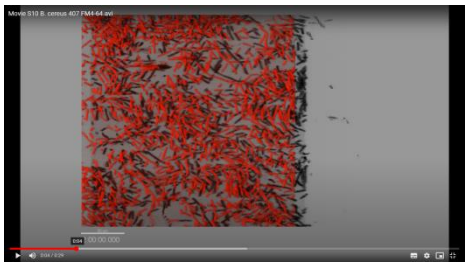

Movie S10. *B.cereus* 407 labelled with the red membrane vital dye FM4-64 (1 image every 15 min for 15 hours, each image 246 x 246 µm).

Movie S11. *B. licheniformis* LMG7559 labelled with the red membrane vital dye FM4-64 (1 image every 15 min for 15 hours, each image 246 x 246 µm).

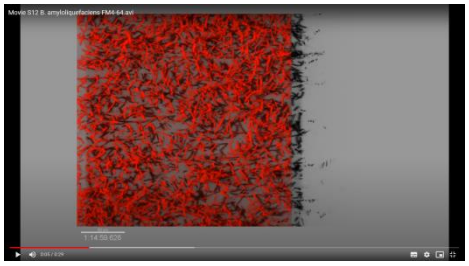

Movie S12. *B. amyloliquefaciens* 20P6 labelled with the red membrane vital dye FM4-64 (1 image every 15 min for 7 hours, each image 246 x 246 µm).

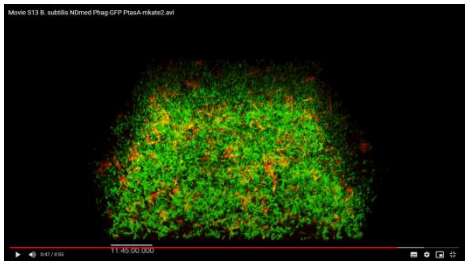

Movie S13 4D-CLSM of submerged biofilm of *B. subtilis* NDmed547 *[Phag-GFP PtapA-mkate2]* reporting the expression of *hag* (motility) in green and the expression of *tapA* (matrix) in red. (1 image every 15 min for 15 hours, Imaris 3D projection, each image 246 x 246 µm).

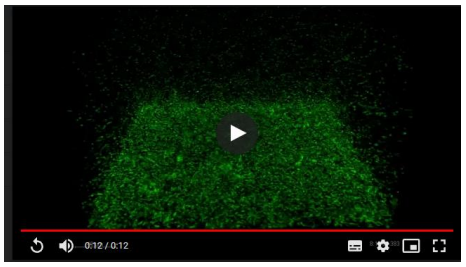

Movie S14 4D-CLSM of submerged biofilm of *B. subtilis* NDmed GM3361 *[Pfnr-gfpmut3]* reporting the expression of *fnr* (anaerobiosis). (1 image every 15 min for 15 hours, each image 246 x 246 µm).

Chapter 3. "Multi-scale spatial transcriptome unveils the heterogeneity between subpopulations of *Bacillus subtilis* surface-associated communities"

This contribution is the first description of spatial transcriptomic profiles for 9 subpopulations of B. subtilis captured in liquid, semi-solid and solid medium with the same strain and the same growth medium. This analysis allowed us to define the specificities of i) cells from the different laboratory biofilm models for B. subtilis (colony, floating pellicle and submerged biofilms); ii) cell physiologies of free cells depending on their history. Taking advantage of the global RNAseq analysis, we could select a subset of genes of interest and fluorescently report their expression in situ. This reveals unexpected spatio-temporal patterns of gene expression and the importance of successive waves of death cells in the system dynamic.

The work presented in this chapter reflects the core of my PhD project. It was the first time for the team to perform RNAseq on biofilm subpopulations, and it took me around 9 months the first year to develop a reproducible protocol to capture the biofilm subpopulations and to extract RNA of the requested quality. It took me an extra year to analyse the huge quantity of data (9 biological samples x 3 independent replicates) with the help of Pierre Nicolas, INRAE specialist of such large scale transcriptomic dataset. In parallel, I also constructed the fluorescent transcriptional fusions, and we could take advantage of a fantastic image analysis software BiofilmQ, released this year by the lab of Knut Descher which allowed us to synthesise a 48h 3D+time CLSM movie in a comprehensive kymograph. Once published, this paper will be the "signature" paper of my PhD.

"Multi-scale spatial transcriptome unveils the heterogeneity between subpopulations of *Bacillus subtilis* surface-associated communities"

(Paper 3)

Yasmine Dergham[1, 2], Dominique Le Coq[1, 3], Pierre Nicolas[4], Julien Deschamps[1], Eugénie Huillet[1], Pilar Sanchez-Vizuete[1], Kassem Hamze[2], Romain Briandet[1]

[1] Université Paris-Saclay, INRAE, AgroParisTech, Micalis Institute, 78350 Jouy-en-Josas, France. yasmin.dorghamova-dergham@inrae.fr (Y.D.); julien.deschamps@inrae.fr (J.D.); eugenie.huillet@inrae.fr (E.H.); pilarsanviz@gmail.com (P.S.V.)

[2] Faculty of Science, Lebanese University, 1003 Beirut, Lebanon. kassem.hamze@ul.edu.lb

[3] Université Paris-Saclay, Centre National de la Recherche Scientifique (CNRS), INRAE, AgroParisTech, Micalis Institute, 78350 Jouy-en-Josas, France. dominique.le-coq@inrae.fr (D.L.C.)

[4] Université Paris-Saclay, INRAE, MAIAGE, 78350 Jouy-en-Josas, France. pierre.nicolas@inrae.fr (P.N.)

Keywords: *Bacillus subtilis*, biofilm, swarming, transcriptome, CLSM (confocal laser scanning microscopy), fluorescent transcriptional fusions, heterogeneity.

ABSTRACT

Many bacterial species adapt to the environmental fluctuations by forming multicellular heterogeneous communities surrounded by a complex matrix of exopolymeric substances which are collectively referred to as biofilms. Over the last decades, *Bacillus subtilis*, a Gram-positive bacterium, has been extensively used as a model for molecular studies on biofilm formation. These studies encompassed the development of complex macro-colonies on either solid or semi-solid agar, the formation of pellicles at the air-liquid interface, and lately the formation of submerged architectural biofilms at the solid-liquid interface. Beside similarities, these multicellular communities also display considerable differences at the structural, chemical and biological heterogeneity levels. In this study, we used RNA-seq to analyze nine different spatio-physiological conditions, including the three biofilm models (colony, pellicle, and submerged). The transcriptome data give a global landscape characterization of gene expression profiles for each of the differently localized selected populations, from which we have selected and transcriptionally reported genes involved in the different physiological states found in the heterogeneous biofilms. By confocal laser scanning microscopy, we were able to visualize *in situ* gene expression at a cell level and its correlation with the RNA-seq results. Furthermore, a temporal scale (4D-CLSM) observation of the submerged model showed spatio-temporal expression patterns of genes (i.e., *epsA-O*, *tapA*, *bslA*, *srfAA*, *ypqP*, *capE*, *hag*, *ctaA*, *narG-I*, *ackA*, *aprE*, *comGA*, *skfA*, *spoIIGA*, *spoVC*) required for the various cellular differentiations during biofilm development.

INTRODUCTION

Biofilms are extremely complex multicellular communities, on the structural and dynamical level, enveloped in a self-produced extracellular matrix [1]. In a biofilm, bacteria respond differently to local chemical environmental conditions (*i.e.* concentration gradient of nutrient, oxygen, waste products and bacterial-signalling compounds), leading to physiological heterogeneity [2]. The microscale gradient of these chemical heterogeneities depends on the biofilm type. For instance, mature submerged biofilms typically have declining oxygen and nutrient concentration along with the biofilm depth. In contrast, the metabolic products are more

concentrated in the core of the biofilm than on the interface with the medium. Hence, as the biofilm develops, bacteria have to adapt to these local environmental changes resulting in subpopulations of cells with considerable structural, biological and chemical heterogeneity over spatial and temporal scales [2]. Understanding how these surface-bound communities are formed and interact is crucial for the development of suitable strategies for their control.

Bacillus subtilis has long served as a model organism for genetic studies on the formation of different types of biofilms [3]–[6]. *B. subtilis* is a Gram-positive, motile, spore-forming ubiquitous bacterium frequently found in the rhizosphere in close proximity to plants, but also in the gastrointestinal tract (GI) [7]–[9]. It is commercially used to produce proteins and fermented food products (*i.e.* Japanese natto [10]), and also as a biocontrol agent [11] or probiotic [12]–[14]. On the other hand, an undomesticated *B. subtilis* strain (NDmed), isolated from a hospital endoscope washer-disinfector, was found to form a striking biofilm structure that is able to resist to the action of oxidizing agents, such as peracetic acid used for endoscopes disinfection, and to protect pathogenic bacteria such as *Staphylococcus aureus* in mixed-species biofilms [15], [16]. Thus, in an ever-changing environment, *B. subtilis* develops different adaptation strategies to survive including motility, sporulation, as well as induction of other stress responses [17]–[19]. These cell-level adaptations are often accompanied by the formation of surface communities associated with matrix production [1]. In the laboratory, *B. subtilis* biofilm studies were typically based on the development of a pellicle at the liquid-air interface, on a submerged biofilm at the solid-liquid interface, and on the development of complex macro-colony at the solid-air interface [4], [5], [20]. In specific conditions, such as on a semi-solid surface, *B. subtilis* cells forming the colony can become highly motile and swarm over the surface by an organized, reproducible and collective movement while proliferating and consuming nutrients [21]. On a synthetic minimal medium, *B. subtilis* swarms from a multilayered colony in a branched, monolayer, dendritic pattern that continues to grow up to 1.5 cm from the swarm front. A transition from monolayer swarm to a multilayered biofilm occurs in response to environmental cues, which could be simply a physical barrier [22]–[26]. In these contributions, comparative phenotypic studies of *B. subtilis* NDmed strain have shown to display highly structured 3D structures and swarms rather efficiently when compared to the *B. subtilis* reference strains NCIB3610 and 168 [4], [6], [27].

An axenic culture of *B. subtilis* forming a biofilm contains different cell phenotypes, at least seven different cell types have been described: motile, surfactin producers, matrix producers, protease producers, cannibal, competent and spore forming [1], [19], [28], [29]. Motile *B. subtilis* cells have the ability to either swim in liquid culture or swarm over an agar semi-solid surface by means of flagella, partly encoded by the large *fla/che* operon that contains also *sigD* and genes involved in chemotaxis [30]. Surfactin is a surfactant intervening in several biological activities, *i.e.* reducing water surface tension, contributing to the genetic competence, and triggering matrix production [5], [31]–[33]. Extracellular matrix-producers secrete an exopolysaccharide (EPS) and an amyloid fiber protein (TasA), synthesized by the product of the 15-gene *epsA-O* operon and encoded by the *tapA-sipW-tasA* operon, respectively [5]. The small BslA secreted protein operates in cooperation with both the EPS and TasA during biofilm formation matrix assembly. BslA also serves as the hydrophobin-like protein which provides the aerial interface of a biofilm with a hydrophobic layer preventing its disruption by wetting agents [34]–[36]. Protease-producers secreting extracellular proteases, such as subtilisin encoded by *aprE*, can degrade proteins present in the environment or released from the dead cells [37]. Under stress conditions such as nutrient depletion, *B. subtilis* cells produce bacteriocins, *i.e.* sporulation-killing factor and sporulation-delaying proteins encoded by the *skfA-H* and *sdpABC* operons, respectively. These toxic proteins aim to cause a reduction in the number of susceptible viable cells (which do not produce Spo0A) [38]. The alive cells can then cannibalize sister cells and use them as a nutrient source. Competent cells, representing a minor subpopulation of cells during the transition to stationary phase, cease their growth ability to become capable of taking exogenous DNA from the extracellular medium [19], [30], [39]. Both of the later physiological cell states, cannibalism and competence, delay the entry into the irreversible sporulation process that leads to the formation of the highly stress-resistant spore [19]. This heterogeneity in the biofilm population is a need to adapt for the environmental fluctuations, permitted by the division of labor between different cell types expressing different metabolic pathways, migration over a solid surface seeking for nutrient source, or sharing public goods with a minimal cost of energy [19], [40]. Therefore, genetically identical cells growing in biofilms are not only physiologically distinct from planktonic cells, but also differ from each other both spatially and temporally.

Temporal transcriptional analysis has been used to follow the developmental strategies that *B. subtilis* undergo to form a complex biofilm. Pisithkul *et al.* [41] performed an analysis of the metabolic changes over a temporal scale on the *B. subtilis* pellicle formation and its development by using the metabolomic, transcriptomic, and proteomic measurements. All these measurements have indicated that metabolic remodeling during biofilm development is largely controlled at the transcriptional level [41]. Recently, the ontogeny of a growing *B. subtilis* macrocolony on agar has been shown to be correlated with the evolutionary measures by recapitulating the phylogeny at the expression level [42]. More recently, we have performed a transcriptional study for the *B. subtilis* NDmed, in which a whole static liquid culture in a microplate well was collected on a temporal scale [43]. The results contributed to identify genetic profiles related to the submerged biofilm development, followed by the pellicle development at the liquid-air interface after several hours of incubation [43], to end up by at least three different populations in the liquid culture after 24 hours of incubation.

In this study, transcriptional spatial analysis has been used in order to identify genes that are specifically expressed in different localized biofilm populations, on solid, semi-solid or liquid surfaces. RNA-seq for the different populations has been performed at a mesoscopic scale, and transcriptome analysis results have provided a global landscape characterization of gene expression for each of the differently localized selected populations. A deeper comparison between the transcriptome profiles of the spatially localized biofilm models and their adjacent compartments allowed us to select and fluorescently report for 3D imaging differentially expressed genes, including *epsA-O, tapA, bslA, srfAA, ypqP, capE, hag, ctaA, narG-I, ackA, aprE, comGA, skfA, spoIIGA, spoVC*. Furthermore, taking advantage of 4D-CLSM, we monitored these genes over time to get access to single cell scale dynamics in the submerged biofilm model.

RESULTS

RNA sequencing show spatially resolved populations with distinct patterns of gene expression

RNA-seq was used to compare transcription between different biofilm models formed by the *B. subtilis* NDmed, a strain in close proximity (less than 100 SNPs) to the reference 168 strain [44]. All selected compartments are summarized in Figure 1. We have considered a 24 hour static

liquid culture where we have collected separately the submerged biofilm (SB) formed on the solid-liquid interface, the floating pellicle (PL) at the liquid-air interface, and the free detached cells (DC) inhabitant between the submerged and the pellicle. In addition, we have collected separately from a 24 hour semi-solid swarming plate four differently localized populations, (i) the mother colony (MC) is the original colony from which the swarm migrates, (ii) the base (BS) of the dendrite in the early biofilm form, (iii) the dendrites (DT) as monolayer cells ready to start producing matrix to form later the biofilm, and (iv) the tips (TP) that are the motile and highly dividing cells. As references, we have collected from a liquid planktonic culture the exponential (EX) and the stationary (ST) phase, the latter being used as an inoculum to initiate the different biofilm models (liquid and swarming, all being cultured with the same growth medium). For each compartment, three independent samples were taken as biological replicates (experimental setup described in detail in the Materials and Methods part).

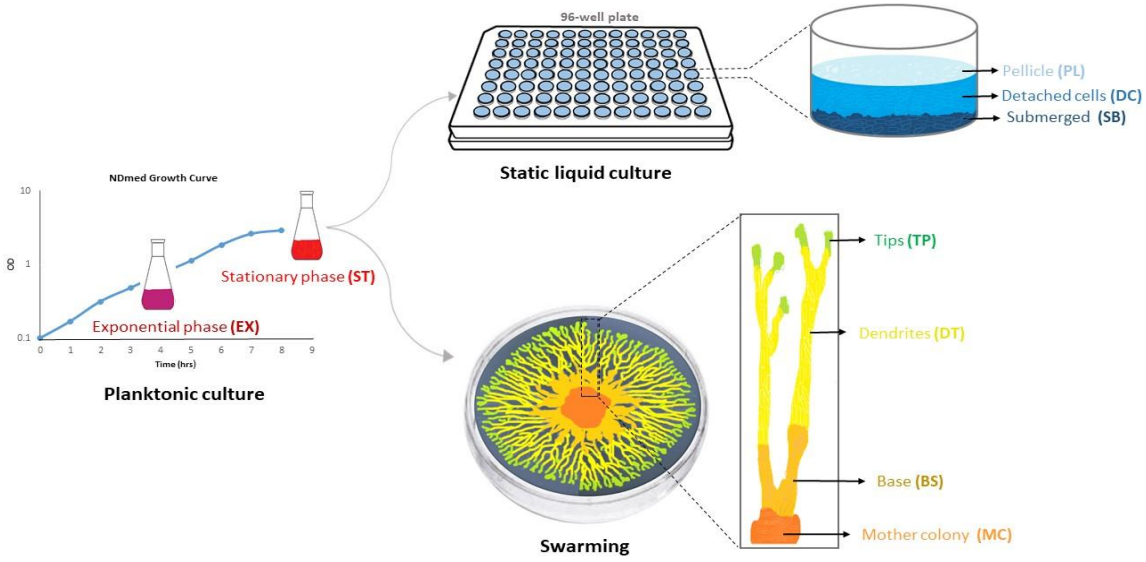

Figure 1: Schematic drawing for the different localized spatial selected compartments. *From the planktonic culture, the exponential (EX) and the stationary (ST) phase were selected. The culture in the stationary phase was used to inoculate the two models, the liquid static culture in a well of microplate and the swarming plate on semi-solid agar, which were incubated at 30°C for 24 hours. From the liquid model, the pellicle (PL), the detached cells (DC) and the submerged biofilm (SB) were collected separately. From the semi-solid medium swarming plate, four localized compartments were captured separately, each corresponding to a different physiological state from its adjacent ones, the mother colony (MC, the inoculation site from which the swarm has developed), the base (BS), the dendrites (DT), and the tips (TP).*

To assess the quality and reproducibility of the RNA dataset obtained, a hierarchical clustering analysis for the different samples was performed (Figure 2a). This clustering analysis clearly shows that the cell transcriptomic profiles within the different spatial compartments are quite distinct from each other with the three biological replicates being mostly grouped together. Exception is for the adjacent swarming compartments, where the three samples of the dendrites are clustered with either the base or the tips. This could be due to technical issues, essentially the difficulty to clearly differentiate the limit between these adjacent compartments, and/or the physiology of the cells in the dendrites that could be very similar to that of the base and the tips. Figure 2a, emphasises the closeness in the RNA-seq profile of the three spatial compartments of the static liquid culture (SB, DC and PL). Moreover, this clustering shows how the adjacent swarming compartments (BS, DT and TP) are very close to each other, and also share a very close genetic profile with the exponential phase. Interestingly, both of the mother colony (MC) and the stationary phase (ST) are not only very distinct from each other but also from all the other selected compartments.

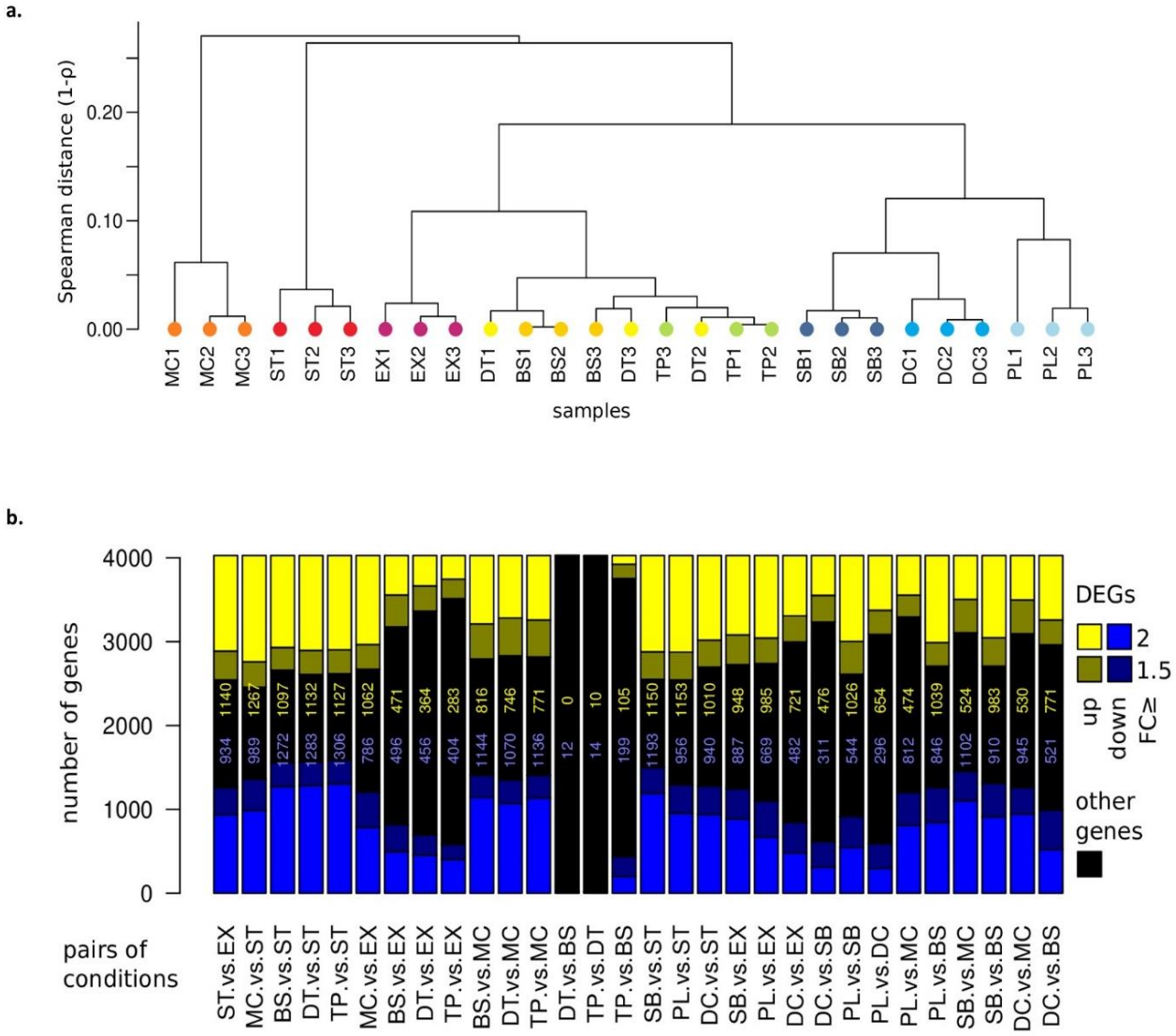

Figure 2: Evaluation of the RNA-seq data followed by differentially expressed genes (DEGs) comparisons across the different selected samples of B. subtilis. *(a) Pairwise distance (Spearman) between RNA-seq profiles are summarized by a hierarchical clustering tree. (b) Out of 4028 genes, the numbers of DEGs in pairwise comparison of different B. subtilis spatial compartments (q-value≤0.05, | Log2FC≥1) are reported in yellow (up-regulated) and in blue (down-regulated).*

To identify deeply the physiology of the cells, a differentially expressed genes (DEGs) analysis has been performed for the different localized populations selected. This DEG analysis allowed the identification of a number of genes statistically upregulated (yellow) or downregulated (blue) in a condition as compared to another taken as a reference (Figure 2b). For instance, comparing the stationary phase to the exponential one (ST vs. EX) shows that 1140 and 934 genes

are significantly upregulated and downregulated with a minimum Log2FC, respectively. At the stationary phase several physiological changes take place, involving complex interconnected regulatory networks. Comparing the stationary phase to the exponential one (ST vs. EX) shows 1140 genes upregulated, among which around 36% related to sporulation, biofilm formation (*tasA operon*, *epsA-O*, as well as *bslA*), coping with stress, or carbon metabolism, and 30% to other minor functions; the remaining (approximately 34%) are of unknown function, e.g. *ydhF*, *ywcI*, *yycP*, *yjdB*, *yycO*, and *yycQ* which show the highest upregulation, all above 7log2FC. Although genetic and physiological studies have been able to decipher some different regulatory pathways taking place, much remains unknown [45], [46].

As for the adjacent spatially selected compartments in the swarming model, the DEG analysis shows that 12 genes are downregulated in the dendrites compared to the base (DT vs. BS). Moreover, 14 genes were downregulated and 10 genes were upregulated in the tips compared to the dendrites (TP vs DT). Interestingly, even though between very close compartments only a few genes display some differential changes, 105 genes are upregulated in the tips compared to the base (TP vs. BS) and 199 genes are downregulated. For the liquid culture, 654 genes are upregulated and 296 are downregulated in the pellicle compared to the detached cells (PL vs. DC). Moreover, 476 genes are upregulated and 311 genes downregulated in the detached cells compared to the submerged (DC vs SB). To better visualize the genetic expression level among the adjacent compartments and to highlight the different functional categories encoded by the differentially expressed genes on a spatial level, models were analyzed sequentially.

A retrospective view on the adjacent spatial compartments of a swarm shows differential gene expression

Swarming of *B. subtilis* on a semi-solid medium is a sequential process where cells cooperatively move in a coordinated way before the transition to a biofilm upon the exposure to any stress, which could be either chemical or physical [274]. A careful examination of global transcription in the swarming model would allow us to better understand the sequential gene regulations occurring through surface colonization to biofilm formation. From the 4028 genes of the *B. subtilis* NDmed, 2371 genes are differentially expressed between the four localized

compartments of a swarm and grouped according to the similarity of their gene expression, represented as a heatmap in Figure 3a. There are 47 groups of genes differentially expressed within the swarming model (GS1 to GS47) (supplementary data **S1**). Figure 3b, represents a functional category percentage of the 2371 genes across the different conditions of a swarm.

GS1 is a large group of genes (1082) highly expressed in the mother colony and repressed through the swarm (Figure 3a), corresponding to the different functions occurring at the same time in this biofilm model. Approximately 80% of the known genes are related to the functional group of the 'Electron transport and ATP synthesis' from which 22 out of 33 are genes encoding functions related to respiration *i.e. fnr, arfM, narG-I, cydBCD, nasD, cccA, qcrABC, ccdA, ctaC-G,* and *ythAB* with a significant upregulation of minimum Log2FC in the mother colony compared to the base (supplementary data **S1**). Moreover, 222 genes encode other metabolic pathways related to carbon metabolism (*i.e. yjmCDF* with 8Log2FC upregulated in the MC compared to the BS, *acoAB* with a 7Log2FC, *licABCH* with a 4Log2FC, *gapB* with a 4Log2FC, *pckA* with a 3Log2FC, *alsDS* with a 2Log2FC), lipid metabolism (*fadA-R* with a 4Log2FC), nucleotide metabolism (*pucH* with a 3Log2FC), miscellaneous metabolic pathways (*glgA* with a 5Log2FC and *ntdABC* with a 7Log2FC), and nitrogen metabolism (*mmgA-F* with approximately 6Log2FC), and genes related to coping with stress (e.g. 5Log2FC for *skfA* and a 6Log2FC for *oxdC*). Sporulation is the function that is majorly differentially expressed in this group by 98%, for example, 5Log2FC for both *spoIIGA* and *spoVD*, 2Log2FC for *ypqP*, upregulated in the mother colony compared to the base.

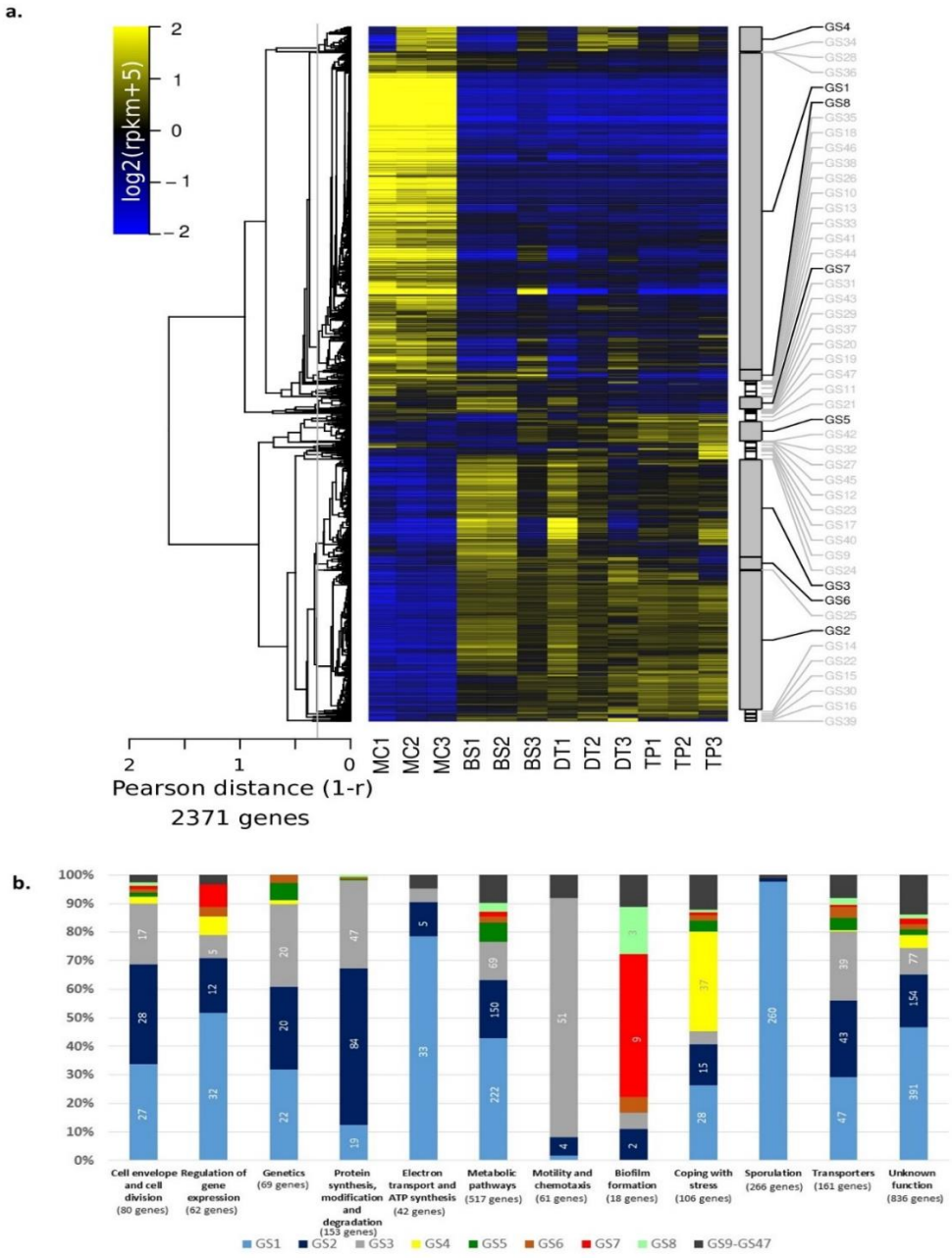

Figure 3: Transcriptome remodeling of differentially expressed genes during swarming. *(a) Heatmap representation of the relative variations of expression level across samples for DEGs (2371) identified in the 6 pairwise comparisons of 4 different localizations (MC, BS, DT, TP). The color code reflects the comparison to the mean computed for each gene across the 12 samples (log2 ratio). The hierarchical clustering tree shown on the left side of the heatmap (average link) was cut at average Pearson correlation of 0.7 (vertical gray line) to define the expression clusters shown on the right side of the heatmap. Clusters were named (from GS1 to GS59) by decreasing*

sizes and those containing more than 30 genes are highlighted (name printed in black). (b) Distribution into expression clusters for genes in Subtiwiki-derived functional categories.

The heatmap (Figure 4a) shows an upregulation in both the mother colony and the base in both swarming groups, GS7 and GS8. These groups contain many genes involved in biofilm formation (Figure 4b). Genes of the *eps* operon (*epsF-N)* and *slrR* are in GS7, the *tapA* operon (*tapA-sipW-tasA*) is in GS8, and all are significantly downregulated by Log2FC in the tips compared to the base (TP vs. BS). A comparison between the tips and the mother colony (TP vs MC) shows a slight downregulation of the *eps* and *slrR* genes (less than a Log2FC), however, the *tasA* operon is downregulated by approximately 1.5Log2FC. No significant difference in gene expression is observed between the adjacent compartments of a swarm (through the different comparisons BS vs. MS, DT vs. BS, or TP vs DT; supplementary data **S1**). Genes related to motility and chemotaxis present in GS3 and GS2 (representing 90% of this functional category) are downregulated in the mother colony and upregulated during the swarm. The *fla/che* operon is upregulated by 2Log2FC, in which the *hag* gene is the highest differentially expressed by 5Log2FC in the tips compared to the mother colony (Tp vs. MC). Several genes poorly characterized or totally unknown like *ywdK, yhoC, yuzM, yodT, yqfX,* or *ydgB* are highly expressed (more than 7Log2FC) in the mother colony compared to the swarm, while on the other hand, *ylxF, yscB,* and *yxkC* are expressed with a 3Log2FC in the swarming compartments compared to the mother colony. An upregulation by 4Log2FC is observed for the *ydgGH* (probable) operon in the tips compared to the other swarming compartments (supplementary data **S1**).

Comparison between adjacent compartments of a swarm, highlights some genes that are differentially expressed (Figure 2b). Between the base and the mother colony (BS vs MC) there are 815 genes upregulated and 1140 genes downregulated, most of which have been described in the GS1. In the dendrites, 12 genes are downregulated compared to the base (DT vs BS), *ppsD-E, rpsNB, yxeG, yrpE, folEB-yciB* and the *znuACB* and *pftAB* operons. In addition, 14 genes are downregulated (*veg, ykoY, ydzJ, spoVS, yydF, sspF, yqzM, tRNA-Met, tRNA-Thr, tRNA- Ser, tRNA-Asp, tRNA-Val, and 2 genes tRNA-Arg*) and 10 upregulated (*tRNA-His, ytbE, ytbD, rbsD, melE, melR, ldh, cydA, ydgH and ydgG*) in the tips when compared to the dendrites (TP vs. DT). The *ycdA* gene, encoding a lipoprotein required for swarming motility, shows gradual upregulation by

a Log2FC from one localized compartment to its adjacent one going from the mother colony to the tips.

Half of the genome is differentially expressed between the floating pellicle and the submerged biofilms coexisting in the same microplate well

Biofilm formation by NDmed has been shown to be a sequential process. In the first few hours the submerged biofilm is formed, followed by the pellicle formation at the air-liquid interface after a few hours of culture, to end up by two different biofilm populations in the same model [43]. In this study, we have separately collected the submerged (SB), the pellicle (PL) as well as the detached cells (DC), a compartment between the SB and PL. From the 4028 genes, 1916 are differentially expressed between the three localized compartments clustered by 26 groups (GL1 to GL26) with functional category percentage, represented in Figure 4.

Groups GL6, GL9 and GL8 (Figure 4a) shows an upregulation in the gene expression profile for the detached cells compared to the pellicle and the submerged. Classification by functional categories (Figure 4b) shows that 85 % of the motility and chemotaxis genes are in group GL9. This group contains genes of the *fla/che* operon and *hag*, the latter showing an upregulation by approximately 3Log2FC and 1.5Log2FC in the detached cells compared to the submerged and the pellicle, respectively. Interestingly, belonging to the *fla/che* operon in GL9, *swrD* encodes a swarming protein (SwrD) used to promote flagellar power [47]. The *swrD* gene is the highest downregulated gene in the pellicle compared to the detached cells by a 2Log2FC (PL vs. DC), which means it is a gene highly upregulated in the detached cells compared to the pellicle. This could suggest that the liquid culture is rather viscous, requiring a swarming-like process to efficiently migrate in the liquid column.

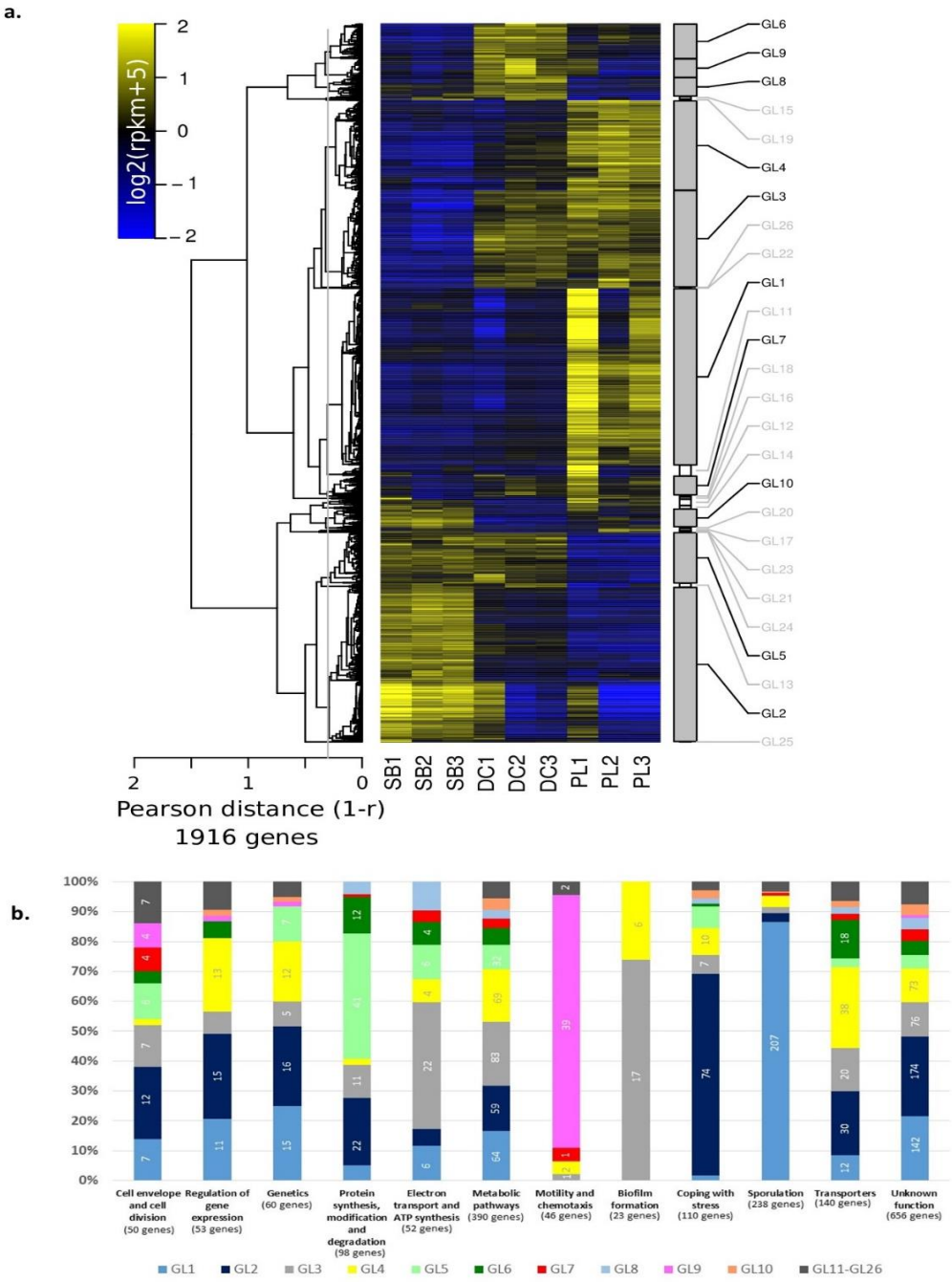

Figure 4: Transcriptome remodeling of differentially localized compartments in a static liquid culture. *(a) Heatmap representation of the relative variations of expression level across samples for DEGs (1916) identified in the 3 pairwise comparisons of 3 different localizations (SB, DC, PL). Clusters were named (from GL1 to GL26) by decreasing sizes and those containing more than 30 genes are highlighted. (b) Distribution into expression clusters for genes in Subtiwiki-derived functional categories.*

GL3 and GL4 groups contain most of the already known genes involved in biofilm formation (Figure 4b), which are upregulated mainly in the pellicle (PL) and partially in the detached cells (DC) (Figure 4a). Biofilm genes in these groups are the *tapA* and *epsA-O* operons, *dhbACB*, *slrR*, *sinI*, *bslA*, and *spo0A* (supplementary data **S1**). Comparison between the matrix genes for the two biofilm populations after 24 hours for the liquid model indicates that the *tapA* operon is upregulated by 4Log2FC, the *epsA-O* operon by approximately 3Log2FC, and the *bslA* by a Log2FC in the pellicle compared to the submerged (PL vs SB). As for the regulators encoding genes in this group, *slrR* and *sinI* show an upregulation by 2LogFC and *spo0A* by a Log2FC in the pellicle compared to the submerged. Sporulation genes, of which about 87% are present in GL1 (Figure 4), show a higher upregulation in the pellicle compared to the other two populations present, detached and submerged, like the *cge*, *cot*, *cwl*, *spoII*, *spoIII* , *spoIV*, *spoV* operons and genes (supplementary data **S1**). The most highly expressed genes in the pellicle compared to the submerged (PL vs. SB) by around 3Log2FC, are *ysxE*, *spoVID*, *spoIVA*, as those compared to the detached cells (PL vs. DC) are *cotC*, *yxeD*, *cotU*. The *ypqP* gene, potentially involved in the synthesis of polysaccharide, has been suggested to be involved in the addition of polysaccharides to the spore envelope [48]. This gene is upregulated by 1.6Log2FC and 1.9Log2FC in the pellicle compared to the submerged or the detached cells, respectively.

GL5, a group clustering 135 genes, is upregulated in the detached cells (DC) and submerged (SB) (Figure 4a). The *narG-I* operon, involved in nitrate respiration, is highly upregulated by a 5Log2FC in both detached and submerged cells compared to pellicle (PL vs. DC, and PL vs. SB). Carbon metabolism related genes, *i.e.*, *lctP*, *gapA*, *eno*, *cggR*, *ackA*, *pgm*… are all upregulated by more than Log2FC in the submerged compartments (SB and DC) compared to the pellicle (PL) (supplementary data **S1**). Figure 4a, shows a high expression in the submerged population compared to the pellicle and the detached one in the GL2 clustering group. This group contains around 70% of genes related to the functional category coping with stress (Figure 4b), most of which are regulated by the SigB regulon *i.e.*, *yjgD*, *ygxB*, *csbx*, *ydbD*, *ktaE*, *yhxD*,... that are upregulated by 3Log2FC and 2Log2FC in the submerged compared to the pellicle or to the detached cells, respectively (downregulated in the comparisons PL vs. SB and DC vs. SB).

About 34 % of the differentially expressed genes between the different populations of the liquid model are poorly characterized or of unknown function (Figure 4b, supplementary data **S1)**. Thus, in the comparison between the pellicle and the submerged (PL vs. SB), among others genes like *yoaC*, *yitJ*, and *ywcL* are upregulated while *yjgC*, *ydaC*, and *yxlE* are downregulated by 3Log2FC. Moreover, genes such as *ydjJ*, *yoxB*, and *yycD* are downregulated by more than 2Log2FC in the detached cells compared to the submerged (DC vs. SB). The *ywmC* and *ypzD* genes are upregulated by approximately 3Log2FC and *yclD*, *ybfA*, *yhbD*, and others are downregulated by more than 2Log2FC in the pellicle compared to the detached cells (PL vs. DC).

3D microscopic observations of the different communities with fluorescent transcriptional fusions reveals local patterns of gene expression

Harvesting the whole population of a biofilm compartment is a useful technique to estimate the mean differential gene expression of cells in this community, which are in a range of particular physiological states. However, we were interested in going beyond the mesoscale analysis by visualizing *in situ* at a single cell level the gene expression in the different biofilm populations. From the transcriptome data, we have selected genes representing the different cell types present in a biofilm (genes showing a well scattered representation in the global heatmap, Supplementary data S2), and constructed transcriptional reporter fusion to fluorescent protein genes *gfp* or *mCherry*. Figure 5, represents quantitative data of the transcriptome results followed by confocal imaging for the reported genes in the different models, swimming and liquid biofilm. The matrix genes are represented by *epsA-O*, *tapA*, *bslA*, *srfAA*, *ypqP* and *capB-E*, motility by *hag*, exoprotease by *aprE*, competence by *comGA*, cannibalism by *skfA*, respiration by *ctaA* and *narG-I*, and sporulation by *spoIIGA* and *spoVC*.

The major matrix genes *epsA-O*, and *tapA* show as expected similar transcriptional patterns, a 4Log2FC downregulation in the submerged biofilm (SB), a 2Log2FC upregulation in the mother colony (MC) and an average expression for the pellicle (PL). Confocal imaging reflects these transcriptional data, with roughly a gradual decrease of expression in the swarming compartments starting from the mother colony to the tips, expression in the pellicle quite similar to that in the mother colony, and very low in the submerged biofilm compared to the other spatial structures

(Figure 5). The *bslA* gene is very highly expressed in all the different aerial models compared to the submerged biofilm (Figure 5). Comparison of its transcription between the different compartments gives a narrow scale range, with nearly a similar expression in the mother colony (a 0.6Log2FC) and the pellicle (a 0.3Log2FC), and a downregulation by only one Log2FC in the submerged biofilm.

The surfactin synthetase encoding gene *srfAA* has a similar expression with a small scale range across all the spatially selected compartments. Even though this gene is described as required during swarming to reduce the surface tension, it shows a higher expression in the pellicle (a 0.7Log2FC). However, deletion of this gene (*ΔsrfAA*) in the *B. subtilis* strain NCIB3610 indicated that it is not essential for the pellicle development [49], and its functionality in the NDmed context did not confer any visible advantage neither on swarming, nor on submerged biofilm and pellicle development [6]. The *ypqP* gene (renamed *spsM* [48]), disrupted by the SPβ prophage in the reference strains NCIB310 and 168, is potentially required for polysaccharide synthesis and has been shown to be involved in the strong spatial organization of *B. subtilis* NDmed biofilms [27]. The microscopic images of the *ypqP* clearly represent the transcriptome data obtained, with ~2.5Log2FC in the pellicle followed by the submerged and the mother colony. Similar observation for the *capB-E* operon, involved in secretion of a polymeric substance, shows a highest expression in the pellicle compared to the other compartments (Figure 5). By the cross section (through the xz plane), one can observe that after 24h hours of incubation at 30 °C, all the matrix genes in the different biofilm models are mainly expressed on the top section of the mother colony and the pellicle, while on the bottom for the submerged biofilm (except for the *tapA* operon that shows expression on both the bottom and the top of the submerged biofilm).

Motility is downregulated in the three biofilm models, mother colony (MC), submerged (SB) and pellicle (PL), compared to the steep expression of the *hag* gene through the swarming compartments, base (BS), dendrites (DT) and the tips (TP) (Figure 5). In the mother colony the few motile cells are present both near to the top and at the bottom of the colony, while for the submerged biofilm these cells are present mainly on the bottom in close contact with the solid surface. In the pellicle, genes involved in motility are highly expressed on the bottom layer at the interface with liquid (Figure 5).

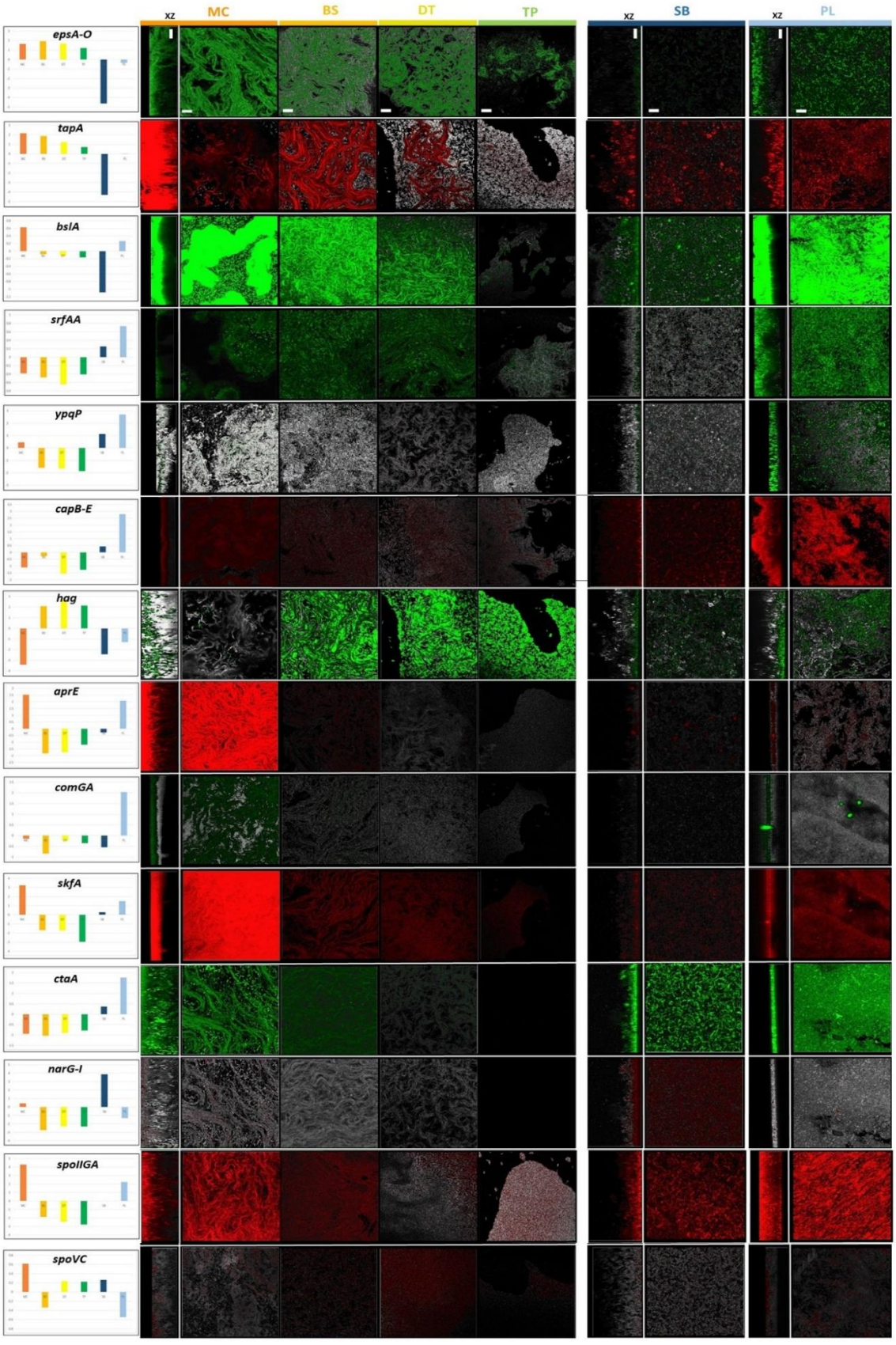
xz
MC
BS
DT
TP
xz
SB
xz
PL
epsA-O
tapA
bslA
srfAA
ypqP
capB-E
hag
aprE
comGA
skfA
ctaA
narG-I
spoIIGA
spoVC

Figure 5: From mesoscopic to microscopic scale. *The transcriptome is represented on the most left panels with a Log2FC scale of an average of the three biological replicates compared to the average of all presented conditions together. The transcriptome results of epsA, capA and narG are used as representatives for the operon epsA-O, capB-E and narG-I, respectively. For confocal imaging contrast was by chemical staining or an oppositely expressed reporter gene fusion. For swarming plates (MC, Mother Colony; BS, Base; DT, Dendrites; TP, Tips) and static liquid cultures (SB, Submerged; PL, Pellicle) images represent a section (x and y 50µm and z 30µm); the scale bar represents 20µm. For the biofilm models (MC, SB and PL), a projection through the xz plane is presented on the left of each image; the vertical scale bars indicate the bottom level of the surface associated communities, in contact with the agar surface, solid surface or liquid surface, respectively. Images are representatives of the majority of the phenotype from at least three replicates for each condition.*

The *aprE* gene, encoding a major extracellular alkaline protease, appears to be expressed in a localized subpopulation in the biofilm models (Figure 5). In the mother colony, this gene is highly expressed on the top most subpopulation with an upregulation by 2.5Log2FC that sharply decreases through the swarming populations, with only few basal and specific subpopulations still expressing it. As for the *comGA* gene, encoding a late competence protein, is more spatially expressed near the top of the mother colony (Figure 5). In the pellicle, this gene shows a moderate expression from a subpopulation with an extreme high stochastic expression for few cells. The latter could explain the results obtained by the transcriptome with a 2Log2FC upregulation in the pellicle compared to the mother colony or other compartments. A correlation between the transcriptome data and imaging is clearly obtained with the *skfA* gene, involved in the production of a spore killing factor. Figure 5, shows a high intensity of gene expression in the mother colony with a gradual decrease in the intensity through the swarm. In the liquid culture, this gene is expressed slightly in the submerged and highly in the pellicle.

For respiration, the *ctaA* gene, encoding heme A synthase, and the *narG-I* operon, encoding nitrate reductase, have been reported and observed (Figure 5). The intensity of *ctaA* gene expression appears to be the highest in the pellicle, followed by the submerged biofilm, and then in the mother colony which shows few cells expressing above the basal level. As for the anaerobic respiration, after 24 hours of incubation, the *narG-I* operon has recorded 4Log2FC of upregulation in the submerged compartment, which could be clearly seen in confocal images (Figure 5). In the mother colony and the pellicle only a few cells are expressing the *narG-I.* However, during the swarm this intensity decreases to record very low to no expression in the tips for both *ctaA* and *narG-I*.

Moreover, *spoIIGA*, a sporulation related genes encoding a protease required for the maturation of SigE involved in early sporulation steps, is highly upregulated in the mother colony and in the pellicle by 4Log2FC and 2Log2FC, respectively. As for the *spoVC* gene, encoding peptidyl-tRNA hydrolase induced under stress conditions and involved in the spore coat formation, is expressed rather similarly in all the conditions with roughly a Log2FC range between the highest (mother colony) and the lowest (pellicle) expression. By confocal imaging spatial localization of this subpopulation appeared to be expressed on top of the mother colony, the pellicle, and near to the adherent cells in the submerged biofilm (Figure 5).

All the reported genes in Figure 5, except for the *narG-I* operon, show a moderate or low expression in the submerged biofilm compared to the colony or the pellicle after 24 hours of incubation at 30°C. This suggests that these genes could either be poorly expressed in the submerged biofilm, or are either expressed before or after the 24 hours of incubation, which led us to monitor temporally the reported genes for 48 hours.

4D spatio-temporal patterns of gene expression in submerged biofilms

From a real-time movie of Gfp expression in the NDmed-GFP strain, drawing of a kymograph allows to illustrate the morphological dynamics of biofilm formation as a function of time and space (Figure 6a). In the first few hours, *B. subtilis* cells adhere to the surface, stop dividing and form sessile chains followed by a sudden differentiation of a subpopulation into motile cells (between 5 and 10 hours of incubation). Only in a second kinetic sessile cells colonize the surface to form the highly structured submerged biofilm (Supplementary movie S1).

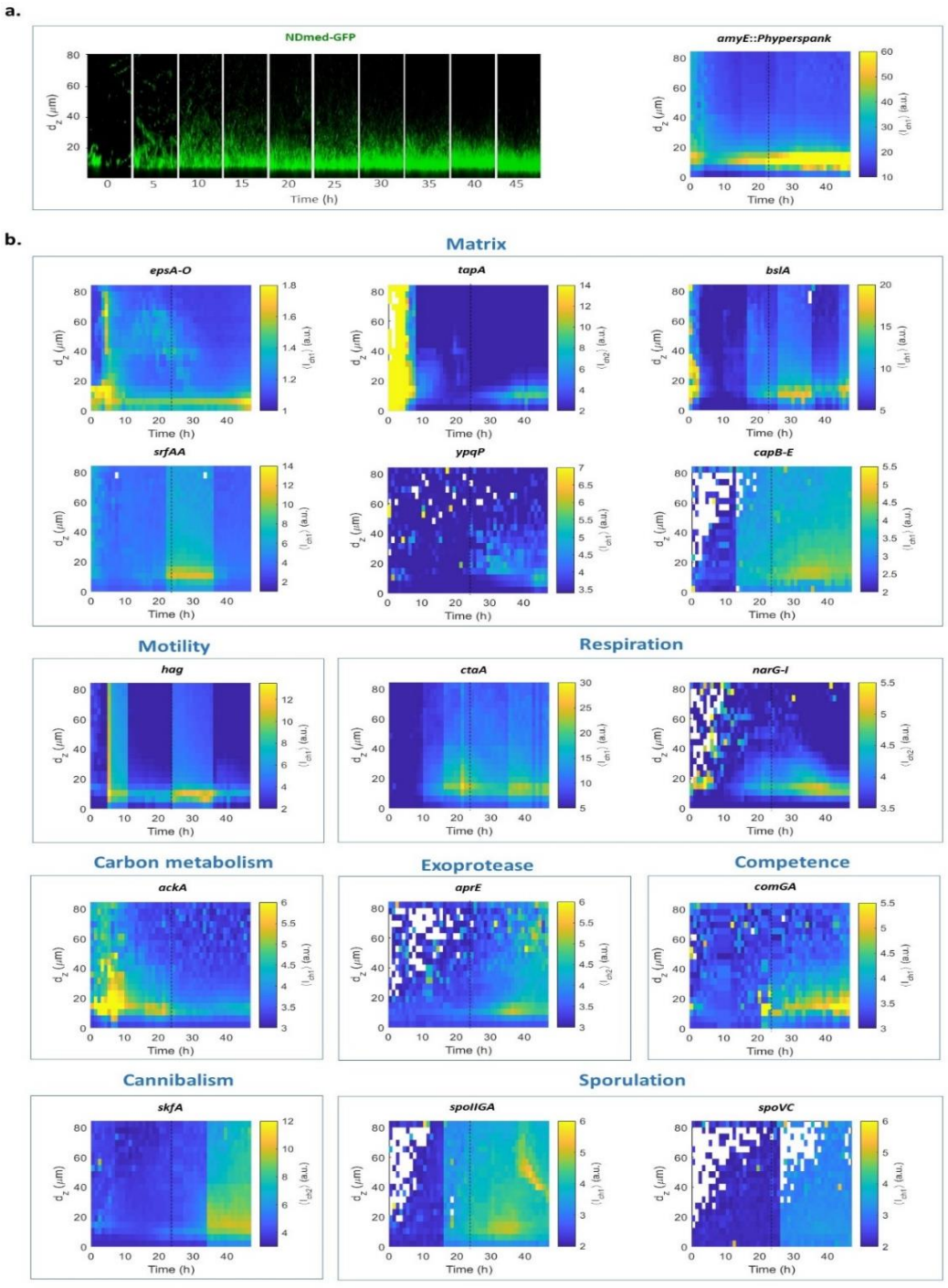

Figure 6: Spatio-temporal monitoring of gene expression in submerged biofilm. *(a) On the left is presented 4D confocal imaging (x 50µm, y 50µm, z 30µm) for the NDmed-GFP strain. A kymograph showing the intensity of Gfp expression as a function of time and space is presented on the right. (b) Kymographs representing spatio-temporal expression of 15 transcriptional reporter fusions to genes potentially involved in biofilm development.*

For all the reported gene representatives of the main functions active in different cell types present in a biofilm, a temporal scale monitoring intensity of gene expression is represented as kymographs in Figure 6b. Expression of the *epsA-O* and *tapA* operons, involved in the synthesis of the major matrix components in a biofilm, are downregulated at 24 hours in submerged biofilm compared to colony and pellicle (Figure 5). On a temporal scale, these genes show higher expression mainly during the first few hours of submerged biofilm formation, and then a gradual decrease with only a small subpopulation with low expression present at 24 hours, in accordance to the corresponding transcriptome data (Figure 6b). This suggests that these matrix genes are expressed essentially in the first stages of biofilm development, whereas after 24 hours, when the biofilm has been raised, high expression of these genes is no longer required for matrix production. Only after 37 hours these genes appear to be further slightly expressed. Expression of *epsA-O* is very low, compared to *tapA*, but still with a basal level in the submerged biofilm. BslA, another structural protein in the biofilm matrix encoded by *bslA*, acts synergistically with both TasA and the EPS [34]. In the submerged biofilm, expression of *bslA* is upregulated in a few cells during the first 3 hours, and then down-regulated till around 17 hours to be gradually upregulated afterwards. The *srfAA* gene, showing roughly no expression for the first 18 hours, is expressed mainly in a time frame between 21 and 36 hours of incubation, to be downregulated afterwards. The *ypqP* gene, involved potentially in the synthesis of polysaccharides participating in the strong spatial organization [27], shows some stochastic expression by very few cells at the beginning of biofilm formation (before 24 hours); after 24 hours *ypqP* is expressed but only in a very small subpopulation. In a similar manner *capB-E* seems to be a late matrix operon, whose expression gradually increases after around 15 hours of incubation. The spatio-temporal heterogeneities observed in the patterns of expression of various genes involved in matrix formation indicate the complexity of this process during biofilm development.

The extracellular protein TasA has been found to act as a developmental signal in the biofilm, stimulating a subpopulation to switch to a motile phenotype, which contributes to the dispersion of a biofilm colony on a surface [50]. Indeed, we could observe a sudden increase of *hag* expression occurring after 5 hours of incubation, synchronized with the beginning of down-regulation of the *tapA* operon (which includes also the *sipW* and *tasA* genes) (Figure 6b), indicating

the switch at that time of a subpopulation from chain forming sessile cells to motile planktonic ones. A gradual decrease of *hag* expression in this subpopulation is then observed, followed by another wave of expression of motility genes between 24 and 37 hours of incubation, before a slight re-expression of the matrix genes *tapA* and *epsA-O* (Figure 6b, and Supplementary movie S2).

The *ctaA* gene, encoding a heme A synthase, is one of several genes involved in aerobic respiration regulated by ResD [51]. Its expression starts after 10 hours of incubation, followed by two waves of high expression by a subpopulation in the submerged biofilm model. The anaerobic genes monitored by the *narG-I* operon show stochastic expression by very few cells during the early first hours of incubation (around 5 hours), but starting at around 21 hours, this operon shows rather a continuous gradual expression with time.

For carbon metabolism, *ackA*, encoding acetate kinase, shows an upregulation in a subpopulation for the first 10 hours, and is systematically downregulated after. In a coordinated manner this downregulation is faced by an upregulation of the *aprE* gene, that is expressed gradually afterwards (Figure 6b, supplementary movie S3).

Tracking the *comGA* gene shows some stochastic expression in single cells in the first hours of incubation. A brutal expression in countable cells is seen after 21 hours, giving the high expression appearing on the kymograph (Figure 6b). This is then accompanied by an increase of the size of the subpopulation expressing *comGA* (supplementary movie S4). Only a few cells express *skfA* during the first 20 hours, followed by a noticeable increase in intensity of gene expression after 31 hours of incubation, and accompanied with an increase in the size of the subpopulation of cells involved in the production of surfactin (supplementary movie S4).

Finally, we have monitored the expression of genes participating in the sporulation process: *spoIIGA* involved in early sporulation steps, and *spoVC* participate in late sporulation steps in spore coat formation. Figure 6b, shows that *spoIIGA* starts to be expressed at around 18 hours of incubation, indicating the beginning of sporulation. The late sporulation gene *spoVC* mainly starts to be expressed after 24 hours of incubation (in the minimal synthetic medium we used).

Two successive waves of localized death remodel the biofilm organization

To further understand the heterogeneity fluctuations of the different functions during *B. subtilis* biofilm development, a Live/Dead tracking was performed. Figure 7a, represents kinetic images for the live cells of *B. subtilis* reported by their expression of green fluorescent protein (GFP, green), while the dead cells and eDNA were contrasted with propidium iodide staining (PI, red). A multidimensional kymograph representing the intensity of dead cells (obtained by a ratio of dead/live cells) as a function of their spatial localization and time is presented in Figure 7b. Bacteria adhere to the surface and form chains of sessile cells in the first few hours of incubation and thereafter, between 13 and 24 hours, clusters of dead cells are observed over the formed biofilm (Figure 7, supplementary movie S1). After this first wave, the dead cells density decreases (Figure 7), faced by a slight increase in the live population until around 42 hours where a second wave of dead cells occurs (Figure 7a, supplementary movie S1). Interestingly, by comparing the kymographs in Figures 6a and 7b, it appears that these dead cells subpopulations are mainly spatially localized as a layer on the top of the submerged biofilm live cells.

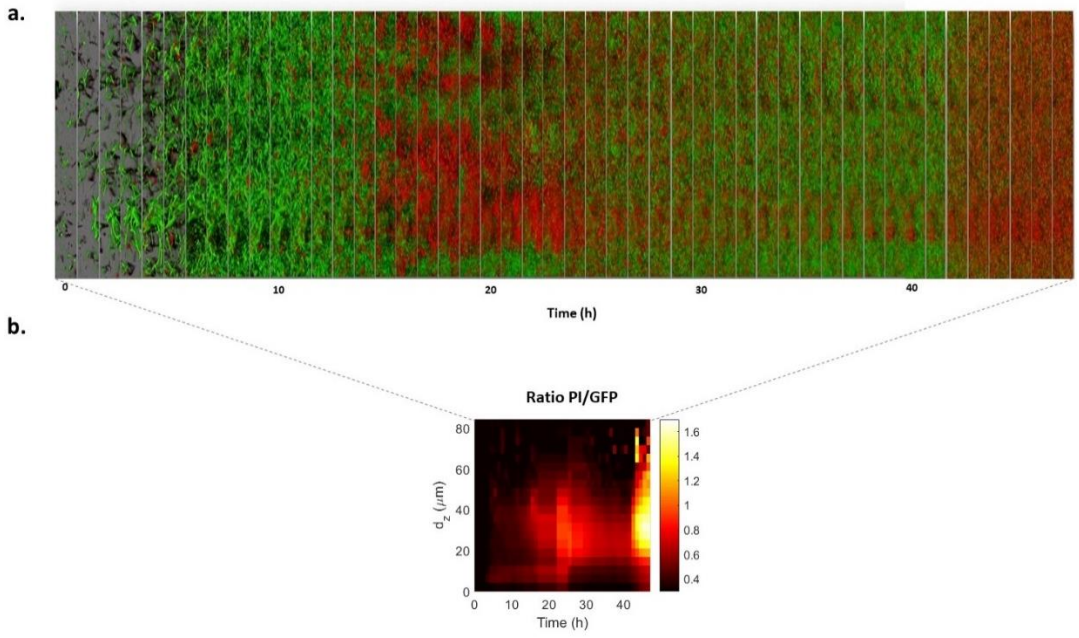

Figure 7: Temporal observation for the submerged biofilm development reveals oscillations of spatial dead cell localization. *(a) Sections from a real-time confocal imaging using NDmed-GFP and IP for permeable cell staining with an image representing an overview projection 250 x 30µm slice. (b) Kymograph representation of the ratio of dead cells/live ones.*

DISCUSSION

Transcriptome remodeling uncovers major differences in patterns of gene expression between colony, pellicle and submerged biofilms

The transcriptomic data generated in this study put forward a global view on the variation of gene expression profiles for the different biofilm models *i.e.* mother colony (MC), pellicle (PL) and submerged (SB). A global hierarchical clustering of the RNAseq analysis points out that the colony formed on agar showed a very distinct transcriptome profile compared to the pellicle and the submerged biofilms. Indeed, most of the genes involved in sporulation are strongly upregulated in colonies and poorly expressed in the submerged communities. In the liquid model, while sporulation genes are mainly expressed in the floating pellicle, a specific counting of spores on agar plates (after heat treatment of the captured populations) demonstrated a higher quantity of spore in the submerged fraction than in the pellicle (data not shown). Indeed, it has been shown recently that the spore surface of *B. subtilis* was covered with legionaminic acid, required for the crust assembly and enhancing hydrophilicity of the spore [52]. All together these observations suggest that, in the timeframe explored here, spores which are essentially produced in the floating pellicle, can sediment as hydrophilic colloids down the well and accumulate on the submerged fraction.

Another striking difference between these models is the dominant anaerobic respiration metabolism detected in the submerged biofilm compared to the other aerial biofilm models. In liquid culture, the coexistence in a well of two interfacial communities of *B. subtilis* present with distinct respiration metabolisms is pointed out here: the submerged biofilm (and the detached cells) mainly under anaerobic, and the pellicle under aerobic respiration. Although the pellicle and the colony are in contact with the air, the existence of a small subpopulation of cells expressing anaerobic genes is still observed. We also showed by RNA-seq that at 24h, the major extracellular matrix genes (*i.e. epsA-O*, *tapA* operon, and *bslA*) are expressed the most in the colony and very weakly in the submerged biofilm. Taking advantage of transcriptional fusions and microscopy, we could observe a minor expression of *tapA* and *bslA* forming small dispersed clusters of expressing cells in submerged biofilm, while the expression of the same genes are dominant and intense in

colonies and pellicles. This diversity in the spatial repartition of cells producing each of these matrix components suggests a variety in the biochemical matrix composition associated with specific local micro-rheological properties.

At the population level (RNA-seq), the *hag* gene encoding flagellin and reporting motility is downregulated in the three biofilm models compared to the other compartments explored (free cells, swarm tips...). However, microscopy observations of fluorescent transcriptional fusion allow to contrast minor subpopulations of cell expressing motility genes with a spatial organisation. This was described previously with other strains in colonies on agar but it is the first report for the pellicle and the submerged biofilms. In the three models, these transcriptional activities associated with cell motility occur mainly on the interfacial layers of the community embedded under matrix-producing subpopulation; in the layer near to the agar surface for the colony; the inner immersed layer for the floating pellicle, and the layer in contact with the substratum for the submerged model. Expression of flagella could also be present within the biofilm indicating the migration of cells by chemotaxis toward a zone richer in oxygen and nutrients, allowing the vascularization of the biofilm matrix to increase diffusion/reaction throughout the biofilm [53].

Swarming as a mosaic landscape of adjacent segregated populations of bacteria with differential genes expression

Swarming is a multicellular behavior during which cells migrate coordinately through chemical, mechanical and bioelectrical interactions [54]. *B. subtilis* swarming initiates from a multilayered colony by migration and dispersion on the minimal synthetic medium in a monolayer form before switching to biofilm form, due to any stressful environmental signal that could be simply a physical barrier [22]–[26]. Transcriptome analysis of four different spatial compartments of the process allowed to highlight the sequential gene regulations taking place during bacterial surface colonization. A huge divergence in gene expression is observed between the mother colony (MC) and the swarming compartments, including its adjacent compartment (base, BS). Although the swarming takes place on an aerial interface, both aerobic and anaerobic respiration genes are upregulated in the mother colony, compared to the other swarming compartments. Confocal imaging showed that the anaerobic *narG-I* operon is expressed by only a few cells distributed in

the mother colony, suggesting that a co-metabolism could occur between cells expressing aerobic and other undergoing anaerobic respiration sharing the same environment. Moreover, a high upregulation of genes related to carbon metabolism (gluconeogenic) and sporulation in the mother colony compared to the base (BS), indicates that stress signals such as nutrient and oxygen depletion initiated the sporulation process to face the harsh environmental conditions. As expected, matrix related genes are more upregulated in the mother colony and the base compared to the dendrites and tips, which is clearly observed by confocal imaging of the distribution of these subpopulations during a swarm. In contrast, the motility and chemotaxis is observed higher during the swarm compared to the mother colony (Figure 5).

Swarming adjacent compartments of the base, dendrites and tips are very close to each other, and only few genes are differentially expressed. For instance, 12 genes are downregulated in the dendrites when compared to the base (DT vs. BS); these genes are the *znuACB*, *ppsD-E*, *folEB-yciB*, and *pftAB* operons, *rpsNB* and two other genes with unknown function, *yxeG*, and *yrpE*. The *znuACB* operon encodes a high-affinity zinc transporter that mediates zinc incorporation. It has been suggested to play a role in regulation of competency development after activation of ComF that follows post-transcriptional control of ComK [55]. In addition, *rpsND* and *folEB* are two genes encoding proteins replacing RpsN and FolE, respectively, under conditions of zinc limitation. After the end of the exponential growth phase, *B. subtilis* can secrete plipastatins, strong antifungal compounds encoded by the *ppsA-E* operon [56]. The *pftAB* operon encodes a facilitated transport system specific for pyruvate import/export, derepressed when glucose is exhausted to re-import and utilize as a carbon source pyruvate exported as overflow metabolite [57], [58]. Obviously, the cell density in the base (closest localized region to biofilm) is much higher than that in the dendrites, thus, the signal for cell density ComX induces there the autophosphorylation of ComP, the sensor kinase of the ComP/A two component system, which activates the response regulator ComA and thus induces expression of the *srfA* operon, encoding the biosurfactant surfactin [59]. Surfactin is required to reduce surface tension, for triggering matrix production and also contributes to development of genetic competence [5], [31]–[33] by activation of ComK, which in turn induces expression of several genes including late competence genes (*comC*, *comE*, *comF*, and *comG*) and protein components required for uptake of exogenous DNA [60]. Hence, the gene expression

profile in the base corresponds to a higher cell density and lower primary carbon source (glucose) availability, leading to induction of genes related to gluconeogenic carbon metabolism, competence development and biofilm formation.

Among the 14 genes downregulated in the tips compared to the dendrites (TP vs DT) is the *veg* gene, encoding a negative effector of SinR activity independently from both SinI and SlrR, thus acting positively on the matrix production and stimulating biofilm formation [61]. Moreover, two genes involved in late sporulation stages, *spoVS* and *sspF*, are more expressed in the dendrites than the tips, in concordance with observation by confocal microscopy of expression of the late sporulation gene *spoVC* (Figure 5). The swarming medium contains low amounts of manganese, yet, genes required to prevent manganese intoxication are upregulated in the dendrites, such as *ykoY* encoding a manganese resistance protein of the TerC family [62]. Moreover, 10 genes were upregulated in the tips compared to the dendrites, including *rbsD*, *melR*, *melE* and *idh*, involved in carbon utilization as encoding ABC transporters to uptake a carbon source from the medium, or enzymes to metabolize this source. Two operons, *ytbDE* and *ydgGH*, specifically upregulated in the tips compared to the dendrites are of unknown function, but could be putatively involved in drug export and detoxification [63]. Further studies aiming at determining their precise function might be of great interest. Taken together, these results highlight the close physiological state proximity of the dendrites with both the base and the tips, reflecting their physical localization between these compartments.

Even though between the adjacent swarming compartments only few genes are differentially expressed (12 genes for DT vs. BS, and 24 genes for TP vs DT), much more differential expression occurs between the base and the tips (304 genes for TP vs BS). Among these, the *ytbDE* and *ydgGH* operons show an upregulation in the tips compared to the base by 2Log2FC and 4Log2FC, respectively. This indicates that expression of these unknown genes is gradually increasing from the base to the tips all along the swarming process. Expression of motility, ribosomal protein genes and *ycdA* gene, encoding a lipoprotein required for swarming motility [64], show a gradual upregulation along the swarm to reach the highest in the tips, confirming previous observation [25], [65]. There is a strong downregulation of genes involved in biofilm formation such as *veg*, *slrR*, *tapA* and *eps* operons in the tips when compared to the base

(TP vs BS). All these gene regulations indicate that cells in the tips express rather more transporters to explore the environment and to incorporate nutrients from the medium, and not the proteins involved in biofilm formation or sporulation, contrary to cells in the base. Thus each compartment is formed by cells under different physiological states with higher cellular heterogeneity as we go toward the mother colony.

Free-cells harvested between the submerged biofilm and the floating pellicle are not similar to exponential nor stationary cells from planktonic cultures

Detached cells have been long considered as a state similar to planktonic culture. Phenotypic and transcriptomic studies on various bacterial species, such as *Klebsiella pneumoniae* or *Streptococcus pneumoniae,* have shown that detached cells exhibit different gene expression patterns, distinct from both sessile and planktonic lifestyles [66]-[69]. Our results with *B. subtilis* confirm these previous observations. The transcriptome profile of the detached cells revealed a distinct state compared to both exponential and stationary planktonic phases and the two biofilm models in the liquid culture. For instance, the *tasA* and *epsA-O* operons are downregulated in the detached cells compared to both the stationary (ST) or to the exponential (EX) phases, indicating the higher expression of major matrix genes in a planktonic culture than in these detached cells.

In other aspects, the detached cells seem to be closer to the exponential phase rather than the stationary phase, as suggested by the clustering. This is illustrated by the extremely strong upregulation (around 9Log2FC) of the *pst* and *tuaA-H* operons in the stationary phase compared to the detached cells or the exponential phase. These operons, involved in high-affinity phosphate uptake and teichuronic acid biosynthesis, respectively, are induced upon phosphate starvation [70], which indicates that cells in stationary phase suffer such conditions more than the detached cells or the exponential phase culture.

Expression of *B. subtilis* matrix genes is finely tuned both spatially and temporally

Previous studies have shown that gene expression is heterogeneous within cells encountering a biofilm [43], [71]. Matrix components are energetically costly to produce and therefore are shared within the population during biofilm development, in which cells have

different expression levels leading to different production of matrix components [71], [72]. In this study we revealed spatiotemporal patterns of gene expression linked to the phenotypic heterogeneity observed during the different stages of submerged biofilm development. We could highlight the heterogeneous expression of the different matrix genes (*epsA-O, tapA, bslA, srfAA, ypqP*, and *capB-E*) over both spatial and temporal levels. EPS and TasA are highly produced in the first few hours of incubation during the adhesion and development of the biofilm to the surface. The latter matrix components are assembled by BslA, required for biofilm architecture and biofilm hydrophobicity of the colony and pellicle [34], [73]. In a previous study, we reported that *bslA* inactivation had an impact on the 3D structure of the colony and also on the stability of the pellicle, while no effect was observed for the submerged biofilm model after 24 hours of incubation [6]. 4D-CLSM allowed to demonstrate that *bslA* is expressed during the first 3 hours of submerged biofilm development (together with the *epsA-O* and *tapA* operons) and then again in late stage of biofilm maturation after 17 hours, when the biofilm is already formed. A strong correlation between biofilm development and surfactin production was suggested within different *Bacillus* species. For instance, in *B. velezensis* FZB42 and *B. amyloliquefaciens* UMAF6614 defect in surfactin production has been shown to cause partial or severe biofilm defects [74], [75]. However, in the *B. subtilis* context (NCIB 3610 and NDmed) surfactin operon mutation was reported not to have any effect on biofilm formation (pellicle, colony and submerged) [6], [49]. As an external signal, surfactin induces cells to express matrix genes [1]. The *srfAA* gene is expressed mainly in a temporal window between 21 and 36 hours during biofilm incubation after which one can re-observe expression of the EPS and TasA. In addition, mutation of the *ypqP* gene and *capB-E* operon had only a slight effect on the biofilm formation after 24 hours [6], since these genes are mainly late expressed. Only a subpopulation of the submerged biofilm expresses the different matrix genes. Hence, heterogeneous spatiotemporal expression of matrix genes indicates specific requirements of the expensive matrix products through the different stages of biofilm development.

Waves of localized cell death correlate with patterns of genes expression

In a medium containing carbon and nitrogen excess, a major overflow pathway takes place through the conversion of pyruvate to acetate by the phosphotransacetylase-acetate kinase pathway to generate ATP. This pathway is positively regulated by a major regulator for the carbon

metabolism CcpA which for instance activates the *ackA* gene, encoding an acetate kinase [76]. In this study we could see that *ackA* was highly expressed during the first 10 hours, before being gradually downregulated, indicating that carbon source started to be limited afterwards. Interestingly, this corresponded with the beginning of the first wave of dead cells that was clearly observed after 13 hours, followed by the initiation of sporulation (reported by *spoIIGA*). Hence, these observations could indicate that carbon source limitation triggered cell death which by turn provided carbon source for the initiation of the irreversible sporulation process. Cell death is also followed by competent and cannibalism cells types, tagged by *comGA* and *skfA* genes, overexpressed at around 20 hours, pointing out the capability of these cells to uptake exogenous DNA from the medium and produce spore-killing factors both of which are involved to delay sporulation [19]. Another expression of the *hag* motility gene is observed after 24 hours in a small subpopulation of the submerged biofilm. This could correspond to pore forming swimmer cells as previously observed [53]. Surfactin, reported by *srfAA*, is overproduced around the same spatiotemporal window. Surfactin is involved in genetic competence and triggers matrix production [5], [31]–[33], in accordance with the upregulation of the genes *epsA-O*, *tapA*, *bslA*, *ypqP*, *capB-E* and *comGA* after 24 hours of incubation. Motility could also allow to increase the diffusion and activity of exoproteases (product of the *aprE* gene, among others) within the matrix biofilm. Moreover, cells undergoing sporulation are also present at that time as indicated by the overexpression of late sporulation genes (such as *spoVC*). A highly structured colony has wrinkles, formed by mechanical forces due to increased cell density. Dead cells localized under these wrinkles, at the base of the biofilm and near the agar, lead to formation of channels that facilitate liquid transport within the biofilm [77], [78]. In the submerged biofilm, *B. subtilis* dead cells are clustered mainly on the top of the biofilm during the first wave (between 13 and 24 hours), while they are more evenly distributed in the second wave (after 42 hours). As discussed above, detached cells from a submerged biofilm at 24h are in a physiological state closer to cells in exponential rather than stationary phase. This could result from the abundant concentration of nutrients liberated by cell death on the upper interface of submerged biofilm.

CONCLUSION

This report presents the first comparative description of the transcriptomic profiles of 9 subpopulations of *B. subtilis* captured on solid, semi-solid and liquid cultures with the same strain and nutrient source. It allowed us to specify the singularities of each biofilm model and to pinpoint the fineness of their spatio-temporal regulation down to the single scale. The presented data give novel insights on the development and dispersal of *B. subtilis* surface-associated communities, which will serve as a unique resource for future studies on biofilm physiology to further investigate genetic determinants required for its control.

MATERIAL AND METHODS

Bacterial strains and growth conditions

The *B. subtilis* strains used during this study are listed in Table 1. NDmed derivatives were obtained by transformation with various plasmids or chromosomal DNA of various strains to introduce the corresponding suitable reporter fusion. The transcriptional fusions of the *gfpmut3* gene to the *ackA*, *hag*, *bslA* or *srfAA* promoter were constructed previously within the pBSB2 plasmid (pBaSysBioII) using ligation-independent cloning [79], prior to integration into the chromosome of BSB168 in a non-mutagenic manner, resulting in strains BBA0093, BBA0231, BBA0290 and BBA0428, respectively (kind gifts from Pr. M. Jules, University Paris-Saclay, AgroParisTech, INRAE). Similarly, fragments corresponding to the promoter regions of *epsA*, *ypqP*, *ctaA*, *narG*, *skfA*, *comGA*, *aprE*, *spoIIGA*, *spoVC*, and *tapA*, or to a region in the 3' part of *capE*, were amplified by PCR from genomic DNA using appropriate pairs of primers (Table S1 in the supplemental material). These fragments were inserted by ligation-independent cloning in pBSB2 or in pBSB8, a pBSB2 derivative with the *gfpmut3* and *spec* (spectinomycin resistance) genes replaced by *mCherry* (codon-optimized for *B. subtilis*) and *cm* (chloramphenicol resistance), respectively. The resulting plasmids were then used to integrate each corresponding transcriptional fusion into the chromosome of *B. subtilis* through single recombination. Transformation of *B. subtilis* was performed according to standard procedures and the transformants were selected on Luria-Bertani (LB, Sigma, France) plates supplemented with appropriate antibiotics at the following concentrations: spectinomycin, 100µg/mL; chloramphenicol, 5 µg/mL. Before each experiment,

cells were cultured on Tryptone Soya Agar (TSA, BioMérieux, France). Bacteria were then grown in synthetic B-medium composed of (all final concentrations) 15 mM $(NH_4)_2SO_4$, 8 mM $MgSO_4.7H_2O$, 27 mM KCl, 7 mM sodium citrate.$2H_2O$, 50 mM Tris/HCl (pH 7.5), and 2 mM $CaCl_2.2H_2O$, 1 µM $FeSO_4.7H_2O$, 10 µM $MnSO_4.4H_2O$, 0.6 mM KH_2PO_4, 4.5 mM glutamic acid (pH 8), 862 µM lysine, 784 µM tryptophan, 1 mM threonine and 0.5% glucose were added before use [80]. Cultures for planktonic inoculum were prepared in 10 mL B-medium inoculated with a single colony and shaken overnight at 37 °C. The culture was then diluted to an OD_{600nm} of approximately 0.1 and grown until it reached an OD_{600nm} of approximately 0.2. The procedure was repeated twice and finally the culture was grown to reach stationary phase, which was then used to inoculate swarming and liquid biofilm assays (Figure 1).

Table 1. *B. subtilis* strains used in this study

Strain	Relevant genotype or isolation source	Construction or Reference [a]
NDmed	Undomesticated, isolated from endoscope washer-disinfectors	[15]
NDmed-GFP	NDmed *amyE*::*Phyperspank-gfpmut2* (spec)	[81]
BSB168	*trp*+ derivative of 168	[82], [83]
BBA093	BSB168 *PackA-gfpmut3* (spec)	M. Jules
BBA0231	BSB168 *Phag-gfpmut3* (spec)	M. Jules
BBA0290	BSB168 *PbslA-gfpmut3* (spec)	M. Jules
BBA0428	BSB168 *PsrfAA-gfpmut3* (spec)	M. Jules
GM3346	NDmed *Phag-gfpmut3* (spec)	BBA0231→NDmed

GM3348	NDmed *PackA-gfpmut3* (spec)	BBA0093→NDmed
GM3401	NDmed *PbslA-gfpmut3* (spec)	BBA0290→NDmed
GM3402	BSB168 *PepsA-gfpmut3* (spec)	pBSB2epsA→BSB168
GM3403	NDmed *PsrfAA-gfpmut3* (spec)	BBA0428 →NDmed
GM3423	NDmed *PepsA-gfpmut3* (spec)	GM3402→NDmed
GM3461	BSB168 *PypqP-gfpmut3* (spec)	pBSB2ypqP→BSB168
GM3476	NDmed *PypqP-gfpmut3* (spec)	GM3461→NDmed
GM3816	NDmed *PctaA-gfpmut3* (spec)	pBSB2ctaA→NDmed
GM3820	NDmed *PnarG-mCherry* (cm)	pBSB8narG→NDmed
GM3823	NDmed *PskfA-mCherry* (cm)	pBSB8skfA→NDmed
GM3838	NDmed *PcomGA-gfpmut3* (spec)	pBSB2comGA→NDmed
GM3841	NDmed *PaprE-mCherry* (cm)	pBSB8aprE→NDmed
GM3862	NDmed *capE-mCherry* (cm)	pBSB8capE→NDmed
GM3864	NDmed *PspoIIGA-mCherry* (cm)	pBSB8spoIIGA→NDmed
GM3867	NDmed *PspoVC-mCherry* (cm)	pBSB8spoVC→NDmed
GM3872	NDmed *PtapA-gfpmut3* (spec)	pBSB2tapA→NDmed
GM3874	NDmed *PtapA-mCherry* (cm)	pBSB8tapA→NDmed

GM3903	NDmed *PaprE-mCherry* (cm)*/PackA-gfpmut3* (spec)	GM3841→GM3348
GM3907	NDmed *PnarG-mCherry* (cm)/*PctaA-gfpmut3* (spec)	GM3820→GM3816
GM3912	NDmed *PskfA-mCherry* (cm)*/PcomGA-gfpmut3* (spec)	GM3838→GM3823
GM3924	NDmed *PtapA-mCherry* (cm)*/Phag-gfpmut3* (spec)	GM3346→GM3874

[a] Arrows indicate transformation of pointed strain with indicated plasmid or chromosomal DNA of indicated strain

Swarming culturing condition

The OD_{600} was measured and the culture was diluted, and 2µL of diluted bacterial culture (adjusted to an OD_{600nm} of 0.01, ~10^4 CFU) were inoculated at the center of B-medium agar plate and incubated for 24hrs at 30°C with 50% relative humidity. Plates (9cm diameter, Greiner bio-one, Austria) containing 25mL agar medium (0.7% agar) were prepared 1hr before inoculation and dried with lids open for 5 minutes before inoculation.

Liquid biofilm culturing condition

A 3ml and 150µl of stationary phase bacterial culture adjusted to an OD_{600nm} of 0.01 has been cultured in 12-well microplate (Greiner bio-one, Germany) and 96-well microscopic grade microplate (µclear, Greiner bio-one, Germany), respectively. The plates were incubated at 30°C for 24hrs, to be followed by either local cell harvesting or microscopic imaging. The 96-well plate was used for kinetic monitoring of the submerged biofilm, as for the pellicle observation it was collected from a 12-well plate. When necessary, the medium was supplemented with 200 µM isopropyl-β-d-thiogalactopyranoside (IPTG) to induce Gfp expression from the *Phyperspank* promoter.

Local mesoscopic cell harvest for RNA-seq

For exponential and stationary cultures (OD_{600} ~0.6 and ~2.8, respectively), 6ml culture was collected for each sample. We transferred 2ml of each culture to an Eppendorf tube (CLEARline microtubes, Italy) and collected the cells by centrifugation at 8,000 X g at 4°C for 30 seconds. The

supernatant was drawn off, and the pellet was homogenized by 500µl TRIzol reagent (Invitrogen, Carlsbad, CA, USA) that helps in stabilizing the RNA in the cell. A centrifugation step (8,000 X g at 4°C for 30 seconds) was done again and the supernatant was drawn off and then the pellet was snap-frozen in liquid nitrogen and then stored at -80°C for further usage.

From 24hr swarming plates, four spatially localized compartments were collected (the mother colony, the base of the dendrites, the dendrites and the tips of the dendrites). 16 plates were used to collect one localized sample compartment. The cells were collected in an Eppendorf tube containing 500 µl TRIzol reagent. Collection was done manually by using a scraper (SARSTEDT, USA) starting from the tips down to reach the mother colony (that was collected by a loop). Cells were collected after the centrifugation step (8,000 X g at 4°C for 30 seconds), supernatant drowned off, pellet was snap-frozen in liquid nitrogen and then stored at -80°C for later use.

For a 24hr liquid biofilm, 6 wells (from a 12-well microplate) were used to collect one sample. By using a scraper, pellicles were collected in 6ml water. For detached cells, 1ml from the supernatant was collected from 6 wells. As for the submerged cells collection, after discarding all the rest of the liquid culture, add 1ml water in a well to be scratched by a pipet tip to be collected. All collected liquid samples were centrifuged rapidly for 30 seconds (8,000 X *g* at 4°C) and then an addition of 500µl TRIzol. A centrifugation step for 1 minute to discard the TRIzol reagent was done and then samples were snap-frozen by liquid nitrogen to be transferred to -80°C to be ready for the RNA extraction step.For each of the 9 samples, 3 biological replicates were done.

RNA extraction for RNA-seq

For all nine different conditions, a washing step for the pellets of the *B. subtilis* NDmed was done with 1ml TE + 60µl EDTA (10mM Tris, 1mM EDTA, pH=8) followed by centrifugation for 30 seconds (8,000 X g at 4°C). Cell pellets were thawed and suspended in 1ml TRIzol reagent. Cell suspension was transferred to a Fastprep screw cap tube containing 0.4 g of glass beads (0.1mm). By the use of a FastPrep-24 instrument (MP Biomedicals, United states), cells were disrupted by bead beating for 45 seconds at 6.5m/s. The supernatant was transferred to an Eppendorf tube and chloroform (Sigma-Aldrich, France) was added in a ratio of 1:5, followed by centrifugation on 8,000 X g for 15 minutes at 4°C. The chloroform step was repeated twice. The aqueous phase was

transferred to new Eppendorf, where sodium acetate (pH=5.8) was added to a final volume of 10% and 500µl of isopropanol (Sigma-Aldrich, France). Samples were left overnight at -20°C and a centrifugation step was followed for 20 minutes. Pellets were washed twice by Ethanol 75% followed by centrifugation for 15 minutes at 4°C. Then pellets were dried for 5 minutes under the hood. A RNA cleanup kit (Monarch RNA Cleanup Kit (T2050), New England Biolabs, France) was used to further clean the RNA samples. Nanodrop and Bioanalyzer instruments were used for quantity and quality controls. Library preparation including ribosomal RNA depletion (RiboZero) and sequencing was performed by I2BC platform (Gif-sur-Yvette, France). Sequencing was conducted on an Illumina NextSeq machine using NextSeq 500/550 High Output Kit v2 to generate stranded single end reads (1 x 75bp).

RNA-seq data analysis

Primary data processing was performed by I2BC platform and consisted of: demultiplexing (with bcl2fastq2-2.18.12), adapter trimming (Cutadapt 1.15), quality control (FastQC v0.11.5), mapping (BWA v0.6.2-r126) against NDmed genome sequence (NCBI WGS project accession JPVW01000000, [44]). This generated between 13M and 29M of uniquely mapped reads per sample and counts for 4028 genes after discarding 7 loci whose sequences also matched External RNA Controls Consortium (ERCC) references. The downstream analysis was performed using R programming language. Samples were compared by computing pairwise Spearman correlation coefficients (ρ) and distance (1-ρ) on raw counts which were summarized by a hierarchical clustering tree (average-link). Detection of DEGs used R package "DESeq2" (v1.30.1) to estimate p-values and log2 fold-changes. To control the false discovery rate, for each pair of conditions compared, the vector of p-values served to estimate q-values with R package "fdrtool" (v1.2.16). DEGs reported for pairwise comparisons of *B. subtilis* stapial compartments were based on a q-value≤0.05 and, unless stated otherwise, |log2FC|≥1. Fragment counts normalized per kilobase of feature length per million mapped fragments (fpkm) computed by DESeq2 based on robust estimation of library size were used as values of expression levels for each gene in each sample. Genes were compared for their expression profiles across samples for selected sets of conditions based on pairwise Pearson correlation coefficients (r) and distance (1-r) computed on log2(fpkm+5) and average-link hierarchical clustering of the distance matrix. Accordingly, the associated

heatmaps represent gene-centered variations of log2(fpkm+5) values across samples. Gene clusters defined by cutting the hierarchical clustering trees at height 0.3 (corresponding to average Pearson correlation coefficient within group of 0.7) were numbered by decreasing number of the genes coupled in the same group, GS1 and GL1 being respectively the largest for differentiation on solid medium and on liquid medium. The resulting gene clusters were systematically compared to *Subtiwiki* functional categories [63] (from hierarchical level 1 to level 5) and regulons using exact Fisher test applied to 2x2 matrices. The results of the comparisons with Subtiwiki functional categories were summarized in the form of stacked bar plots after manually assigning each gene to the most relevant category in the context of this study (when the same gene belonged to several categories) and a grouping of categories corresponding to hierarchical level 2 excepted for "Metabolism" (level 1), and "motility and chemotaxis" and "biofilm formation" (level 3). The whole transcriptomic data set has been deposited in GEO (accession number XXX).

CLSM

The biofilm models were observed using a Leica SP8 AOBS inverted laser scanning microscope (CLSM, LEICA Microsystems, Wetzlar, Germany) at the INRAE MIMA2 platform (www6.jouy.inra.fr/mima2_eng/). For observation, strains were tagged fluorescently in green with SYTO 9 (0.5:1000 dilution in water from a stock solution at 5µM in DMSO; Invitrogen, France) and SYTO 61 (1:1000 dilution in water from a stock solution at 5µM in DMSO; Invitrogen, France), a nucleic acid markers. After 15 to 20 minutes of incubation in the dark at 30 °C to enable fluorescent labeling of the bacteria, plates were then mounted on the motorized stage of the confocal microscope. Biofilms on the bottom of the wells were scanned using a HC PL APO CS2 63x/1.2 water immersion objective lens. SYTO 9, Gfp and IP excitation was performed at 488 nm with an argon laser, and the emitted fluorescence was recorded within the range 500–550 nm on hybrid detectors. SYTO 61 or mCherry excitation was performed at 561 nm with an argon laser, and the emitted fluorescence was recorded within the range 600–750 nm on hybrid detectors. The 3D (xyz) acquisitions were performed (512 × 512 pixels, pixel size 0.361 µm, 1 image every z = 1 µm with a scan speed of 600 Hz). For 4D (xyzt) acquisitions an image was taken every 1 hour for 48 hours. Easy 3D and 4D projections were constructed from Z-series images using IMARIS v9.0 software (Bitplane AG, Zurich, Switzerland).

Image analysis

Projections of the biofilm structural dynamic were constructed from xyzt images series using IMARIS 9.3 (Bitplane, Switzerland). Space-time kymographs were constructed with the BiofilmQ visualisation toolbox from 4D-CLSM series [84].

ACKNOWLEDGMENTS

This work was supported by INRAE. Y. Dergham is the recipient of fundings from the Union of Southern Suburbs Municipalities of Beirut, INRAE, Campus France PHC CEDRE 42280PF and Fondation AgroParisTech. P. Sanchez-Vizuete was the recipient of a PhD grant from the Région Ile-de-France (DIM ASTREA). M. Jules is acknowledged for the gift of plasmids pBSB2 and pBSB8, and of strains BBA0093, BBA0231, BBA0290 and BBA0428. M. Calabre (INRAE) is acknowledged for technical assistance. This work is performed under the umbrella of the European Space Agency Topical Team: Biofilms from an interdisciplinary perspective.

REFERENCES

[1] H. Vlamakis, Y. Chai, P. Beauregard, R. Losick, and R. Kolter, "Sticking together: Building a biofilm the *Bacillus subtilis* way," *Nature Reviews Microbiology*, vol. 11, no. 3. pp. 157–168, Mar-2013.

[2] P. S. Stewart and M. J. Franklin, "Physiological heterogeneity in biofilms," *Nat. Rev. Microbiol.*, vol. 6, no. 3, pp. 199–210, 2008.

[3] K. P. Lemon, A. M. Earl, H. C. Vlamakis, C. Aguilar, and R. Kolter, "Biofilm Development with an Emphasis on *Bacillus subtilis*," *Curr Top Microbiol Immunol*, vol. 322, no. 1, pp. 1–16, 2008.

[4] A. Bridier, D. Le Coq, F. Dubois-Brissonnet, V. Thomas, A. Stéphane, and R. Briandet, "The Spatial Architecture of *Bacillus subtilis* Biofilms Deciphered Using a Surface-Associated Model and In Situ Imaging," *PLoS One*, vol. 6, no. 1, p. e16177, 2011.

[5] S. S. Branda, J. E. G. Lez-Pastor, S. Ben-Yehuda, R. Losick, and R. Kolter, "Fruiting body formation by *Bacillus subtilis*," *PNAS*, vol. 98, no. 2, pp. 11621–26, 2001.

[6] Y. Dergham *et al.*, "Comparison of the Genetic Features Involved in *Bacillus subtilis* Biofilm Formation Using Multi-Culturing Approaches," *Microorganisms*, vol. 9, no. 633, 2021.

[7] T. M. Barbosa, C. R. Serra, R. M. La Ragione, M. J. Woodward, and A. O. Henriques, "Screening for *Bacillus* Isolates in the Broiler Gastrointestinal Tract," *Appl. Environ. Microbiol.*, vol. 71, no. 2, pp. 968–978, 2005.

[8] N. K. M. Tam *et al.*, "The intestinal life cycle of *Bacillus subtilis* and close relatives," *J. Bacteriol.*, vol. 188, no. 7, pp. 2692–2700, 2006.

[9] H. A. Hong *et al.*, "*Bacillus subtilis* isolated from the human gastrointestinal tract," *Res. Microbiol.*, vol. 160, pp. 134–143, 2008.

[10] Y. Inatsu, N. Nakamura, Y. Yuriko, T. Fushimi, L. Watanasiritum, and S. Kawamoto, "Characterization of *Bacillus subtilis* strains in Thua nao, a traditional fermented soybean food in northern Thailand," *Lett Appl Microbiol*, vol. 43, no. 3, pp. 237–42, 2006.

[11] H. P. Bais, R. Fall, and J. M. Vivanco, "Biocontrol of *Bacillus subtilis* against Infection of Arabidopsis Roots by Pseudomonas syringae Is Facilitated by Biofilm Formation and Surfactin Production," *Plant Physiol.*, vol. 134, pp. 307–319, 2004.

[12] M. Marzorati *et al.*, "*Bacillus subtilis* HU58 and *Bacillus coagulans* SC208 probiotics reduced the effects of antibiotic-induced gut microbiome dysbiosis in an M-SHIME® model," *Microorganisms*, vol. 8, no. 7, pp. 1–15, 2020.

[13] H. A. Hong, H. D. Le, and S. M. Cutting, "The use of bacterial spore formers as probiotics," *FEMS Microbiol. Rev.*, vol. 29, no. 4, pp. 813–835, 2005.

[14] M. Lefevre *et al.*, "Safety assessment of *Bacillus subtilis* CU1 for use as a probiotic in humans," *Regul. Toxicol. Pharmacol.* vol. 83, pp. 54–65, 2017.

[15] D. J. H. Martin, S. P. Denyer, G. McDonnell, and J. Y. Maillard, "Resistance and cross-resistance to oxidising agents of bacterial isolates from endoscope washer disinfectors," *J. Hosp. Infect.*, vol. 69, no. 4, pp. 377–383, 2008.

[16] A. Bridier *et al.*, "Biofilms of a *Bacillus subtilis* Hospital Isolate Protect Staphylococcus aureus from Biocide Action," *PLoS One*, vol. 7, no. 9, 2012.

[17] W. Klein, M. H. W. Weber, and M. A. Marahiel, "Cold shock response of *Bacillus subtilis*: Isoleucine-dependent switch in the fatty acid branching pattern for membrane adaptation to low temperatures," *J. Bacteriol.*, vol. 181, no. 17, pp. 5341–5349, 1999.

[18] T. Hoffmann and E. Bremer, "Protection of *Bacillus subtilis* against cold stress via compatible-solute acquisition," *J. Bacteriol.*, vol. 193, no. 7, pp. 1552–1562, 2011.

[19] D. Lopez, H. Vlamakis, and R. Kolter, "Generation of multiple cell types in *Bacillus subtilis*," *FEMS Microbiol. Rev.*, vol. 33, no. 1, pp. 152–163, 2009.

[20] M. A. Hamon and B. A. Lazazzera, "The sporulation transcription factor Spo0A is required for biofilm development in *Bacillus subtilis*," 2001.

[21] R. M. Harshey, "Bacterial motility on a surface: many ways to a common goal," *Annu. Rev. Microbiol*, vol. 57, pp. 249–73, 2003.

[22] D. Julkowska, M. Obuchowski, I. B. Holland, and S. J. Séror, "Branched swarming patterns on a synthetic medium formed by wild-type *Bacillus subtilis* strain 3610: Detection of different cellular morphologies and constellations of cells as the complex architecture develops," *Microbiology*, vol. 150, no. 6, pp. 1839–1849, 2004.

[23] D. Julkowska *et al.*, "Comparative Analysis of the Development of Swarming Communities of *Bacillus subtilis* 168 and a Natural Wild Type: Critical Effects of Surfactin and the Composition of the Medium," *Society*, vol. 187, no. 1, pp. 65–76, 2005.

[24] K. Hamze *et al.*, "Identification of genes required for different stages of dendritic swarming in *Bacillus subtilis*, with a novel role for *phrC*," *Microbiology*, vol. 155, no. 2, pp. 398–412, 2009.

[25] L. Hamouche *et al.*, "*Bacillus subtilis* Swarmer Cells Lead the Swarm, Multiply, and Generate a Trail of Quiescent Descendants," *MBio*, vol. 8, no. 1, pp. 1–14, 2017.

[26] I. Grobas, M. Polin, and M. Asally, "Swarming bacteria undergo localized dynamic phase transition to form stress-induced biofilms," *Elife*, vol. 10, pp. 1–22, 2021.

[27] P. Sanchez-Vizuete, D. Le Coq, A. Bridier, J.-M. Herry, S. Aymerich, and R. Briandet, "Identification of *ypqP* as a New *Bacillus subtilis* Biofilm Determinant That Mediates the Protection of *Staphylococcus aureus* against Antimicrobial Agents in Mixed-Species Communities," *Appl Env. Microbiol*, vol. 81, no. 1, pp. 109–118, 2015.

[28] H. Vlamakis, C. Aguilar, R. Losick, and R. Kolter, "Control of cell fate by the formation of an architecturally complex bacterial community," *Genes Dev.*, vol. 22, no. 7, pp. 945–953, 2008.

[29] D. López and R. Kolter, "Extracellular signals that define distinct and coexisting cell fates in *Bacillus subtilis*," *FEMS Microbiol. Rev.*, vol. 34, no. 2, pp. 134–149, 2010.

[30] D. B. Kearns and R. Losick, "Cell population heterogeneity during growth of Bacillus subtilis," *Genes Dev.*, vol. 19, no. 24, pp. 3083–3094, 2005.

[31] D. López, M. A. Fischbach, F. Chu, R. Losick, and R. Kolter, "Structurally diverse natural products that cause potassium leakage trigger multicellularity in *Bacillus subtilis*," *Proc. Natl. Acad. Sci. U. S. A.*, vol. 106, no. 1, pp. 280–285, 2009.

[32] M. M. Nakano, R. Magnuson, A. Myers, J. Curry, A. D. Grossman, and P. Zuber, "srfA is an operon required for surfactin production, competence development, and efficient sporulation in *Bacillus subtilis*," *J. Bacteriol.*, vol. 173, no. 5, pp. 1770–1778, 1991.

[33] C. D'Souza, M. M. Nakano, and P. Zuber, "Identification of *comS*, a gene of the *srfA* operon that regulates the establishment of genetic competence in *Bacillus subtilis*," *Proc. Natl. Acad. Sci. U. S. A.*, vol. 91, no. 20, pp. 9397–9401, 1994.

[34] A. Ostrowski, A. Mehert, A. Prescott, T. B. Kiley, and N. R. Stanley-Wall, "YuaB Functions Synergistically with the Exopolysaccharide and TasA Amyloid Fibers To Allow Biofilm Formation by *Bacillus subtilis*," *J. Bacteriol.*, vol. 193, no. 18, pp. 4821–4831, 2011.

[35] K. Kobayashi and M. Iwano, "BslA(YuaB) forms a hydrophobic layer on the surface of *Bacillus subtilis* biofilms," *Mol. Microbiol.*, vol. 85, no. 1, pp. 51–66, 2012.

[36] L. Hobley *et al.*, "BslA is a self-assembling bacterial hydrophobin that coats the *Bacillus subtilis* biofilm," *PNAS*, vol. 98, no. 20, pp. 11621–11626, Aug. 2013.

[37] J. W. Veening, O. A. Igoshin, R. T. Eijlander, R. Nijland, L. W. Hamoen, and O. P. Kuipers, "Transient heterogeneity in extracellular protease production by *Bacillus subtilis*," *Mol. Syst. Biol.*, vol. 4, no. February, 2008.

[38] C. D. Ellermeier, E. C. Hobbs, J. E. Gonzalez-Pastor, and R. Losick, "A three-protein signaling pathway governing immunity to a bacterial cannibalism toxin," *Cell*, vol. 124, no. 3, pp. 549–559, 2006.

[39] B.-J. Haijema, ² J Hahn, J. Haynes, and D. Dubnau, "A ComGA-dependent checkpoint limits growth during the escape from competence," 2001.

[40] J. van Gestel, H. Vlamakis, and R. Kolter, "From Cell Differentiation to Cell Collectives: *Bacillus subtilis* Uses Division of Labor to Migrate," *PLoS Biol.*, vol. 13, no. 4, pp. 1–29, 2015.

[41] T. Pisithkul *et al.*, "Metabolic Remodeling during Biofilm Development of *Bacillus subtilis*," *MBio*, vol. 10, no. 3, 2019.

[42] M. Futo *et al.*, "Embryo-Like Features in Developing *Bacillus subtilis* Biofilms," *Mol. Biol. Evol.*, vol. 38, no. 1, pp. 31–47, 2020.

[43] P. Sanchez-Vizuete *et al.*, "The coordinated population redistribution between *Bacillus subtilis* submerged biofilm and liquid-air pellicle," *Biofilm*, 100065, 2021.

[44] P. Sanchez-Vizuete *et al.*, "Genome Sequences of Two Nondomesticated *Bacillus subtilis* Strains Able To Form Thick Biofilms on Submerged Surfaces," *Genome Announc.*, vol. 25, no. 2, p. 5, 2014.

[45] Z. E. V. Phillips and M. A. Strauch, "*Bacillus subtilis* sporulation and stationary phase gene expression," *Cell. Mol. Life Sci.*, vol. 59, no. 3, pp. 392–402, 2002.

[46] M. Ratnayake-Lecamwasam, P. Serror, K. W. Wong, and A. L. Sonenshein, "*Bacillus subtilis* CodY represses early-stationary-phase genes by sensing GTP levels," *Genes Dev.*, vol. 15, no. 9, pp. 1093–1103, 2001.

[47] A. N. Hall, S. Subramanian, R. T. Oshiro, A. K. Canzoneri, and D. B. Kearns, "SwrD (YlzI) promotes swarming in *Bacillus subtilis* by increasing power to flagellar motors," *J. Bacteriol.*, vol. 200, no. 2, 2018.

[48] K. Abe *et al.*, "Developmentally-Regulated Excision of the SPβ Prophage Reconstitutes a Gene Required for Spore Envelope Maturation in *Bacillus subtilis*," *PLoS Genet.*, vol. 10, no. 10, 2014.

[49] M. Thérien *et al.*, "Surfactin production is not essential for pellicle and root-associated biofilm development of *Bacillus subtilis*," *Biofilm*, vol. 2, p. 100021, Dec. 2020.

[50] N. Steinberg *et al.*, "The extracellular matrix protein TasA is a developmental cue that maintains a motile subpopulation within *Bacillus subtilis* biofilms," *Sci. Signal*, vol. 13, p. 8905, 2020.

[51] S. Paul, X. Zhang, and F. M. Hulett, "Two ResD-controlled promoters regulate *ctaA* expression in *Bacillus subtilis*," *J. Bacteriol.*, vol. 183, no. 10, pp. 3237–3246, 2001.

[52] T. Dubois *et al.*, "The *sps* genes encode an original legionaminic acid pathway required for crust assembly in *Bacillus subtilis*," *MBio*, vol. 11, no. 4, pp. 1–17, 2020.

[53] A. Houry *et al.*, "Bacterial swimmers that infiltrate and take over the biofilm matrix," *PNAS*, vol. 109, no. 32, 2012.

[54] S. Srinivasan, C. Nadir Kaplan, and L. Mahadevan, "A multiphase theory for spreading microbial swarms and films," *Elife*, vol. 8, pp. 1–28, 2019.

[55] M. Ogura, "ZnuABC and ZosA zinc transporters are differently involved in competence development in *Bacillus subtilis*," *J. Biochem.*, vol. 150, no. 6, pp. 615–625, 2011.

[56] F. Coutte *et al.*, "Effect of *pps* disruption and constitutive expression of *srfA* on surfactin productivity, spreading and antagonistic properties of *Bacillus subtilis* 168 derivatives," *J. Appl. Microbiol.*, vol. 109, no. 2, pp. 480–491, 2010.

[57] T. Charbonnier *et al.*, "Molecular and physiological logics of the pyruvate-induced response of a novel transporter in *Bacillus subtilis*," *MBio*, vol. 8, no. 5, pp. 1–18, 2017.

[58] M. H. van den Esker, Á. T. Kovács, and O. P. Kuipers, "YsbA and LytST are essential for pyruvate utilization in *Bacillus subtilis*," *Environ. Microbiol.*, vol. 19, no. 1, pp. 83–94, 2017.

[59] P. Cosmina *et al.*, "Sequence and analysis of the genetic locus responsible for surfactin synthesis in *Bacillus subtilis*," *Mol. Microbiol.*, vol. 8, no. 5, pp. 821–831, 1993.

[60] B. Maier, "Competence and transformation in *Bacillus subtilis*," *Curr. Issues Mol. Biol.*, vol. 37, pp. 57–76, 2020.

[61] Y. Lei, T. Oshima, N. Ogasawara, and S. Ishikawa, "Functional analysis of the protein Veg, which stimulates biofilm formation in *Bacillus subtilis*," *J. Bacteriol.*, vol. 195, no. 8, pp. 1697–1705, 2013.

[62] S. Paruthiyil, A. Pinochet-Barros, X. Huang, and J. D. Helmann, "*Bacillus subtilis* TerC family proteins help prevent manganese intoxication," *J. Bacteriol.*, vol. 202, no. 2, pp. 1–13, 2020.

[63] B. Zhu and J. Stülke, "SubtiWiki in 2018: From genes and proteins to functional network annotation of the model organism *Bacillus subtilis*," *Nucleic Acids Res.*, vol. 46, no. D1, pp. D743–D748, 2018.

[64] M. Ogura and K. Tsukahara, "SwrA regulates assembly of *Bacillus subtilis* DegU via its interaction with N-terminal domain of DegU," *J. Biochem.*, vol. 151, no. 6, pp. 643–655, 2012.

[65] K. Hamze *et al.*, "Single-cell analysis in situ in a *Bacillus subtilis* swarming community identifies distinct spatially separated subpopulations differentially expressing hag (flagellin), including specialized swarmers," *Microbiology*, vol. 157, no. 9, pp. 2456–2469, 2011.

[66] C. Guilhen *et al.*, "Colonization and immune modulation properties of *Klebsiella pneumoniae* biofilm-dispersed cells," *npj Biofilms Microbiomes*, vol. 5, no. 1, 2019.

[67] C. Guilhen *et al.*, "Transcriptional profiling of *Klebsiella pneumoniae* defines signatures for planktonic, sessile and biofilm-dispersed cells," *BMC Genomics*, vol. 17, no. 1, 2016.

[68] S. L. Chua *et al.*, "Dispersed cells represent a distinct stage in the transition from bacterial biofilm to planktonic lifestyles," *Nat. Commun.*, vol. 5, 2014.

[69] M. M. Pettigrew, L. R. Marks, Y. Kong, J. F. Gent, H. Roche-Hakansson, and A. P. Hakansson, "Dynamic changes in the *Streptococcus pneumoniae* transcriptome during transition from biofilm formation to invasive disease upon influenza A virus infection," *Infect. Immun.*, vol. 82, no. 11, pp. 4607–4619, 2014.

[70] D. C. Ellwood and D. W. Tempest, "Control of teichoic acid and teichuronic acid biosyntheses in chemostat cultures of *Bacillus subtilis* var. *niger*.," *Biochem. J.*, vol. 111, no. 1, pp. 1–5, 1969.

[71] S. B. Otto *et al.*, "Privatization of Biofilm Matrix in Structurally Heterogeneous Biofilms," *mSystems*, vol. 5, no. 4, 2020.

[72] W. D. Hamilton, "The genetical evolution of social behavior," *Gr. Sel.*, pp. 23–43, 2017.

[73] S. Arnaouteli *et al.*, "Bifunctionality of a biofilm matrix protein controlled by redox state," *Proc. Natl. Acad. Sci. U. S. A.*, vol. 114, no. 30, pp. E6184–E6191, 2017.

[74] H. Zeriouh, A. de Vicente, A. Pérez-García, and D. Romero, "Surfactin triggers biofilm formation of *Bacillus subtilis* in melon phylloplane and contributes to the biocontrol activity," *Environ. Microbiol.*, vol. 16, no. 7, pp. 2196–2211, 2014.

[75] X. H. Chen *et al.*, "Genome analysis of *Bacillus amyloliquefaciens* FZB42 reveals its potential for biocontrol of plant pathogens," *J. Biotechnol.*, vol. 140, no. 1–2, pp. 27–37, 2009.

[76] R. P. Shivers, S. S. Dineen, and A. L. Sonenshein, "Positive regulation of *Bacillus subtilis ackA* by CodY and CcpA: Establishing a potential hierarchy in carbon flow," *Mol. Microbiol.*, vol. 62, no. 3, pp. 811–822, 2006.

[77] M. Asally *et al.*, "Localized cell death focuses mechanical forces during 3D patterning in a biofilm," *Proc. Natl. Acad. Sci. U. S. A.*, vol. 109, no. 46, pp. 18891–18896, 2012.

[78] J. N. Wilking, V. Zaburdaev, M. De Volder, R. Losick, M. P. Brenner, and D. A. Weitz, "Liquid transport facilitated by channels in *Bacillus subtilis* biofilms," *PNAS*, vol. 110, no. 3, pp. 848–852, 2013.

[79] E. Botella *et al.*, "pBaSysBioII: An integrative plasmid generating *gfp* transcriptional fusions for high-throughput analysis of gene expression in *Bacillus subtilis*," *Microbiology*, vol. 156, no. 6, pp. 1600–1608, 2010.

[80] H. Antelmann, S. Engelmann, R. Schmid, A. Sorokin, A. Lapidus, and M. Hecker, "Expression of a stress- and starvation-induced *dps/pexB*-homologous gene is controlled by the alternative sigma factor σ(B) in *Bacillus subtilis*," *J. Bacteriol.*, vol. 179, no. 23, pp. 7251–7256, 1997.

[81] A. Bridier *et al.*, "Biofilms of a *Bacillus subtilis* Hospital Isolate Protect Staphylococcus aureus from Biocide Action," *PLoS One*, vol. 7, no. 9, 2012.

[82] P. Nicolas *et al.*, "Condition-dependent transcriptome reveals high-level regulatory architecture in *Bacillus subtilis*," *Science (80-.).*, vol. 335, no. March, pp. 1103–1106, 2012.

[83] J. M. Buescher *et al.*, "Global network reorganization during dynamic adaptations of *Bacillus subtilis* metabolism," *Science (80-.)*, vol. 335, no. 6072, pp. 1099–1103, 2012.

[84] R. Hartmann *et al.*, "Quantitative image analysis of microbial communities with BiofilmQ," *Nat. Microbiol.*, vol. 6, no. 2, pp. 151–156, 2021.

SUPPLEMENTARY MATERIAL

Data S1 Raw RNA-seq data for the nine different conditions selected with three biological replicates each (EX, ST, MC, BS, DT, TP, SB, DC and PL)

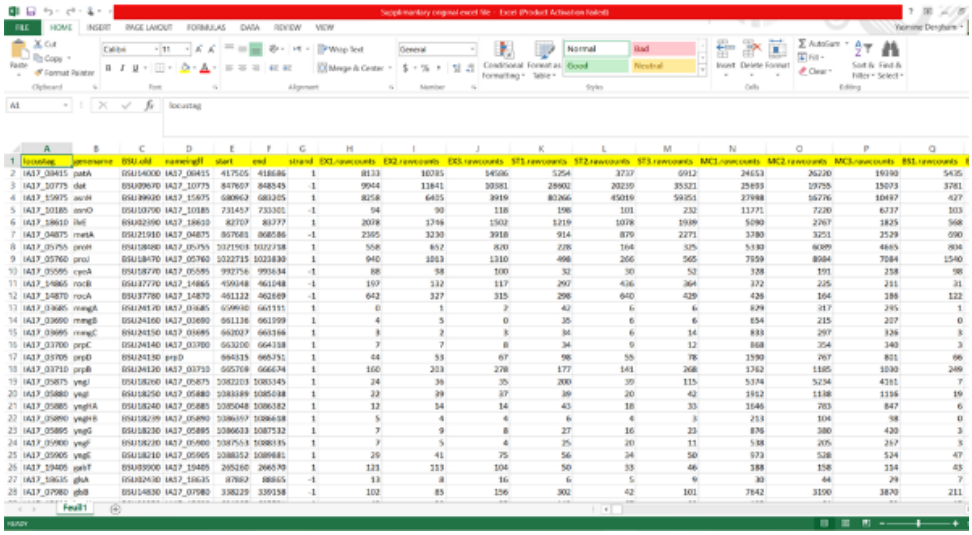

Data S2 Global heatmap for all the different conditions selected pinpointing reported genes selected

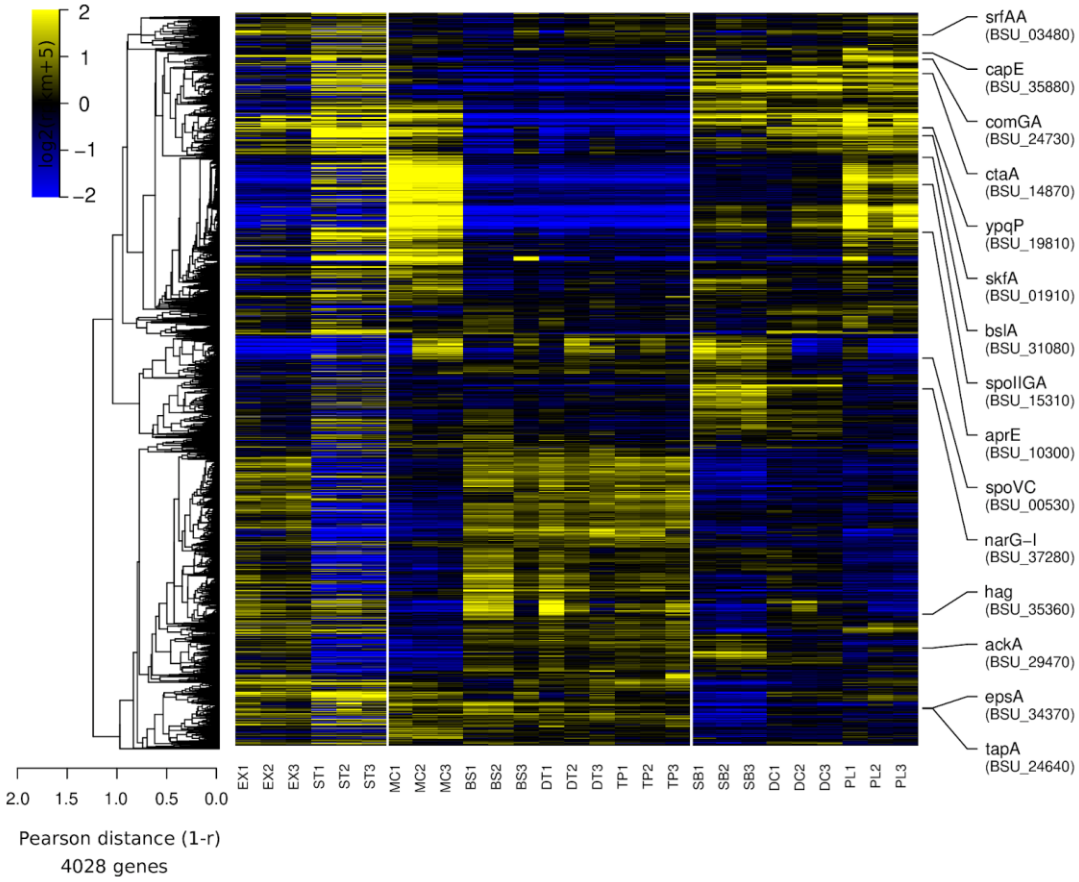

Movie S1: Submerged biofilm dynamics of *B. subtilis* NDmed-GFP with propidium iodide (1 image every 1 hour for 48 hours, Imaris Easy 4D projection representation)

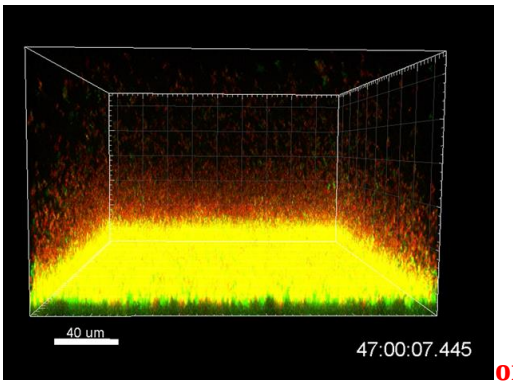

or

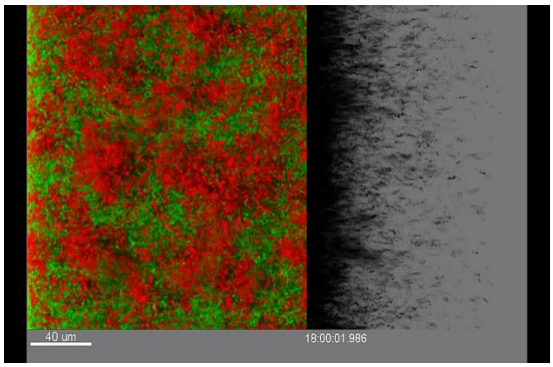

Movie S2: Spatio-temporal observation of strain GM3924, reporting transcription of *hag* by Gfp (in green) and of *tapA* by mCherry (in red) during the submerged biofilm development. (1 image every 1 hour for 48 hours, Imaris Easy 4D projection representation)

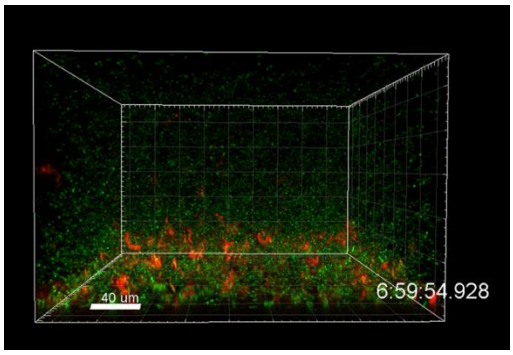

Movie S3: Spatio-temporal observation of strain GM3903, reporting transcription of *ackA* by Gfp (in green) and of *aprE* by mCherry (in red) during the submerged biofilm development. (1 image every 1 hour for 48 hours, Imaris Easy 4D projection representation)

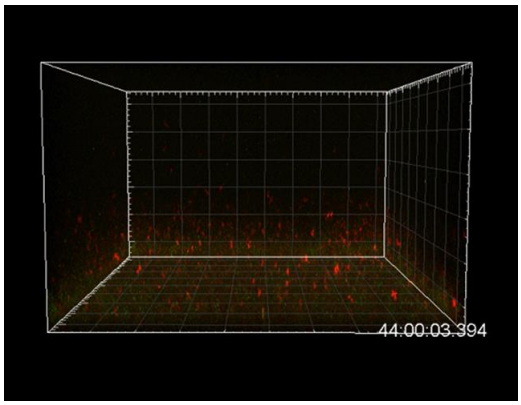

Movie S4: Spatio-temporal observation of strain GM3912, reporting transcription of *comGA* by Gfp (in green) and of *skfA* by mCherry (in red) during the submerged biofilm development. (1 image every 1 hour for 48 hours, Imaris Easy 4D projection representation)

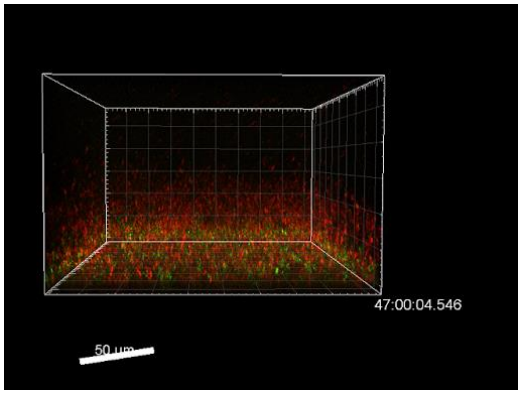

TABLE S1. Forward (F) and reverse (R) primers used for the construction of plasmids with reporter fusions.

Fusion	Primers	Plasmid
PepsA-gfpmut3	F: CCGCGGGCTTTCCCAGCCCTTTAACCGATCATC R: GTTCCTCCTTCCCACCTTCAGCCTTCCCGCG	pBSB2epsA
PypqP-gfpmut3	F: CCGCGGGCTTTCCCAGCTTGCCAAACTCATAAGAATG R: GTTCCTCCTTCCCACCTCCAACTCTCGTTTCTCTAC	pBSB2ypqP
PctaA-gfpmut3	F: CCGCGGGCTTTCCCAGCGTAAGAAGAACGGTGTTTATATTGCC R: GTTCCTCCTTCCCACCCATACTGCTGCAATTTTATATACGTTC	pBSB2ctaA
PnarG-mCherry	F: CCGCGGGCTTTCCCAGCGGCAGTGTCCGTTTTATGGACAC R: GTTCCTCCTTCCCACCCGAGTCAGGTGATGCTAAGTTCAC	pBSB8narG
PskfA-mCherry	F: CCGCGGGCTTTCCCAGCGCTGCCCTGCATCTCGGTTGTG R: GTTCCTCCTTCCCACCAATTTTTGCATAGAGTCTATTGACATAG	pBSB8skfA
PcomGA-gfpmut3	F: CCGCGGGCTTTCCCAGCTCCGATTACAGCTCTGGGTGCC R: GTTCCTCCTTCCCACCCGCATATTGTAGAAAAAGAAGAAAAGG	pBSB2comGA
PaprE- mCherry	F: CCGCGGGCTTTCCCAGCCTGCTATCAAAATAACAGACTCGTG R: GTTCCTCCTTCCCACCAATTCAGAGTAGACTTACTTAAAAGAC	pBSB8aprE
capE- mCherry	F: CCGCGGGCTTTCCCAGCCAAGAGTATGACAATGATCCAAATG R: GTTCCTCCTTCCCACCTGAATTATTTATTGGCGTTTACCGG	pBSB8capE
PspoIIGA- mCherry	F: CCGCGGGCTTTCCCAGCCGTTTACCATTCGTATGCCGCTGA R: GTTCCTCCTTCCCACCCTTGCCTCACGCTGTTCCCCTTC	pBSB8spoIIGA
PspoVC- mCherry	F: CCGCGGGCTTTCCCAGCGAAGTTCCGATTCATCTGACCGGAG R: GTTCCTCCTTCCCACCTCACATAACTCCCGTCTTCATAAAC	pBSB8spoVC
PtapA-gfpmut3 *PtapA- mCherry*	F: CCGCGGGCTTTCCCAGCGGTCCTTCAAAAAATGGAGGACC R: GTTCCTCCTTCCCACCACACTGTAACTTGATATGACAATCG	pBSB2tapA pBSB8tapA

Complement to Paper 3. "Preliminary results on the spatio-temporal heterogeneity of central carbon metabolic fluxes during surface associated multicellular assemblages of *Bacillus subtilis*"

The glycolysis and gluconeogenesis are two oppositely regulated carbon metabolism pathways. In the presence of glycolytic source, B. subtilis will enter into glycolytic pathway where genes such as gapA will intervene, but in the absence of glycolytic source gluconeogenic pathway will be on where genes such as gapB will intervene. When digging through the huge transcriptome data, we have found that in all the spatially selected compartments these regulation were oppositely regulated, except in the submerged both of the genes related for these opposite pathways were upregulated. This had grabbed our curiosity to go further and observe in situ their spatial localization and expression. For this purpose, and with the help of Dominique Le Coq, we were able not only to make individual transcriptional fusions for those genes, but also we have constructed a B. subtilis NDmed strain in which both pathways are reported with a different color (cggR (repressor of the auto-regulated glycolytic cggR-gapA operon) reported by mCherry and gapB by Gfp). Preliminary results by real-time confocal imaging were performed on both the swarming and static liquid culture after 24 hours. Moreover, 4D acquisition for spatio-temporal monitoring has been done for the submerged model for 3 days. We envision to use this first description of the spatio-temporal pattern of expression of these genes as a base of a possible 4th article.

"Preliminary results on the spatio-temporal heterogeneity of central carbon metabolic fluxes during surface associated multicellular assemblages of *Bacillus subtilis*"

In order to grow in a given environment in an optimal manner, bacteria must be able to efficiently use the resources present, among which carbon sources are particularly important. They make it possible to manufacture the precursors essential for the development of the cell, and are also the main source of energy. In *Bacillus subtilis*, the use of these carbon sources is very finely regulated, whether specifically (induction by the source present in the medium of its transporter, as well as of the enzymes involved in its use, and maintenance of the homeostasis of this source in the cell for optimal use), or more generally by a prioritization of preferential use when several glycolytic and/or gluconeogenic carbon sources are present concomitantly. A hierarchy is established giving priority to the most rapidly metabolizable sources by the cell, at the top of which appear glucose and malate (Kleijn et al., 2010). Thus carbon sources can repress the utilization of other less favourable sources by mechanisms of catabolic repression, involving the regulatory protein CcpA for repression by glucose (and by other glycolytic carbon sources), but also by malate (Meyer et al., 2011). Repression by the latter (and possibly by other gluconeogenic carbon sources) also occurs through a mechanism independent of CcpA (Charbonnier et al., 2017). When glucose and malate are both present, these carbon sources can be used together, glucose being metabolized through the glycolysis up to pyruvate, and malate fueling essentially the Krebs cycle (Kleijn et al., 2010). When present as a sole carbon source, glucose or malate generates a glycolytic or gluconeogenic metabolic flux, respectively, which involves essentially the same enzymes having the ability to function reversibly, both in the glycolytic (catabolic) and gluconeogenic (anabolic) direction. However, some enzymes catalyze the reaction only in one direction, due to their expression and activity depending on particular physiological and environmental conditions. Thus, *B. subtilis* possesses two similar but distinct glyceraldehyde-3-phosphate dehydrogenases (GAPDH) (EC 1.2.1.12) catalyzing the oxidative phosphorylation of glyceraldehyde-3-phosphate into 1,3-diphosphoglycerate or the reverse reaction: (i) GapA, a strictly NAD-dependent GAPDH involved in glycolysis, and (ii) GapB, involved in gluconeogenesis and exhibiting a cofactor specificity for NADP (Fillinger et al., 2000). These two GAPDHs are encoded respectively by the

gapA and *gapB* genes, whose expression is subjected to opposite regulation: *gapA* transcription is induced in glycolytic conditions and is repressed during gluconeogenesis by the self-regulated CggR repressor of the *cggR-gapA* operon, whereas gapB is transcribed only during gluconeogenesis and strongly repressed under glycolytic conditions by the CcpN repressor (Fillinger *et al*., 2000; Ludwig *et al*., 2001; Servant et al., 2005). Thus, this key step for both glycolysis and gluconeogenesis is catalyzed in *B. subtilis* by two enzymes specialized either in catabolism (GapA) or in anabolism (GapB), both through their enzymatic characteristics and regulation of their synthesis. The first specific step of the gluconeogenic pathway is catalyzed by the PEP-carboxykinase (PckA) which decarboxylates oxaloacetate from the Krebs cycle, to phosphoenolpyruvate (PEP), above the pyruvate node. This enzyme, absolutely required for gluconeogenesis, belongs to the same CcpN regulon as GapB (Servant et al., 2005). Since the pioneer works of Monod on diauxie (Monod, 1942), most if not all of these physiological and genetic studies on regulation of carbon central metabolism and glycolysis/gluconeogenesis have been performed with planktonic liquid cultures in defined media. Although this allows deciphering several main regulation pathways, these laboratory conditions do not reflect the complexity of the regulations involved in nature.

Bacterial cells are mostly living in mono- or plurispecies communities under different forms, biofilms on solid or semi-solid surfaces, immersed or not, or as floating pellicles at the liquid/air interface, thus leading to different interactions with environment, as well as competition or cooperation between cells for optimal utilization of resources. Studies on *B. subtilis* biofilms have been devoted to their formation and structure, and aiming at identifying genes involved in different aspects of this mode of life: synthesis of matrix, flagella, surfactin or chemotaxis (Dergham *et al.*, 2021). In our global transcriptional analysis, we identified genes differentially and specifically expressed in various differently localized populations of several experimental biofilm models (Dergham *et al.*, in preparation) (Figure1). Although cultures for this study were performed in purely glycolytic conditions, we observed that in the three biofilm models (the mother colony, MC; the submerged biofilm, SB; and the pellicle, PL) expression of *gapB* and *pckA* was derepressed, indicating depletion of the carbon source (glucose) in these compartments. In all the spatial compartments studied, purely glycolytic genes *cggR* and *gapA* were strongly oppositely

regulated to gluconeogenic genes *gapB* and *pckA,* except in the submerged biofilm (SB) in which all were up-regulated (Figure 1A). This suggested that different subpopulations in the same biofilm could adopt different carbon metabolic regimes. ”Waves” of dead cells appearing mainly on top of submerged biofilms could serve as a nutrient for resuming growth of cells, with a metabolic regime locally different from that in cells utilizing only the medium. This led us to take an interest in observation *in situ* of the spatial localization of these subpopulations stratified, segregated, or intertwined) (Figure 1B).

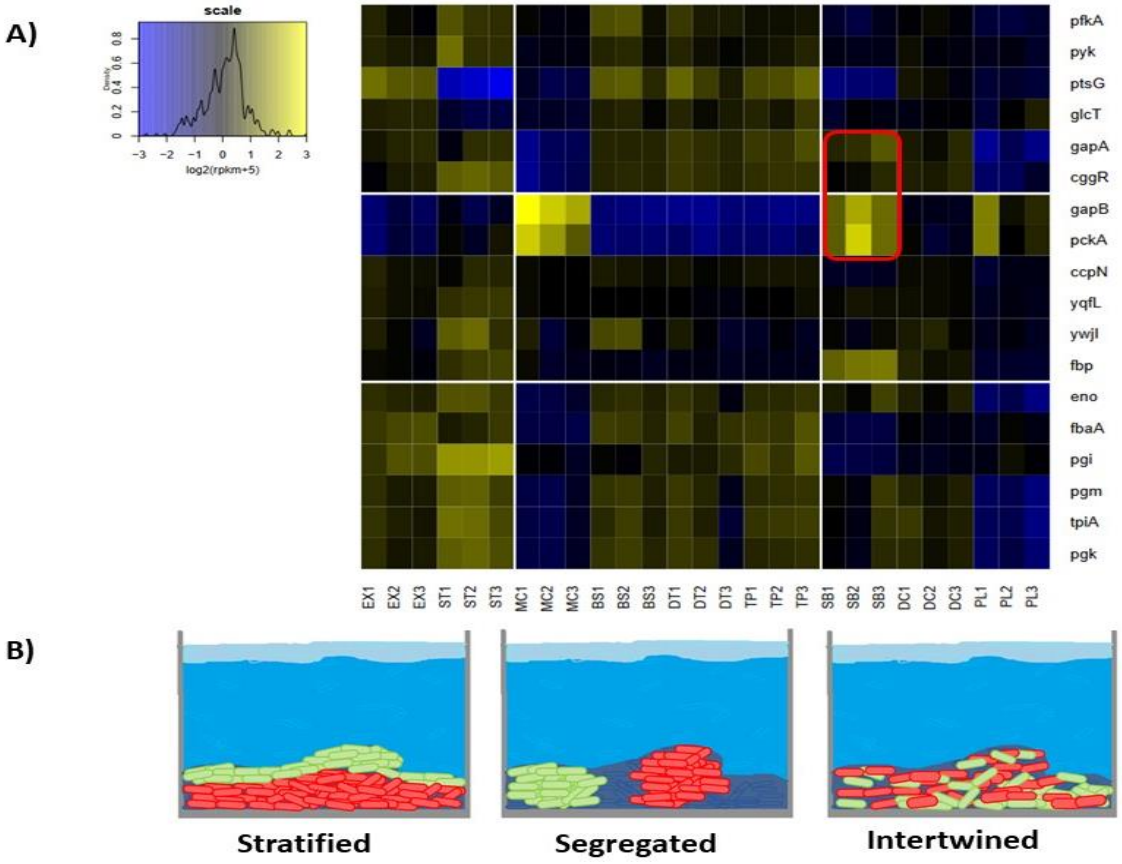

Figure 1: Transcriptome remodeling for carbon metabolism differential expression along the nine spatially localized compartments. A) *Heatmap representation of the relative variations of expression level across samples. The color code reflects the comparison to the mean computed for each gene across all the samples, except the planktonic (EX and ST) (log2 ratio). Genes were selected from Subtiwiki categories for glycolysis and gluconeogenesis (level 3). The yellow box highlights the joint upregulation of both glycolytic and gluconeogenic genes in the same compartment (submerged biofilm, SB).* ***B)*** *Schematic drawing of the different hypothesis proposed for the distribution of subpopulations adopting different carbon metabolic regimes in the submerged biofilm.*

A co-expression of both gluconeogenic and glycolytic genes in the same cell is prevented by their antagonist regulation, and if occurring (*e.g.* in a *ccpN* mutant under glycolytic condition) leads to severe growth defects due to extensive futile cycling through PycA (pyruvate carboxylase), PckA, and PykA (pyruvate kinase) (Tännler *et al.*, 2008). We thus undertook spatio-temporal observations at the single cell level, with a strain reporting expression of both *gapA* and *gapB* by different fluorescent transcriptional fusions to these genes (Table 1).

Table 1. *B. subtilis* strains used in this study

Strain	Relevant genotype	Construction or Reference [a]
BBA9006	BSB168 *PgapB-gfpmut3* (spec)	Botella *et al.*, 2010
GM3378	NDmed *PgapB-gfpmut3* (spec)	BBA9006→NDmed
GM3859	NDmed *PcggR-mCherry* (cm)	pBSB8cggR→NDmed
GM3900	NDmed *PgapB-gfpmut3* (spec),*PcggR-mCherry* (cm)	GM3859→GM3378

[a] *Arrows indicate transformation of pointed strain with indicated plasmid or chromosomal DNA of indicated strain. The transcriptional fusions of the gfpmut3 gene to the gapB promoter was constructed previously within the pBSB2 plasmid (pBaSysBioII) using ligation-independent cloning, prior to integration into the chromosome of BSB168 in a non-mutagenic manner, resulting in strain BBA9006. Plasmid pBSB8cggR derived from pBSB2cggR (Botella et al., 2010) by replacement of the gfpmut3 and spec (spectinomycin resistance) genes by mCherry (codon-optimized for B. subtilis) and cm (chloramphenicol resistance), respectively. BBA9006 and pBSB2cggR are kind gifts from Pr. M. Jules, University Paris-Saclay, AgroParisTech, INRAE).*

Expression of both transcriptional fusions present in strain GM3900 were observed in planktonic liquid cultures in microplates in a microplate reader (Biotek) recording the OD_{600} (growth) and fluorescence emitted by Gfp or mCherry. Conditions of cultures, either glycolytic (B medium) or gluconeogenic (B medium with malate replacing glucose) allowed to validate this strain as expressing specifically either *PcggR-mCherry* or *PgapB-gfpmut3* during exponential phase in the specific condition corresponding for each fusion to its known regulation.

Thus, monitoring transcription of these reporter fusions indicates expression of either glycolytic or gluconeogenic antagonist enzymatic activities (G3PDHs with GapA or GapB, but also PEP-CK with PckA), and therefore the direction of the metabolic flux occurring in a particular cell of a particular compartment and at a particular time.

Using real-time confocal imaging we could observe *in situ* expression of both GapA and GapB in the different spatially localized compartments. Figures 2 and 3 represent a real-time spatial observation of the different compartments of a swarming plate (MC, BS, DT, and TP) and a liquid culture (PL, DC, and SB), respectively.

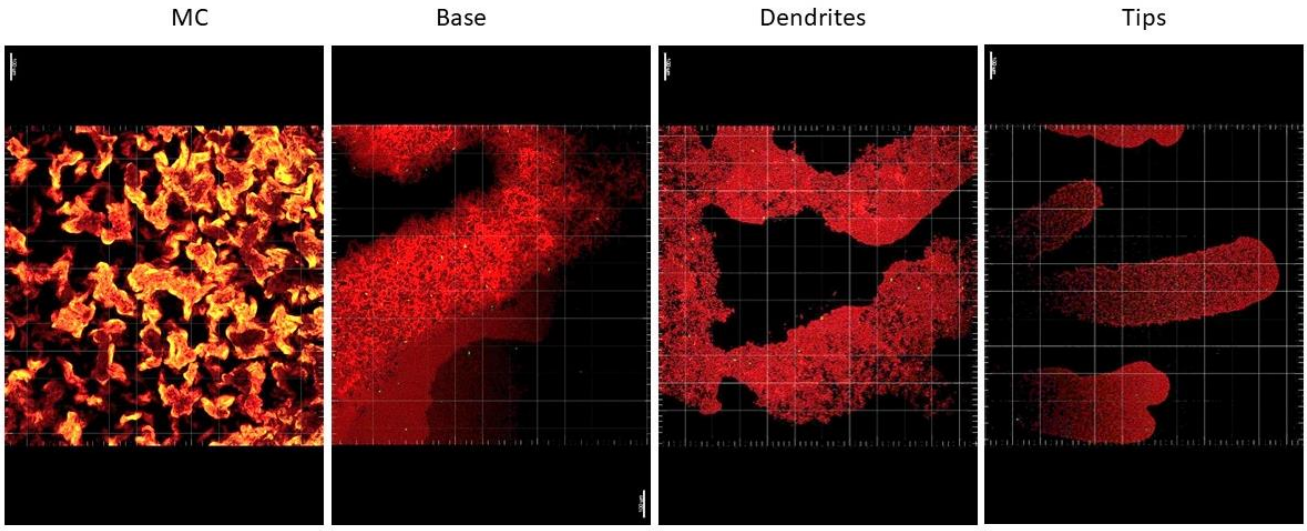

Figure 2: Spatial confocal imaging for the four different compartments in a swarming model. *The mother colony (MC), base (BS), Dendrites (DT) and tips (TP). Using strain GM3900 reporting transcription of cggR(gapA) by mCherry (in red) and gapB by Gfp (in green), with the same protocol as for the transcriptome analysis. After 24 hours of incubation the slice from the plate was transferred to a slide and observed by confocal microscopy. Gfp and mCherry excitation was performed at 488 and 561 nm, respectively, with an argon laser and the emitted fluorescence was recorded within the range 500–550 nm for Gfp and 600-750 nm on hybrid detectors. The 3D (xy) acquisitions were performed by a HC PL FLUOTAR 10x /0.3 DRY objective (512 × 512 pixels, pixel size 0.361 µm, with a scan speed of 600 Hz, and a pinhole 70µm). The scale bar represents 100 µm.*

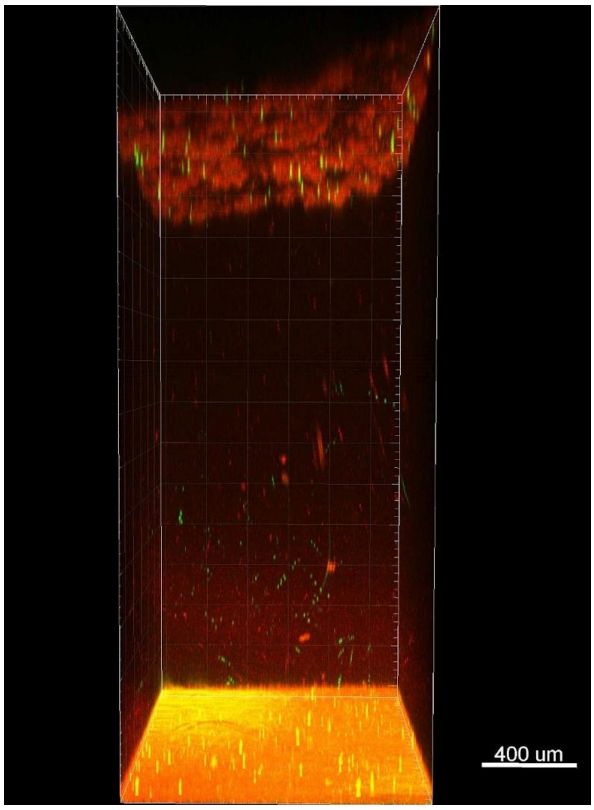

Figure 3: 3D confocal imaging for the static liquid culture after 24 hours of incubation. *Using strain GM3900 reporting transcription of cggR (gapA) by mCherry (in red) and gapB by Gfp (in green), with the same protocol as for the transcriptome analysis, except the usage of 96-well microplates instead of the 12-well. The pellicle (PL), detached cells (DT) and the submerged biofilm (SB) were imaged. Gfp and mCherry excitation was performed at 488 and 561 nm, respectively, with an argon laser and the emitted fluorescence was recorded within the range 500–550 nm for Gfp and 600-750 nm on hybrid detectors. The 3D (xyz) acquisitions were performed by a HC PL FLUOTAR 10x /0.3 DRY objective (512 × 512 pixels, pixel size 0.361 µm, 1 image every z = 20 µm with a scan speed of 600 Hz, and a pinhole70µm). The scale bar represents 400 µm.*

Observation of GM3900 swarming on a glycolytic medium clearly confirmed our previous transcriptome data, from which the glycolytic genes *gapA* and *cggR* appeared upregulated all along the swarming compartments (BS, DT, and TP) and are rather downregulated in the mother colony. On the contrary, expression of the gluconeogenic genes *gapB* and *pckA* was completely repressed in the swarming compartments, and highly upregulated in the mother colony. In liquid culture, gluconeogenic genes were upregulated in both the pellicle and the submerged biofilm models. Interestingly, an upregulation of glycolytic genes was also observed in both the submerged and the detached cells compartments. Microscopy observations using strain GM3900 allowed to display

the coexistence of subpopulations following either a glycolytic or gluconeogenic metabolic regime in all the three biofilm models (PL, SB and MC). We then performed *in situ* spatio-temporal scale observations for the submerged model with a higher resolution (Figure 4).

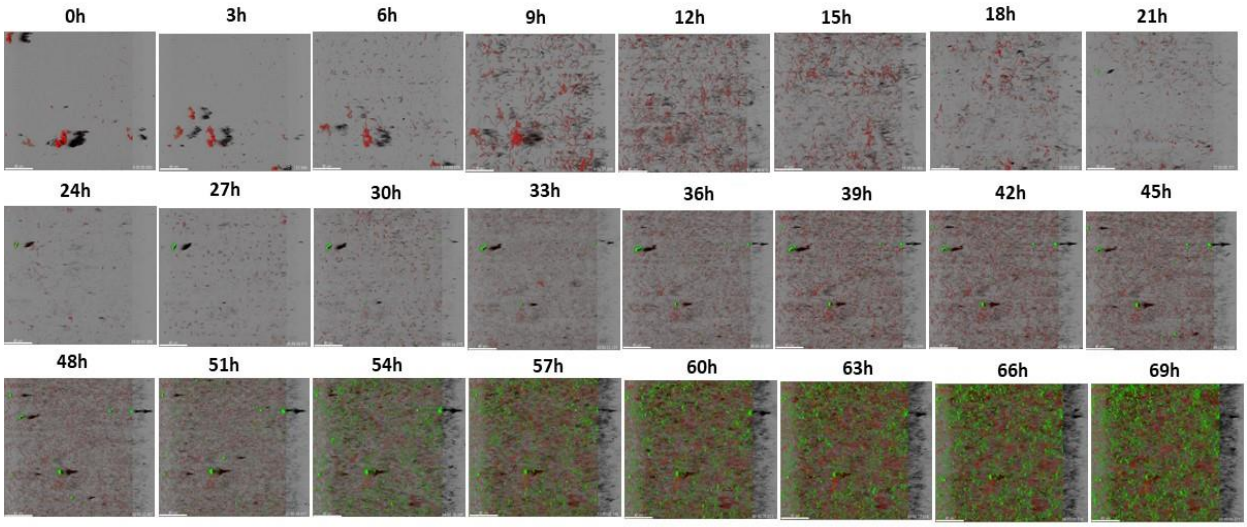

Figure 4: Spatio-temporal 4D imaging for the submerged biofilm model. *Using strain GM3900 reporting transcription of cggR (gapA) by mCherry (in red) and gapB by Gfp (in green), with the same protocol used for the transcriptome analysis, except the usage of 96-well microplates instead of the 12-well. GFP and mCherry excitation was performed at 488 and 561 nm, respectively, with an argon laser and the emitted fluorescence was recorded within the range 500–550 nm for GFP and 600-750 nm on hybrid detectors. The 4D (xyzt) acquisitions were performed by a HC PL FLUOTAR 63x /WATER objective (512 × 512 pixels, pixel size 0.361 µm, 1 image every z = 1 µm with a scan speed of 600 Hz, and a pinholeAiry 1AU) for 3 days. The scale bar represents 40 µm.*

4D confocal imaging of GM3900 shows expression of glycolytic genes (reported by *PcggR-mCherry*) in bacteria growing in a glycolytic minimal medium, gradually decreasing as nutrients become limiting over time. This is faced by a burst of expression of gluconeogenic genes (reported by *PgapB-gfpmut3*) by a few cells, at around 24 hours (Figure 4). After 24 hours, one can observe a slight increase in the number of cells of both subpopulations expressing either glycolytic or gluconeogenic genes, followed after 48 hours by an increase in the cooperative subpopulations expressing opposite carbon metabolism regulatory pathways. These observations could be highly correlated with the oscillations of waves of cell death, the first wave taking place between 13 and 24 hours, followed by a higher second wave of dead cells starting at around 42 hours.

These preliminary data show the coexistence of spatially mixed subpopulations growing either under a glycolytic or gluconeogenic regime in all the three biofilm models: colony, pellicle and submerged biofilm. This observation opens further doors to figure out: *What are the environmental factors that determine this distribution? Are there some metabolite exchanges between these subpopulations? What metabolites do the dead cells provide in the medium?*

References

[1] Botella, E. *et al.* (2010) "pBaSysBioII: An integrative plasmid generating *gfp* transcriptional fusions for high-throughput analysis of gene expression in *Bacillus subtilis*," *Microbiology* **156**(6): 1600–1608, 2010.

[2] Charbonnier, T., Le Coq, D., McGovern, S., Calabre, M., Delumeau, O., Aymerich, S. and Jules, M. (2017) Molecular and Physiological Logics of the Pyruvate-Induced Response of a Novel Transporter in *Bacillus subtilis*. mBio **8**:e00976-17.

[3] Dergham, Y., Sanchez-Vizuete, P., Le Coq, D., Deschamps, J., Bridier, A., Hamze, K. and Briandet, R. (2021) Comparison of the Genetic Features Involved in *Bacillus subtilis* Biofilm Formation Using Multi-Culturing Approaches. *Microorganisms* **9**, 633.

[4] Fillinger, S., Boschi-Muller, S., Azza, S., Dervyn, E., Branlant, G. and Aymerich, S. (2000) Two Glyceraldehyde-3-Phosphate Dehydrogenases with Opposite Physiological Roles in a Nonphotosynthetic Bacterium . *J. Biol. Chem.* **275**(19):14031-14037.

[5] Kleijn, R.J., Buescher, J.M., Le Chat, L., Jules, M., Aymerich, S. and Sauer, U. (2010) Metabolic Fluxes during Strong Carbon Catabolite Repression by Malate in *Bacillus subtilis*. *J. Biol. Chem.* **285**(3): 1587–1596.

[6] Ludwig, H., Homuth, G., Schmalisch, M., Dyka, F.M., Hecker, M. and Stülke, J. (2001) Transcription of Glycolytic Genes and Operons in *Bacillus subtilis*: Evidence for the Presence of Multiple Levels of Control of the *gapA* operon. *J. Mol. Microbiol.* **41**(2):409-422.

[7] Meyer, F.M., Jules, M., Mehne, F.M.P., Le Coq, D., Landmann, J.J., Görke, B., Aymerich, S. and Stülke, J. (2011) Malate-Mediated Carbon Catabolite Repression in *Bacillus subtilis* Involves the HPrK/CcpA Pathway. *J. Bacteriol.* **193**(24):6939-6949.

[8] Monod, J. (1942) Recherches sur la Croissance des Cultures Bactériennes. Thèse. Université de Paris, France.

[9] Servant, P., Le Coq, D. and Aymerich, S. (2005) CcpN (YqzB), a Novel Regulator for CcpA-Independent Catabolite Repression of *Bacillus subtilis* Gluconeogenic Genes. *Molec. Microbiol.* **55**(5), 1435–1451

[10] Tännler, S., Fischer, E., Le Coq, D., Doan, T., Jamet, E., Sauer, U. and Aymerich, S. (2008) CcpN Controls Central Carbon Fluxes in *Bacillus subtilis***.** *J. Bacteriol.* **190**(18): 6178–6187.

GENERAL DISCUSSION & PERSPECTIVES

1. *Bacillus subtilis* is able to form different spatially localized surface-associated communities

B. subtilis, an ubiquitous and non-pathogenic bacterium, is the best studied model organism of Gram-positive bacteria as being naturally transformable, fast growing, easy cultivated, and with an extremely powerful genetic toolbox. In the past two decades, it has been an important model system for studies on the genetic regulations of multicellular behaviors. In this field, most of the studies has been done on two spatially organized communities formed at the air interface (colony and pellicle), and only recently few studies were performed on submerged bacterial communities associated with an inert surface. The latter model was not studied frequently due to the strains specificities and the requirement of more sophisticated techniques of observation and quantification. However, certain specificities are associated with this model (*i.e.* concentration gradient of oxygen, nutrient, waste products, and surface contact, etc.) that could mimic the surface-bounded communities of *B. subtilis* found in natural and industrial environments (in the submerged soil, fermentation of *natto*, pipes, water recovery systems of spacecraft and space station etc. [2], [11], [143]), which makes it a relevant model to consider.

The study of the architecture of the submerged biofilm for *B. subtilis* was made feasible, thanks to former PhD students who optimized the protocol, by coupling an experimental system of biofilm growth in a microplate, a wild type strain (NDmed) capable of forming highly structured biofilms, and confocal microscopy [12]–[14]. The questions that arose were "*Are the genetic regulatory circuits previously described for aerial surface-attached communities, colony and pellicle, the same for the B. subtilis submerged biofilm? What about the expression of the genes described to be required for biofilm formation and its dispersal, are they expressed similarly and do they have the same impact on the three spatially localized surface-bounded communities?"*

By multi-culturing approaches (colony, pellicle, swarming, and submerged models) we have analyzed and compared the structure of the *B. subtilis* multicellular bounded communities using the NDmed strain and series of derivative mutants affected in genes required for motility and biofilm formation. The results obtained in the NDmed context allowed us to visualize that similar behavior could be exhibited between the different surface-associated communities, however some genetic mechanisms could also differ accordingly. For example, we have shown that matrix gene mutants for *tasA*, *epsA-O*, *bslA*, *cap*, and *ypqP* all formed less structured colonies and pellicles with

more efficient swarming motility on semi-agar surface compared to the wild type strain. However, on the submerged level, only major matrix genes (*tasA* and *espA-O*) were able to negatively influence the biofilm development, while the *bslA* mutation has no visible effect on the structure after 24 hours of incubation. A mutant affected in *hag*, a gene required for motility, showed failure to swarm and to form highly structured biofilms. In the NDmed context and in the growth conditions we have used, a *sinR* mutant showed a less wrinkled macrocolony, swarmed all over the plate with multilayered dendritic biofilm, very thin pellicle, and was negatively affected in the submerged model. These observations were opposite to phenotypic observation by Kearns *et al.*, 2005 [216] (except for the submerged model that was not tested in their work); on the other hand, a similar phenotype of the pellicle was observed by Kobayashi *et al.*, 2008 using another *B. subtilis* strain and another medium after 24 hours of incubation [228]. These phenotypic observations point out the specificity linked to the microenvironmental conditions of *B. subtilis* cells encountering these spatially localized communities, in particular:

- The parallel nutrient and oxygen gradients in the submerged, and antiparallel in both the colony and the pellicle models, induce specific cellular behaviors associated with each model [2], [6]. *B. subtilis* is able to grow in both aerobic and anaerobic conditions [133]. In the latter condition, Kolodkin-Gal *et al.*, 2013 have shown that oxygen limitation triggers exopolymer production [218]. Thus, complex spatial organized biofilms formed on the submerged levels under oxygen-deficient conditions could promote matrix production by a subpopulation of cells [163].

- The nature of the substratum on which these surface-bounded communities reside, *i.e.* on solid surface, a nutrient gel or a liquid-air interface modulates the physiology of adherent bacterial cells, as shown by Guégan *et al.*, 2014 [275]. Upon contact with the surface, *B. subtilis* cells sense its proximity by its flagellar rotation acting as a mechanosensor that activates signal transduction cascades for polymer production and biofilm development [193], [208], [276].

Biofilm molecular studies, by phenotypic observation of mutants or temporal transcriptional studies of classical biofilm models (colony or pellicle) led to identification of genetic determinants required for biofilm formation. However, these multicellular communities could display similar genetic expression profiles, but which could also differ considerably. Hence, we have performed a spatial transcriptome analysis on different localized biofilm compartments,

in addition to others, under the same growth conditions to identify a global view on the genetic profile behind the different spatial multicellular communities. This allowed us to pinpoint genes differentially expressed between the different models, with the fineness of their spatio-temporal regulation. Our data give novel insights on the development and dispersal of *B. subtilis* surface-associated communities that will serve as a unique resource for future studies on biofilm physiology to further investigate genetic determinants required for its control.

2. Massive population redistribution and diversification in liquid model

The submerged biofilm model offers the experimental possibility to observe *in situ* the development of biofilm over time. This type of observation is possible by coupling real-time confocal imaging through the bottom of a microplate and the use of virtual fluorescent genetic (GFP, mCherry, mKate2) or chemical (Syto9, Syto61, FM4-64) markers. The 4D acquisition on this type of system revealed that *B. subtilis* biofilm development is a discontinuous biphasic process, which was unexpected and unlike observations on other species, *i.e.* other *Bacilli*, *S. aureus, P. aeruginosa, L. lactis*...

In the first few hours of culture in a rich medium (TSB) bacteria attach to the surface and form long chains of sessile cells producing an extracellular matrix (reported by *tapA* operon). Shortly after, around 3 to 4 hours, a sudden massive fragmentation occurs through differentiation from sessile to motile cells (reported by *hag* gene). This cell differentiation is correlated with oxygen depletion as an environmental trigger leading the cells to become motile and swim to the air interface to form the pellicle after around 7 hours. A similar dynamic observation of population relocalization and cell differentiation has been observed for *B. subtilis* cultured in a minimal medium (B synthetic medium), with temporal variations. During the first 5 hours of submerged biofilm development *B. subtilis* cells highly express major matrix genes (*epsA-O*, *tapA*, and *bslA)*, that are then gradually downregulated in accordance with a sudden fragmentation of sessile cells to motile individual ones. Anaerobic respiration reported by the *narG-I* operon is stochastically expressed by few cells indicating that oxygen depletion stress triggered the cell fragmentation to form afterward the pellicle at the air-liquid interface. The impaired respiration as an environmental signal has already been shown to trigger matrix production (TasA) in *B. subtilis* for colony and pellicle[218]. Spatio-temporal observations on the submerged level confirm such observation in

which *tapA* was expressed in accordance with the *narG-I* operon, however, it seems that at a certain level of oxygen depletion, coordinated cells differentiate from sessile to motile planktonic state seeking for oxygen. This differentiation is correlated with the initiation of the pellicle at the liquid-air interface, observed after an hour from this process. Thus, leading to a biphasic biofilm formation one static liquid culture, on the solid-liquid and liquid-air interfaces.

By temporal monitoring, localized cell death has been observed early during biofilm formation. A correlation between carbon source limitation and cell death has been observed, which was then followed by a heterogeneity in cell types including the initiation of sporulation. We propose (Figure 24) to introduce the subpopulation of dead cells, as an important player, within the life cycle of *B. subtilis* submerged biofilm. In the 48 hours of monitoring different cell types, 6 stages appeared: **i)** Adhesion to the inert surface; **ii)** Biofilm initiation (sessile cells multiplication and matrix production; cells expressing *eps*, *tasA*, *bslA*, *ackA*, and *narG-I*); **iii)** Massive population redistribution (cell differentiation from sessile to motile due to extreme oxygen limitation; reduction in matrix producing cells, a burst of expression of *hag*, reporting motility, with *ackA*, reporting carbon metabolism, still expressed); **iv)** Submerged reorganization and pellicle development (submerged biofilm associated with localized cell death mainly clustered on top and initiation of sporulation, as reported by *spoIIGA*); **v)** Maturation of the two coexisting biofilm models (cellular heterogeneity in motility (*hag*), matrix production (*eps*, *tapA*, *bslA*, *srfAA*, *ypqP*, and *capE-B*), respiration (*ctaA* and *narG-I*), sporulation (*spoIIGA* and *spoVC*), exoprotease production (*aprE*), competency (*comGA*) and cannibalism (*skfA*), all accompanied with a slight revival of growth; **vi)** Emergence of a second wave of dead cells, accompanied with the different cell types (spores, competent cells, cannibals, exoprotease producers and anaerobically respirating cells). The system might not be at equilibrium at this stage: Waves of dead cells could continue to oscillate before a gradual stabilisation; the floating pellicle could sink after longer incubation time, redistributing nutrient resources in the well. Long term monitoring would be necessary to explore a full cycle of population dynamic and heterogeneity inside such an apparently simple microtiter well system.

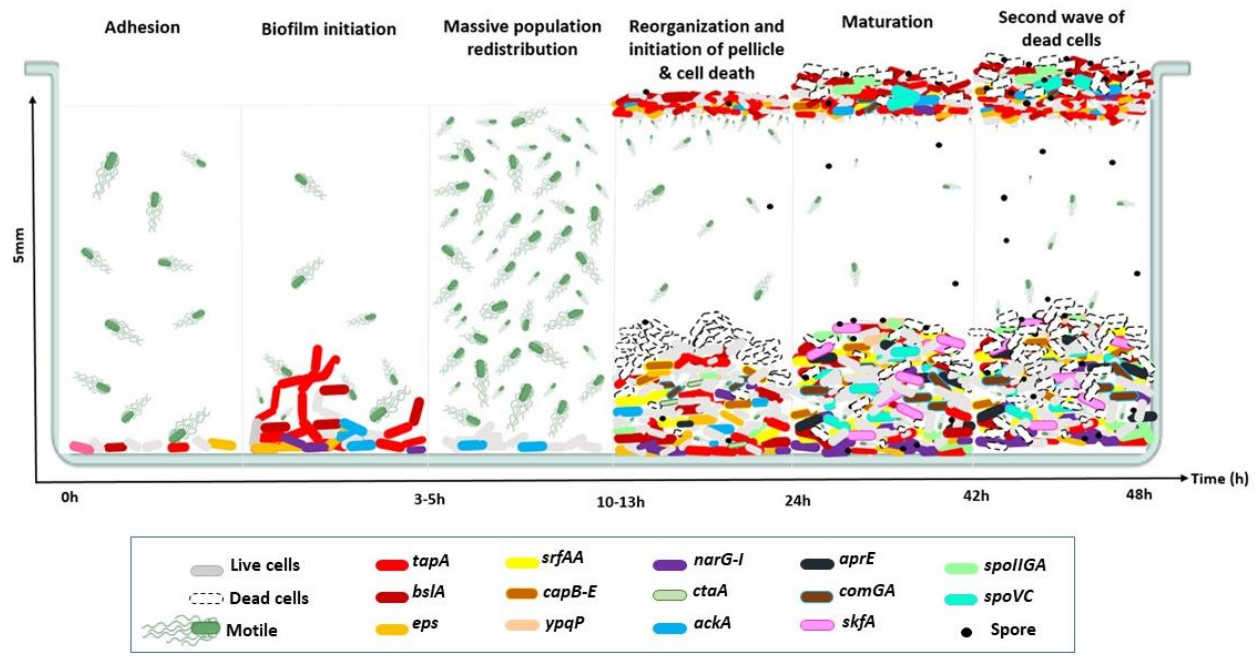

Figure 24: Spatio-temporal diversification of B. subtilis cell types in a well of microplate. *A schematic illustration poposed for the static liquid biofilm dynamics over 48 hours, using a microplate and different reporting techniques. First, cells adhere to the submerged surface, followed by biofilm initiation where adherent sessile cells proliferate expressing matrix genes (i.e. tapA and eps). This is followed by a massive population redistribution, during which a sudden cell differentiation from sessile to motile cells occurs within a 15 minutes range. Then the submerged biofilm is reorganized and the formation of a pellicle is initiated at the air-liquid interface. This is accompanied by a 1st localized cell death wave (between 13 and 24 hours). Maturation of biofilm, associated with a slight increase in the live population is followed by a 2nd wave of cell death (after around 42 hours).*

4D monitoring not only allowed us to observe the different subpopulations of matrix-producing cells that are delightfully controlled and selectively expressed over both spatial and temporal level, but also we were able to detect coexistence of oppositely regulated bacterial cell types, *i.e.* that required for respiration or carbon metabolism. For instance, the spatial transcriptome data displayed the domination of anaerobic respiration in the submerged model compared to the pellicle and the colony in contact with oxygen. Interestingly, confocal imaging showed the coexistence of a small subpopulation under anaerobic respiration within the pellicle and colony, biofilms with air contact. Moreover, as presented in the perspectives for paper 3 (Chapter 3), from the transcriptome data we were able to detect the upregulation of two oppositely regulated pathways, glycolytic and gluconeogenic, in the submerged population. *In situ* spatial observations indicated the coexistence of these two subpopulations in close spatial proximity in all the biofilm

models (colony, pellicle and submerged); even when cultured in pure glycolytic conditions a small subpopulation can adopt a gluconeogenic metabolism, raising questions, *i.e. "Is there exchange of metabolites between these subpopulations? What are these metabolites? What is the relation with the dead cells population?"*

Hence, future attachment is to formally demonstrate the metabolic cooperation between these subpopulations in a biofilm, by putting in use biochemical analysis for the media over time (High-performance liquid chromatography (HPLC) or mass spectrometry…).

3. *B. subtilis* is able to form very different free/migrating cells in laboratory models

Environmental signals, *i.e.* cell density, nutrients or oxygen limitations, trigger cells within the surface-associated multicellular communities to disperse motile cells seeking for better conditions. This requires flagella to move towards favourable or away from unfavourable conditions, a process known as chemotaxis. Subsequently, bacterial cells exhibiting a biofilm must undergo differentiation to become highly motile and able to swim or swarm over different surfaces. By spatial transcriptome study (Chapter 3), we have shown that in liquid static culture the detached cells, formed between the submerged and the pellicle, display a gene expression profile distinct from that of cells in exponential or stationary phase of a planktonic culture, similarly to previous observations on other bacterial species [65]-[68]. Moreover, swarmers (detached cells on agar surface) are not only genetically very distinct from the original mother colony but also distinct from exponential, stationary and detached cells in liquid culture. Although the detached cells, either on agar surface or liquid culture, are distinct from each other, they are both closer to the exponential phase cells than the stationary phase ones. This pinpointed the specificity of the cell population in the stationary phase that is likely an assemblage of very heterogeneous subpopulations.

4. Future perspectives

Even though in a monoculture microbial cells exhibit the same set of genes, only a fraction of these genes are used by any given cell at any given time and space. Thus, within a population cells exhibit heterogeneous gene expression profiles as a consequence of environmental factors, leading to differences between individual cells, which characterizes the structural phenotype of a microbial community. Transcriptome analysis is a powerful tool to identify a global view of the

gene expression profiles for the different studied conditions, guiding for a new understanding of the genetic regulatory pathways associated with these conditions.

Transcriptional analysis to identify new genetic determinants. For an insight into the transcriptome of a cell, RNA sequencing (RNA-seq) provides a higher coverage and a greater resolution of the dynamic nature using the capability of high-throughput sequencing methods. Comparison between different transcriptome analysis profiles, *i.e.* treated and non treated, samples over a temporal scale, samples selected from different spatial localizations…, allows to quantify gene expression and to identify new genetic determinants that could be good candidates to answer certain biological questions of interest. In our study for example, the low expression of matrix genes in the submerged biofilm compared to the other spatially different biofilm models have driven our curiosity to go further, to find that expression of these genes is very heterogeneous with spatio-temporal differences. Beyond the known genes, RNA-seq facilitates the studies of genes poorly characterized or of unknown function. These genes represent a significant number (~30%), differentially expressed between the spatially localized compartments either in a swarming or in the static liquid model. Among those we can mention the *ydgGH* and *ytbDE* operons, which display a gradual increase in their expression going from the base to the tips, or even the *ylxF* and *yscB* genes, which are upregulated in the swarming compartments compared to the mother colony. Similarly, between the adjacent compartments of the static liquid culture we have identified the *ydjJ* and *yoxB* genes downregulated in the detached compared to the submerged, the *yclD* and *ybfA* genes upregulated in the detached compared to the pellicle, and *yjgC* and *ydaC* upregulated in the submerged compared to the pellicle. Moreover, the *yxkC* gene has shown an upregulation in the exponential phase, swarmers (BS, DT, and TP), and in the detached cells compared to stationary or to the three spatial biofilm models studied. Hence, observing *in situ* the spatio-temporal expression of these genes under the microscope, as well as the structural phenotypes of corresponding mutants, could help to assign them to a role at the different specific stages of the swarming process or biofilm development. To expand further our knowledge, we are interested in determining the proteome profiles for the spatial compartments of *B. subtilis* NDmed, which could be compared to the transcriptome results and give some clues on how the transcript levels determine the absolute protein levels.

Advanced methodology for spatial transcriptome. A possibility to get access to more precision in the sampling of biofilm spatial subpopulation is Laser capture microdissection (LCM) [278]. This method allows microscopic scale design of the regions of interest, and is compatible with transcriptomic analysis as long as the sample contains sufficient quantity of RNA. To get access to single cell scale analysis, a recent methodology named par-seqFISH (parallel sequential fluorescence *in situ* hybridization) was developed [277]. This method captures gene expression profiles at a high-throughput level in both planktonic and biofilm models. By par-seqFISH gene expression is detected with preservation of the physical context of individual cells within the spatially structured environments. Interestingly such approach allows to determine transcriptional profiles for hundred thousand bacteria in dozens different conditions, to capture cell biological parameters (*i.e.* cell size), and could be further integrated with specific dyes allowing to measure the chromosome copy number in the same cells.

CRISPR interference screen approach to identify genes whose repression affects biofilm fitness. CRISPRi (CRISPR interference) is a versatile method for silencing gene expression using a catalytically inactive Cas9 protein (dCas9) and single gene-targeting guide RNAs (sgRNAs). CRISPRi has emerged as a powerful genetic tool to dissect the functions of essential and non-essential genes in various bacterial species. Combined with NGS sequencing technologies, CRISPRi is now used successfully to screen large groups of genes using gRNA libraries. These screens allow to quickly identify genes whose repression confers an advantage or a disadvantage or in a particular physiological condition (gene fitness). Marie-Françoise Noirot-Gros in the B3D team is engaged in the construction of the genetic tools to implement this system in *B. subtilis* NDmed. The initial selection of the subset of target genes was based on the RNAseq data generated in this study. This approach will allow us to pinpoint the direct relationships between a gene and a biofilm phenotype, in various conditions.

From laboratory models to applications of *B. subtilis* biofilms: *B. subtilis*, due to its status as a GRAS bacterium and its strong enzymatic potential, is a species with many applications, in particular in the agricultural, industrial and food sectors. Some of these applications exploit the capacity of *B. subtilis* to form biofilms: production of a fermented soy food widely consumed in Japan and having probiotic properties (*natto*); bio-remineralization of monuments or degraded concrete and bioremediation of contaminated soils; bio-control of the persistence of pathogens on

plant crops. A PhD program starting in the B3D team with an industrial partnership aims to develop the protective biofilm concept in livestock buildings. This program includes *B. subtilis* strains and will benefit from the use of the fluorescent transcriptional fusions constructed here to decipher interspecies interactions in various biofilm models.

***B. subtilis* NDmed macrocolony on agar.**

REFERENCES

[1] W. J.Costerton, Z. Lewandowski, D. E. Caldwell, D. R. Korber, and H. M. Lappin-Scott, "Microbial biofilms," *Annu Rev. Microbiol*, no. 49, pp. 711–45, 1995.
[2] H. C. Flemming, J. Wingender, U. Szewzyk, P. Steinberg, S. A. Rice, and S. Kjelleberg, "Biofilms: An emergent form of bacterial life," *Nat. Rev. Microbiol.*, vol. 14, no. 9, pp. 563–575, 2016.
[3] J. W. Costerton, P. S. Stewart, and E. P. Greenberg, "Bacterial biofilms: A common cause of persistent infections," *Science (80-.).*, vol. 284, no. 5418, pp. 1318–1322, 1999.
[4] M. R. Parsek and P. K. Singh, "Bacterial Biofilms: An Emerging Link to Disease Pathogenesis," *Annu. Rev. Microbiol.*, vol. 57, pp. 677–701, 2003.
[5] J. D. Bryers, "Medical biofilms," *Biotechnol. Bioeng.*, vol. 100, no. 1, pp. 1–18, 2008.
[6] P. S. Stewart and M. J. Franklin, "Physiological heterogeneity in biofilms," *Nat. Rev. Microbiol.*, vol. 6, no. 3, pp. 199–210, 2008.
[7] D. Lopez, H. Vlamakis, and R. Kolter, "Generation of multiple cell types in *Bacillus subtilis*," *FEMS Microbiol. Rev.*, vol. 33, no. 1, pp. 152–163, 2009.
[8] H. Vlamakis, C. Aguilar, R. Losick, and R. Kolter, "Control of cell fate by the formation of an architecturally complex bacterial community," *Genes Dev.*, vol. 22, no. 7, pp. 945–953, 2008.
[9] H. Vlamakis, Y. Chai, P. Beauregard, R. Losick, and R. Kolter, "Sticking together: Building a biofilm the *Bacillus subtilis* way," *Nature Reviews Microbiology*, vol. 11, no. 3. pp. 157–168, Mar-2013.
[10] D. López and R. Kolter, "Extracellular signals that define distinct and coexisting cell fates in *Bacillus subtilis*," *FEMS Microbiol. Rev.*, vol. 34, no. 2, pp. 134–149, 2010.
[11] D. J. H. Martin, S. P. Denyer, G. McDonnell, and J. Y. Maillard, "Resistance and cross-resistance to oxidising agents of bacterial isolates from endoscope washer disinfectors," *J. Hosp. Infect.*, vol. 69, no. 4, pp. 377–383, 2008.
[12] A. Bridier, D. Le Coq, F. Dubois-Brissonnet, V. Thomas, A. Stéphane, and R. Briandet, "The Spatial Architecture of *Bacillus subtilis* Biofilms Deciphered Using a Surface-Associated Model and In Situ Imaging," *PLoS One*, vol. 6, no. 1, p. e16177, 2011.
[13] A. Bridier *et al.*, "Biofilms of a *Bacillus subtilis* Hospital Isolate Protect *Staphylococcus aureus* from Biocide Action," *PLoS One*, vol. 7, no. 9, 2012.
[14] P. Sanchez-Vizuete, D. Le Coq, A. Bridier, J.-M. Herry, S. Aymerich, and R. Briandet, "Identification of *ypqP* as a New *Bacillus subtilis* Biofilm Determinant That Mediates the Protection of *Staphylococcus aureus* against Antimicrobial Agents in Mixed-Species Communities," *Appl Env. Microbiol*, vol. 81, no. 1, pp. 109–118, 2015.
[15] L. Hall-Stoodley, J. W. Costerton, and P. Stoodley, "Bacterial biofilms: From the natural environment to infectious diseases," *Nat. Rev. Microbiol.*, vol. 2, no. 2, pp. 95–108, 2004.
[16] L. Hobley, C. Harkins, C. E. MacPhee, and N. R. Stanley-Wall, "Giving structure to the biofilm matrix: An overview of individual strategies and emerging common themes," *FEMS Microbiol. Rev.*, vol. 39, no. 5, pp. 649–669, 2015.
[17] M. T. Costerton JW, Cheng KJ, Geesey GG, Ladd TI, Nickel JC, Dasgupta M, "Bacterial biofilms in nature and disease," *Ann. Rev. Microbiol.*, vol. 41, pp. 435–464, 1987.
[18] H. C. Flemming *et al.*, "Who put the film in biofilm? The migration of a term from wastewater engineering to medicine and beyond," *NPJ Biofilms Microbiomes*, vol. 7, no. 1, pp. 1–5, 2021.
[19] M. Wainwright, "An alternative view of the early history of microbiology," *Adv. Appl. Microbiol.*, vol. 52, pp. 333–355, 2003.
[20] L. Hall-Stoodley and P. Stoodley, "Evolving concepts in biofilm infections," *Cell.*

Microbiol., vol. 11, no. 7, pp. 1034–1043, 2009.
[21] N. Høiby, "A short history of microbial biofilms and biofilm infections," *APMIS*, vol. 125, pp. 272–275, 2017.
[22] M. H. Michel Vert, Yoshiharu Doi, Karl-Heinz Hellwich and and F. S. Philip Hodge, Przemyslaw Kubisa, Marguerite Rinaudo, "Terminology for biorelated polymers and applications (IUPAC Recommendations 2012)," *Pure Appl. Chem.*, vol. 84, no. 2, pp. 377–410, 2012.
[23] H. C. Flemming and S. Wuertz, "Bacteria and archaea on Earth and their abundance in biofilms," *Nat. Rev. Microbiol.*, vol. 17, no. 4, pp. 247–260, 2019.
[24] P. Stoodley, K. Sauer, D. G. Davies, and J. W. Costerton, "Biofilms as complex differentiated communities," *Annu. Rev. Microbiol.*, vol. 56, pp. 187–209, 2002.
[25] M. E. Davey and G. A. O'toole, "Microbial Biofilms: from Ecology to Molecular Genetics," *Microbiol. Mol. Biol. Rev.*, vol. 64, no. 4, pp. 847–867, 2000.
[26] M. A. Hassani, P. Durán, and S. Hacquard, "Microbial interactions within the plant holobiont," *Microbiome*, p. 6:58, 2018.
[27] W. K. Mousa, C. Shearer, V. Limay-Rios, C. L. Ettinger, J. A. Eisen, and M. N. Raizada, "Root-hair endophyte stacking in finger millet creates a physicochemical barrier to trap the fungal pathogen *Fusarium graminearum*," *Nat. Microbiol.*, vol. 1, no. December, 2016.
[28] E. G. Ruby and M. J. Mcfall-Ngai, "A Squid That Glows in the Night: Development of an Animal-Bacterial Mutualism," 1992.
[29] E. R. Rotman *et al.*, "Natural Strain Variation Reveals Diverse Biofilm Regulation in Squid-Colonizing Vibrio fischeri," *J Bacteriol*, vol. 201, pp. 33–52, 2021.
[30] Y. Chen *et al.*, "Biocontrol of tomato wilt disease by *Bacillus subtilis* isolates from natural environments depends on conserved genes mediating biofilm formation," 2012.
[31] B. Halan, K. Buehler, and A. Schmid, "Biofilms as living catalysts in continuous chemical syntheses," *Trends Biotechnol.*, vol. 30, no. 9, pp. 453–465, 2012.
[32] R. Singh, D. Paul, and R. K. Jain, "Biofilms: implications in bioremediation," *Trends Microbiol.*, vol. 14, no. 9, pp. 389–397, 2006.
[33] B. Erable, M. A. Roncato, W. Achouak, and A. Bergel, "Sampling natural biofilms: A new route to build efficient microbial anodes," *Environ. Sci. Technol.*, vol. 43, no. 9, pp. 3194–3199, 2009.
[34] E. Rosenberg, E. F. Delong, S. Lory, E. Stackebrandt and F. Thompson, *The Prokaryotes - Mycobacterium*. 2006.
[35] I. B. Beech and J. Sunner, "Biocorrosion: Towards understanding interactions between biofilms and metals," *Curr. Opin. Biotechnol.*, vol. 15, no. 3, pp. 181–186, 2004.
[36] H. C. Flemming, M. Meier, and T. Schild, "Mini-review: Microbial problems in paper production," *Biofouling*, vol. 29, no. 6, pp. 683–696, 2013.
[37] D. Davies, "Understanding biofilm resistance to antibacterial agents," *Nat. Rev. Drug Discov.*, vol. 2, no. 2, pp. 114–122, Feb. 2003.
[38] C. Moser *et al.*, "Immune Responses to *Pseudomonas aeruginosa* Biofilm Infections," *Front. Imunol.*, vol. 12, no. 625597, 2021.
[39] V. E. Wagner and B. H. Iglewski, "*P. aeruginosa* Biofilms in CF Infection," *Clinical reviews in allergy & immunology*, 35(3), 124–134. 2008.
[40] C. W. Hall and T.-F. Mah, "Molecular mechanisms of biofilm-based antibiotic resistance and tolerance in pathogenic bacteria," *FEMS Microbiol. Rev.*, vol. 010, pp. 276–301, 2017.
[41] A. D. Verderosa, M. Totsika, and K. E. Fairfull-Smith, "Bacterial Biofilm Eradication Agents: A Current Review," *Front. Chem.*, vol. 7, no. November, pp. 1–17, 2019.

[42] M. R. Parsek and T. Tolker-Nielsen, “Pattern formation in *Pseudomonas aeruginosa* biofilms,” *Curr. Opin. Microbiol.*, vol. 11, no. 6, pp. 560–566, 2008.
[43] N. Høiby *et al.*, “The clinical impact of bacterial biofilms,” *Int. J. Oral Sci.*, vol. 3, no. 2, pp. 55–65, 2011.
[44] N. Høiby, T. Bjarnsholt, M. Givskov, S. Molin, and O. Ciofu, “Antibiotic resistance of bacterial biofilms,” *Int. J. Antimicrob. Agents*, vol. 35, no. 4, pp. 322–332, 2010.
[45] R. A. Fasani and M. A. Savageau, “Unrelated toxin-antitoxin systems cooperate to induce persistence,” *J. R. Soc. Interface*, vol. 12, no. 108, 2015.
[46] R. Wolcott, J. W. Costerton, D. Raoult, and S. J. Cutler, “The polymicrobial nature of biofilm infection,” *Clin. Microbiol. Infect.*, vol. 19, no. 2, pp. 107–112, 2013.
[47] I. Pastar *et al.*, “Interactions of Methicillin Resistant *Staphylococcus aureus* USA300 and *Pseudomonas aeruginosa* in Polymicrobial Wound Infection,” *PLoS One*, vol. 8, no. 2, pp. 1–11, 2013.
[48] B. M. Peters, M. A. Jabra-Rizk, M. A. Scheper, J. G. Leid, J. W. Costerton, and M. E. Shirtliff, “Microbial interactions and differential protein expression in *Staphylococcus aureus* -Candida albicans dual-species biofilms,” *FEMS Immunol. Med. Microbiol.*, vol. 59, no. 3, pp. 493–503, 2010.
[49] K. T. Elvers, K. Leeming, and H. M. Lappin-Scott, “Binary and mixed population biofilms: Time-lapse image analysis and disinfection with biocides,” *J. Ind. Microbiol. Biotechnol.*, vol. 29, no. 6, pp. 331–338, 2002.
[50] S. Behnke, A. E. Parker, D. Woodall, and A. K. Camper, “Comparing the chlorine disinfection of detached biofilm clusters with those of sessile biofilms and planktonic cells in single- and dual-species cultures,” *Appl. Environ. Microbiol.*, vol. 77, no. 20, pp. 7176–7184, 2011.
[51] P. M. Alves, E. Al-Badi, C. Withycombe, P. M. Jones, K. J. Purdy, and S. E. Maddocks, “Interaction between *Staphylococcus aureus* and *Pseudomonas aeruginosa* is beneficial for colonisation and pathogenicity in a mixed biofilm,” *Pathog. Dis.*, vol. 76, no. 1, pp. 1–10, 2018.
[52] M. Habash and G. Reid, “Microbial Biofilms: Their Development and Significance for Medical Device—Related Infections,” 1999.
[53] I. Francolini and G. Donelli, “Prevention and control of biofilm-based medical-device-related infections,” *FEMS Immunol Med Microbiol*, vol. 59(3):227-, 2010.
[54] M. Haque, M. Sartelli, J. Mckimm, and M. Abu Bakar, “Health care-associated infections-an overview,” *Infect. Drug Resist.*, vol. 11, no. 1, pp. 2321–2333, 2018.
[55] F. Quignon, M. Sardin, L. Kiene, and L. Schwartzbrod, “Poliovirus-1 inactivation and interaction with biofilm: A pilot-scale study,” *Appl. Environ. Microbiol.*, vol. 63, no. 3, pp. 978–982, 1997.
[56] M. I. Thoulouze and A. Alcover, “Can viruses form biofilms?,” *Trends Microbiol.*, vol. 19, no. 6, pp. 257–262, 2011.
[57] R. G. Von Borowski, “Biofilms and Coronavirus Reservoirs : a Perspective Review,” vol. 87, no. 18, pp. 1–14, 2021.
[58] J. A. Otter *et al.*, “Surface-attached cells, biofilms and biocide susceptibility: Implications for hospital cleaning and disinfection,” *J. Hosp. Infect.*, vol. 89, no. 1, pp. 16–27, 2015.
[59] J. E. Nett, K. M. Guite, A. Ringeisen, K. A. Holoyda, and D. R. Andes, “Reduced biocide susceptibility in Candida albicans biofilms,” *Antimicrob. Agents Chemother.*, vol. 52, no. 9, pp. 3411–3413, 2008.
[60] P. S. Stewart and J. W. Costerton, “Antibiotic resistance of bacteria in biofilms,” *Lancet*,

vol. 358, no. 9276, pp. 135–138, 2001.
[61] P. Stoodley and P. Dirckx, “Biofilm formation in 3 steps.,” *In http://www.biofilm.montana.edu/resources/images/multicellularextracellular/biofilm–formation–3–steps.html.*; Center for Biofilm Engeneering, Montana State University, Bozeman, 2003.
[62] J. K. Hyun, J. Q. Boedicker, W. C. Jang, and R. F. Ismagilov, “Defined spatial structure stabilizes a synthetic multispecies bacterial community,” *Proc. Natl. Acad. Sci. U. S. A.*, vol. 105, no. 47, pp. 18188–18193, 2008.
[63] C. D. Nadell, K. Drescher, and K. R. Foster, “Spatial structure, cooperation and competition in biofilms,” *Nat. Rev. Microbiol.*, vol. 14, no. 9, pp. 589–600, 2016.
[64] H. J. Gilbert and G. P. Hazlewood, “Bacterial cellulases and xylanases,” *J. Gen. Microbiol.*, vol. 139, no. 2, pp. 187–194, 1993.
[65] S. D. Allison, “Cheaters, diffusion and nutrients constrain decomposition by microbial enzymes in spatially structured environments,” *Ecol. Lett.*, vol. 8, no. 6, pp. 626–635, 2005.
[66] W. W. Driscoll and J. W. Pepper, “Theory for the evolution of diffusible external goods,” *Evolution (N. Y).*, vol. 64, no. 9, pp. 2682–2687, 2010.
[67] B. Allen, J. Gore, and M. A. Nowak, “Spatial dilemmas of diffusible public goods,” *Elife*, vol. 2013, no. 2, pp. 1–11, 2013.
[68] C. D. Nadell, K. R. Foster, and J. B. Xavier, “Emergence of spatial structure in cell groups and the evolution of cooperation,” *PLoS Comput. Biol.*, vol. 6, no. 3, 2010.
[69] T. Pfeiffer, S. Schuster, and S. Bonhoeffer, “Cooperation and competition in the evolution of ATP-producing pathways,” *Science (80-.).*, vol. 292, no. 5516, pp. 504–507, 2001.
[70] G. D’Souza, S. Shitut, D. Preussger, G. Yousif, S. Waschina, and C. Kost, “Ecology and evolution of metabolic cross-feeding interactions in bacteria,” *Nat. Prod. Rep.*, vol. 35, no. 5, pp. 455–488, 2018.
[71] G. P. Dubey and S. Ben-Yehuda, “Intercellular nanotubes mediate bacterial communication,” *Cell*, vol. 144, no. 4, pp. 590–600, 2011.
[72] A. Ducret, B. Fleuchot, P. Bergam, and T. Mignot, “Direct live imaging of cell-cell protein transfer by transient outer membrane fusion in *Myxococcus xanthus*,” *Elife*, vol. 2013, no. 2, pp. 1–15, 2013.
[73] A. T. Jan, “Outer Membrane Vesicles (OMVs) of gram-negative bacteria: A perspective update,” *Front. Microbiol.*, vol. 8, no. JUN, pp. 1–11, 2017.
[74] O. Hallatschek and D. R. Nelson, “Gene surfing in expanding populations,” *Theor. Popul. Biol.*, vol. 73, no. 1, pp. 158–170, 2008.
[75] J. D. Van Dyken, M. J. I. Müller, K. M. L. MacK, and M. M. Desai, “Spatial population expansion promotes the evolution of cooperation in an experimental prisoner’s dilemma,” *Curr. Biol.*, vol. 23, no. 10, pp. 919–923, 2013.
[76] E. R. Oldewurtel, N. Kouzel, L. Dewenter, K. Henseler, and B. Maier, “Differential interaction forces govern bacterial sorting in early biofilms,” *Elife*, vol. 4, no. September, pp. 1–21, 2015.
[77] S. Ishii, T. Kosaka, K. Hori, Y. Hotta, and K. Watanabe, “Coaggregation facilitates interspecies hydrogen transfer between *Pelotomaculum thermopropionicum* and *Methanothermobacter thermautotrophicus*,” *Appl. Environ. Microbiol.*, vol. 71, no. 12, pp. 7838–7845, 2005.
[78] S. S. Branda, Å. Vik, L. Friedman, and R. Kolter, “Biofilms: The matrix revisited,” *Trends Microbiol.*, vol. 13, no. 1, pp. 20–26, 2005.
[79] A. Persat *et al.*, “The mechanical world of bacteria,” *Cell*, vol. 161, no. 5, pp. 988–997, 2015.

[80] D. O. Serra, A. M. Richter, and R. Hengge, "Cellulose as an architectural element in spatially structured *Escherichia coli* biofilms," *J. Bacteriol.*, vol. 195, no. 24, pp. 5540–5554, 2013.
[81] G. E. Pinchuk *et al.*, "Utilization of DNA as a sole source of phosphorus, carbon, and energy by Shewanella spp.: Ecological and physiological implications for dissimilatory metal reduction," *Appl. Environ. Microbiol.*, vol. 74, no. 4, pp. 1198–1208, 2008.
[82] H. Mulcahy, L. Charron-Mazenod, and S. Lewenza, "*Pseudomonas aeruginosa* produces an extracellular deoxyribonuclease that is required for utilization of DNA as a nutrient source," *Environ. Microbiol.*, vol. 12, no. 6, pp. 1621–1629, 2010.
[83] B. B. Christensen *et al.*, "Establishment of new genetic traits in a microbial biofilm community," *Appl. Environ. Microbiol.*, vol. 64, no. 6, pp. 2247–2255, 1998.
[84] F. de la Cruz and J. Davies, "Horizontal gene transfer and the origin of species: lessons from bacteria," *Trends Microbiol.*, vol. 8, no. 3, pp. 128–133, 2000.
[85] D. M. Cornforth *et al.*, "Combinatorial quorum sensing allows bacteria to resolve their social and physical environment," *Proc. Natl. Acad. Sci. U. S. A.*, vol. 111, no. 11, pp. 4280–4284, 2014.
[86] M. K. Kim, F. Ingremeau, A. Zhao, B. L. Bassler, and H. A. Stone, "Local and global consequences of flow on bacterial quorum sensing," *Nat. Microbiol.*, vol. 1, no. 1, pp. 1–5, 2016.
[87] M. R. Parsek and E. P. Greenberg, "Acyl-homoserine lactone quorum sensing in Gram-negative bacteria: A signaling mechanism involved in associations with higher organisms," *Proc. Natl. Acad. Sci. U. S. A.*, vol. 97, no. 16, pp. 8789–8793, 2000.
[88] Matthew R. Parsek, D. L. Val, B. L. Hanzelka, J. E. C. Jr., and E. P. Greenberg, "Acyl homoserine-lactone quorum-sensing signal generation," *Proc. Natl. Acad. Sci. U. S. A.*, vol. 96, no. April, pp. 4360–4365, 1999.
[89] B. A. Annous, P. M. Fratamico, and J. L. Smith, "Scientific status summary: Quorum sensing in biofilms: Why bacteria behave the way they do," *J. Food Sci.*, vol. 74, no. 1, 2009.
[90] J. Schluter, A. P. Schoech, K. R. Foster, and S. Mitri, "The Evolution of Quorum Sensing as a Mechanism to Infer Kinship," *PLoS Comput. Biol.*, vol. 12, no. 4, pp. 1–18, 2016.
[91] C. D. Nadell, J. B. Xavier, S. A. Levin, and K. R. Foster, "The evolution of quorum sensing in bacterial biofilms," *PLoS Biol*, vol. 6, no. 1, p. 14, 2008.
[92] P. A. Risøen, M. B. Brurberg, V. G. H. Eijsink, and I. F. Nes, "Functional analysis of promoters involved in quorum sensing-based regulation of bacteriocin production in *Lactobacillus*," *Mol. Microbiol.*, vol. 37, no. 3, pp. 619–628, 2000.
[93] L. Fontaine *et al.*, "Quorum-sensing regulation of the production of Blp bacteriocins in S*treptococcus thermophilus*," *J. Bacteriol.*, vol. 189, no. 20, pp. 7195–7205, 2007.
[94] D. M. Cornforth and K. R. Foster, "Competition sensing: The social side of bacterial stress responses," *Nat. Rev. Microbiol.*, vol. 11, no. 4, pp. 285–293, 2013.
[95] K. Sauer, A. K. Camper, G. D. Ehrlich, J. W. Costerton, and D. G. Davies, "*Pseudomonas aeruginosa* displays multiple phenotypes during development as a biofilm," *J. Bacteriol.*, vol. 184, no. 4, pp. 1140–1154, 2002.
[96] A. Raj and A. van Oudenaarden, "Nature, Nurture, or Chance: Stochastic Gene Expression and Its Consequences," *Cell*, vol. 135, no. 2, pp. 216–226, 2008.
[97] M. B. Elowitz, A. J. Levine, E. D. Siggia, and P. S. Swain, "Stochastic gene expression in a single cell," *Science (80-.).*, vol. 297, no. 5584, pp. 1183–1186, 2002.
[98] A. D. Co, S. Van Vliet, and M. Ackermann, "Emergent microscale gradients give rise to metabolic cross-feeding and antibiotic tolerance in clonal bacterial populations," *Philos. Trans. R. Soc. B Biol. Sci.*, vol. 374, no. 1786, 2019.

[99] A. Dal Co, M. Ackermann, and S. Van Vliet, "Metabolic activity affects the response of single cells to a nutrient switch in structured populations," *J. R. Soc. Interface*, vol. 16, no. 156, 2019.
[100] J. van Gestel, H. Vlamakis, and R. Kolter, "From Cell Differentiation to Cell Collectives: *Bacillus subtilis* Uses Division of Labor to Migrate," *PLoS Biol.*, vol. 13, no. 4, pp. 1–29, 2015.
[101] H. Jeckel, N. Matthey, and K. Dresher, "Common concepts for bacterial collectives," *Elife*, vol. 8, pp. 8–10, 2019.
[102] Y. W. Chang, A. A. Fragkopoulos, S. M. Marquez, H. D. Kim, T. E. Angelini, and A. Fernández-Nieves, "Biofilm formation in geometries with different surface curvature and oxygen availability," *New J. Phys.*, vol. 17, 2015.
[103] D. de Beer, P. Stoodley, F. Roe, and Z. Lewandowski, "Effects of biofilm structures on oxygen distribution and mass transport," *Biotechnol. Bioeng.*, vol. 43, no. 11, pp. 1131–1138, 1994.
[104] S. A. Rani *et al.*, "Spatial patterns of DNA replication, protein synthesis, and oxygen concentration within bacterial biofilms reveal diverse physiological states," *J. Bacteriol.*, vol. 189, no. 11, pp. 4223–4233, 2007.
[105] P. S. Stewart, "Diffusion in Biofilm," *J. Bacteriol.*, vol. 185, no. 5, pp. 1485–1491, 2003.
[106] C. Von Ohle, A. Gieseke, L. Nistico, E. M. Decker, D. Debeer, and P. Stoodley, "Real-time microsensor measurement of local metabolic activities in ex vivo dental biofilms exposed to sucrose and treated with chlorhexidine," *Appl. Environ. Microbiol.*, vol. 76, no. 7, pp. 2326–2334, 2010.
[107] A. Bridier, F. Hammes, A. Canette, T. Bouchez, and R. Briandet, "Fluorescence-based tools for single-cell approaches in food microbiology," *Int. J. Food Microbiol.*, vol. 213, pp. 2–16, 2015.
[108] A. Houry *et al.*, "Bacterial swimmers that infiltrate and take over the biofilm matrix," *PNAS*, vol. 109, no. 32, 2012.
[109] A. Bridier, F. Dubois-Brissonnet, G. Greub, V. Thomas, and R. Briandet, "Dynamics of the action of biocides in *Pseudomonas aeruginosa* biofilms," *Antimicrob. Agents Chemother.*, vol. 55, no. 6, pp. 2648–2654, 2011.
[110] A. Bridier, R. Briandet, V. Thomas, and F. Dubois-Brissonnet, "Comparative biocidal activity of peracetic acid, benzalkonium chloride and ortho-phthalaldehyde on 77 bacterial strains," *J. Hosp. Infect.*, vol. 78, no. 3, pp. 208–213, 2011.
[111] A. Bridier *et al.*, "Biofilms of a *Bacillus subtilis* Hospital Isolate Protect *Staphylococcus aureus* from Biocide Action," *PLoS One*, vol. 7, no. 9, 2012.
[112] A. Bridier, T. Meylheuc, and R. Briandet, "Realistic representation of *Bacillus subtilis* biofilms architecture using combined microscopy (CLSM, ESEM and FESEM)," *Micron*, vol. 48, pp. 65–69, 2013.
[113] B. Zippel and T. R. Neu, "Characterization of glycoconjugates of extracellular polymeric substances in tufa-associated biofilms by using fluorescence lectin-binding analysis," *Appl. Environ. Microbiol.*, vol. 77, no. 2, pp. 505–516, 2011.
[114] T. R. Neu, G. D. W. Swerhone, and J. R. Lawrence, "Assessment of lectin-binding analysis for in situ detection of glycoconjugates in biofilm systems," *Microbiology*, vol. 147, no. 2, pp. 299–313, 2001.
[115] D. Romero, C. Aguilar, R. Losick, and R. Kolter, "Amyloid fibers provide structural integrity to *Bacillus subtilis* biofilms.," *Proc. Natl. Acad. Sci. U. S. A.*, vol. 107, no. 5, pp. 2230–4, Feb. 2010.

[116] N. Steinberg *et al.*, "The extracellular matrix protein TasA is a developmental cue that maintains a motile subpopulation within *Bacillus subtilis* biofilms," *Sci. Signal*, vol. 13, p. 8905, 2020.
[117] P. Sanchez-Vizuete, B. Orgaz, S. Aymerich, D. Le Coq, and R. Briandet, "Pathogens protection against the action of disinfectants in multispecies biofilms," *Front. Microbiol.*, vol. 6, no. JUN, pp. 1–12, 2015.
[118] T. Thurnheer, R. Gmür, and B. Guggenheim, "Multiplex FISH analysis of a six-species bacterial biofilm," *J. Microbiol. Methods*, vol. 56, no. 1, pp. 37–47, 2004.
[119] R. Amann and B. M. Fuchs, "Single-cell identification in microbial communities by improved fluorescence in situ hybridization techniques," *Nat. Rev. Microbiol.*, vol. 6, no. 5, pp. 339–348, 2008.
[120] P. Servais, J. Prats, J. Passerat, and T. Garcia-Armisen, "Abundance of culturable versus viable *Escherichia coli* in freshwater," *Can. J. Microbiol.*, vol. 55, no. 7, pp. 905–909, 2009.
[121] J. Baudart, A. Olaizola, J. Coallier, V. Gauthier, and P. Laurent, "Assessment of a new technique combining a viability test, whole-cell hybridization and laser-scanning cytometry for the direct counting of viable Enterobacteriaceae cells in drinking water," *FEMS Microbiol. Lett.*, vol. 243, no. 2, pp. 405–409, 2005.
[122] R. Almstrand, H. Daims, F. Persson, F. Sörensson, and M. Hermansson, "New methods for analysis of spatial distribution and coaggregation of microbial populations in complex biofilms," *Appl. Environ. Microbiol.*, vol. 79, no. 19, pp. 5978–5987, 2013.
[123] C. Almeida, N. F. Azevedo, C. Iversen, S. Fanning, C. W. Keevil, and M. J. Vieira, "Development and application of a novel peptide nucleic acid probe for the specific detection of Cronobacter genomospecies (*enterobacter sakazakii*) in powdered infant formula," *Appl. Environ. Microbiol.*, vol. 75, no. 9, pp. 2925–2930, 2009.
[124] G. Grégori *et al.*, "Resolution of Viable and Membrane-Compromised Bacteria in Freshwater and Marine Waters Based on Analytical Flow Cytometry and Nucleic Acid Double Staining," *Appl. Environ. Microbiol.*, vol. 67, no. 10, pp. 4662–4670, 2001.
[125] S. Jiang, S. Chen, C. Zhang, X. Zhao, X. Huang, and Z. Cai, "Effect of the biofilm age and starvation on acid tolerance of biofilm formed by *Streptococcus* mutans isolated from caries-active and caries-free adults," *Int. J. Mol. Sci.*, vol. 18, no. 4, pp. 1–12, 2017.
[126] J. P. Biggerstaff *et al.*, "New methodology for viability testing in environmental samples," *Mol. Cell. Probes*, vol. 20, no. 2, pp. 141–146, 2006.
[127] S. M. Stocks, "Mechanism and use of the commercially available viability stain, BacLight," *Cytom. Part A*, vol. 61, no. 2, pp. 189–195, 2004.
[128] M. Berney, F. Hammes, F. Bosshard, H. U. Weilenmann, and T. Egli, "Assessment and interpretation of bacterial viability by using the LIVE/DEAD BacLight kit in combination with flow cytometry," *Appl. Environ. Microbiol.*, vol. 73, no. 10, pp. 3283–3290, 2007.
[129] C. E. M. Krämer, W. Wiechert, and D. Kohlheyer, "Time-resolved, single-cell analysis of induced and programmed cell death via non-invasive propidium iodide and counterstain perfusion," *Sci. Rep.*, vol. 6, no. January, pp. 1–13, 2016.
[130] A. Bridier, R. Briandet, V. Thomas, and F. Dubois-Brissonnet, "Resistance of bacterial biofilms to disinfectants: A review," *Biofouling*, vol. 27, no. 9, pp. 1017–1032, 2011.
[131] F. Cohn, "Untersuchungen über bacterien," *Beiträge zur Biol der Pflanz*, pp. 124–224, 1872.
[132] A. L. McLoon, S. B. Guttenplan, D. B. Kearns, R. Kolter, and R. Losick, "Tracing the domestication of a biofilm-forming bacterium," *J. Bacteriol.*, vol. 193, no. 8, pp. 2027–2034, 2011.
[133] T. Hoffmann, B. Troup, A. Szabo, C. Hungerer, and D. Jahn, "The anaerobic life of *Bacillus*

subtilis: Cloning of the genes encoding the respiratory nitrate reductase system," *FEMS Microbiol. Lett.*, vol. 131, no. 2, pp. 219–225, 1995.
[134] M. M. Nakano and P. Zuber, "ANAEROBIC GROWTH OF A ' Strict Aerobe ' (*Bacillus Subtilis*)," *Annu. Rev. Microbiol.*, vol. 52, pp. 165–1990, 1998.
[135] M. M. Nakano, Y. P. Dailly, P. Zuber, and D. P. Clark, "Characterization of anaerobic fermentative growth of *Bacillus subtilis*: Identification of fermentation end products and genes required for growth," *Anal. Biochem.*, vol. 217, no. 2, pp. 220–230, 1994.
[136] M. Lacelle, M. Kumano, K. Kurita, K. Yamane, P. Zuber, and M. M. Nakano, "Oxygen-controlled regulation of the flavohemoglobin gene in *Bacillus subtilis*," *J. Bacteriol.*, vol. 178, no. 13, pp. 3803–3808, 1996.
[137] Yun Chen *et al.*, "Biocontrol of tomato wilt disease by *Bacillus subtilis* isolates from natural environments depends on conserved genes mediating biofilm formation," *Env. Microbiol.*, vol. 15, no. 3, pp. 848–864, 2013.
[138] Y. Deng *et al.*, "Complete genome sequence of *Bacillus subtilis* BSn5, an endophytic bacterium of Amorphophallus konjac with antimicrobial activity for the plant pathogen Erwinia carotovora subsp. carotovora," *J. Bacteriol.*, vol. 193, no. 8, pp. 2070–2071, 2011.
[139] T. M. Barbosa, C. R. Serra, R. M. La Ragione, M. J. Woodward, and A. O. Henriques, "Screening for *Bacillus* isolates in the broiler gastrointestinal tract," *Appl. Environ. Microbiol.*, vol. 71, no. 2, pp. 968–978, 2005.
[140] N. K. M. Tam *et al.*, "The intestinal life cycle of *Bacillus subtilis* and close relatives," *J. Bacteriol.*, vol. 188, no. 7, pp. 2692–2700, 2006.
[141] H. A. Hong *et al.*, "*Bacillus subtilis* isolated from the human gastrointestinal tract," *Res. Microbiol.*, vol. 160, no. 2, pp. 134–143, 2009.
[142] A. M. Earl, R. Losick, and R. Kolter, "Ecology and genomics of *Bacillus subtilis*," *Trends Microbio*, vol. 16, no. 6, p. 269, 2008.
[143] M. Fujita, K. Nomura, K. Hong, Y. Ito, A. Asada, and S. Nishimuro, "Purification and characterization of a strong fibrinolytic enzyme (nattokinase) in the vegetable cheese natto, a popular soybean fermented food in Japan. Biochem Biophys Res Commun." pp. 1340–1347, 1993.
[144] H. P. Bais, R. Fall, and J. M. Vivanco, "Biocontrol of *Bacillus subtilis* against Infection of *Arabidopsis* Roots by *Pseudomonas syringae* Is Facilitated by Biofilm Formation and Surfactin Production," *Plant Physiol.*, vol. 134, pp. 307–319, 2004.
[145] M. Marzorati *et al.*, "*Bacillus subtilis* HU58 and bacillus coagulans SC208 probiotics reduced the effects of antibiotic-induced gut microbiome dysbiosis in an M-SHIME® model," *Microorganisms*, vol. 8, no. 7, pp. 1–15, 2020.
[146] P. J. Piggot and D. W. Hilbert, "Sporulation of *Bacillus subtilis*," *Curr. Opin. Microbiol.*, vol. 7, no. 6, pp. 579–586, 2004.
[147] L. S. Cairns, L. Hobley, and N. R. Stanley-Wall, "Biofilm formation by *Bacillus subtilis*: New insights into regulatory strategies and assembly mechanisms," *Mol. Microbiol.*, vol. 93, no. 4, pp. 587–598, 2014.
[148] P. R. Burkholder and N. H. Giles, "Induced biochemical mutations in *Bacillus subtilis*," *Am. J. Bot.*, vol. 34, no. 6, pp. 345–348, 1947.
[149] C. Anagnostopoulos and J. Spizizen, "Requirements for Transformation in *Bacillus Subtilis*," *J. Bacteriol.*, vol. 81, no. 5, pp. 741–746, 1961.
[150] J. Spizizen, "Transformation of Biochemically Deficient Strains of *Bacillus Subtilis* By Deoxyribonucleate," *Proc. Natl. Acad. Sci.*, vol. 44, no. 10, pp. 1072–1078, 1958.
[151] F. Kunst *et al.*, "The complete genome sequence of the Gram-positive bacterium *Bacillus*

subtilis," *Nature*, vol. 390, no. 6657, pp. 249–256, 1997.
[152] A. Otto *et al.*, "Systems-wide temporal proteomic profiling in glucose-starved *Bacillus subtilis*," *Nat. Commun.*, vol. 1, no. 9, 2010.
[153] M. Hecker and U. Völker, "Towards a comprehensive understanding of *Bacillus subtilis* cell physiology by physiological proteomics," *Proteomics*, vol. 4, no. 12, pp. 3727–3750, 2004.
[154] S. Wolff *et al.*, "Towards the entire proteome of the model bacterium *Bacillus subtilis* by gel-based and gel-free approaches," *J. Chromatogr. B Anal. Technol. Biomed. Life Sci.*, vol. 849, no. 1–2, pp. 129–140, 2007.
[155] P. Nicolas *et al.*, "Condition-dependent transcriptome reveals high-level regulatory architecture in *Bacillus subtilis*," *Science (80-.).*, vol. 335, no. March, pp. 1103–1106, 2012.
[156] Y. K. Oh, B. O. Palsson, S. M. Park, C. H. Schilling, and R. Mahadevan, "Genome-scale reconstruction of metabolic network in *Bacillus subtilis* based on high-throughput phenotyping and gene essentiality data," *J. Biol. Chem.*, vol. 282, no. 39, pp. 28791–28799, 2007.
[157] B. Zhu and J. Stülke, "SubtiWiki in 2018: From genes and proteins to functional network annotation of the model organism *Bacillus subtilis*," *Nucleic Acids Res.*, vol. 46, no. D1, pp. D743–D748, 2018.
[158] H. J. Conn, "The identity of *Bacillus subtilis*," *J. Infect. Dis.*, vol. 46, no. 4, pp. 341–350, 1930.
[159] D. R. Zeigler *et al.*, "The origins of 168, W23, and other *Bacillus subtilis* legacy strains," *J. Bacteriol.*, vol. 190, no. 21, pp. 6983–6995, 2008.
[160] D. B. Kearns, F. Chu, R. Rudner, and R. Losick, "Genes governing swarming in *Bacillus subtilis* and evidence for a phase variation mechanism controlling surface motility," *Mol. Microbiol.*, vol. 52, no. 2, pp. 357–369, 2004.
[161] T. Stein, "*Bacillus subtilis* antibiotics: Structures, syntheses and specific functions," *Mol. Microbiol.*, vol. 56, no. 4, pp. 845–857, 2005.
[162] W. Liu and J. N. Hansen, "Conversion of *Bacillus subtilis* 168 to a Subtilin Producer by Competence," *Am. Soc. Microbiol.*, vol. 173, no. 22, pp. 7387–7390, 1991.
[163] S. S. Branda, J. E. G. Lez-Pastor, S. Ben-Yehuda, R. Losick, and R. Kolter, "Fruiting body formation by *Bacillus subtilis*," *PNAS*, vol. 98, no. 2, pp. 11621–26, 2001.
[164] G. O. Toole, H. B. Kaplan, and R. Kolter, "Biofilm Formation as Microbial Development," *Annu. Rev. Microbiol.*, vol. 54, pp. 49–79, 2000.
[165] A. L. McLoon, S. B. Guttenplan, D. B. Kearns, R. Kolter, and R. Losick, "Tracing the domestication of a biofilm-forming bacterium," *J. Bacteriol.*, vol. 193, no. 8, pp. 2027–2034, 2011.
[166] M. A. Konkol, K. M. Blair, and D. B. Kearns, "Plasmid-encoded comi inhibits competence in the ancestral 3610 strain of *Bacillus subtilis*," *J. Bacteriol.*, vol. 195, no. 18, pp. 4085–4093, 2013.
[167] D. B. Kearns and R. Losick, "Swarming motility in undomesticated *Bacillus subtilis*," *Mol. Microbiol.*, vol. 49, no. 3, pp. 581–590, 2003.
[168] K. Hamze *et al.*, "Single-cell analysis in situ in a *Bacillus subtilis* swarming community identifies distinct spatially separated subpopulations differentially expressing *hag* (flagellin), including specialized swarmers," *Microbiology*, vol. 157, no. 9, pp. 2456–2469, 2011.
[169] D. Julkowska, M. Obuchowski, I. B. Holland, and S. J. Séror, "Comparative analysis of the development of swarming communities of *Bacillus subtilis* 168 and a natural wild type: Critical effects of surfactin and the composition of the medium," *J. Bacteriol.*, vol. 187, no.

1, pp. 65–76, 2005.
[170] D. Julkowska, M. Obuchowski, I. B. Holland, and S. J. Séror, "Branched swarming patterns on a synthetic medium formed by wild-type *Bacillus subtilis* strain 3610: Detection of different cellular morphologies and constellations of cells as the complex architecture develops," *Microbiology*, vol. 150, no. 6, pp. 1839–1849, 2004.
[171] L. Hamouche *et al.*, "*Bacillus subtilis* Swarmer Cells Lead the Swarm, Multiply, and Generate a Trail of Quiescent Descendants," *MBio*, vol. 8, no. 1, pp. 1–14, 2017.
[172] P. Stefanic, B. Kraigher, N. A. Lyons, R. Kolter, and I. Mandic-Mulec, "Kin discrimination between sympatric *Bacillus subtilis* isolates," *Proc. Natl. Acad. Sci. U. S. A.*, vol. 112, no. 45, pp. 14042–14047, 2015.
[173] D. Debois *et al.*, "In situ localisation and quantification of surfactins in a *Bacillus subtilis* swarming community by imaging mass spectrometry," *Proteomics*, vol. 8, no. 18, pp. 3682–3691, 2008.
[174] K. Hamze *et al.*, "Identification of genes required for different stages of dendritic swarming in *Bacillus subtilis*, with a novel role for phrC," *Microbiology*, vol. 155, no. 2, pp. 398–412, 2009.
[175] M. A. Hamon and B. A. Lazazzera, "The sporulation transcription factor Spo0A is required for biofilm development in *Bacillus subtilis*," 2001.
[176] M. A. Hamon, N. R. Stanley, R. A. Britton, A. D. Grossman, and B. A. Lazazzera, "Identification of AbrB-regulated genes involved in biofilmformation by *Bacillus subtilis*," *Mol Microbiol.*, vol. 52, no. 3, pp. 847–860, 2004.
[177] N. R. Stanley and B. A. Lazazzera, "Defining the genetic differences between wild and domestic strains of *Bacillus subtilis* that affect poly-γ-DL-glutamic acid production and biofilm formation," *Mol. Microbiol.*, vol. 57, no. 4, pp. 1143–1158, 2005.
[178] N. R. Stanley, R. A. Britton, A. D. Grossman, B. A. Lazazzera, S. E. T. Al, and J. B. Acteriol, "Identification of Catabolite Repression as a Physiological Regulator of Biofilm Formation by *Bacillus subtilis* by Use of DNA Microarrays," *J. Bacteriol.*, vol. 185, no. 6, pp. 1951–1957, 2003.
[179] R. Terra, N. R. Stanley-Wall, G. Cao, and B. A. Lazazzera, "Identification of *Bacillus subtilis sipw* as a bifunctional signal peptidase that controls surface-adhered biofilm formation," *J. Bacteriol.*, vol. 194, no. 11, pp. 2781–2790, 2012.
[180] Y. Dergham *et al.*, "Comparison of the Genetic Features Involved in *Bacillus subtilis* Biofilm Formation Using Multi-Culturing Approaches," *Microorganisms*, vol. 9, no. 633, 2021.
[181] M. Asally *et al.*, "Localized cell death focuses mechanical forces during 3D patterning in a biofilm," *Proc. Natl. Acad. Sci. U. S. A.*, vol. 109, no. 46, pp. 18891–18896, 2012.
[182] J. N. Wilking, V. Zaburdaev, M. De Volder, R. Losick, M. P. Brenner, and D. A. Weitz, "Liquid transport facilitated by channels in *Bacillus subtilis* biofilms," *PNAS*, vol. 110, no. 3, pp. 848–852, 2013.
[183] A. Bridier, F. Dubois-Brissonnet, A. Boubetra, V. Thomas, and R. Briandet, "The biofilm architecture of sixty opportunistic pathogens deciphered using a high throughput CLSM method," *J. Microbiol. Methods*, vol. 82, no. 1, pp. 64–70, 2010.
[184] P. Sanchez-Vizuete, "Biofilms immergés de *Bacillus subtilis*: architecture, résistance aux biocides et protection de pathogènes," *Thèse de Doctorat (AgroParisTech).*, 2014.
[185] S. Arnaouteli, N. C. Bamford, N. R. Stanley-Wall, and Á. T. Kovács, "*Bacillus subtilis* biofilm formation and social interactions," *Nat. Rev. Microbiol.*, vol. 19, no. 9, pp. 600–614, 2021.

[186] D. T. Verhamme, E. J. Murray, and N. R. Stanley-Wall, "DegU and Spo0A jointly control transcription of two loci required for complex colony development by *Bacillus subtilis*," *J. Bacteriol.*, vol. 91, no. 1, pp. 100–108, 2009.
[187] A. K. Epstein, B. Pokroy, A. Seminara, and J. Aizenberg, "Bacterial biofilm shows persistent resistance to liquid wetting and gas penetration," *Proc. Natl. Acad. Sci. U. S. A.*, vol. 108, no. 3, pp. 995–1000, 2011.
[188] S. S. Branda, J. E. González-Pastor, E. Dervyn, S. D. Ehrlich, R. Losick, and R. Kolter, "Genes involved in formation of structured multicellular communities by *Bacillus subtilis*," *J. Bacteriol.*, vol. 186, no. 12, pp. 3970–3979, 2004.
[189] S. S. Branda, F. Chu, D. B. Kearns, R. Losick, and R. Kolter, "A major protein component of the *Bacillus subtilis* biofilm matrix," *Mol. Microbiol.*, vol. 59, no. 4, pp. 1229–1238, 2006.
[190] J. Gerwig, T. B. Kiley, K. Gunka, N. Stanley-Wall, and J. Stülke, "The protein tyrosine kinases EpsB and PtkA differentially affect biofilm formation in *Bacillus subtilis*," *Microbiol. (United Kingdom)*, vol. 160, no. PART 4, pp. 682–691, 2014.
[191] A. K. W. Elsholz, S. A. Wacker, and R. Losick, "Self-regulation of exopolysaccharide production in *Bacillus subtilis* by a tyrosine kinase," *Genes Dev.*, vol. 28, no. 15, pp. 1710–1720, 2014.
[192] K. M. Blair, L. Turner, J. T. Winkelman, H. C. Berg, and D. B. Kearns, "A molecular clutch disables flagella in the *Bacillus subtilis* biofilm," *Science (80-.).*, vol. 320, no. 5883, pp. 1636–1638, 2008.
[193] S. B. Guttenplan, K. M. Blair, and D. B. Kearns, "The EpsE flagellar clutch is bifunctional and synergizes with EPS biosynthesis to promote *bacillus subtilis* biofilm formation," *PLoS Genet.*, vol. 6, no. 12, pp. 1–12, 2010.
[194] C. R. Kaundinya, H. S. Savithri, K. K. Rao, and P. V. Balaji, "EpsM from *Bacillus subtilis* 168 has UDP-2,4,6-trideoxy-2-acetamido-4-amino glucose acetyltransferase activity in vitro," *Biochem. Biophys. Res. Commun.*, vol. 505, no. 4, pp. 1057–1062, 2018.
[195] D. Romero, H. Vlamakis, R. Losick, and R. Kolter, "An Accessory Protein Required for Anchoring and Assembly of Amyloid Fibers in *B. subtilis* Biofilms," *Mol Microbiol.*, vol. 80, no. 5, pp. 1155–1168, 2011.
[196] N. El Mammeri *et al.*, "Molecular architecture of bacterial amyloids in *Bacillus* biofilms," *FASEB J.*, vol. 33, no. 11, pp. 12146–12163, 2019.
[197] D. Romero, H. Vlamakis, R. Losick, and R. Koltera, "Functional analysis of the accessory protein TapA in *Bacillus subtilis* amyloid fiber assembly," *J. Bacteriol.*, vol. 196, no. 8, pp. 1505–1513, 2014.
[198] E. Erskine, C. E. MacPhee, and N. R. Stanley-Wall, "Functional Amyloid and Other Protein Fibers in the Biofilm Matrix," *J Mol Biol*, vol. 430, no. 20, pp. 3642–3656, 2018.
[199] M. Serrano, R. Zilhao, E. Ricca, A. J. Ozin, C. P. Moran, and A. O. Henriques, "A *Bacillus subtilis* secreted protein with a role in endospore coat assembly and function," *J. Bacteriol.*, vol. 181, no. 12, pp. 3632–3643, 1999.
[200] J. Cámara-Almirón *et al.*, "Dual functionality of the amyloid protein TasA in *Bacillus* physiology and fitness on the phylloplane," *Nat. Commun.*, vol. 11, no. 1, 2020.
[201] K. Kobayashi and M. Iwano, "BslA(YuaB) forms a hydrophobic layer on the surface of *Bacillus subtilis* biofilms," *Mol. Microbiol.*, vol. 85, no. 1, pp. 51–66, 2012.
[202] S. Arnaouteli *et al.*, "Bifunctionality of a biofilm matrix protein controlled by redox state," *Proc. Natl. Acad. Sci. U. S. A.*, vol. 114, no. 30, pp. E6184–E6191, 2017.
[203] L. Hobley *et al.*, "BslA is a self-assembling bacterial hydrophobin that coats the *Bacillus subtilis* biofilm," *PNAS*, vol. 98, no. 20, pp. 11621–11626, Aug. 2013.

[204] A. Ostrowski, A. Mehert, A. Prescott, T. B. Kiley, and N. R. Stanley-Wall, "YuaB Functions Synergistically with the Exopolysaccharide and TasA Amyloid Fibers To Allow Biofilm Formation by *Bacillus subtilis*," *J. Bacteriol.*, vol. 193, no. 18, pp. 4821–4831, 2011.
[205] N. Peng, P. Cai, M. Mortimer, Y. Wu, C. Gao, and Q. Huang, "The exopolysaccharide-eDNA interaction modulates 3D architecture of *Bacillus subtilis* biofilm," *BMC Microbiol.*, vol. 20, no. 1, pp. 1–12, 2020.
[206] M. Ashiuchi and H. Misono, "Biochemistry and molecular genetics of poly-γ-glutamate synthesis," *Appl. Microbiol. Biotechnol.*, vol. 59, no. 1, pp. 9–14, 2002.
[207] M. Morikawa *et al.*, "Biofilm formation by a *Bacillus subtilis* strain that produces γ-polyglutamate," *Microbiology*, vol. 152, no. 9, pp. 2801–2807, 2006.
[208] J. M. Chan, S. B. Guttenplan, and D. B. Kearns, "Defects in the flagellar motor increase synthesis of poly-γ-glutamate in *bacillus subtilis*," *J. Bacteriol.*, vol. 196, no. 4, pp. 740–753, 2014.
[209] K. Kobayashi, "*Bacillus subtilis* pellicle formation proceeds through genetically defined morphological changes," *J. Bacteriol.*, vol. 189, no. 13, pp. 4920–4931, 2007.
[210] Y. Yu, F. Yan, Y. Chen, C. Jin, J. H. Guo, and Y. Chai, "Poly-γ-glutamic acids contribute to biofilm formation and plant root colonization in selected environmental isolates of *Bacillus subtilis*," *Front. Microbiol.*, vol. 7, no. NOV, pp. 1–15, 2016.
[211] D. López, M. A. Fischbach, F. Chu, R. Losick, and R. Kolter, "Structurally diverse natural products that cause potassium leakage trigger multicellularity in *Bacillus subtilis*," *Proc. Natl. Acad. Sci. U. S. A.*, vol. 106, no. 1, pp. 280–285, 2009.
[212] H. Zeriouh, A. de Vicente, A. Pérez-García, and D. Romero, "Surfactin triggers biofilm formation of *Bacillus subtilis* in melon phylloplane and contributes to the biocontrol activity," *Environ. Microbiol.*, vol. 16, no. 7, pp. 2196–2211, 2014.
[213] M. Thérien *et al.*, "Surfactin production is not essential for pellicle and root-associated biofilm development of *Bacillus subtilis*," *Biofilm*, vol. 2, p. 100021, Dec. 2020.
[214] T. Danevčič, A. Dragoš, M. Spacapan, P. Stefanic, I. Dogsa, and I. Mandic-Mulec, "Surfactin Facilitates Horizontal Gene Transfer in *Bacillus subtilis*," *Front. Microbiol.*, vol. 12, no. May, pp. 1–8, 2021.
[215] B. Mielich-süss and D. Lopez, "Molecular mechanisms involved in *Bacillus subtilis* biofilm formation," *Environ. Microbiol.*, vol. 17, no. 3, pp. 555–565, 2015.
[216] D. B. Kearns, F. Chu, S. S. Branda, R. Kolter, and R. Losick, "A master regulator for biofilm formation by *Bacillus subtilis*," *Mol. Microbiol.*, vol. 55, no. 3, pp. 739–749, 2005.
[217] I. Dogsa, M. Brloznik, D. Stopar, and I. Mandic-Mulec, "Exopolymer Diversity and the Role of Levan in *Bacillus subtilis* Biofilms," *PLoS One*, vol. 8, no. 4, pp. 2–11, 2013.
[218] I. Kolodkin-Gal, A. K. W. Elsholz, C. Muth, P. R. Girguis, R. Kolter, and R. Losick, "Respiration control of multicellularity in *Bacillus subtilis* by a complex of the cytochrome chain with a membrane-embedded histidine kinase," *Genes Dev.*, vol. 27, no. 8, pp. 887–899, 2013.
[219] M. Shemesh, R. Kolter, and R. Losick, "The biocide chlorine dioxide stimulates biofilm formation in *Bacillus subtilis* by activation of the histidine kinase KinC," *J. Bacteriol.*, vol. 192, no. 24, pp. 6352–6356, 2010.
[220] M. Jiang, W. Shao, M. Perego, and J. A. Hoch, "Multiple histidine kinases regulate entry into stationary phase and sporulation in *Bacillus subtilis*," *Mol. Microbiol.*, vol. 38, no. 3, pp. 535–542, 2000.
[221] A. L. McLoon, I. Kolodkin-Gal, S. M. Rubinstein, R. Kolter, and R. Losick, "Spatial regulation of histidine kinases governing biofilm formation in *Bacillus subtilis*," *J.*

Bacteriol., vol. 193, no. 3, pp. 679–685, 2011.
[222] M. Fujita, J. E. González-Pastor, and R. Losick, "High- and low-threshold genes in the Spo0A regulon of *Bacillus subtilis*," *J. Bacteriol.*, vol. 187, no. 4, pp. 1357–1368, 2005.
[223] V. Molle *et al.*, "The Spo0A regulon of *Bacillus subtilis*," *Mol. Microbiol.*, vol. 50, no. 5, pp. 1683–1701, 2003.
[224] H. Takada *et al.*, "Cell motility and biofilm formation in *Bacillus subtilis* are affected by the ribosomal proteins, S11 and S21," *Biosci. Biotechnol. Biochem.*, vol. 78, no. 5, pp. 898–907, 2014.
[225] Y. Chai, F. Chu, R. Kolter, and R. Losick, "Bistability and Biofilm Formation in *Bacillus subtilis*," *Mol. Microbiol.*, vol. 67, no. 2, pp. 254–263, 2008.
[226] Y. Chai, R. Kolter, and R. Losic, "Paralogous Antirepressors Acting on the Master Regulator for Biofilm Formation in *Bacillus subtilis*," *Mol Microbiol.*, vol. 74, no. 4, pp. 876–887, 2009.
[227] Y. Chai, T. Norman, R. Kolter, and R. Losick, "An epigenetic switch governing daughter cell separation in *Bacillus subtilis*," *Genes Dev.*, vol. 24, pp. 754–765, 2010.
[228] K. Kobayashi, "SlrR/SlrA controls the initiation of biofilm formation in *Bacillus subtilis*," *Mol. Microbiol.*, vol. 69, no. 6, pp. 1399–1410, 2008.
[229] Y. Chai, P. B. Beauregard, H. Vlamakis, R. Losick, and R. Kolter, "Galactose metabolism plays a crucial role in biofilm formation by *Bacillus subtilis*," *MBio*, vol. 3, no. 4, pp. 1–10, 2012.
[230] J. A. Newman, C. Rodrigues, and R. J. Lewis, "Molecular basis of the activity of SinR Protein, the master regulator of biofilm formation in *bacillus subtilis*," *J. Biol. Chem.*, vol. 288, no. 15, pp. 10766–10778, 2013.
[231] L. M. Cozy *et al.*, "SlrA/SinR/SlrR inhibits motility gene expression upstream of a hypersensitive and hysteretic switch at the level of σ D in *Bacillus subtilis*," *Mol. Microbiol.*, vol. 83, no. 6, pp. 1210–1228, 2012.
[232] J. T. Winkelman, A. C. Bree, A. R. Bate, P. Eichenberger, R. L. Gourse, and D. B. Kearns, "RemA is a DNA-binding protein that activates biofilm matrix gene expression in *Bacillus subtilis*," *Mol Microbiol.*, vol. 88, no. 5, 2013.
[233] J. T. Winkelman, K. M. Blair, and D. B. Kearns, "RemA (YlzA) and RemB (YaaB) regulate extracellular matrix operon expression and biofilm formation in *Bacillus subtilis*," *J. Bacteriol.*, vol. 191, no. 12, pp. 3981–3991, 2009.
[234] E. J. Murray, T. B. Kiley, and N. R. Stanley-Wall, "A pivotal role for the response regulator DegU in controlling multicellular behaviour," *Microbiology*, vol. 155, no. 1, pp. 1–8, 2009.
[235] V. L. Marlow *et al.*, "Phosphorylated DegU manipulates cell fate differentiation in the *Bacillus subtilis* biofilm," *J. Bacteriol.*, vol. 196, no. 1, pp. 16–27, 2014.
[236] F. A. Davidson, C. Seon-Yi, and N. R. Stanley-Wall, "Selective heterogeneity in exoprotease production by *bacillus subtilis*," *PLoS One*, vol. 7, no. 6, 2012.
[237] D. T. Verhamme, T. B. Kiley, and N. R. Stanley-Wall, "DegU co-ordinates multicellular behaviour exhibited by *Bacillus subtilis*," *Mol. Microbiol.*, vol. 65, no. 2, pp. 554–568, 2007.
[238] K. Kobayashi, "Gradual activation of the response regulator DegU controls serial expression of genes for flagellum formation and biofilm formation in *Bacillus subtilis*," *Mol. Microbiol.*, vol. 66, no. 2, pp. 395–409, 2007.
[239] P. Margot, M. Pagni, and D. Karamata, "*Bacillus subtilis* 168 gene *lytF* encodes a γ-D-glutamate-meso-diaminopimelate muropeptidase expressed by the alternative vegetative sigma factor, σ(D)," *Microbiology*, vol. 145, no. 1, pp. 57–65, 1999.
[240] R. Chen, S. B. Guttenplan, K. M. Blair, and D. B. Kearns, "Role of the σD-dependent

autolysins in *Bacillus subtilis* population heterogeneity," *J. Bacteriol.*, vol. 191, no. 18, pp. 5775–5784, 2009.
[241] F. M. P. Mehne, K. Gunka, H. Eilers, C. Herzberg, V. Kaever, and J. Stülke, "Cyclic Di-AMP homeostasis in *bacillus subtilis*: Both lack and high level accumulation of the nucleotide are detrimental for cell growth," *J. Biol. Chem.*, vol. 288, no. 3, pp. 2004–2017, 2013.
[242] Y. Oppenheimer-Shaanan, E. Wexselblatt, J. Katzhendler, E. Yavin, and S. Ben-Yehuda, "C-di-AMP reports DNA integrity during sporulation in *Bacillus subtilis*," *EMBO Rep.*, vol. 12, no. 6, pp. 594–601, 2011.
[243] J. Gundlach, H. Rath, C. Herzberg, U. Mäder, and J. Stülke, "Second messenger signaling in *Bacillus Subtilis*: Accumulation of cyclic di-AMP inhibits biofilm formation," *Front. Microbiol.*, vol. 7, no. MAY, pp. 1–8, 2016.
[244] Loni Townsley, S. M. Yannarell, T. N. Huynh, J. J. Woodward, and E. A. Shank, "Cyclic di-AMP Acts as an Extracellular Signal That Impacts *Bacillus subtilis* Biofilm Formation and Plant Attachment," *MBio*, vol. 9, no. 2, pp. 1–13, 2018.
[245] Y. Chen, Y. Chai, J. hua Guo, and R. Losick, "Evidence for cyclic Di-GMP-mediated signaling in *Bacillus subtilis*," *J. Bacteriol.*, vol. 194, no. 18, pp. 5080–5090, 2012.
[246] T. Abee, Á. T. Kovács, O. P. Kuipers, and S. van der Veen, "Biofilm formation and dispersal in Gram-positive bacteria," *Curr. Opin. Biotechnol.*, vol. 22, no. 2, pp. 172–179, 2011.
[247] D. McDougald, S. A. Rice, N. Barraud, P. D. Steinberg, and S. Kjelleberg, "Should we stay or should we go: Mechanisms and ecological consequences for biofilm dispersal," *Nat. Rev. Microbiol.*, vol. 10, no. 1, pp. 39–50, 2012.
[248] J. B. Kaplan, "Biofilm Dispersal: Mechanisms, Clinical Implications, and Potential Therapeutic Uses," *J. Dent. Res.*, vol. 89, no. 3, pp. 205–218, 2010.
[249] M. Bartolini *et al.*, "Regulation of biofilm aging and dispersal in *Bacillus subtilis* by the alternative sigma factor SigB," *J. Bacteriol.*, vol. 201, no. 2, 2019.
[250] E. Nadezhdin, N. Murphy, N. Dalchau, A. Phillips, and J. C. W. Locke, "Stochastic pulsing of gene expression enables the generation of spatial patterns in *Bacillus subtilis* biofilms," *Nat. Commun.*, vol. 11, no. 1, pp. 1–12, 2020.
[251] M. Kalamara, M. Spacapan, I. Mandic-Mulec, and N. R. Stanley-Wall, "Social behaviours by *Bacillus subtilis*: quorum sensing, kin discrimination and beyond," *Mol. Microbiol.*, vol. 110, no. 6, pp. 863–878, 2018.
[252] J. Van Gestel, H. Vlamakis, and R. Kolter, "Division of Labor in Biofilms : the Ecology of Cell Differentiation," *Microbiol. Spectr.*, vol. 3, 2015.
[253] T. Domazet-Lošo and D. Tautz, "A phylogenetically based transcriptome age index mirrors ontogenetic divergence patterns," *Nature*, vol. 468, no. 7325, pp. 815–819, 2010.
[254] H. G. Drost, P. Janitza, I. Grosse, and M. Quint, "Cross-kingdom comparison of the developmental hourglass," *Curr. Opin. Genet. Dev.*, vol. 45, no. Box 1, pp. 69–75, 2017.
[255] M. Quint, H. G. Drost, A. Gabel, K. K. Ullrich, M. Bönn, and I. Grosse, "A transcriptomic hourglass in plant embryogenesis," *Nature*, vol. 490, no. 7418, pp. 98–101, 2012.
[256] N. Irie and S. Kuratani, "Comparative transcriptome analysis reveals vertebrate phylotypic period during organogenesis," *Nat. Commun.*, vol. 2, no. 1, 2011.
[257] A. T. Kalinka *et al.*, "Gene expression divergence recapitulates the developmental hourglass model," *Nature*, vol. 468, no. 7325, pp. 811–816, 2010.
[258] M. Futo *et al.*, "Embryo-Like Features in Developing *Bacillus subtilis* Biofilms," *Mol. Biol. Evol.*, vol. 38, no. 1, pp. 31–47, 2020.
[259] T. Pisithkul *et al.*, "Metabolic Remodeling during Biofilm Development of *Bacillus*

subtilis," *MBio*, vol. 10, no. 3, 2019.
[260] D. Dubnau, "The regulation of genetic competence in *Bacillus subtilis*," *Mol. Microbiol.*, vol. 5, no. 1, pp. 11–18, 1991.
[261] D. Dubnau and R. Provvedi, "Internalizing DNA," *Res. Microbiol.*, vol. 151, no. 6, pp. 475–480, 2000.
[262] C. D. Ellermeier, E. C. Hobbs, J. E. Gonzalez-Pastor, and R. Losick, "A three-protein signaling pathway governing immunity to a bacterial cannibalism toxin," *Cell*, vol. 124, no. 3, pp. 549–559, 2006.
[263] P. J. Piggot and D. W. Hilbert, "Sporulation of *Bacillus subtilis*," *Curr. Opin. Microbiol.*, vol. 7, no. 6, pp. 579–586, 2004.
[264] D. Z. Rudner and R. Losick, "Morphological Coupling in Development: Lessons from Prokaryotes," *Dev. Cell*, vol. 1, no. 6, pp. 733–742, 2001.
[265] J. A. Shapiro, "Thinking about bacterial populations as multicellular organisms," *Annu. Rev. Microbiol.*, vol. 52, pp. 81–104, 1998.
[266] D. B. Kearns, "Division of labour during *Bacillus subtilis* biofilm formation," *Mol. Microbiol.*, vol. 67, no. 2, pp. 229–231, 2008.
[267] S. Tasaki, M. Nakayama, and W. Shoji, "Morphologies of *Bacillus subtilis* communities responding to environmental variation," *Dev. Growth Differ.*, vol. 59, no. 5, pp. 369–378, 2017.
[268] A. Bridier, P. Sanchez-Vizuete, M. Guilbaud, J. C. Piard, M. Naïtali, and R. Briandet, "Biofilm-associated persistence of food-borne pathogens," *Food Microbiol.*, vol. 45, no. PB, pp. 167–178, 2015.
[269] A. K. Deva *et al.*, "Detection of persistent vegetative bacteria and amplified viral nucleic acid from in-use testing of gastrointestinal endoscopes," *J. Hosp. Infect.*, vol. 39, no. 2, pp. 149–157, 1998.
[270] A. P. Machado, A. T. M. Pimenta, P. P. Contijo, S. Geocze, and O. Fischman, "Microbiologic profile of flexible endoscope disinfection in two Brazilian hospitals," *Arq. Gastroenterol.*, vol. 43, no. 4, pp. 255–258, 2006.
[271] P. Sanchez-Vizuete *et al.*, "Genome Sequences of Two Nondomesticated *Bacillus subtilis* Strains Able To Form Thick Biofilms on Submerged Surfaces," *Genome Announc.*, vol. 25, no. 2, p. 5, 2014.
[272] K. Abe *et al.*, "Developmentally-Regulated Excision of the SPβ Prophage Reconstitutes a Gene Required for Spore Envelope Maturation in *Bacillus subtilis*," *PLoS Genet.*, vol. 10, no. 10, 2014.
[273] M. Arumugam *et al.*, "Enterotypes of the human gut microbiome," *Nature*, vol. 473, no. 7346, pp. 174–180, 2011.
[274] I. Grobas, M. Polin, and M. Asally, "Swarming bacteria undergo localized dynamic phase transition to form stress-induced biofilms," *Elife*, vol. 10, pp. 1–22, 2021.
[275] C. Guégan *et al.*, "Alteration of bacterial adhesion induced by the substrate stiffness," *Colloids Surfaces B Biointerfaces*, vol. 114, pp. 193–200, 2014.
[276] L. S. Cairns, V. L. Marlow, E. Bissett, A. Ostrowski, and N. R. Stanley-Wall, "A mechanical signal transmitted by the flagellum controls signalling in *Bacillus subtilis*," *Mol. Microbiol.*, vol. 90, no. 1, pp. 6–21, 2013.
[277] D. Dar, N. Dar, L. Cai, and D. K. Newman, "Spatial transcriptomics of planktonic and sessile bacterial populations at single-cell resolution," *Science (80-.).*, vol. 373, no. 6556, 2021.
[278] A. C. Pérez-Osorio, and M. J. Franklin, "Isolation of RNA and DNA from biofilm samples obtained by laser capture microdissection microscopy," *CSH protocols*, pdb.prot5065, 2008

THESIS SUMMARY IN FRENCH

COURTE INTRODUCTION

Les assemblages multicellulaires associés aux surfaces se rencontrent dans tous les habitats

Les bactéries jouent un rôle bénéfique essentiel au maintien de la vie sur cette planète. Avec les fluctuations environnementales constantes, les bactéries doivent développer des stratégies adaptatives pour survivre, souvent par la formation d'agrégats multicellulaires associés à des surfaces, spatialement structurés et entourés d'une matrice extracellulaire autoproduite, appelés biofilms [1], [2]. Ce comportement microbien collectif génère plusieurs propriétés émergentes importantes, telles que des interactions physiques et sociales, un taux accru d'échanges génétiques et une tolérance accrue aux antimicrobiens, ce qui questionne le rôle fondamental joué par la matrice extracellulaire du biofilm [2]. Cette matrice - principalement composée d'eau, de polysaccharides, de protéines, de lipides et d'ADN extracellulaire - n'est pas seulement impliquée dans l'établissement et le maintien de l'architecture spatiale d'un biofilm, mais contribue également à la protection des cellules contre des conditions environnementales difficiles telles que la déshydratation, et à la tolérance contre l'action des agents antimicrobiens.

Dans la nature, la cohabitation du microbiote (archées, bactéries, champignons et protistes) avec les plantes a des effets bénéfiques sur leur santé en supprimant les maladies, en renforçant leur système immunitaire, en augmentant leur tolérance aux stress abiotiques et aux variations environnementales [3]. Par exemple, la rhizosphère de l'éleusine, une céréale africaine ancestrale, est habitée par des microcolonies médiées par un biofilm d'une bactérie endophyte (*Enterobacter sp.*) qui constitue à la fois des barrières chimiques et physiques contre la colonisation par une bactérie pathogène (*Fusarium graminearum*) [4]. Un autre exemple de biofilm symbiotique est la colonisation d'un calmar hôte par la bactérie bioluminescente *Vibrio fischeri*, ce qui permet au calmar de camoufler son ombre au clair de lune en modulant la lumière émise par les bactéries [5], [6]. De plus, il a été avancé que les biofilms seraient à l'origine de cycles biogéochimiques impliqués dans le traitement de la matière organique ou la dégradation des contaminants [7].

Dans plusieurs applications d'ingénierie, les biofilms sont essentiels et jouent un rôle utile, notamment dans le traitement des eaux usées, la bioremédiation, la préservation des bâtiments historiques, dans l'industrie alimentaire, la production d'électricité à l'aide de batteries microbiennes ou en tant qu'agents de biocontrôle [8]–[12]. D'autre part, ces communautés microbiennes sont responsables d'effets néfastes sur les activités humaines tels que le colmatage

et la biocorrosion des canalisations industrielles, entraînant chaque année d'énormes pertes économiques [13], [14]. Les bactéries résidant dans le biofilm sont bien connues pour être résistantes aux mécanismes de défense de l'hôte, ont un niveau élevé de résistance aux antimicrobiens et à d'autres traitements.

Malheureusement, les biofilms bactériens deviennent un problème de société important, avec des effets indésirables sur les activités humaines à savoir le colmatage délétère ou la biocorrosion des canalisations industrielles, et même pour des problèmes de santé publique dramatiques. On estime que près de 80% des infections chroniques humaines et de la pathogénicité bactérienne sont liées à la formation de biofilms bactériens, c'est-à-dire les infections récurrentes des voies urinaires par *Escherichia coli* entéropathogène, la rhinosinusite chronique ou la colonisation des plaies chroniques par *Staphylococcus aureus*, les otites moyennes chroniques par *Haemophilus influenzae* ou *Streptococcus pneumoniae*, et la pneumonie à mucoviscidose par *Pseudomonas aeruginosa* [15]-[19]. De plus, avec les progrès de la science médicale, de plus en plus de dispositifs et/ou d'organes artificiels sont appliqués dans le traitement des maladies humaines. En conséquence, les infections associées aux biofilms sont également devenues fréquentes, où il a été estimé qu'environ 60 à 70 % des infections nosocomiales sont dues à la présence de biofilms à la surface des dispositifs médicaux à demeure [20]. Par exemple, les biocides utilisés pour désinfecter les surfaces sont très efficaces sur les microbes planctoniques, bien que leur efficacité diminue de mille fois lorsqu'ils sont appliqués sur un biofilm mature organisé spatialement [21]-[23]. Pour un meilleur contrôle, de nouvelles stratégies sont donc nécessaires pour désinfecter les surfaces, traiter les biofilms et empêcher leur dispersion. L'intérêt des communautés de biofilm ne cesse de croître pour une meilleure compréhension des mécanismes moléculaires impliqués dans ce mode de vie.

L'organisation spatiale 3D complexe engendre des propriétés émergentes

Dans l'organisation spatiale d'un biofilm, les cellules réagissent différemment à leurs conditions environnementales locales, c'est-à-dire à différents gradients de concentration de produits chimiques et de nutriments, entraînant une hétérogénéité physiologique [24]. Les gradients microscopiques dépendent de la localisation spatiale d'un biofilm, par exemple avec un gradient de nutriments à travers un biofilm immergé adhérant à une surface abiotique orienté de manière opposée à celui pour une colonie cultivée sur une surface de gélose nutritive. À mesure qu'une

culture pure évolue vers la formation d'un biofilm, les cellules doivent s'adapter à ces altérations microenvironnementales, ce qui entraîne des différenciations physiologiques cellulaires, chaque type cellulaire affichant un phénotype distinct. Ainsi, un même biofilm génétiquement homogène peut inclure des producteurs de surfactine, des producteurs de matrice, des producteurs de protéase, des cellules cannibales, des cellules compétentes ainsi que des cellules sporulantes [25]–[28]. Par une telle hétérogénéité, les cellules pourraient s'adapter aux fluctuations environnementales, permises par la division du travail entre différents types cellulaires exprimant différentes voies métaboliques régulées par des réseaux sophistiqués de régulation génique.

Bacillus subtilis, un organisme modèle à Gram positif

B. subtilis est un micro-organisme aérobie en forme de bâtonnet qui peut également se développer de manière anaérobie en respirant du nitrate ou du nitrite comme accepteur d'électrons ou en faisant fermenter du pyruvate ou du glucose comme source de carbone [29]–[32]. Cet organisme mobile possède des flagelles péritriches sur toute la surface cellulaire et est omniprésent dans diverses niches écologiques.

Dans la nature, *B. subtilis* se trouve en abondance dans le sol, considéré comme son principal réservoir. En tant que rhizobactérie, elle favorise la croissance des plantes en limitant le développement des espèces pathogènes [33], [34]. *B. subtilis* n'est pas seulement un micro-organisme du sol, mais est également un membre de la microflore intestinale chez les animaux et les humains, car sa capacité à former des spores et des biofilms permet à cette espèce de traverser les rudes conditions de l'environnement gastrique pour atteindre l'intestin et y persister [35]–[37]. En l'absence de pathogénicité ni d'effets toxiques enregistrés à son contact, *B. subtilis* est considéré comme un organisme GRAS (Generally Recognized As Safe) par la FDA (Food and Drug Administration). De plus, avec une excellente capacité de sécrétion de protéines, il a été largement utilisé comme usine cellulaire pour produire des protéines hétérologues. *B. subtilis* est utilisé dans l'industrie agricole en tant qu'agent de lutte biologique et également dans l'industrie alimentaire en tant que probiotique et en tant que ferment des *natto* dans la nourriture japonaise traditionnelle à partir de graines de soja [38]–[41]. La formation des biofilms entraîne des effets secondaires problématiques dans le colmatage et l'encrassement biologique des canalisations industrielles. Mais le plus dangereux pour la santé humaine est leur persistance en milieu médical et leur résistance aux biocides où les biofilms de *B. subtilis* peuvent protéger les bactéries pathogènes

[42]-[44]. Pour toutes ces raisons, combinées au fait que *B. subtilis* est naturellement compétent, facile et sûr à manipuler en laboratoire, il est devenu le modèle d'études sur les régulations génétiques de la sporulation, du métabolisme du carbone et de la formation de biofilms pour les bactéries Gram-positives [45]-[47].

Les différents modèles de laboratoire de communautés associées à des surfaces pour *B. subtilis*

Au laboratoire, plusieurs conditions de culture artificielle sont utilisées pour étudier les formations de biofilm de *B. subtilis*, notamment les colonies à l'interface air-solide et la pellicule à l'interface air-liquide [48], [49]. Entre les conditions de culture solide et liquide il existe un milieu semi-solide, sur la surface duquel la bactérie mobile de type sauvage de *B. subtilis* a la capacité d'essaimer par un mouvement collectif organisé tout en proliférant et en consommant des nutriments. Sur un milieu riche, comme le LB, *B. subtilis* essaime sous la forme d'une masse cellulaire multicouche à partir du site d'inoculation bactérienne [50]. En revanche, dans des conditions de milieu synthétique et de température bien optimisées, *B. subtilis* essaime sur une gélose semi-solide sous la forme d'un motif dendritique monocouche hautement ramifié qui recouvre la boîte de Pétri en quelques heures à un taux constant (jusqu'à 10 mm/h) [51]–[54]. Le milieu B défini optimal est utilisé pour imiter les conditions d'une croissance lente des cellules dans la nature et permet un développement hautement reproductible de l'essaim aux niveaux spatial et temporel [54]. Le processus d'essaimage est le suivant : (i) au site d'inoculation les bactéries se multiplient d'abord et forment une colonie mère multicouche, (ii) après plusieurs heures d'incubation les bactéries sécrètent de la surfactine, ce qui réduit la tension superficielle et facilite la translocation des bactéries à la surface, (iii) puis plusieurs petites structures monocouches ressemblant à des bourgeons migrent vers l'extérieur à partir des bords de la colonie mère et s'allongent pour former des dendrites [55]. Ces derniers continuent de s'étendre sous forme monocouche jusqu'à au moins 1,5 cm des pointes des dendrites, avant un basculement vers une forme de biofilm multicouche qui commence à se produire de la base des dendrites jusqu'aux pointes [52], [53], [56]. Les pointes des dendrites, les derniers 1 à 2 mm, comprennent des essaims hyper-flagellés et très mobiles [51].

Les agrégats multicellulaires associés à la surface ont été principalement étudiés à l'interface avec l'air, et seules quelques études se sont concentrées sur le développement de biofilms submergés.

De telles études de biofilms associés à la surface à l'interface solide-liquide ont d'abord été menées par Lazazzera et ses collaborateurs [57]–[61] suivis par Briandet et ses collaborateurs [44], [62]-[64]. Les études se sont focalisées sur des modèles aériens pour la simplicité technique permettant d'observer des différences de phénotypes (dues à des différences génétiques) entre les souches, sans nécessiter d'outils complexes pour les analyser. D'un autre côté, la surveillance du biofilm immergé nécessitait l'utilisation d'outils de laboratoire plus personnalisés tels que des chambres à circulation, des circuits microfluidiques, des microplaques spécifiques ou des techniques de coloration. Des techniques avancées, telles que la microscopie électronique ou confocale, et des logiciels élaborés sont essentiels pour la visualisation de ces biofilms et permettent une analyse plus approfondie, jusqu'à la quantification de la structure 3D (épaisseur, rugosité et biovolume), la localisation de la matrice extracellulaire *in situ*, ainsi que le suivi de l'expression génique aux niveaux spatio-temporels. Un cadre optimisé pour un tel système, développé par Briandet et ses collaborateurs, consistant en la croissance de biofilms immergés dans des microplaques, combiné à une technique de microscopie confocale, permet une surveillance à la fois spatiale et temporelle des biofilms immergés au niveau de la cellule unique [62], [63], [65]. Dans ce contexte, une étude architecturale comparative du biofilm immergé a été réalisée sur différentes souches de *B. subtilis* dont la souche de référence 168, dans laquelle la souche *B. subtilis* NDmed s'est avérée former le biovolume le plus élevé au niveau immergé [62].

B. subtilis NDmed, un hyper biofilm formateur isolé d'un dispositif médical

Les communautés associées à la surface sont à l'origine de nombreux problèmes dans un grand nombre de milieux écologiques, industriels et hospitaliers, y compris des problèmes de santé publique tels que les infections nosocomiales [66], [67]. Par exemple, même après les procédures de nettoyage et de désinfection, certaines études ont rapporté la persistance de bactéries associées à la surface sur un endoscope [68], [69]. Dans ce contexte, la souche non domestiquée de *B. subtilis* NDmed isolée à partir d'un laveur-désinfecteur d'endoscope d'un hôpital en Angleterre [42], s'est avérée hyper-résistante à l'action des biocides, à savoir l'acide peracétique (PAA), un désinfectant fréquemment utilisé pour désinfecter les endoscopes [70].

Au sein d'une collection d'isolats de *B. subtilis*, Bridier *et al.* ont montré que la souche NDmed présentait le biovolume de biofilm le plus élevé formant des structures en forme de «tige de haricot » pouvant atteindre une hauteur allant jusqu'à 300 µm, au niveau immergé [62]. En utilisant des

techniques de microscopie confocale et électronique, la souche NDmed a été caractérisée pour former des biofilms architecturaux dans l'espace, immergés et en colonies, avec des quantités élevées de substances exopolymères par rapport à la souche de référence *B. subtilis* 168 [70]. De plus, la visualisation en temps réel de la perte d'intégrité des membranes par fluorescence a indiqué une inactivation cellulaire après un traitement à l'acide peracétique (PAA) dans les 30 secondes pour les cellules du biofilm formées par la souche *B. subtilis* 168, tandis que la perte était beaucoup plus progressive dans le biofilm formé par souche NDmed, où des poches de cellules survivantes étaient encore visibles même après 10 minutes d'exposition [70].

Génétiquement, la séquence NDmed est très similaire à celle de la souche de référence 168, avec moins de 100 polymorphismes mononucléotidiques (SNP) et moins de 50 insertions/délétions [71]. Les gènes défectueux dans la souche 168 (*sfp, epsC, swrA et degQ*) sont fonctionnels à la fois dans NDmed et NCIB3610. Semblablement à d'autres souches de type sauvage, NDmed possède un gène *ypqP* fonctionnel (renommé par la suite *spsM* dans [72]), alors que ce gène est disrupté par le prophage SPβ à la fois dans 168 et NCIB3610. Le gène *ypqP*, potentiellement impliqué dans la synthèse du polysaccharide, est impliqué dans la structure 3D spatiale mucoïde du biofilm et participe à la résistance à l'action du biocide [63].

NDmed n'est pas une bactérie pathogène mais s'est avérée capable de protéger des bactéries pathogènes telles que *Staphylococcus aureus* de l'action de biocides lorsqu'elles sont cultivées ensemble dans des biofilms mixtes. Un mutant *ypqP* a perdu la majeure partie de sa capacité à protéger les agents pathogènes [63]. En d'autres termes, cela signifie que dans un biofilm d'espèces mixtes exposé à un biocide, un gène responsable de la persistance du pathogène a été identifié, mais ce gène (*ypqP*) provient du génome du partenaire, pas du pathogène. Cette observation ouvre des perspectives d’approches métagénomiques dans ce domaine du contrôle des biofilms comme déjà exploré dans le microbiote humain [73].

Par conséquent, pour pouvoir développer des stratégies appropriées pour contrôler ces communautés limitées en surface, une compréhension plus approfondie des similitudes et des différences de leur nature moléculaire est nécessaire. L'objectif principal de ce projet de thèse est de « Comparer les différents modèles de biofilm de *B. subtilis* et identifier les déterminants génétiques impliqués dans l'hétérogénéité des sous-populations ».

Cela est présenté en trois chapitres : 1) Différenciation phénotypique à travers les différents modèles de biofilm (Article 1, publié) ; 2) Étude de la dynamique de la colonisation de surface de *B. subtilis* poussant dans une culture liquide statique (Article 2, publié) ; 3) Analyse spatiale du transcriptome pour 9 sous-populations collectées à partir de milieux liquides, semi-solides et solides, en utilisant la même souche (*B. subtilis* NDmed) et le même milieu (Article 3, en préparation).

RÉSULTATS

Chapitre 1 : « Comparaison des caractéristiques génétiques impliquées dans la formation de biofilm de *Bacillus subtilis* à l'aide d'approches multiculturales » (article 1, publié).

Dans l'étude de leur contribution à la différenciation phénotypique, nous nous sommes intéressés à l'effet de mutations de plusieurs génes sur les différents modèles de biofilm (macrocolonie, essaimage, pellicule et sur le biofilm immergé), en utilisant la souche *B. subtilis* NDmed et 15 dérivés mutés pour des gènes dont il a déjà été démontré qu'ils étaient nécessaires à la motilité et à la formation de biofilm. Les résultats de cet article ont été discutés en termes de pertinence pour déterminer si les gènes impliqués dans la formation de colonies et de pellicules régissent également la formation de biofilms submergés, en tenant compte des spécificités de chaque modèle. Généralement, pour les 15 souches NDmed mutées étudiées, toutes ont montré un phénotype altéré pour au moins un des différents tests de de culture de laboratoire. Par exemple, la mutation de gènes impliqués dans la production de matrice (c'est-à-dire *tasA, epsA-O, cap, ypqP*) a un impact négatif sur tous les phénotypes de biofilm, cependant, a favorise la motilité de l'essaimage sur les surfaces semi-solides. A partir des gènes de la matrice, il a été démontré que la mutation de *bslA* (un gène codant pour une protéine amphiphile) affecte la stabilité de la pellicule à l'interface air-liquide sans impact sur le modèle de biofilm immergé. De plus, la mutation de *lytF*, un gène d'autolysine requis pour la séparation cellulaire, a un effet plus important sur le modèle de biofilm immergé que celui formé au niveau aérien, contrairement à l'observation pour le mutant *lytABC*. De plus, *B. subtilis*NDmed avec la mutation *sinR* forme une macrocolonie moins ridée, que celle formée par le type sauvage, mais ne peut former ni une pellicule épaisse ni un biofilm submergé structuré. Par conséquent, les mutations géniques peuvent soit avoir un impact similaire sur tous les différents modèles de biofilm formés dans différentes conditions de culture, soit peuvent

également montrer quelques différences. Cependant, on sait peu de choses sur la dynamique de la colonisation de surface dans une culture liquide statique.

Chapitre 2 : «Redistribution coordonnée de population entre le biofilm submergé de *Bacillus subtilis* et la pellicule liquide-air » (article 2, publié)

Dans cette contribution, nous nous sommes intéressés à étudier la dynamique de la colonisation de surface de *B. subtilis* en croissance statique dans un puits de microplaque, en profitant de la 4D-CLSM. La souche NDmed a été marquée par une fusion fluorescente transcriptionnelle (mCherry ou GFP) et observée par microscopie confocale 4D. Nous avons d'abord pu observer une construction de cellules sessiles au niveau immergé puis après plusieurs heures (environ 7 à 8 heures) l'intensité de fluorescence augmente à l'interface liquide-air correspondant à la formation de la pellicule (Figure 1). Un examen plus approfondi du niveau immergé a montré qu'au premier stade, les cellules sessiles prolifèrent sous la forme d'un réseau dense de longs filaments couvrant la surface. Après 2 à 4 heures de prolifération, on observe une fragmentation soudaine des chaînes allongées et la libération de nuages de courtes cellules nageant librement (Figure 2A).

Pour comprendre le mécanisme à l'origine de la fragmentation des cellules sessiles en cellules hautement mobiles, une analyse du transcriptome à l'échelle temporelle a été effectuée sur l’ensemble des cellules de *B. subtilis* du puits. Une vue globale des résultats a indiqué que les gènes codant pour les fonctions de base essentielles à la croissance cellulaire (c.à.d. les gènes liés à la réplication, la transcription, la traduction ou le métabolisme central du carbone) sont exprimés à un taux constant durant les premières heures (de 1h à 7h), indiquant que le processus de fragmentation se produit pendant que les cellules se développent à un rythme constant. Les gènes liés à l'autolysine et à la motilité (Figure S1) ont montré une régulation positive après 3 heures d'incubation pour atteindre un niveau maximum après 4 heures d'incubation (le temps pendant lequel les chaînes sessiles allongées se fragmentent en cellules courtes mobiles), confirmant ce qui avait été observé en microscopie confocale. Les gènes liés à la respiration, et non ceux liés aux nutriments, sont exprimés de manière variable à travers les différents temps choisis, suggérant que la fragmentation était déclenchée suite à une limitation en oxygène. La fragmentation est suivie par l'expression de gènes liés au biofilm (c'est-à-dire les gènes de la matrice) après environ 7 heures, suivie par les gènes tardifs liés au biofilm et les gènes de sporulation (après 24 et 48 heures).

NDmed rapportant par fusion GFP au promoteur l'expression de *hag* (un gène responsable de la motilité) et par fusion mKate l'expression de *tapA* (nécessaire pour assembler et ancrer la protéine TasA à la paroi cellulaire qui est à son tour impliquée dans la synthèse de la matrice extracellulaire) a été observée spatialement et temporellement (Figure 3 et 4A, B). De plus, une fusion transcriptionnelle au promoteur de *fnr* permet également de rapporter l'expression de ce gène codant pour un régulateur de la réponse globale à l'appauvrissement en oxygène (Figure 4C). En parallèle, la concentration en oxygène dans un puits a été mesurée physiquement par une microélectrode (Figure 4D). Les résultats ont montré qu'au cours des 3 premières heures, les chaînes sessiles de cellules exprimant *tapA* augmentent avec le temps et coexistant avec une sous-population mobile décroissante exprimant *hag* et l'oxygène étant toujours détecté. Après 3 heures, les chaînes cellulaires exprimant *tapA* se fragmentent et se différencient de manière soudaine et coordonnée en cellules individuelles mobiles exprimant *hag*. Entre-temps, une diminution stricte de la concentration en oxygène, en dessous de la limite de détection, est enregistrée. Ensuite, une reprise de l'expression de *tapA* (après 7 heures), indique une relocalisation et une structuration du biofilm immergé en saillie typique associé à la surface et initiant la pellicule flottante de *B. subtilis*, ce qui conduit à deux biofilms dans un même puits de culture liquide statique. Ainsi, la dynamique de culture statique liquide n'est pas un processus linéaire mais biphasique avec une relocalisation brutale de population entre les deux interfaces (liquide-solide et air-liquide) entraînant la coexistence à la fois du biofilm immergé et d'une pellicule flottante dans la même microplaque.

Chapitre 3 : « Le transcriptome spatial multi-échelle dévoile l'hétérogénéité entre les sous-populations des communautés associées à la surface de *Bacillus subtilis* » (Article 3, en préparation)

Pour mieux comprendre le coeur du réseau transcriptionnel actif pendant le développement du biofilm, une analyse de l'expression génique au niveau spatial a été réalisée pour les différentes localisations des compartiments hétérogènes de différents modèles de biofilms. Nous avons choisi d'étudier une culture liquide statique de 24 heures où nous avons séparé les pellicules des cellules détachées du compartiment immergé. De plus, nous avons utilisé une boite de swarming semi-solide de 24 heures et séparé 4 compartiments aux différentes localisations : la colonie mère, qui ressemble au biofilm formé par une macrocolonie mature sur une interface gélose-air ; la base de la dendrite, qui est une forme précoce de biofilm ; les dendrites, formées par des cellules en

monocouches s'apprêtant à produire des substances matricielles pour former plus tard le biofilm ; et enfin les pointes qui sont les cellules mobiles et à forte division ; comme référence, nous avons collecté la phase exponentielle et stationnaire d'une culture planctonique. Après la sélection, des échantillons ont été collectés, et finalement nous avons eu 9 conditions différentes avec 3 répétitions biologiques pour chacune. Il est important de noter que toutes les cultures ont été réalisées dans le même milieu minimum B-glucose. Pour les 27 échantillons collectés, une extraction d'ARN par lyse mécanique a été réalisée suivie d'évaluations quantitatives et qualitatives, respectivement par nanodrop et bioanalyseur.

Après le séquençage, une analyse par regroupement (« *clustering* ») hiérarchique a été effectuée pour évaluer la qualité et la reproductibilité de l'énorme ensemble de données d'ARN. L'analyse par *clustering* (Figure 2a) est basée sur une certaine notion de « similitude », dans laquelle elle montre comment les différents compartiments spatiaux sont distincts les uns des autres avec leurs trois réplicats biologiques tous regroupés. Ceci est vrai pour toutes les conditions à l'exception des trois réplicas biologiques de la population de dendrites qui sont répartis entre les compartiments adjacents, la base et les pointes Cela pourrait être dû soit techniquement à la difficulté de séparer les différents compartiments d'essaimage, soit à la proximité de l'état physiologique des cellules adjacentes. Pour identifier en profondeur la physiologie des cellules, une analyse des gènes différentiellement exprimés (DEG) a été réalisée qui a permis d'identifier un certain nombre de gènes statistiquement régulés à la hausse ou à la baisse dans une condition par rapport à une autre prise comme référence (Figure 2b). Les comparaisons entre les compartiments d'essaimage adjacents (dendrites vs base ou pointes vs dendrites) montrent peu d'expressions différentielles de gènes, suggérant que la proximité physiologique des cellules.

Afin de mieux visualiser le niveau d'expression génétique parmi les compartiments adjacents, les modèles de biofilm ont été analysés séquentiellement. Pour l'essaimage, 2371 sur 4028 gènes sont différentiellement exprimés entre les quatre compartiments localisés d'un swarm (Figure 3a). Les gènes sont regroupés selon la similitude de leur profil d'expression génique en 47 groupes (numérotés en fonction de la quantité de gènes regroupés dans un ordre décroissant) et sont systématiquement comparés et classés selon les catégories fonctionnelles Subtiwiki (c'est-à-dire enveloppe cellulaire et division cellulaire, synthèse des protéines, motilité et formation de biofilm) qui sont présentés en pourcentage des gènes trouvés dans un groupe en fonction du nombre total

de gènes constituant cette catégorie fonctionnelle (Figure 3b). Par exemple, le groupe 1 regroupe 1082 gènes régulés à la hausse dans la colonie mère et régulés à la baisse dans les compartiments d'essaimage. Ce groupe contient des gènes liés à la sporulation, à différentes voies métaboliques telles que celles du métabolisme du carbone, du métabolisme des lipides et autres, et des gènes codant pour le transport des électrons et la synthèse de l'ATP comme les gènes liés à la respiration (à la fois pour les anaérobies ou les aérobies). Les gènes liés à la formation de biofilm, c'est-à-dire les opérons *eps*, *tapA* et *slrR* sont principalement régulés à la hausse dans la colonie mère et la base (GS7 et GS8) et, comme prévu, les gènes de motilité et de chimiotaxie sont régulés à la hausse de manière différentielle dans les compartiments d'essaimage et non dans la colonie mère (GS2 et GS3). La même étude a été fait pour la culture liquide statique, dans laquelle 1916 des 4028 gènes sont exprimés de manière différentielle entre compartiments adjacents (environ la moitié du génome), regroupés en 26 groupes (Figure 4). Par exemple, les gènes liés à la motilité et à la chimiotaxie (Groupe GL1) montrent une régulation positive dans les cellules détachées par rapport à celles en biofilm submergé ou dans la pellicule. Les gènes liés au biofilm sont plus exprimés dans la pellicule et les cellules détachées que dans les cellules submergées. Les gènes liés à la sporulation sont plus exprimés dans la pellicule que dans les 2 autres compartiments et environ 70 % des gènes liés à l'adaptation au stress (sous le régulon *sigB*) sont régulés à la hausse uniquement dans le biofilm immergé. Les données du transcriptome représentent l'expression génique différentielle moyenne des cellules dans une population de biofilm.

Cependant, nous étions intéressés à aller au-delà et à visualiser *in situ* à un niveau cellulaire unique l'expression des gènes dans les différentes populations de biofilm. En utilisant les données du transcriptome, nous avons sélectionné des gènes représentant les différents types cellulaires présents dans un biofilm, 17 gènes (c'est-à-dire ceux liés à la matrice, à la motilité, au métabolisme du carbone et autres...) et construit des fusions transcriptionnelles rapportices de l’expression de gènes d’intérêt par des protéines fluorescentes Gfp ou mCherry. L'imagerie confocale a révélé des profils locaux d'expression génique, non seulement parmi les différents compartiments spatiaux étudiés, mais aussi au sein de chaque population de biofilm. Étonnamment, les gènes liés à la matrice (c'est-à-dire *eps, tapA et bslA*) se sont révélés fortement régulés à la baisse par rapport aux 2 autres populations de biofilm (la pellicule et la colonie mère). Un suivi spatio-temporel 4D pour les différents gènes sélectionnés a dévoilé des profils hétérogènes d'expression génique (pour les 17 gènes testés) dans des biofilms immergés (Figure 6). Cette expression génique liée à la matrice

n'est pas uniforme mais comme une mosaïque dynamique avec différents types spatio-temporels d'expression génique. Par exemple, *eps* et *tapA* sont principalement exprimés dans les premiers stades du développement du biofilm submergé, suivis d'un stade de transition où *bslA* et *srfAA* sont exprimés et, à un stade tardif, les gènes liés à la matrice *ypqP* et *capE*. De plus, l'eDNA est un autre composant matriciel, également essentiel pour l'architecture 3D d'un biofilm. Pour observer l'eDNA, nous avons utilisé la souche Ndmed-GFP et l'iodure de propodium, un colorant fluorescent rouge imperméable qui se lie aux cellules endommagées par la membrane et à l'ADN. Fait intéressant, nous avons pu observer 2 oscillations principales de vagues de mortalité, la première entre et 13-24 heures et la seconde commençant après 42 heures (Figure 7) et semblant être principalement localisée au-dessus des cellules vivantes d'un biofilm. Ces oscillations de mortalité cellulaire sont interrompues par une légère augmentation de la population de cellules vivantes. Ainsi, toutes ces données permettent de préciser les singularités de chaque modèle de biofilm et de souligner la finesse de leur régulation spatio-temporelle jusqu'au niveau d'une seule cellule.

Complément au chapitre 3. « Résultats préliminaires sur l'hétérogénéité spatio-temporelle des flux métaboliques centraux de carbone lors d'assemblages multicellulaires associés à la surface de *Bacillus subtilis* »

La glycolyse et la gluconéogenèse sont 2 voies régulées de manière opposée, où pour *B. subtilis* se développant dans des conditions glycolytiques (c'est-à-dire avec du glucose comme source de carbone), le processus de glycolyse est activé et l'opéron *cggR-gapA* est induit et il est réprimé dans des conditions gluconéogèniques, tandis que dans ces conditions purement gluconéogéniques, les gènes *pckA* et *gapB* sont déréprimés. Ainsi, GapA et GapB sont deux enzymes régulées de manière opposée, en fonction du flux métabolique et ne peuvent pas être exprimées ensemble dans la même cellule à un moment donné. En creusant dans les données du transcriptome, la voie du métabolisme du carbone a attiré notre attention (Figure 1). Les 2 groupes de gènes (*cggR* et *gapA*, ou *pckA* et *gapB*) sont régulés de manière opposée dans la colonie mère, dans un essaim, ainsi que dans la pellicule, cependant, pour le biofilm immergé, ces 2 groupes sont tous deux régulés à la hausse. Cela suggère que dans le même biofilm, différentes sous-populations entrent dans différentes voies métaboliques. La question qui se pose ici est de savoir comment ces

sous-populations s'organisent spatialement dans un biofilm, sont-elles stratifiées, ségrégées ou entrelacées ?

Pour mieux comprendre ce qui se passe dans le temps et dans l'espace, une souche rapportant l'expression de *gapA* et de *gapB* par différentes fusions transcriptionnelles fluorescentes à ces gènes dans la même souche a été construite et observée *in situ* au niveau d'une seule cellule. Les résultats ont clairement confirmé les différences rapportées par l'analyse du transcriptome pour l'expression des gènes entre les compartiments adjacents. Par exemple, dans la colonie mère où le glucose est limité, l'intensité d'expression du gène mCherry rapportant un flux glycolytique (*cggR-gapA*) est inférieure à celle dans la base, tandis que l'intensité d'expression du gène GFP rapportant la gluconéogenèse (*gapB*) est clairement fortement régulée à la hausse (Figure 2). Une observation similaire a été faite pour une culture liquide statique de 24 heures (Figure 3), montrant que dans la pellicule, la plupart de la population exprime les gènes glycolytiques avec certaines cellules exprimant brutalement *gapB*, un gène purement gluconéogenique. Cependant, pour les cellules submergées, les deux sous-populations semblent co-exister.

L'imagerie confocale spatio-temporelle 4D durant 3 jours pour le biofilm immergé a montré que l'expression des gènes glycolytiques (rapportée par *PcggR-mCherry*) dans des bactéries poussant dans un milieu glycolytique minimal, diminue progressivement à mesure que les nutriments deviennent limitants avec le temps. Ceci est confronté à une explosion d'expression des gènes gluconéogèniques (rapportée par *PgapB-gfpmut3*) par quelques cellules, vers 24 heures (Figure 4). Après 24 heures, on peut observer une légère augmentation du nombre de cellules des deux sous-populations exprimant des gènes glycolytiques ou gluconéogèniques, suivie après 48 heures d'une augmentation des sous-populations coopératives exprimant des voies de régulation opposées du métabolisme du carbone. Ces observations pourraient être fortement corrélées avec les oscillations des vagues de mort cellulaire, la première vague ayant lieu entre 13 et 24 heures, suivie d'une deuxième vague plus élevée de cellules mortes commençant vers 42 heures.

Ces données préliminaires montrent la coexistence de sous-populations spatialement mélangées poussant sous un régime glycolytique ou gluconéogènique dans les trois modèles de biofilm : colonie, pellicule et biofilm immergé. Ce constat ouvre des portes supplémentaires pour comprendre : *quels sont les facteurs environnementaux qui déterminent cette répartition ? Y a-t-il*

des échanges de métabolites entre ces sous-populations ? Quels métabolites les cellules mortes fournissent-elles dans le milieu ?

CONCLUSION ET PERSPECTIVES

Les données de transcriptome obtenues sont massives et de nombreuses investigations sont encore nécessaires

Beaucoup de travail reste à faire pour extraire et digérer toutes les informations des données du transcriptome dont nous disposons. Par exemple, utiliser le modèle de swarming comme outil pour mieux comprendre l'ordre chronologique du développement du biofilm à la surface de la gélose en analysant en profondeur les différents profils d'expression génique entre les compartiments adjacents. Quant à la culture liquide statique, en utilisant 1 souche bactérienne et un modèle unifié, nous avons pu observer des niveaux d'hétérogénéité divergents et différents non seulement entre les différentes populations spatiales localisées mais aussi au sein d'une population, différentes sous-populations hétérogènes sont présentes. Sans oublier qu'environ 35% du génome correspondent à des gènes de fonctions inconnues, hypothétiques ou mal caractérisées, selon les catégories Subtiwiki, à partir desquelles en utilisant les données du transcriptome nous avons sélectionné et rapporté transcriptionnellement 3 gènes inconnus qui ont montré une expression très localisée (dans les pointes, cellules submergées et pellicule) et sont prêts pour de futures investigations.

Diversification spatio-temporelle des types cellulaires de *B. subtilis* dans un puits de microplaque

À partir de toutes les données ci-dessus, nous avons proposé une illustration schématique de la dynamique du biofilm liquide statique. L'adhésion des premières cellules à la surface immergée est suivie de l'initiation du biofilm, où les cellules sessiles adhérentes prolifèrent et produisent la matrice (expression de *tapA* et *eps*). Puis une différenciation cellulaire soudaine des cellules sessiles en cellules mobiles est observée, en milieu riche ou minimum. Cette différenciation cellulaire conduit à une redistribution massive de la population et probablement directement corrélée à la limitation de l'oxygène au niveau submergé.

Suite à cette redistribution massive de la population, il y a réorganisation du biofilm immergé et initiation de la formation de pellicule à l'interface air-liquide. Cela est accompagné de la première vague de mort cellulaire localisée, suivi peu de temps après par l'initiation de la sporulation indiquant que les cellules sont soumises à un stress. La maturation du biofilm se poursuit, associée à une légère augmentation de la population vivante, finalement suivie d'une 2ème vague de mort cellulaire.

Techniques avancées

Pour passer du niveau du transcriptome au niveau fonctionnel, le laboratoire utilise des techniques avancées telles que l'interférence CrispR, ou silencing, une technique basée sur l'utilisation d'une nucléase Cas9 catalytiquement inactive pour neutraliser sélectivement l'expression de gènes, fournissant une relation directe entre un gène et un phénotype lorsqu'elle est appliquée aux communautés associées aux surfaces. Cette approche s'est déjà avérée utile pour étudier la motilité et les phénotypes de biofilm chez les bactéries.

De plus, un projet d'investigation a été lancé dans l'équipe B3D par Marie-Françoise Noirot-Gros par criblage utilisant une approche par interférence CrispR plus précise pour identifier les gènes dont la répression affecte la forme physique de la communauté. L'objectif est de fournir une preuve de principe que cette approche pourrait être utilisée avec succès à l'échelle génomique, pour identifier les gènes impliqués dans la formation de biofilm.

Maintenant, pour une meilleure visualisation des profils d'expression génique, une alternative à l'utilisation de fusions transcriptionnelles, est la technique récente de par-seqFISH qui permet de capturer des profils d'expression génique à un niveau de débit élevé avec la préservation du contexte physique des cellules individuelles au sein d'un biofilm.

RÉFÉRENCES

[1] W. J.Costerton, Z. Lewandowski, D. E. Caldwell, D. R. Korber, and H. M. Lappin-Scott, "Microbial biofilms," *Annu Rev. Microbiol*, no. 49, pp. 711–45, 1995.
[2] H. C. Flemming, J. Wingender, U. Szewzyk, P. Steinberg, S. A. Rice, and S. Kjelleberg, "Biofilms: An emergent form of bacterial life," *Nat. Rev. Microbiol.*, vol. 14, no. 9, pp. 563–575, 2016.
[3] M. A. Hassani, P. Durán, and S. Hacquard, "Microbial interactions within the plant holobiont,"

Microbiome, p. 6:58, 2018.
[4] W. K. Mousa, C. Shearer, V. Limay-Rios, C. L. Ettinger, J. A. Eisen, and M. N. Raizada, "Root-hair endophyte stacking in finger millet creates a physicochemical barrier to trap the fungal pathogen *Fusarium graminearum*," *Nat. Microbiol.*, vol. 1, no. December, 2016.
[5] E. G. Ruby and M. J. Mcfall-Ngai, "A Squid That Glows in the Night: Development of an Animal-Bacterial Mutualism," 1992.
[6] E. R. Rotman *et al.*, "Natural Strain Variation Reveals Diverse Biofilm Regulation in Squid-Colonizing Vibrio fischeri," *J Bacteriol*, vol. 201, pp. 33–52, 2021.
[7] H. C. Flemming and S. Wuertz, "Bacteria and archaea on Earth and their abundance in biofilms," *Nat. Rev. Microbiol.*, vol. 17, no. 4, pp. 247–260, 2019.
[8] Y. Chen *et al.*, "Biocontrol of tomato wilt disease by *Bacillus subtilis* isolates from natural environments depends on conserved genes mediating biofilm formation," 2012.
[9] B. Halan, K. Buehler, and A. Schmid, "Biofilms as living catalysts in continuous chemical syntheses," *Trends Biotechnol.*, vol. 30, no. 9, pp. 453–465, 2012.
[10] R. Singh, D. Paul, and R. K. Jain, "Biofilms: implications in bioremediation," *Trends Microbiol.*, vol. 14, no. 9, pp. 389–397, 2006.
[11] B. Erable, M. A. Roncato, W. Achouak, and A. Bergel, "Sampling natural biofilms: A new route to build efficient microbial anodes," *Environ. Sci. Technol.*, vol. 43, no. 9, pp. 3194–3199, 2009.
[12] E. Rosenberg, E. F. Delong, S. Lory, E. Stackebrandt and F. Thompson, *The Prokaryotes - Mycobacterium*. 2006.
[13] I. B. Beech and J. Sunner, "Biocorrosion: Towards understanding interactions between biofilms and metals," *Curr. Opin. Biotechnol.*, vol. 15, no. 3, pp. 181–186, 2004.
[14] H. C. Flemming, M. Meier, and T. Schild, "Mini-review: Microbial problems in paper production," *Biofouling*, vol. 29, no. 6, pp. 683–696, 2013.
[15] D. Davies, "Understanding biofilm resistance to antibacterial agents," *Nat. Rev. Drug Discov.*, vol. 2, no. 2, pp. 114–122, Feb. 2003.
[16] C. Moser *et al.*, "Immune Responses to *Pseudomonas aeruginosa* Biofilm Infections," *Front. Imunol.*, vol. 12, no. 625597, 2021.
[17] V. E. Wagner and B. H. Iglewski, "*P. aeruginosa* Biofilms in CF Infection," *Clinical reviews in allergy & immunology*, 35(3), 124–134. 2008.
[18] C. W. Hall and T.-F. Mah, "Molecular mechanisms of biofilm-based antibiotic resistance and tolerance in pathogenic bacteria," *FEMS Microbiol. Rev.*, vol. 010, pp. 276–301, 2017.
[19] A. D. Verderosa, M. Totsika, and K. E. Fairfull-Smith, "Bacterial Biofilm Eradication Agents: A Current Review," *Front. Chem.*, vol. 7, no. November, pp. 1–17, 2019.
[20] J. D. Bryers, "Medical biofilms," *Biotechnol. Bioeng.*, vol. 100, no. 1, pp. 1–18, 2008.
[21] J. A. Otter *et al.*, "Surface-attached cells, biofilms and biocide susceptibility: Implications for hospital cleaning and disinfection," *J. Hosp. Infect.*, vol. 89, no. 1, pp. 16–27, 2015.
[22] J. E. Nett, K. M. Guite, A. Ringeisen, K. A. Holoyda, and D. R. Andes, "Reduced biocide susceptibility in Candida albicans biofilms," *Antimicrob. Agents Chemother.*, vol. 52, no. 9, pp. 3411–3413, 2008.
[23] P. S. Stewart and J. W. Costerton, "Antibiotic resistance of bacteria in biofilms," *Lancet*, vol. 358, no. 9276, pp. 135–138, 2001.
[24] P. S. Stewart and M. J. Franklin, "Physiological heterogeneity in biofilms," *Nat. Rev. Microbiol.*, vol. 6, no. 3, pp. 199–210, 2008.
[25] D. Lopez, H. Vlamakis, and R. Kolter, "Generation of multiple cell types in *Bacillus*

subtilis," *FEMS Microbiol. Rev.*, vol. 33, no. 1, pp. 152–163, 2009.
[26] H. Vlamakis, C. Aguilar, R. Losick, and R. Kolter, "Control of cell fate by the formation of an architecturally complex bacterial community," *Genes Dev.*, vol. 22, no. 7, pp. 945–953, 2008.
[27] H. Vlamakis, Y. Chai, P. Beauregard, R. Losick, and R. Kolter, "Sticking together: Building a biofilm the *Bacillus subtilis* way," *Nature Reviews Microbiology*, vol. 11, no. 3. pp. 157–168, Mar-2013.
[28] D. López and R. Kolter, "Extracellular signals that define distinct and coexisting cell fates in *Bacillus subtilis*," *FEMS Microbiol. Rev.*, vol. 34, no. 2, pp. 134–149, 2010.
[29] T. Hoffmann, B. Troup, A. Szabo, C. Hungerer, and D. Jahn, "The anaerobic life of *Bacillus subtilis*: Cloning of the genes encoding the respiratory nitrate reductase system," *FEMS Microbiol. Lett.*, vol. 131, no. 2, pp. 219–225, 1995.
[30] M. M. Nakano and P. Zuber, "ANAEROBIC GROWTH OF A ' Strict Aerobe ' (*Bacillus Subtilis*)," *Annu. Rev. Microbiol.*, vol. 52, pp. 165–1990, 1998.
[31] M. M. Nakano, Y. P. Dailly, P. Zuber, and D. P. Clark, "Characterization of anaerobic fermentative growth of *Bacillus subtilis*: Identification of fermentation end products and genes required for growth," *Anal. Biochem.*, vol. 217, no. 2, pp. 220–230, 1994.
[32] M. Lacelle, M. Kumano, K. Kurita, K. Yamane, P. Zuber, and M. M. Nakano, "Oxygen-controlled regulation of the flavohemoglobin gene in *Bacillus subtilis*," *J. Bacteriol.*, vol. 178, no. 13, pp. 3803–3808, 1996.
[33] Yun Chen *et al.*, "Biocontrol of tomato wilt disease by *Bacillus subtilis* isolates from natural environments depends on conserved genes mediating biofilm formation," *Env. Microbiol.*, vol. 15, no. 3, pp. 848–864, 2013.
[34] Y. Deng *et al.*, "Complete genome sequence of *Bacillus subtilis* BSn5, an endophytic bacterium of Amorphophallus konjac with antimicrobial activity for the plant pathogen Erwinia carotovora subsp. carotovora," *J. Bacteriol.*, vol. 193, no. 8, pp. 2070–2071, 2011.
[35] T. M. Barbosa, C. R. Serra, R. M. La Ragione, M. J. Woodward, and A. O. Henriques, "Screening for *Bacillus* isolates in the broiler gastrointestinal tract," *Appl. Environ. Microbiol.*, vol. 71, no. 2, pp. 968–978, 2005.
[36] N. K. M. Tam *et al.*, "The intestinal life cycle of *Bacillus subtilis* and close relatives," *J. Bacteriol.*, vol. 188, no. 7, pp. 2692–2700, 2006.
[37] H. A. Hong *et al.*, "*Bacillus subtilis* isolated from the human gastrointestinal tract," *Res. Microbiol.*, vol. 160, no. 2, pp. 134–143, 2009.
[38] A. M. Earl, R. Losick, and R. Kolter, "Ecology and genomics of *Bacillus subtilis*," *Trends Microbio*, vol. 16, no. 6, p. 269, 2008.
[39] M. Fujita, K. Nomura, K. Hong, Y. Ito, A. Asada, and S. Nishimuro, "Purification and characterization of a strong fibrinolytic enzyme (nattokinase) in the vegetable cheese natto, a popular soybean fermented food in Japan. Biochem Biophys Res Commun." pp. 1340–1347, 1993.
[40] H. P. Bais, R. Fall, and J. M. Vivanco, "Biocontrol of *Bacillus subtilis* against Infection of *Arabidopsis* Roots by *Pseudomonas syringae* Is Facilitated by Biofilm Formation and Surfactin Production," *Plant Physiol.*, vol. 134, pp. 307–319, 2004.
[41] M. Marzorati *et al.*, "*Bacillus subtilis* HU58 and bacillus coagulans SC208 probiotics reduced the effects of antibiotic-induced gut microbiome dysbiosis in an M-SHIME® model," *Microorganisms*, vol. 8, no. 7, pp. 1–15, 2020.
[42] D. J. H. Martin, S. P. Denyer, G. McDonnell, and J. Y. Maillard, "Resistance and cross-

resistance to oxidising agents of bacterial isolates from endoscope washer disinfectors," *J. Hosp. Infect.*, vol. 69, no. 4, pp. 377–383, 2008.

[43] P. Sanchez-Vizuete, D. Le Coq, A. Bridier, J.-M. Herry, S. Aymerich, and R. Briandet, "Identification of *ypqP* as a New *Bacillus subtilis* Biofilm Determinant That Mediates the Protection of *Staphylococcus aureus* against Antimicrobial Agents in Mixed-Species Communities," *Appl Env. Microbiol*, vol. 81, no. 1, pp. 109–118, 2015.

[44] A. Bridier *et al.*, "Biofilms of a *Bacillus subtilis* Hospital Isolate Protect *Staphylococcus aureus* from Biocide Action," *PLoS One*, vol. 7, no. 9, 2012.

[45] H. Vlamakis, Y. Chai, P. Beauregard, R. Losick, and R. Kolter, "Sticking together: Building a biofilm the *Bacillus subtilis* way," *Nature Reviews Microbiology*, vol. 11, no. 3. pp. 157–168, Mar-2013.

[46] P. J. Piggot and D. W. Hilbert, "Sporulation of *Bacillus subtilis*," *Curr. Opin. Microbiol.*, vol. 7, no. 6, pp. 579–586, 2004.

[47] L. S. Cairns, L. Hobley, and N. R. Stanley-Wall, "Biofilm formation by *Bacillus subtilis*: New insights into regulatory strategies and assembly mechanisms," *Mol. Microbiol.*, vol. 93, no. 4, pp. 587–598, 2014.

[48] S. S. Branda, J. E. G. Lez-Pastor, S. Ben-Yehuda, R. Losick, and R. Kolter, "Fruiting body formation by *Bacillus subtilis*," *PNAS*, vol. 98, no. 2, pp. 11621–26, 2001.

[49] A. L. McLoon, S. B. Guttenplan, D. B. Kearns, R. Kolter, and R. Losick, "Tracing the domestication of a biofilm-forming bacterium," *J. Bacteriol.*, vol. 193, no. 8, pp. 2027–2034, 2011.

[50] D. B. Kearns and R. Losick, "Swarming motility in undomesticated *Bacillus subtilis*," *Mol. Microbiol.*, vol. 49, no. 3, pp. 581–590, 2003.

[51] K. Hamze *et al.*, "Single-cell analysis in situ in a *Bacillus subtilis* swarming community identifies distinct spatially separated subpopulations differentially expressing *hag* (flagellin), including specialized swarmers," *Microbiology*, vol. 157, no. 9, pp. 2456–2469, 2011.

[52] D. Julkowska, M. Obuchowski, I. B. Holland, and S. J. Séror, "Comparative analysis of the development of swarming communities of *Bacillus subtilis* 168 and a natural wild type: Critical effects of surfactin and the composition of the medium," *J. Bacteriol.*, vol. 187, no. 1, pp. 65–76, 2005.

[53] D. Julkowska, M. Obuchowski, I. B. Holland, and S. J. Séror, "Branched swarming patterns on a synthetic medium formed by wild-type *Bacillus subtilis* strain 3610: Detection of different cellular morphologies and constellations of cells as the complex architecture develops," *Microbiology*, vol. 150, no. 6, pp. 1839–1849, 2004.

[54] L. Hamouche *et al.*, "*Bacillus subtilis* Swarmer Cells Lead the Swarm, Multiply, and Generate a Trail of Quiescent Descendants," *MBio*, vol. 8, no. 1, pp. 1–14, 2017.

[55] D. Debois *et al.*, "In situ localisation and quantification of surfactins in a *Bacillus subtilis* swarming community by imaging mass spectrometry," *Proteomics*, vol. 8, no. 18, pp. 3682–3691, 2008.

[56] K. Hamze *et al.*, "Identification of genes required for different stages of dendritic swarming in *Bacillus subtilis*, with a novel role for phrC," *Microbiology*, vol. 155, no. 2, pp. 398–412, 2009.

[57] M. A. Hamon and B. A. Lazazzera, "The sporulation transcription factor Spo0A is required for biofilm development in *Bacillus subtilis*," 2001.

[58] M. A. Hamon, N. R. Stanley, R. A. Britton, A. D. Grossman, and B. A. Lazazzera, "Identification of AbrB-regulated genes involved in biofilmformation by *Bacillus subtilis*,"

Mol Microbiol., vol. 52, no. 3, pp. 847–860, 2004.
[59] N. R. Stanley and B. A. Lazazzera, "Defining the genetic differences between wild and domestic strains of *Bacillus subtilis* that affect poly-γ-DL-glutamic acid production and biofilm formation," *Mol. Microbiol.*, vol. 57, no. 4, pp. 1143–1158, 2005.
[60] N. R. Stanley, R. A. Britton, A. D. Grossman, B. A. Lazazzera, S. E. T. Al, and J. B. Acteriol, "Identification of Catabolite Repression as a Physiological Regulator of Biofilm Formation by *Bacillus subtilis* by Use of DNA Microarrays," *J. Bacteriol.*, vol. 185, no. 6, pp. 1951–1957, 2003.
[61] R. Terra, N. R. Stanley-Wall, G. Cao, and B. A. Lazazzera, "Identification of *Bacillus subtilis sipw* as a bifunctional signal peptidase that controls surface-adhered biofilm formation," *J. Bacteriol.*, vol. 194, no. 11, pp. 2781–2790, 2012.
[62] A. Bridier, D. Le Coq, F. Dubois-Brissonnet, V. Thomas, A. Stéphane, and R. Briandet, "The Spatial Architecture of *Bacillus subtilis* Biofilms Deciphered Using a Surface-Associated Model and In Situ Imaging," *PLoS One*, vol. 6, no. 1, p. e16177, 2011.
[63] P. Sanchez-Vizuete, D. Le Coq, A. Bridier, J.-M. Herry, S. Aymerich, and R. Briandet, "Identification of *ypqP* as a New *Bacillus subtilis* Biofilm Determinant That Mediates the Protection of *Staphylococcus aureus* against Antimicrobial Agents in Mixed-Species Communities," *Appl Env. Microbiol*, vol. 81, no. 1, pp. 109–118, 2015.
[64] Y. Dergham *et al.*, "Comparison of the Genetic Features Involved in *Bacillus subtilis* Biofilm Formation Using Multi-Culturing Approaches," *Microorganisms*, vol. 9, no. 633, 2021.
[65] A. Bridier, F. Dubois-Brissonnet, A. Boubetra, V. Thomas, and R. Briandet, "The biofilm architecture of sixty opportunistic pathogens deciphered using a high throughput CLSM method," *J. Microbiol. Methods*, vol. 82, no. 1, pp. 64–70, 2010.
[66] L. Hall-Stoodley and P. Stoodley, "Evolving concepts in biofilm infections," *Cell. Microbiol.*, vol. 11, no. 7, pp. 1034–1043, 2009.
[67] A. Bridier, P. Sanchez-Vizuete, M. Guilbaud, J. C. Piard, M. Naïtali, and R. Briandet, "Biofilm-associated persistence of food-borne pathogens," *Food Microbiol.*, vol. 45, no. PB, pp. 167–178, 2015.
[68] A. K. Deva *et al.*, "Detection of persistent vegetative bacteria and amplified viral nucleic acid from in-use testing of gastrointestinal endoscopes," *J. Hosp. Infect.*, vol. 39, no. 2, pp. 149–157, 1998.
[69] A. P. Machado, A. T. M. Pimenta, P. P. Contijo, S. Geocze, and O. Fischman, "Microbiologic profile of flexible endoscope disinfection in two Brazilian hospitals," *Arq. Gastroenterol.*, vol. 43, no. 4, pp. 255–258, 2006.
[70] A. Bridier *et al.*, "Biofilms of a *Bacillus subtilis* Hospital Isolate Protect *Staphylococcus aureus* from Biocide Action," *PLoS One*, vol. 7, no. 9, 2012.
[71] P. Sanchez-Vizuete *et al.*, "Genome Sequences of Two Nondomesticated *Bacillus subtilis* Strains Able To Form Thick Biofilms on Submerged Surfaces," *Genome Announc.*, vol. 25, no. 2, p. 5, 2014.
[72] K. Abe *et al.*, "Developmentally-Regulated Excision of the SPβ Prophage Reconstitutes a Gene Required for Spore Envelope Maturation in *Bacillus subtilis*," *PLoS Genet.*, vol. 10, no. 10, 2014.
[73] M. Arumugam *et al.*, "Enterotypes of the human gut microbiome," *Nature*, vol. 473, no. 7346, pp. 174–180, 2011.

SCIENTIFIC VALUATION

Publications

[1] **Y. DERGHAM**, P. SANCHEZ-VIZUETE, D. LE COQ, J. DESCHAMPS, A. BRIDIER, K. HAMZE, R. BRIANDET. Comparison of the Genetic Features Involved in *Bacillus subtilis* Biofilm Formation Using Multi-Culturing Approaches. *Microorganisms*, vol. 9, no. 633, 2021.

[2] P. SANCHEZ-VIZUETE, **Y. DERGHAM,** A. BRIDIER, J. DESCHAMPS, E. DERVYN, K. HAMZE, S. AYMERICH, D. LE COQ, R. BRIANDET. The coordinated population redistribution between *Bacillus subtilis* submerged biofilm and liquid-air pellicle. *Biofilm*, 100065, 2021.

[3] **Y. DERGHAM,** D. LE COQ, P. NICOLAS, J. DESCHAMPS, E. HUILLET, P. SANCHEZ-VIZUETE, K. HAMZE, R. BRIANDET. Multi-scale spatial transcriptome unveils the heterogeneity between subpopulations of *Bacillus subtilis* surface-associated communities. *Under preparation*.

[4] **Y. DERGHAM,** D. LE COQ, K. HAMZE, R. BRIANDET. Spatio-temporal heterogeneity of central carbon metabolic fluxes during surface associated multicellular assemblages of *Bacillus subtilis*. *Under preparation*.

Oral communications

[5] **Y. DERGHAM,** D. LE COQ, K. HAMZE, R. BRIANDET. Multi-scale spatial transcriptome of the surface-associated communities of *Bacillus subtilis* NDmed. *Micalis seminar*, 9 October 2020, Viso-conference.

[6] **Y. DERGHAM,** D. LE COQ, K. HAMZE, R. BRIANDET. Multi-scale spatial transcriptome of the surface-associated communities of *Bacillus subtilis* NDmed. Doc' *Micalis*, 16 October 2020, Jouy-en-Josas, France.

[7] **Y. DERGHAM,** D. LE COQ, K. HAMZE, R. BRIANDET. Multi-scale spatial transcriptome of the surface-associated communities of *Bacillus subtilis* NDmed. *ESA Topical Team 'Biofilms'*, 11 November 2020, Viso-conference.

[8] R. BRIANDET**, Y. DERGHAM**, C. SAINT MARTIN, V. GUENEAU, J. DESCHAMPS, J.C PIARD. « Biofilms dans l'industrie : comment lutter contre ou les utiliser à bon escient ? » Clubster NSL (Nutrition Santé Longevité). Webinar Avril 2021.

[9] R. BRIANDET**, Y. DERGHAM**, D. LE COQ J. DESCHAMPS V. GUENEAU, C. SAINT MARTIN, P. SANCHEZ-VIZUETE. Symposium Pharmaceutique BioMérieux 2021. « Actualité et perspectives en Microbiologie pharmaceutique » 17 juin 2021, Marcy L'Etoile.

ÉCOLE DOCTORALE
Agriculture, alimentation, biologie, environnement, santé (ABIES)

Titre : Analyse spatio-temporelle du transcriptome d'assemblages multicellulaires de *Bacillus subtilis* associés aux surfaces

Mots clés : *Bacillus subtilis*, biofilm, essaimage, transcriptome, MCBL (microscopie confocale à balayage laser) & fusions transcriptionnelles fluorescentes, hétérogénéité.

Résumé : Les cellules microbiennes sont fréquemment associées à diverses surfaces, formant des assemblages multicellulaires complexes, appelées biofilms. Malgré certains effets bénéfiques de ces structures, elles sont souvent impliquées dans des infections chroniques humaines. Une souche non domestiquée de *Bacillus subtilis* (NDmed), récemment isolée d'un hôpital, s'est avérée former des biofilms immergés hautement structurés, hyper-résistants à l'action des biocides et capables de protéger des agents pathogènes lorsqu'ils y sont associés. Ainsi, comprendre comment ces communautés liées aux surfaces se forment est crucial pour leur contrôle. Des études sur les biofilms de *B. subtilis*, principalement sous forme de colonies et de pellicules, avaient permis d'identifier plusieurs gènes impliqués dans la formation et la régulation des structures 3D, mais leur implication dans le modèle de biofilm immergé restait incertaine. Afin de mieux comprendre les stratégies moléculaires se déroulant au cours du développement des biofilms, plus particulièrement le modèle immergé, nous avons réalisé des études génétiques comparatives par différentes approches, notamment le profilage spatio-temporelle du transcriptome, l'identification et la construction de mutants cibles et la MCBL/4D couplée à l'utilisation de fusions transcriptionnelles fluorescentes. Les données obtenues à partir de l'analyse RNA-seq ont offert une vue globale sur les différents profils d'expression génétique pour chacune des populations spatiales associées aux surfaces. La comparaison entre ces profils transcriptomiques a révélé des similitudes et des différences entre des compartiments spatialement distincts. De plus, la visualisation spatio-temporelle *in situ* de l'expression de plusieurs gènes au niveau de la cellule unique a révélé de nouvelles paternes d'expressions suggérant de nouveaux mécanismes de régulation de ces communautés structurées.

Title : Spatio-temporal transcriptome analysis of surface-associated multicellular assemblages of *Bacillus subtilis*

Keywords : *Bacillus subtilis*, biofilm, swarming, transcriptome, CLSM (confocal laser scanning microscopy) & fluorescent transcriptional fusions, heterogeneity.

Abstract : Microbial cells are frequently found associated to various surfaces, forming complex multicellular assemblages, known as biofilms. Despite some beneficial effects provided by these structures, they are often involved in human chronic infections. An undomesticated *Bacillus subtilis* strain (NDmed), lately isolated from a hospital, has been found to form highly structured immersed biofilms hyper-resistant to biocide action and able to protect pathogens when associated with them. Thus, understanding how these surface bounded communities are formed is crucial for their control. *Bacillus subtilis* biofilm studies, mainly on colony and pellicle, had allowed to identify several genes involved in the formation and the regulation of 3D structures, but their involvement in the submerged biofilm model remained unclear. In order to better understand the molecular strategies taking place during biofilm development, we have performed genetic comparative studies using different approaches, including the swarming model, temporal and spatial transcriptome profiling, identification and construction of target mutants and 4D CLSM coupled with the use of fluorescent transcriptional fusions. Data obtained from RNA-seq analysis gave a global view on the different genetic expression profiles for each of the local spatial surface-associated population. Comparison between these transcriptome profiles indicated similarities and differences exhibited between the distinct spatial surface compartments. Moreover, *in situ* spatio-temporal visualization of expression of several genes at single cell level revealed undescribed patterns suggesting new mechanisms of regulation in these structured communities.

Maison du doctorat de l'Université Paris-Saclay
2ème étage aile ouest, Ecole normale supérieure Paris-Saclay
4 avenue des Sciences,
91190 Gif sur Yvette, France